Technical Report

TR-02-12

The Buffer and Backfill Handbook

Part 2: Materials and techniques

Roland Pusch
Geodevelopment AB

December 2001

Svensk Kärnbränslehantering AB
Swedish Nuclear Fuel
and Waste Management Co
Box 5864
SE-102 40 Stockholm Sweden
Tel 08-459 84 00
+46 8 459 84 00
Fax 08-661 57 19
+46 8 661 57 19

The Buffer and Backfill Handbook

Part 2: Materials and techniques

Roland Pusch
Geodevelopment AB

December 2001

Contents

1 Symbols and definitions

a_c	=	activity
a_z	=	swelling index
A	=	cross section, creep parameter, weight percentage
A_s	=	contact area
b	=	soil structure coefficient, load factor
B	=	creep parameter
B_s	=	solid phase modulus
B_w	=	bulk modulus
c, c'	=	cohesion
C	=	heat capacity, concentration
C_c	=	compression index, gradation coefficient
C_u	=	uniformity coefficient
d	=	diameter, distance, sample thickness
d_{10}, d_{60}	=	grain diameters
D_a	=	apparent diff. coefficient
D_e	=	effective diff. coefficient
D_p	=	pore diffusivity
D_s	=	surface diffusion coefficient
e	=	void ratio
E	=	modulus of elasticity
F	=	force
g	=	gravity
g_o	=	organic content
g_1, g_c	=	ignition loss
G	=	shear modulus
h	=	settling distance
i	=	hydraulic gradient, activity
I_P	=	plasticity index
I_C	=	consistency index
I_L	=	liquidity index
k	=	(hydraulic) permeability, colorimeter reading
K	=	hydraulic conductivity, compression modulus
K_d	=	sorption factor
l	=	sample length (height)
l_c	=	content of particles with an equivalent stoke diameter smaller than 2 μm
L_S	=	linear shrinkage
m	=	mass, modulus number
m_j	=	modulus number (ref.)
m_s	=	mass of solid matter
m_w	=	mass of water
M	=	oedometer modulus
M^I, M^{II}, M^{III}	=	metal cations
n	=	porosity
p	=	normal stress
p_S	=	swelling pressure
P	=	vapor pressure
q	=	deviator stress
R	=	molar gas constant, roundness
R_S	=	shrinkage ratio
s	=	salt content of pore fluid, scale factor
S	=	expansion ("rebounce"), sphericity
S_r	=	degree of water saturation, vol %
S_t	=	sensitivity
t	=	time
T	=	temperature
u	=	porewater press.
ν	=	Poisson's ratio
V	=	bulk volume
V_d	=	volume of dry soil sample
V_p	=	pore volume
V_s	=	volume of solid matter
V_S	=	volumetric shrinkage
V_w	=	volume of water
V_g	=	volume of gas
w	=	water content (ratio)
w_L	=	liquid limit
w_P	=	plastic limit
w_S	=	shrinkage limit
x	=	variable
y	=	variable

α	=	heat expansion coefficient	ρ_w	=	density of water
α_s	=	swelling index	σ	=	pressure
β	=	stress exponent	σ'	=	effective press.
ε	=	strain	σ_c'	=	preconsolidation pressure
γ	=	shear strain	σ_j	=	reference stress
ξ	=	constitutional parameter	τ	=	shear stress
η	=	viscosity	τ_{fu}	=	undrained shear strength
λ	=	heat conductivity	τ_r	=	remoulded shear strength
ν	=	Poisson's ratio	ϕ	=	electrical potential
ρ	=	bulk density	ϕ, ϕ'	=	friction angle
ρ_d	=	dry density	Δl	=	shortening of sample with length (height) l
ρ_s	=	density of solid particles			
ρ_{sat}	=	density of fluid-saturated soil			

Note 1 on "Grain size"
In literature the grain size distribution is expressed as "Percentage finer than", "percent finer by weight", weight percent passing etc. They appear in various diagrams quoted from various literature sources.

Note 2 on "Symbols"
Some additional symbols that appear in the Handbook are not included here as they are self-explanatory or defined in the text.

2 Introduction

2.1 General

Buffer is the term for dense clay used for embedment of canisters with highly radioactive waste, while backfill is soil used for filling tunnels and shafts in repositories.

Examples of soil materials of potential use as buffers and backfills in repositories of KBS-3 type are described in this part of the Handbook. They are:

- Smectitic clay materials intended for preparation of buffers (canister-embedding clay) and used as clay component in artificially prepared tunnel and shaft backfills consisting of mixtures of clay and ballast.
- Ballast materials intended for backfilling of tunnels and shafts and used as components of artificially prepared backfills.
- Smectitic natural clay soils intended for use as buffers and backfills.
- Very fine-grained smectite clay used as grout for sealing rock fractures.

In this part of the Handbook for Buffers and Backfills, description of various candidate materials will be made with respect to their mineral composition and physical properties, with respect to the groundwater chemistry that can be expected in a deep repository in Swedish bedrock.

2.2 Scope

Improved technology and prospection yielding more pure and homogeneous raw materials for preparing buffers and backfills will ultimately outdate the clays and ballast materials described in the present part of the Handbook. It describes experimentally investigated materials of potential use in repositories but other, more suitable materials will replace them in the future. The Handbook will hence have to be reviewed regularly, making room for superior materials in future, upgraded Handbook versions.

2.3 Major content of Chapters 3–9

Chapter 3 deals with smectitic clay materials intended for embedment of heat-producing canisters with highly radioactive waste. Focus is on the nature of the buffer constitutents, i.e. the smectite content, the non-expanding clay minerals colloidal and the accessory non-clay minerals as well as amorphous matter and organic substances. The dominant part of the chapter describes the occurrence and origin of commercially smectite-rich clays.

Chapter 4 deals with the non-clay mineral components of mixtures of such material, termed "ballast" here, and smectitic clay. Mixtures of this sort can primarily be used for backfilling shafts and tunnels with less tight soil material than the buffer clay but sufficiently low-conductive and expansive to prevent deposition tunnels from serving as effective hydraulic conductors. The chapter also describes major sources, primarily glacial deposits and crushed rock.

Chapter 5 deals with the granulometric composition of mixtures of smectitic clay and ballast for achieving good compactability and effective filling of clay in the voids between ballast grains. Focus is on the gradation of the ballast and the density of the clay component since it controls the hydraulic conductivity of the mixtures.

Chapter 6 deals with chemical composition and properties of smectitic clays and ballast materials. It is a very comprehensive issue and we will confine ourselves to describe the chemical composition of clays tested by SKB and provide a basis for estimating their chemical stability and physical performance.This latter issue is under investigation and is further treated in Part 3.

Chapter 7 gives the basis of selection of suitable buffers and clay/ballast mixtures with respect to their desired performance in a repository. Major physical properties of common commercial smectite-rich clays and clay/ballast mixtures are described in detail and can serve as reference in designing buffers and backfills.

Chapter 8 deals with methods for preparing buffer materials, primarily blocks of highly compacted smectite-rich clay materials. Also, major physical properties of compacted blocks are given as a basis of determining the performance of the system of blocks applied in deposition holes before hydration, swelling and homogenisation has started.

Chapter 9 describes methods for preparing, applying and compacting clay/ballast mixtures. Examples are given from large-scale field tests like the Stripa and Äspö Projects.

3 Buffer materials

This chapter deals with smectitic clay materials intended for embedment of heat-producing canisters with highly radioactive waste. Focus is on the nature of the buffer constituents, i.e. the smectite content, the non-expanding clay minerals and the accessory non-clay minerals as well as amorphous matter and organic substances. The dominant part of the chapter describes the occurrence and origin of commercially smectite-rich clays.

3.1 Introduction

It was early concluded that clay-based embedment of canisters and backfill in drifts and shafts offers the best isolation through the low hydraulic conductivity and canister-supporting ability of such materials /1, 2/. Also, the ion sorption and its impact on diffusion were identified as important properties and comprehensive systematic laboratory studies have been made for finding suitable clay materials. A major requirement in this respect has been to find source materials of sufficient quantities and homogeneity for commercial use. While these studies were focused on montmorillonite-rich clays because of its particularly low hydraulic conductivity and high potential of becoming homogeneous, a more extensive search has been made in recent years for checking the sealing capacity also of other clay materials. This work, which was made by use of samples prepared by compaction under 100 MPa pressure, led to the following conclusions /3/:

- In addition to MX-80, which has been used as reference clay material in SKB-related R&D through the years, the following clay types: saponite (Mg-rich smectite), mixed-layer (smectite/illite) Friedland Ton, kaolinite, and palygorskite, are all possible buffer candidates and commercially available in large quantities.
- MX-80, representing montmorillonite-rich (>60%) clays, has the lowest hydraulic conductivity of all the investigated clay types, saponite being somewhat more permeable but still tighter than mixed-layer clay, palygorskite and kaolinite. Palygorskite has a very high swelling pressure and buffer can therefore be prepared with a lower density than MX-80 clay. MX-80 and saponite have the highest cation sorption capacity. Palygorskite and very finely ground kaolinite have an appreciable anion sorption potential. Kaolinite and mixed-layer clay are concluded to have the highest thermal conductivity. Kaolinite and palygorskite are concluded to show less creep than MX-80 and mixed-layer clay. This means that the firstmentioned buffer clays minimize canister movement.
- Assessment of the various properties has led to the conclusion that smectite-rich clays are most suitable for preparing buffer material with mixed-layer clay coming next and being preferable for certain purposes. These clays are represented by autochtonous and allochthonous bentonites and certain sedimentary clay deposits. For backfilling of drifts and shafts one can consider mixed-layer clay as a primary candidate but artificially prepared mixtures of very smectite-rich clay and ballast material may be equally good.

3.2 Smectite constitution

3.2.1 General

Clay minerals are described in detail in Part 1 /4/. Here, we will confine ourselves to summarize their constitution and fundamental physico/chemical properties as a basis of selection of suitable clays for practical use as seals in repositories. As indicated by the preceding text the document will focus on smectitic clays and rock material that can be used for preparing mixtures with such clay materials.

The major smectite species, which are present in different proportions in many natural bentonite layers, are generalized as:

- Montmorillonite: Only Si in the tetrahedrons and Al in the octahedrons.
- Beidellite: Si and Al in the tetrahedrons and Al in the octahedrons.
- Nontronite: Si and Al in the tetrahedrons and Fe in the octrahedrons.
- Hectorite: Si in the tetrahedrons and Mg and Li in the octahedrons.
- Saponite: Si and Al in the tetrahedrons and Mg in the octrahedrons.

3.2.2 Hydration properties

The hydration of the interlamellar space depends on the crystal lattice constitution since it determines the charge and coordination of adsorbed cations and water molecules. A water hull, one monolayer thick and containing cations, is sorbed on the basal surfaces of practically all minerals and plays a role in diffusive ion transport and in osmotic swelling of smectites. The interlamellar hydrates largely determine the swelling potential, plasticity and rheological behavior and are hence of fundamental importance /4/. Figure 3-1 shows a generalized section of a montmorillonite particle consisting of two lamellae (flakes), while Figure 3-2 shows a schematic picture of the organisation of water molecules in the interlamellar space. The coordination of interlamellar cations, the crystal lattice and the water molecules depends strongly on the size and charge of the cations and of the charge distribution in the lattice. 3 hydrate layers can only be formed in some of the smectite species and normally only when sodium, lithium or magnesium are in interlamellar positions (Table 3-1). One finds from this table that montmorillonite is the only smectite mineral that can expand by forming 3 interlamellar hydrates.

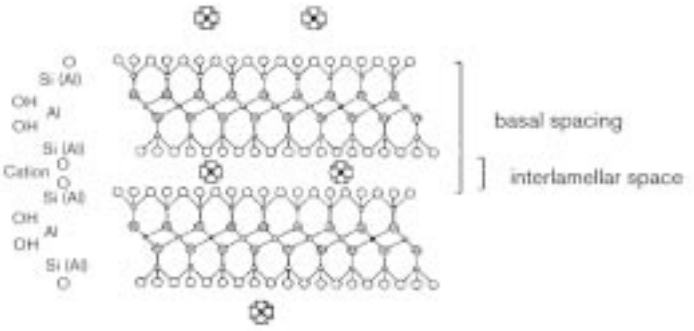

Figure 3-1. *A montmorillonite particle consisting of two lamellae. Hydrated cations are in the interlamellar space and at the free basal surfaces.*

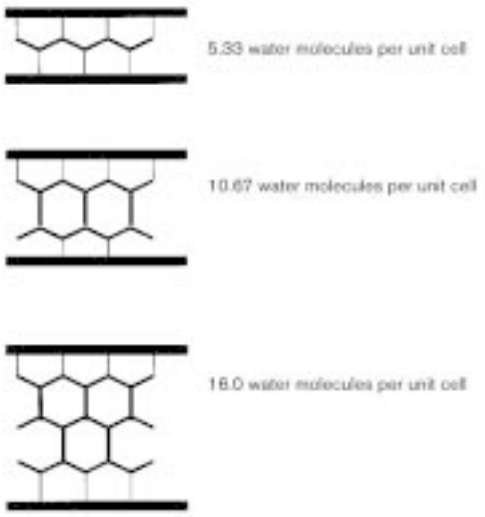

Figure 3-2. *Hydrate configuration in interlamellar montmorillonite (after Forslind).*

Table 3-1. Number and thickness of interlamellar hydrates /5/.

Smectite clay	M[1)]	1 hydrate	2 hydrates	3 hydrates
Montmorillonite (Wyoming)	Mg	3.00	3.03	3.05
	Ca	3.89	2.75	–
	Na	3.03	3.23	3.48
	K	2.42	3.73	–
Beidellite	Mg	2.69	2.69	–
	Ca	2.30	2.30	–
	Na	2.15	2.15	–
	K	2.54	–	–
Nontronite	Mg	2.92	3.00	–
	Ca	3.05	3.37	–
	Na	2.70	2.79	–
	K	2.60	–	–

M[1)] is adsorbed cation in the interlamellar space.

In water, hydration proceeds until the maximum number of interlamellar hydrates is formed, provided that there is no geometrical restraint. In humid air, the number of hydrates depends on the relative humidity (Table 3-2). This latter table shows that one interlamellar hydrate is formed in Na montmorillonite when RH is approximately in the interval 20–40%, while two hydrates require 40<RH<60%. For RH exceeding about 60–70% three interlamellar hydrates are formed.

The expandability of montmorillonite-rich clay is illustrated by experiments with MX-80 powder with a water content of about 10%, compacted to a dry density of 900 kg/m^3 and then submerged in distilled water. The expansion will be more than 100% in three hours, primarily due to establishment of 3 interlamellar hydrate layers from the initial 1–2, but also to release of thin stacks of lamellae that rearrange to form a clay gel between stable aggregates of stacks of lamellae.

Table 3-2. d-spacing and water absorption of Na montmorillonite in atmosphere with different relative humidity (RH) /6/.

RH %	Adsorption area, m^2/g solids	D(001) spacing, Å	Water adsorption in g/g solids, %. Pure clay	Water adsorption in g/g solids, %. MX-80
8	33	10	2.0	1.4
14	33	10	4.5	3.2
19	33	10	6.5	4.6
24	440	12.4	8.0	5.6
32	440	12.5	10.0	7.0
38	440	12.6	11.5	8.1
60	810	14.2	17.0	12.0
70	810	15.0	21.5	15.0
80	810	15.2	24.0	17.0
90	810	15.4	28.0	20.0
95	810	15.4	36.5	26.0

Table 3-2 shows that beidellite and nontronite can form no more than 2 interlamellar hydrate layers irrespective of the type of adsorbed cation, and they therefore have less swelling potential than montmorillonite with sodium or magnesium in the interlamellar exchange positions. With potassium or calcium in these positions a third hydrate does not form in this or any other smectite mineral because of charge and size of these ions. Thus, K^+ is deeply and strongly anchored in the cavities of the siloxane (Si-O) lamella because it fits geometrically and stereochemically /7/.

When Na is in the interlamellar space the coupling to water molecules is weak and the cations relatively free to move. The water molecules can be considered to form its own H^+-bonded interlamellar structure (Figure 3-2), while in Ca-smectite the cations are strongly hydrated and the interlamellar complexes rigid and stable (Figure 3-3). One consequence of this is that the swelling pressure, or the pressure required to expell interlamellar water, is higher for Ca-smectite than for Na-smectite for smaller interlamellar space than about 6 Å, corresponding approximately to a bulk density of about 2000 kg/m^3 at complete water saturation.

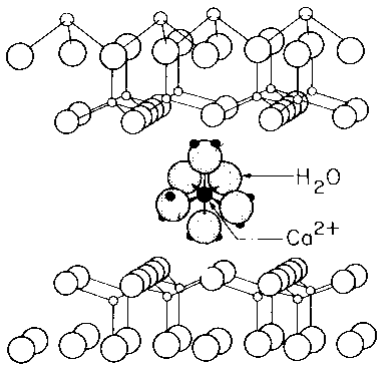

Figure 3-3. *Interlamellar hydrated Ca ion complex with water molecules strongly attached to the cation and interacting also with the siloxane oxygens. It forms the wellknown two-layer hydrate in Ca montmorillonite /7/.*

The consequences of the different hydration properties from a practical point of view is that montmorillonite is superior to the other smectite species as far as expandability is concerned, and that Li and Na as exchangeable cation provides the best expansion properties. This means that, for any given density, the ability to self-seal and become homogeneous is at maximum and the hydraulic conductivity at minimum for Na montmorillonite as buffer material. The effect of changes in porewater composition is obvious: If the clay initially has sodium ions in the exchange positions and the porewater becomes rich in calcium, partial dehydration takes place. The stacks of lamellae contract and the voids between them become larger, which leads to an increase in hydraulic conductivity.

3.2.3 Sorptive properties

Cations

The lattice charge deficit and exposure of structural elements like hydroxyls gives the smectites an ability to adsorb and exchange ions and charged inorganic and organic molecules. This is manifested by i.a. the cation exchange capacity, which is determined by use of the techniques described in Section 1.3.4.3 in Part 1.

Cation exchange studies have shown that, under a given set of conditions, various cations are not equally replaceable and do not have the same replacing power. In principle, the following law of replacement power applies:

$Li < Na < K < Ca < Mg < NH_4$,

which means, for example, that in general Ca^{2+} will more easily replace Na^+ than Na^+ will replace Ca^{2+}.

However, there is no single universal replaceability series. It varies depending on the experimental conditions, the cations involved, and the kind of smectite mineral and it is presently understood that replaceability is controlled by a considerable number of factors. One of them is the ion concentration, as demonstrated by the fact that the replacement of Ca^{2+} and Mg^{2+} by Na^+ in montmorillonite increases as the concentration of Na^+ in the solution increases. This is of course expected since cation exchange is a stoichiometric reaction and the laws of mass action holds, implying that an increased concentration of the replacing cation causes greater exchange by that action. However, the concentration of replacing cations is not the sole factor as demonstrated by the fact that the effects of concentration depend on the kind of cation that is being replaced and also on the valence of the cation.

The complexity of cation exchange processes is indicated by the fact that with cations of about similar replacing power and the same valence, dilution has a relatively small effect on the exchange, while with cations of different replacing power and different valence, for example Na^+ vs Ca^{2+}, dilution produces significant differences in exchange.

Na^+ vs Ca^{2+} represents a particularly important case of competition /8/. Thus, it is a wellknown fact that as the amount of exchangeable calcium on the clay mineral becomes less, it becomes more and more difficult to release. Sodium, on the other hand, tends to become easier to release as the degree of saturation with sodium ions becomes less. Magnesium and potassium are not affected by the degree of saturation to the same extent as calcium and sodium, which is believed to be caused by the charge and size conditions.

One factor that affects the cation exchange is the nature of the anions in replacing solutions. This is obvious from the finding that the replaceability of Na^+ from montmorillonite by Ca^{2+} depends on whether the electrolyte is dissolved calcium hydroxide or calcium sulphate. The issue of the effect of anions is in fact complicated by the possibility of the formation of "basic" salts with the clay and a soluble anion, through which montmorillonite can undergo structural alteration in conjunction with the formation of new compounds.

The most important factor that determines the replaceability power of cations is the valence. The higher the valence of the cation, the higher its replacing power, with the exception of hydrogen, which behaves like a divalent or trivalent ion. For ions of the same valence, the replacing power increases with the size of the ion, meaning that smaller ions are less tightly held than the larger ions. Potassium is an exception, which is explained by the fact that its ionic diameter 2.66 Å is about the same as the diameter of the cavity in the oxygen layer, so that the potassium ion can just fit into one of these cavities. As a consequence, the potassium ion is rather difficult to replace. However, it is commonly stated that it is the size of the hydrated ion, rather than the size of the nonhydrated ion, that controls the replaceability. Thus, it appears that for ions of equal valence, those which are least hydrated have the greatest energy of replacement and are the most difficult to displace when present upon the clay /8/. Li, although being a very small ion, is considered to be strongly hydrated and, therefore, to have a very large hydrated size. The low replacing power of Li^+ and its ready replaceability are thought to be a consequence of this large hydrated size. However, there are a number of indications that Li^+ and Na^+ are only weakly hydrated in interlamellar positions (cf Section 3.1.2), which offers a more reasonable explanation of their replaceability.

Typical cation exchange data of the most common smectite species are given in Table 3-3. For comparison, zeolites have a cation exchange capacity (CEC) in the range of 100–300 meq/100 g and are hence very effective cation catchers. However, they are not considered as buffers because zeolite materials have a very high hydraulic conductivity.

Anions

There are three types of anion exchange in smectites:

1. Replacement of OH ions of clay-mineral surfaces. The extent of the reaction depends on the accessibility of the OH ions; those within the lattice are naturally not involved.
2. Anions that fit the geometry of the clay lattice, like phosphate and arsenate, may be adsorbed by fitting onto the edges of the silica tetrahedral sheets and growing as extensions of these sheets /8/. Other anions, such as sulfate and chloride, do not fit on to the silica tetrahedral sheets because of their geometry and do not adsorb.
3. Local charge deficiencies may form anion-exchange spots on basal plane surfaces.

Table 3-3. Typical CEC ranges for some important smectites /8/.

Mineral	CEC, meq/100 g
Montmorillonite	80–150
Beidellite	80–135
Nontronite	60–120
Saponite	70–85

The latter mechanism is considered to give some contribution to the net anion exchange capacity of smectites. The other two may be important in kaolinite but they are assumed to be rather unimportant in smectite clays. The latter minerals commonly have an anion exchange capacity of 5–10 meq/100 g but it can be considerably higher for very fine-grained kaolinite and palygorskite.

Organic matter

Organic ions and molecules can enter the interlamellar space or be adsorbed on the edges and basal surfaces through hydrophilic groups or hydrogen bonds. It appears from Table 3-4 that the CEC determined with certain organic cations is the same as when barium is adsorbed.

A recent research project has demonstrated the possibility to treat montmorillonite with organic substances for increasing the anion exchange capacity /9/. It showed that adding the chloride salt of the quarternary alkylammonium ion of hexadecylpyridinium ($HDPy^+$) can completely exchange the initially adsorbed cations and also be adsorbed in molecular form. By this, iodide and pertechnetate sorption becomes very important while sorption of i.a. cesium and strontium decreases. For MX-80 such treatment can increase the sorption of iodide by several orders of magnitude. The organisation of $HDPy^+$ in the interlamellar space of smectites can be of the type shown in Figure 3-4.

Table 3-4. CEC of montmorillonite determined for organic cations and barium, respectively /8/.

Species	CEC, meq/100 g
Benzidine	91
p-Aminodimethylaniline	90
p-Phenylenediamine	86
α-Napthylamine	85
2.7-Diaminofluorence	95
Piperidine	90
Barium	90–94

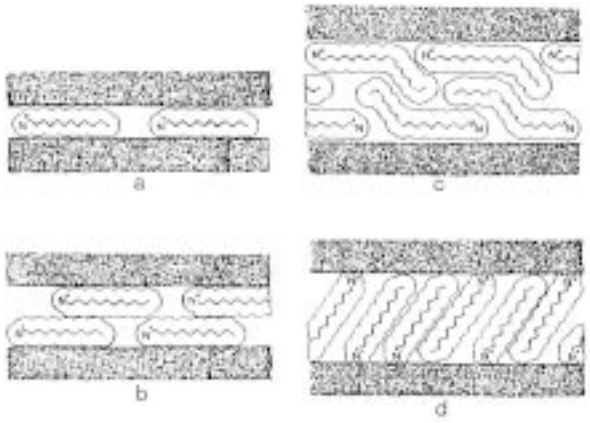

Figure 3-4. *Generalized picture of organic positively charged ions or molecules in the interlamellar space of smectites /10/. a) Monomolecular, b) Bimolecular, c) Pseudomeolecular, d) Paraffin-type.*

3.3 Non-expanding clay minerals

3.3.1 General

No buffer material source contains solely smectite. Usually, both other clay minerals, rock forming minerals, amorphous constituents and organic matter are present in various amounts. The most common non-expanding clay minerals are illite (hydrous mica, hydro-mica), chlorite, and kaolinite (cf Section 1.3 in Part 1). Here, we will confine ourselves to give basic data on the hydration and sorption properties.

The three phyllosilicate[1] non-smectitic clay minerals of practical importance in composing buffers and backfills have the following characteristic compositions /4, 8/:

Illite: $M^{I}ySi_{(8-y)}Al_yO_{20}(OH)_4(M^{III},M^{II})_4$

Chlorite: $(Si,Al)_4O_{10}(Mg,Fe,Al)_6O_{10}(OH)_8$

Kaolinite: $Si_2Al_2O_5(OH)_4$

where M^{I} = monovalent cations (K^+ in illite)
M^{II} = Mg and Fe^{3+}
M^{III} = Al and Fe^{2+}

These compositions imply different intraparticle bond strengths and hence different particle dimensions, which affects the specific surface area and the hydration potential.

3.3.2 Hydration properties

Illite

The non-expanding clay minerals commonly represent particles smaller than 2 μm, which means that while the specific surface area is smaller than that of smectites it is significant compared to non-clay minerals and hence important to the water uptake and retention. Typical size distribution histograms of illite particles in natural clays are shown in Figure 3-5, the histograms also being representative of chlorite particles. The corresponding specific surface area is in the range of 25–100 m^2/g, or about 5–10% of that of the smectites and is similar to the external surface area of the latter clay type.

The hydration potential is hence significantly lower than that of the smectites. Still, expressed in terms of the activity number a_c, which is a simple practical measure of the hydration potential, it is as high as 0.90 while Ca-montmorillonite has about a_c=1.5 and Na-montmorillonite a_c~7 /4/.

The reason why the hydration of illite clay is not too different from that of Ca montmorillonite is that the large size of the stacks of lamellae in the latter clay is similar to the thickness of illite crystals, yielding a relatively small surface area, and also that interlamellar hydration is not extensive in any of these minerals.

For comparison, the size distribution (longest diameter) of dispersed MX-80 particles is shown in Figure 3-6. It should be noticed that the average size range of the longest diameter (*a*) of the smectite particles is similar to that of illite particles (0.01 to 0.3 μm), but that there are illite particles that are up to 2 μm long in contrast to smectite crystals

[1] From the Greek word meaning “leaf”.

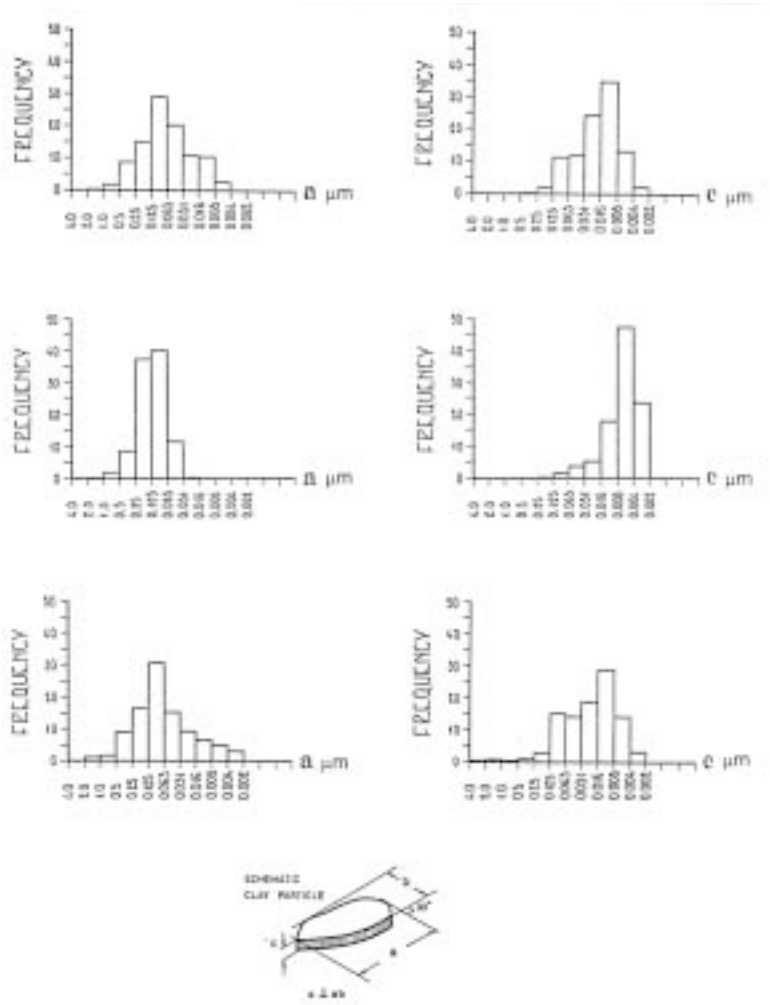

Figure 3-5. *Size parameters of illite particles and their distribution (frequency in percent) in three illitic clay samples from different sites in Sweden. a represents the maximum diameter and c the minimum, which is usually equal to the total number of sheets (flakes) /11/.*

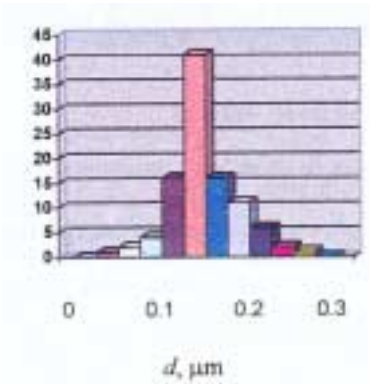

Figure 3-6. *Size distribution (longest diameter) of MX-80 bentonite dispersed in distilled water based on transmission electron microscopy.*

that are never larger than about 0.3 μm. The major geometrical difference is that smectite particles have a thickness (*c*) of no more than about 30 to 200 Å while the majority of the illite particles are 100 to 1000 Å thick. The smectite particles consist of 10 Å lamellae separated by a variable interlamellar space and hence have a reactive surface area that is about 10 to 20 times larger than that of illite particles. This explains the very significant difference in water adsorption and retainment.

As for smectites, the crystal lattice is characterized by vacancies and atom substitution that yield a net electric charge of illite particles. This means that the interparticle force field depends on the porewater chemistry in approximately the same way for both clay types. Thus, electrolyte-poor water yields a more dispersed arrangement of illite particles than saline conditions, cf Figure 3-7. Also, there is limited spontaneous transfer from dispersed to aggregated structure when the porewater chemistry is changed, which is a major reason for the development of quick clays /12/. Thus, the aggregated structure in marine clay is largely preserved at fresh-water leakage and hence also the strength of the clay except when mechanical disturbance takes place and separates the equally charged aggregates, yielding fluid conditions. Similarly, there is rather little spontaneous micro-structural reorganization on percolation of matured low-electrolyte smectite clay with moderately strong Ca solution, which is a reason for using Na bentonite rather than Ca bentonite as buffer and as backfill component even if it is known that the groundwater is salt and Ca-rich.

In general, the hydration capacity of illite and chlorite is sufficiently high to make them maintain their plastic and ductile properties both at high and low densities, which makes it possible to use such clay materials as buffer and backfill components.

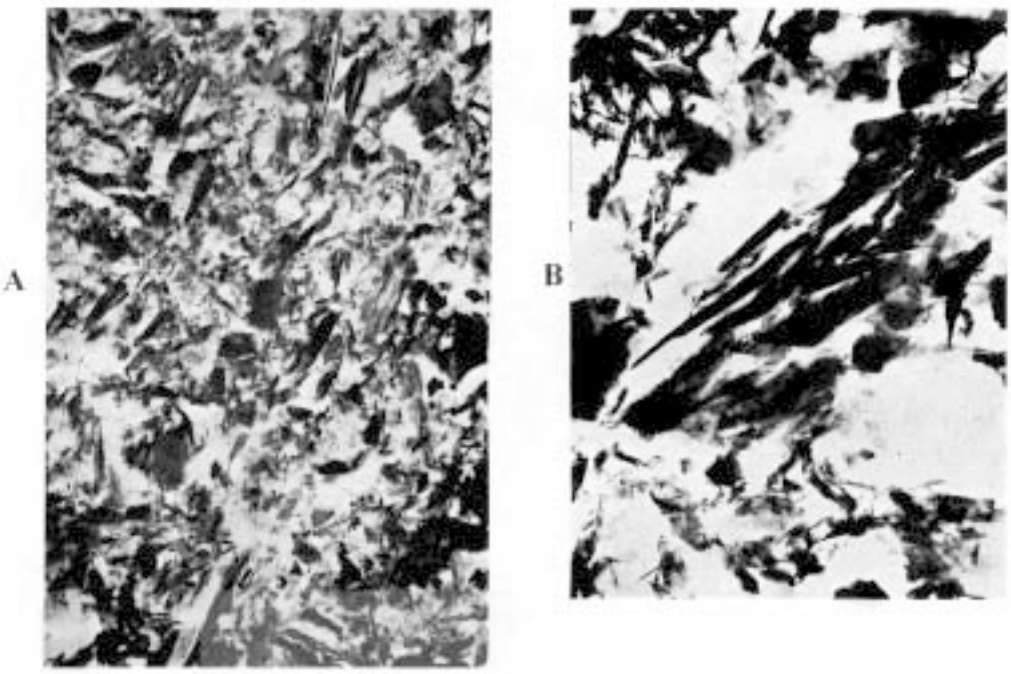

Figure 3-7. *Electron micrograph of glacial clays with a density of about 1600 kg/m³. A) Clay deposited in fresh water having relatively porous aggregates and small voids. B) Marine clay with large, dense aggregates separated by large voids. (TEM of ultrathin sections of acrylate-treated clay).*

Chlorite

Chlorite particles can have a particle size ranging from a few tenths of a micrometer to several millimeters, depending on whether the clay emanates from weathered rock or from neoformation in clay sediments. It never occurs as homogeneous zones of sedimented, fine-grained material but is a frequent component of glacial and postglacial clays in which the chlorite content commonly amounts to 1–3% by weight. The specific surface area of clay-sized chlorite particles is comparable to that of illite particles and they can be regarded as having similar hydration properties. Both are usually more or less weathered as revealed by XRD spectra and are occasionally somewhat expansive.

Kaolinite

The large diameter of the booklet-like kaolinite particles usually ranges from 0.3 to 4 μm while the thickness is 0.05 to 2 μm /8/. Numerous 7 Å thick lamellae form very thick, coherent stacks that make up the particles and this causes a small specific surface area, i.e. around 15 m^2/g. Kaolinite therefore has a low hydration capacity, which gives kaolin clays low plasticity and ductility with only a small difference between the Atterberg plastic and liquid limits (cf Part 1), much like very fine silt consisting of quartz grains. The porewater salinity has only a very small effect on the consistency and even at very low electrolyte contents kaolin clay does not form a coherent paste at lower densities than about 1600 kg/m^3 (dry density 1100 kg/m^3).

3.3.3 Sorptive properties

Cations

In illite, cation exchange takes place mainly on external surfaces, and the cation exchange capacity is therefore relatively low. Since the grain size determines the specific surface area it is expected that very fine-grained illite has a significantly higher CEC than coarser material. This is verified by classical experiments /8/, showing that CEC is typically 15–20 meq/100 g for illite clay with a particle size of 0.1–1.0 μm while it increases to 30–40 meq/100 g when the particle size is smaller than 0.06 μm.

Chlorite exhibits properties that are similar to those of illite. Thus, it is reported in the literature that CEC is in the range of 10–40 meq/100 g /8/.

Kaolinite is a poor cation exchanger; CEC commonly is in the interval 3–4 meq/100 g due to the small specific surface area and to a low frequency of lattice substitutions. Grinding to a particle size of 0.1–0.05 μm increases CEC to about 10 meq/100 g.

Anions

Replacement of hydroxyls by anions is thought to be the main reason for anionic exchange. In montmorillonite the cation exchange is due mostly to lattice substitutions, while the anion capacity depends on the frequency of exposed hydroxyls, which is controlled by the ratio of edge and basal surfaces. It is hence a small fraction of the CEC for smectite, while, for kaolinite, with larger exposure of hydroxyls on the basal surfaces, the opposite conditions prevail. Thus, the anion exchange capacity can exceed 10 meq/100g. It is appreciably lower for illite and chlorite.

3.4 Non-clay minerals

3.4.1 Types

Non-clay minerals are present in all sorts of natural smectitic clays. They may represent minerals formed in conjunction with the birth of smectite minerals like in the evolution of bentonites, or mixed in during transportation and sedimentation of smectites particles in allochthonous bentonites, or evolved from chemical degradation of ancient smectites. They may also represent unaltered grains in clay formed by hydrothermal processes in volcanic rock. In raw material with a higher smectite content than about 30% the smectite constitutes a matrix in which rock-forming minerals and non-smectite clay minerals are distributed. They therefore do not have a very significant influence on the physical properties of the buffer. However, the chemical impact of certain minerals on canister corrosion, smectite conversion and cementation processes may be important and the content of such minerals needs to be considered. They are listed in Table 3-5.

It should be added that heavy minerals like amphiboles and pyroxenes are apt to undergo degradation under hydrothermal conditions and be transformed to smectite as documented by the numerous examples in amphibolite rock in Gothenburg, Sweden and many other areas. Naturally, this process improves the isolation potential of clays and backfills containing such minerals.

Very often mica grains and larger chlorite particles are more or less weathered as revealed by XRD spectra and are occasionally somewhat expansive. A typical example is given in Figure 3-8.

3.4.2 Hydration

Unweathered rock-forming minerals have a low hydration potential and only a one-hydrate layer is formed on their surfaces.

3.4.3 Ion exchange and sorption

The cation and anion exchange capacities of rock-forming minerals is negligible. However, as constituents in ancient sediments they are often partly weathered and thereby have some ability to sorb cations. The matter is further discussed in Chapter 4.

Table 3-5. Accessory minerals of major importance in buffers and in the clay component of backfills.

Mineral	Effect on buffer and canister
Feldspars	Source of Si and Al for formation of new minerals, colloids and cementing agents. K-feldspar provides K^+ for illitization.
Sulphides	Source of SO_4^{-2} for attack on copper canister. Source of SO_4^{-2} for formation of Ca and Na sulphates in the hottest part of the buffer.
Carbonates	Source of Ca^{2+} for ion exchange of Na smectite to Ca form. pH-enhancement.

Figure 3-8. *Transmission electron micrograph of postglacial clay with mica grain (center) degraded by weathering or shearing, by which a large number of internal surfaces have been exposed. Scale is 100 μm.*

3.5 Inorganic amorphous matter

Dissolved mineral particles yield free silica, aluminum and magnesium in the porewater and some of these elements spontaneously rearrange to form inorganic colloids like Fe and Al compounds (sesquioxides), which are known to be mobile in shallow, natural soils, while it is doubtful whether they can move in the very narrow and tortuous pathways of highly compacted bentonite. Iron and sulfur combine to form colloids with similar mobility /13/. The latter reactions are very redox-sensitive, however, and polysulphide complexes may form instead.

Formation of inorganic amophous matter in smectite buffer clay under hydrothermal conditions may be of great practical importance since it may serve as cement and reduces the expandability of the clay /14/. It may also have a positive effect by clogging voids and fractures in the rock surrounding the buffer.

3.6 Organic material

The various types of organic species in smectitic clay range from millimeter-sized tissues emanating from plants, fungal and animal activities, to organic molecules representing ultimate degradation products of organic life as described in Part 1, Section 1.4. The problem that can arise in the present context is that mobile organic colloids can be formed and adsorb radionuclides, which may be transported to the biosphere. Recent theoretical considerations and laboratory investigations have shown that bacteria of the kind that represent a potential risk of transporting radionuclides do not survive in highly compacted bentonite /15, 16/. This is both because the access to free water is very limited and since the interconnection and size of the voids are very limited as quantified in Chapter 7.

The originally contained organic substance in bentonites can be largely removed by heating the air-dry powder at about 400°C for one hour without significant alteration of the smectite minerals /16/. The matter of acceptable content of organics is therefore not very critical although it has an economic impact. For SKB an organic content of 2000 ppm is considered to be acceptable /17/.

3.7 Occurrence and origin of commercially exploited smectite clay deposits

3.7.1 General

Smectites stem from spontaneous nucleation and growth of crystals in saline water with the glassy components of volcanic ash as source material, as well as from weathering of feldspars and heavy minerals in hydrothermally affected rock. The firstmentioned material is true bentonite, which forms beds of different thickness in many parts of the world, while weathering products are confined to rock masses with a structure that has been sufficiently pervious to let solutions through, like fracture-rich zones in crystalline rock and porous rock of sedimentary or volcanic origin. The present description is a very short overview in order to show the wide-spread occurrence of smectitic material of

Table 3-6. World production and exports of bentonite per 1997 according to DURTEC, 2001.

Country	Production, kilotons	Percentage of world production	Export, kilotons	Percentage of world export
USA	6 390	49.4	1 007	35.9
Germany	1 111	8.6	73	2.6
Greece	950	7.3	12	0.4
Spain*	846	6.5	603	21.5
Italy	543	4.2	182	6.4
Turkey	531	4.1	62	2.2
Japan	496	3.8	2	0.1
India	367	2.8	174	6.2
Korea	167	1.3	6	0.2
Mexico	163	1.3	13	0.5
UK	135	1.0	158	5.6
Argentina	132	1.0	35	1.2
Brazil	110	0.8	–	–
Czech Republic	110	0.8	21	0.7
Cyprus	100	0.8	52	1.9
Senegal	100	0.8	–	–
Others	691	5.3	404	14.4
Total	12 942	100.0	2 804	100.0

* (incl. sepiolite)

potential use. Some North American, Japanese and European bentonites are given somewhat more space than those from other areas since they will be referred to later in the document.

Commercial data on clay manufacturers, and export and import of bentonite materials is found in /18/, which illustrates that clays rich in smectite and other industrially important minerals are found in almost all parts of the world.

3.7.2 North America

The most widely used and mined North American deposits of sodium bentonite were formed during the Cretaceous age through a combination of geological activity and environmental conditions that allowed initiation of bentonite formation. Central North America had been inundated by a shallow brackish sea that varied with time, especially in the northwestern areas (now Alberta and Saskatchewan). Contemporary with this marine episode was extensive volcanic activity in the Western Cordillera by which vast quantities of ash were formed and blown east by the prevailing winds. The result was a series of ash deposits on the inland sea. They gradually settled and became buried by marine or land-derived materials. With time, these deposits were deeply buried and consolidated by the more recent sediments and many of these ancient ash layers later altered to bentonite /19/.

The bentonite beds have a character that depends on the initial ash composition and granularity, as well as on the pore-fluid chemistry of the deposits. Those in the North and West tend to be more "ashy" with a lower smectite content due to their proximity to the volcanic sources of the ash, or to the inclusion of terrestrial material carried into the deposits during sea level fluctuations. The deposits in the central basin tend to be more homogeneous, perhaps as the result of calmer central waters and finer textured material deposited farther from the volcanic ash sources.

The United States have large bentonite resources of Upper Cretaceous and Tertiary ages, the principal producing area being the Black Hills region of South Dakota, Wyoming and Montana, and the Gulf region especially in Texas and Mississippi /20/. Figure 3-9 shows Wyoming bentonite exposures and processing facilities. In the Black Hills area the bentonite beds have a thickness of a few centimeters to a few meters and appear in a series of marine shales, marls and sandstones (Figure 3-10). It is generally assumed that the bentonites in this region have been formed by in situ alteration of volcanic ash, which is believed to have been rhyolitic and stemming from a western source. The best producing horizon has been the "Clay Spur" bed forming the top of the mowry shale. The Wyoming bentonite has a particularly good reputation among the large number of various smectitic clays because it has extraordinarily good colloidal, plastic and bonding properties.

Figure 3-9. *Wyoming bentonite exposures and processing facilities /19/.*

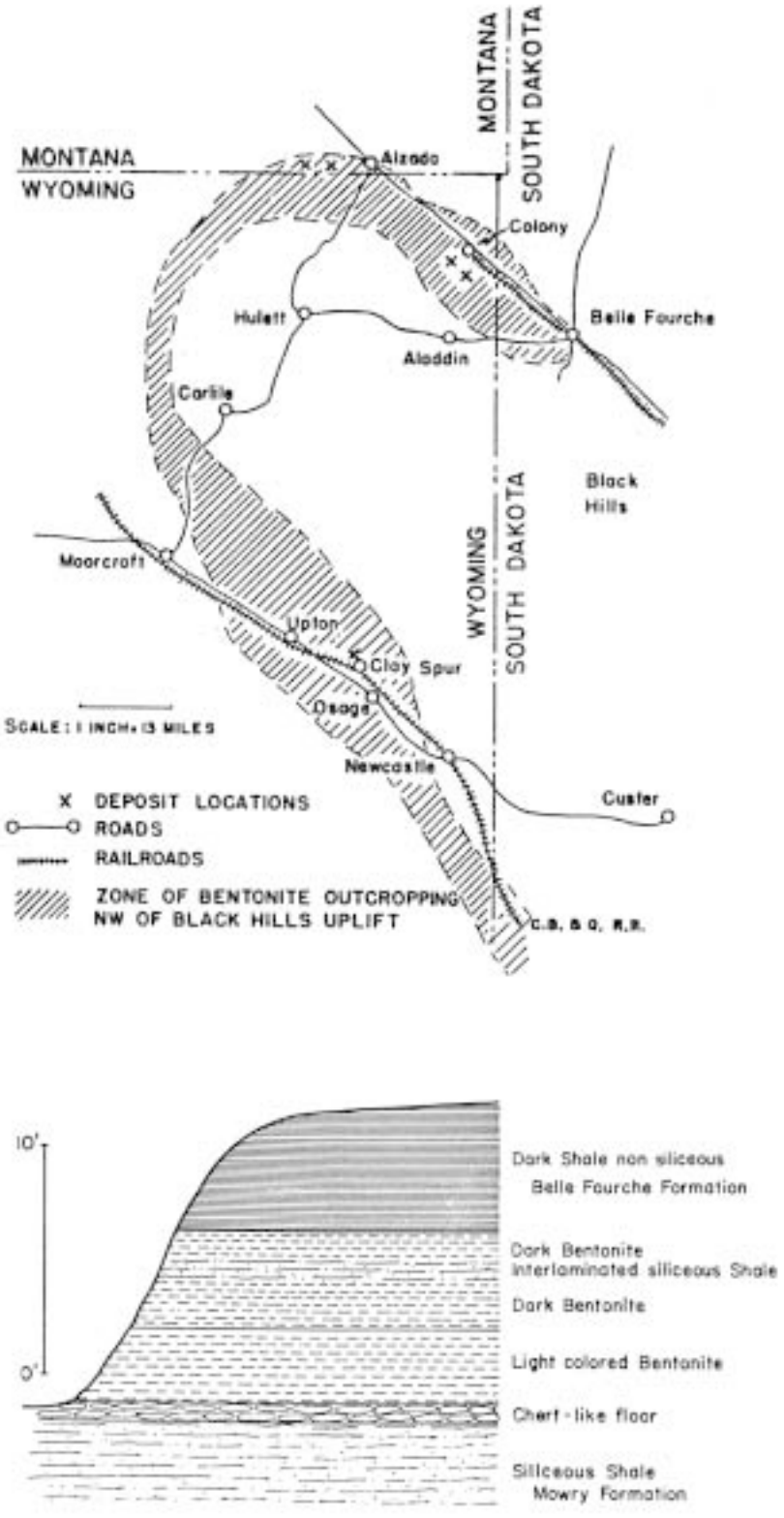

Figure 3-10. *Black Hill region. Upper: Area where the so-called Wyoming bentonite is mined. Lower: Schematic section of Clay Spur Bentonite /21/.*

Very often the beds cover more or less silicified (silicitated) strata, indicating release of silica from the smectite in conjunction with its formation. At the outcrop bentonite is often light yellow or green while it is bluish deeper down, the color shift being due to oxidation of iron or to leaching replacement of exchangeable sodium by calcium. However, sodium is commonly the dominant adsorbed cation in the bentonite from Wyoming and South Dakota. In the Gulf area most bentonites have calcium as major adsorbed cation.

The important question what the controlling factors really are for the type of exchangeable cation in natural bentonites has no definite answer. Marine and lacustrine formations may have either sodium or calcium as dominating cation and it seems as if the composition of the ash is a determinant.

Canada is rich in bentonite, particularly in the Prairie Provinces (Manitoba, Saskatchewan and Alberta). The bentonites, which are similar to those in Wyoming and South Dakota, are of Cretaceous and lower Tertiary ages. They occur in marine shales and limestones and their thickness ranges between a centimeter and a few meters. Alteration of volcanic ash is the generally accepted mode of formation. Most of the Prairie bentonites have calcium as major exchangeable cation but sodium-dominant clays occur as well. Cristobalite is a common accessory mineral that may explain the slight cementation that is characteristic of many of the Prairie bentonites. In fact, they are often shaly and somewhat brittle and fractured as illustrated by Figure 3-11.

3.7.3 South America

South America has bentonites in Argentina, Peru, Uruguay and Brazil. Clay originating from altered tuff are found in older, i.e. Triassic, formations (Mendoza) in Argentina /20/. Cretaceous smectite-rich bentonites formed by ash fall in lacustrine environment occur in Brazil in the Ponta Alfa area of Minas Gerais, and Permian bentonite beds, up to 3.3 m thick, have been found in the Estrada Nova formation at Acegua in Rio Grande do Sul. Both sorts are rich in montmorillonite, while in other Brazilian bentonites the smectite is diluted with substantial amounts of other minerals.

3.7.4 Central America

Mexico is rich in bentonites in the volcanic area /20/. They stem from volcanic ash and have calcium as major adsorbed cation, although natural Na-smectites of high quality have been reported as well, unfortunately not in written form (American Colloid Co). Chalcedony in over- and underlying certain beds may be related to heating, in conjunction with hydrothermal alteration of the ash. The extension and quality of the bentonite sources are poorly known.

Figure 3-11. *Canadian Prairie Bentonite with shaly appearance. Notice the brownish color of the fractures. It is caused by oxidation of iron contained in the bentonite. (Photos by Malcolm Gray, AECL, Canada).*

3.7.5 Africa

Bentonites occur frequently in Algeria and Morocco /20/. Some of them stem from volcanic ash, like those in the Chelif River area in Algeria (Figure 3-12) while others have been formed by hydrothermal alteration of rhyolite rock.

The bentonites formed by ash fall vary in thickness from about 10 centimeters to around 5 meters. They represent Cretaceous and Tertiary sediments with interbedded pyroclastics and lava flow, the complex stratification indicating variation in homogeneity and smectite content. Some of them have a high smectite content with sodium as major adsorbed cation and with no enrichment of silica below or above. A number of these bentonites have been extensively utilized commercially.

In Morocco, bentonites of Miocene age are common, often in the form of layers with a thickness of a few centimeters. They stem from ash fall. An area known to have smectite-rich bentonites of high quality is Camp-Berteaux in the Taourint region. The smectites from this area serves as one of the French reference montmorillonite minerals.

In South Africa bentonite beds of Liassic age occur with a thickness of more than 2 meters in the Karoo system. These beds, which have calcium as major exchangeable cation and do not originate from ash fall, are composed of very pure montmorillonite. In Mozambique, thick bentonite masses, formed by hydrothermal alteration of perlite, occur but they contain rather much unaltered rock fragments and cristobalite.

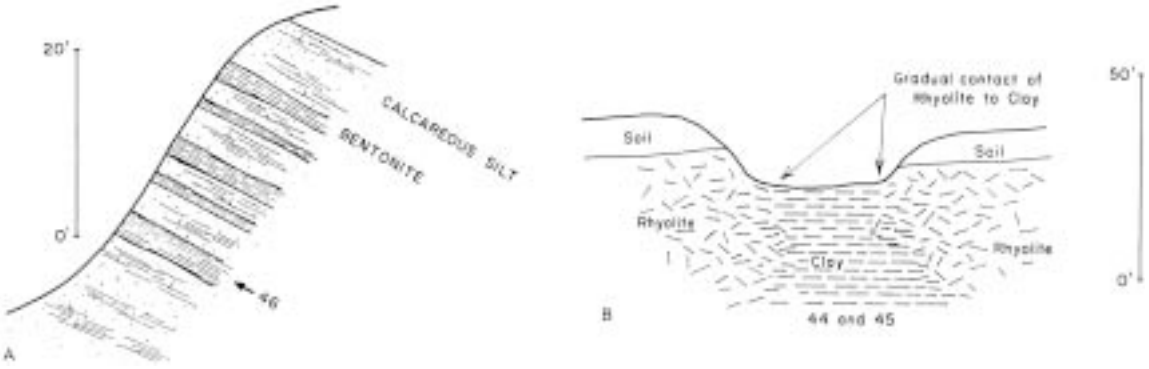

Figure 3-12. *Two profiles from Algerian bentonite deposits formed in different ways: Left sedimentary origin. Right: In-situ weathering /20/.*

3.7.6 Asia

India has quite pure smectite clays of lower Tertiary age /20/. They form large deposits with more than 3 meters thickness and are concluded to stem from in situ weathering of igneous and metamorphic rocks followed by erosion, transportation and deposition in the Barmer Embayment.

One meter thick bentonite beds have been found in the Jamash and Kashmir areas. They seem to have been formed by alteration of volcanic glass in ash.

Japan

Bentonites formed from volcanic ash and by in situ alteration through hydrothermal processes in Tertiary liparites and liparitic tuffs are present on several sites in Honshu and Hokkaido. At Yamagata and in the Tsukinuno area on the main island, the deposits were formed in Early Miocene mostly by hydrothermal processes that gave large clay bodies which are irregular in shape. Depending on the composition of the parent rock, zeolites have also been formed in large amounts. In the Kwanto district of the Gumwa Prefecture there are several beds with a total thickness of up to 5 m, interbedded with mudstones and hence of heterogeneous and relatively poor quality.

A general conclusion is that most of the clays originated from volcanic ash irrespective of the formation process. Since the volcanic activity of Japan has been very significant from the Neogene epoch the amounts of clay are very large /22/. Particularly the submarine sedimentation of the Miocene dacite pumice was very rich and most of the deposits gave huge masses of montmorillonite, zeolite and opal. Still, most of the bentonites that are being exploited commercially are altered tuffs.

At Tsukinuno, the geological profile is as shown in Table 3-7, while it is illustrated in Figure 3-13 for the Yamagata area. This figure also shows a map over a presently mined area at Tsukinuno.

Table 3-7. Geological profile in the Tsukinuno Area /22/.

Age	Formation	Unit	Thickness	Bentonite
Tertiary		Black Mudstone M	170 m	
(Miocene)	Nukumi F	Gray Tuffaceous Sandstone M	80 m	
		Brown Pumiceous Tuff M	30 m	+
		Dark Brown Hard Mudstone M	20 m	
		Gray Pumiceous Tuff M	20 m	+
	Tsukinono F	Dark Brown Hard Mudstone M	290 m	+
		Brown Hard Shale M	100 m	+++
		Pale Green Sandy Tuff M	100 m	+

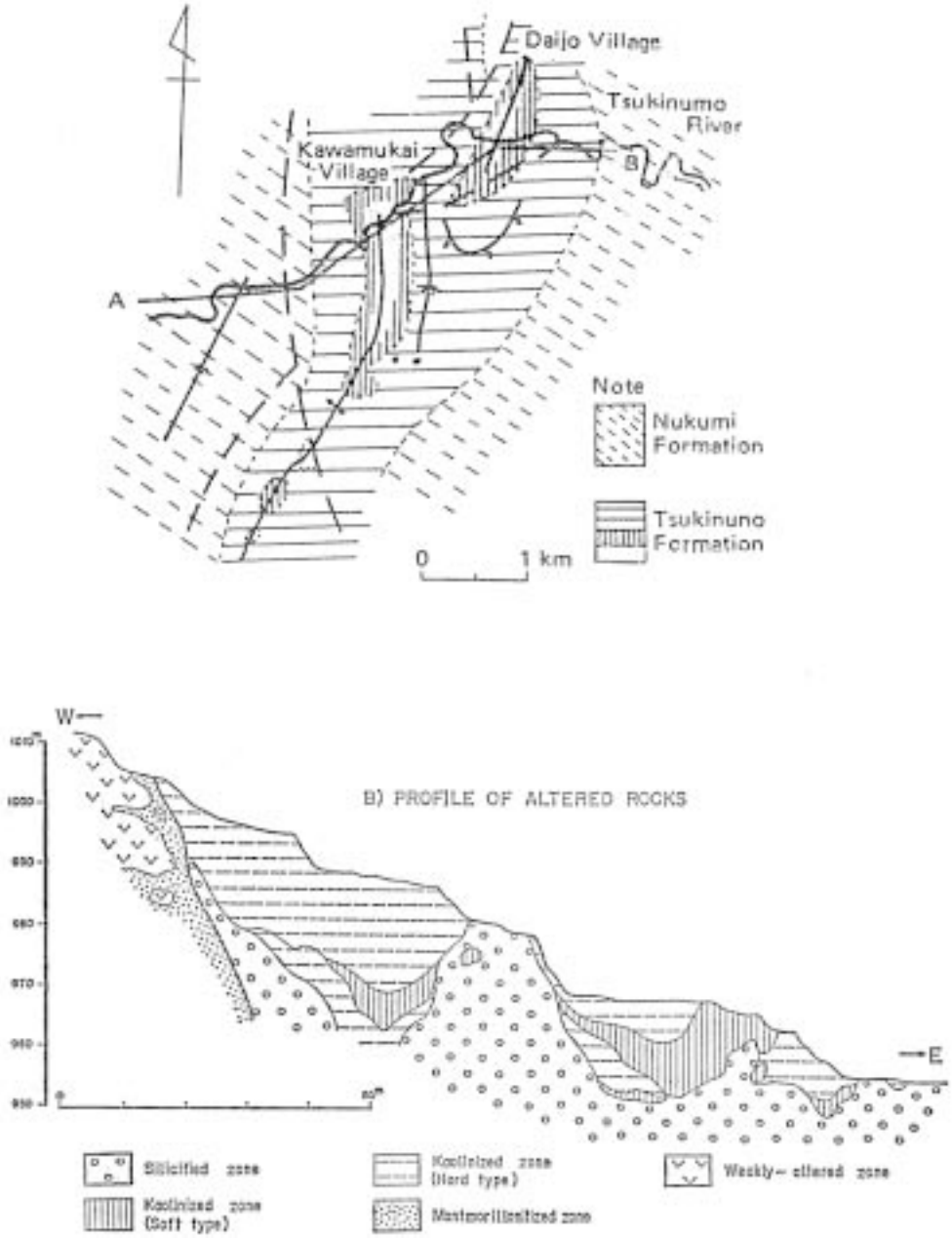

Figure 3-13. *Bentonites at Tsukinono and Yamagata. Upper: Presently mined area at the Tsukinono river. Lower: Profile at the Itaya mine in the Yamagata area /22/.*

Clay formation has been extensively studied in Japan and led to considerable deepening of the understanding of the mechanisms involved in bentonite formation. An important conclusion from this is that it is unlikely that weathering processes were important in the formation of such bentonites in Japan. The studies show that weathering tends to produce a suite of clay minerals rather than a single one and that other clay minerals rather than smectite are likely to be abundant. In most of the bentonites originating from hydrothermal influence on rhyolitic rock, there are frequent quartz phenocrysts and a considerable quantity of plagioclase and biotite. The smectite content is hence not very high.

3.7.7 Europe

European bentonites are well known and easily available in Spain, Germany, Denmark, Hungary, Czech Republic, Italy, Greece and Bulgaria /20/. We will confine ourselves here to mention those in Germany, Italy, Spain, Czech Republic, Greece and Sweden. Those from Germany, Spain and the Czech Republic have all been examined in SKB's R&D work as exemplified in later chapters.

Germany is an important source of commercial bentonites, generally emanating from in situ alteration of acid vitreous tuff. At Moosburg in Bavaria bentonite with calcium as major exchangeable cation forms up to 3 m thick beds in a generally marine section of marls and tuffaceous sands. The purity varies from relatively non-contaminated montmorillonite to material with rather much kaolinite and illite. Typically, there is a distinct boundary between an upper oxidized (yellow) and a lower blue-colored part in one of the pit areas /23/. In the Neubrandenburg region of northern Germany there are huge quantities of smectitic clay that are exploited for isolation of shallow waste piles and that is presently considered as a possible material for backfilling of drifts and shafts in repositories for radioactive and hazardous chemical waste /24/. The clay, which is of Tertiary age, has an average content of expandable minerals of 50–60%, half of which is montmorillonite and the rest being mixed-layer minerals. The clay is termed Friedland Ton and will be used as an example of commercially available relatively smectite-poor European clays that are potentially useful for repository sealing /25/.

Italy is rich in bentonites, particularly in the islands Ponza, Sardinia and Sicily. Most of them originate from alteration of basic rocks, some due to the effect of gases left in intrusions of magma (Figure 3-14), while others appear to be of sedimentary origin. One case of the latter type is concluded to be the presently mined bentonite at Busachi in central Sardinia /26/. Here, molten rhyolite is assumed to have moved in over a more than 7 m thick reddish, rather homogeneous bentonite mass, yielding sintering at the contact but causing very little changes at larger distance from the hot contact than about 2 m. This and similar sites represent rich potential bentonite sources.

Figure 3-15 shows a map of Sardinia with the Uri, Oristano and Cagliari regions representing bentonite-rich areas and processing plants. At Cagliari the bentonite reserves represent tens of millions of cubic meters, a general section of the valley with up to 10 m thick bentonite beds being shown in Figure 3-16 together with a section of the Pedra de Fogu area with up to 25 m thick bentonite beds. At Cagliari the bentonite is a Miocenic alteration product of a more than 13 m thick fine pyroclastic stratum, while at Pedra de Fogu it stems from in situ alteration of rhyolitic rock /27/.

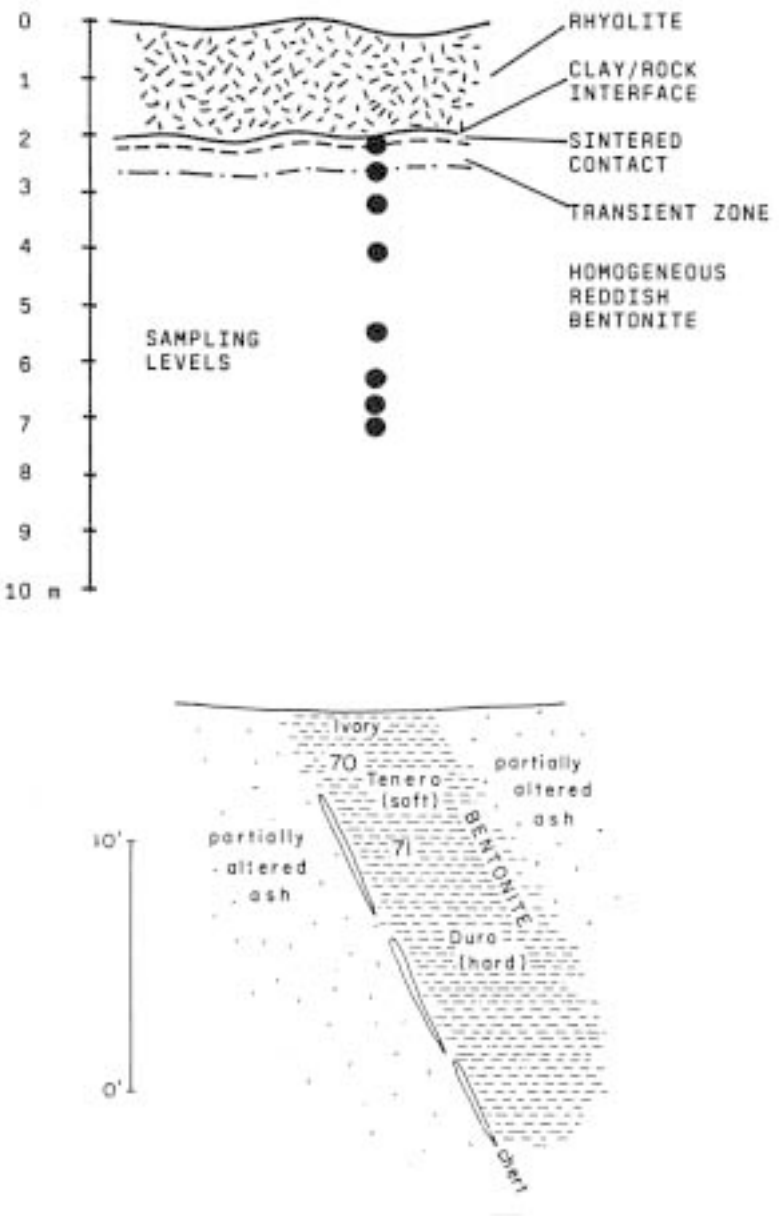

Figure 3-14. *Section at Busachi (upper) and La Forna (Ponza). The dots in the upper picture represent samples that were analyzed with respect to the montmorillonite and cement contents. The samples taken at the depths represented by the lower five dots had a very high smectite content and almost the same composition. Notice the chert formation below the clay zone in the lower picture, indicating release of silica in the smectite-forming process.*

Figure 3-15. *Map of Sardinia. Cagliari is a major coastal city with good harbor facilities. Such facilities are also available at Oristano where shipping of processed bentonite has taken place for decades.*

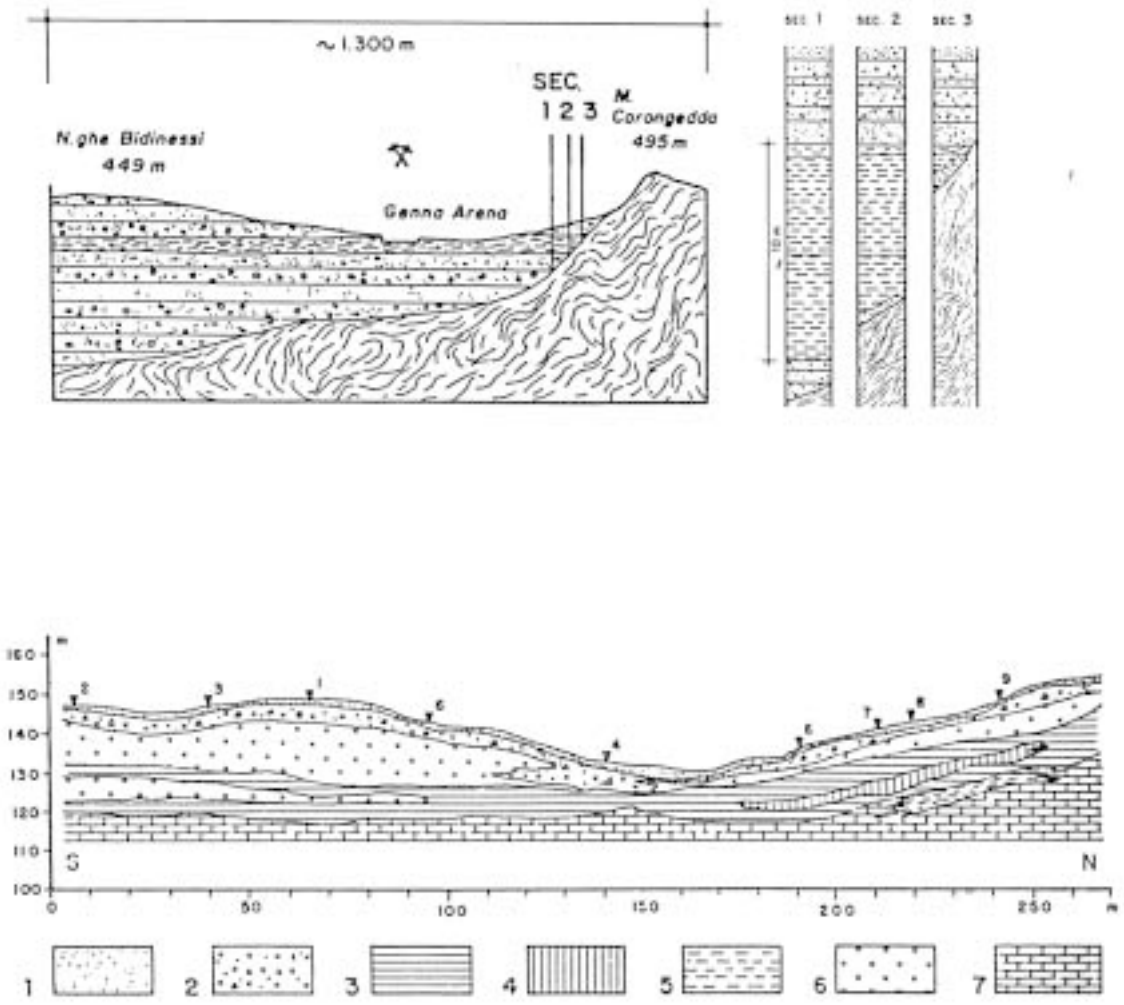

Figure 3-16. *Sections through major bentonite deposits. Upper: Genna at Cagliaria with bentonite beds shown dotted. Lower: Pedra de Fogu with the following legend: 1=detritus; 2=detritus and volcanics; 3=red bentonite; 4=whitish-yellow bentonite; 5=sandy bentonite; 6=rhyolitic volcanics; 7=Jurassic carbonate formation (after Pietracaprina).*

Spain

In recent years systematic prospecting has given a good overview of the Spanish bentonite resources. Three areas have turned out to be of particular practical importance. They have all been formed by alteration of Tertiary rhyolite-dacites through hydrothermal processes or percolation of meteoric water involving removal of some silica and iron, and incorporation of aluminum and magnesium. Concentration of chromium, nickel and cobalt has caused coloring of some of the bentonites /28/.

The Madrid Basin, part of the Tajo Basin, lies in the southern edge of the Sistema Central. The Tajo Basin is a Tertiary depression, located in the middle of the Iberian Peninsula, which became filled with continental sediments, ranging from fluviatile to lacustrine-palustrine environment type deposits. A major characteristic of these deposits is a lateral change of facies from detrital to chemical. Clay materials of saponite type are commonly found in the transition zones and they represent about 500 000 m^3. Three different units have been established: a) a lower unit composed mainly of evaporites, b) an intermediate unit made up of clays, sandstones, limestones and chert, and c) an upper unit of essentially detrital materials, associated with tectonic phases that occurred during the Miocene. The intermediate unit is of particular interest and is made up of materials from lacustrine and fluviatile environments, with some transition zones. Predominating in the transition zone are clay materials associated with silty sands. Biotitic sepiolite deposits, exploited in the Madrid Basin, are found within these clay formations.

Tests performed in the program of ENRESA have shown that the Cerro del Aguila bentonites with a smectite content of more than 85%, have the best characteristics of three deposits identified in the Madrid Basin. Available field data from borings indicate that the potential reserves and an “easy to mine” configuration of the deposits meet the requirements set.

The main Spanish bentonite deposits of hydrothermal origin are located in Cabo de Gata (Almeria, southeastern Spain). The volcanic activity in this area gave rise to calc-alkaline rocks, from basaltic andensites to rhyolites in composition. The volcanic emissions varied from massive lava flows to different types of pyroclastic products. The rocks were heavily fractured and have undergone comprehensive physical and chemical alteration. Most of the pyroclastic materials have experienced hydrothermal alteration. Acid solutions gave rise to the formation of alunite, jarosite and kaolinite but the most extended alteration resulted in the formation of the thick bentonite deposits spread all over the Cabo de Gata region. The bentonites in S de Nijar (Figure 3-17) occupy an area of about 11x1.5 km^2 and extend to at least 20 m depth. The smectite content is in the interval 85–95%, the major species being montmorillonite. Other sites are the montmorillonite-rich zones Los Trancos and Escullos.

The process of alteration of the volcanic materials to bentonite took place with a large loss of matter, in particular silica and alkaline elements, accounting for over 50% of the fresh rock mass. The accompanying decrease in volume gave rise to some morphologic readjustments in the altered pyroclastic bed cover. As a rule the hydrothermal solution supplied Mg to the initial fresh rock. The meteoric waters, heated during their underground southward movement from the metamorphic northern ranges altered the pyroclastic beds into bentonite. Since the hydrolysis reaction of these materials is exothermic, the solutions did not need to reach great depths or high temperature bodies to be heated up. These smectites belong to the montmorillonite-beidellite series and their compositions vary gradually with the degree of alteration and the chemical

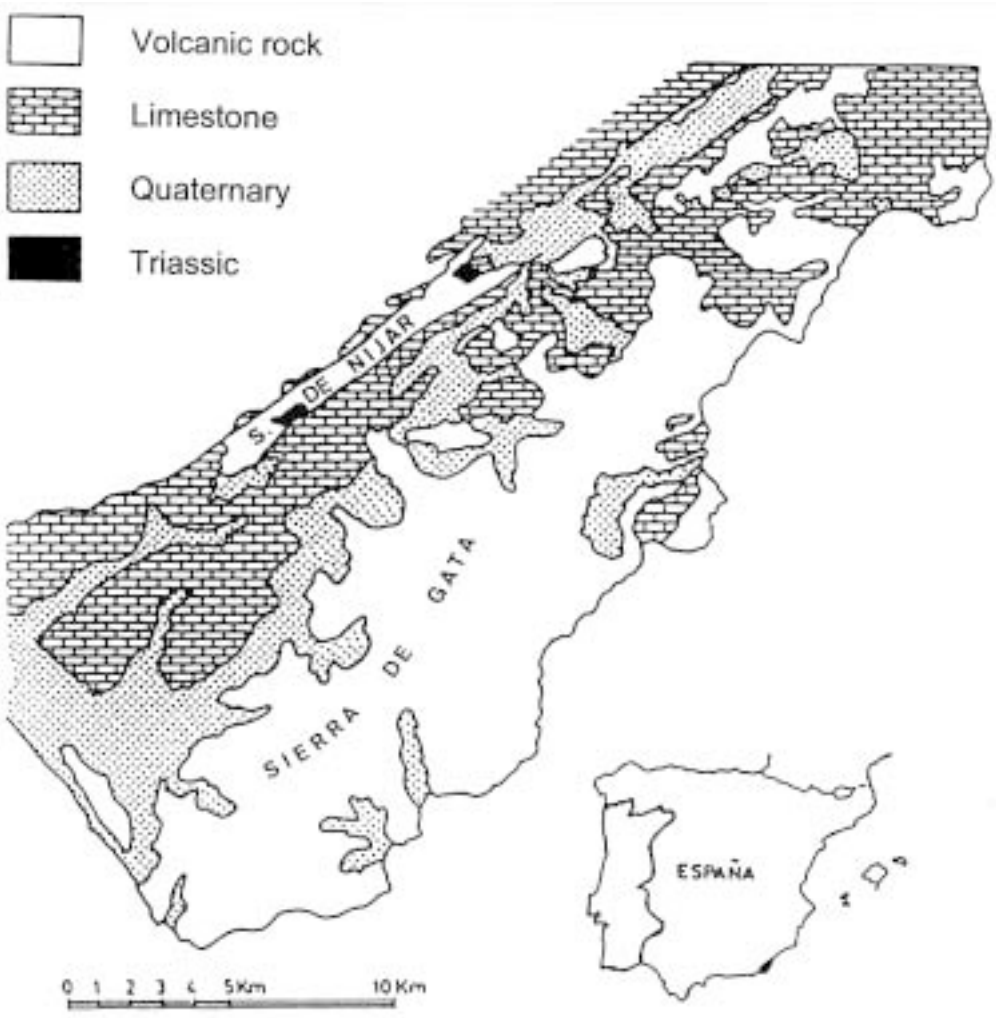

Figure 3-17. *Smectitic material at Almeria ("Rocias Volcanicas" in the Serrata de Nijar) /28/.*

composition of the parent materials. Thus, beidellites correspond to very early alteration stages, especially in acid rocks. The color of the bentonite depends on the content in trace elements of the first transition series; all shades of green, blue, red and white are present. The bentonite deposits are numerous and important all over the region and reserves are estimated to be tens of millions of cubic meters.

Czech Republic

The Bohemian Massif in the Czech Republic is estimated to contain at least 280 million (metric) tons of high-grade bentonites representing 16 sites of which 3 are being mined. One of them is the Zelena clay quarry in the upper Miocene Cheb basin, which holds up to 20 m thick smectitic layers. Both Ca-dominated clay requiring soda activation and Na-dominated clays have been identified and exploited /29/.

Greece

The volcanic islands of Greece were formed by transgressive sedimentation on a crystalline base, a dominant part of the island being covered with sediments of volcanic origin deposited in late-Tertiary and early Quaternary times /30, 31/. Young alluvial sediments are found in tectonically generated depressions. Volcanic activity was initiated in Pliocene forming tuffs and tuffites and proceeded in five phases, which has yielded considerable complexity. The geothermal conditions are still very obvious as demonstrated by the fact that water vapor with 300°C temperature is contained in pores and fractures at less than 1 km depth. The island of Milos represents a major bentonite resource and is briefly commented on here.

The geology of Milos has been described in detail with respect to the presence and extension of smectitic clays /31/. There are several mineralogically and chemically different clay beds, the ones of major practical interest being formed by in situ alteration of andesitic pyroclastic rock characterized by high contents of volcanic glass and plagioclase that were transformed to montmorillonite in many places. The main clay beds in one area, Agrilies, consist of iron-poor smectites with high quartz and mica contents. Xenolites in the original rock are largely preserved here. In the Ano Komia area bentonites with rather little smectite and significant amounts of cristobalite and tridymite were formed from pyroclastic rock. In certain areas, particularly in shallow positions and in shear zones, hydrothermal solutions have percolated and degraded the smectites.

In the area Aspro Chorio, where smectite-rich bentonites are available in very large quantities, the processes involved in the transformation of pyroclastic rock and the evolution of smectites have been studied in detail. It is claimed that percolation of meteoric water of relatively porous rock was a major factor in the smectite formation in this and other areas.

Figure 3-18 shows a section of the underground at the Aspro Chorio site, which demonstrates that the bentonite beds can be very thick. The smectite content is commonly in the range of 50–70% but prospection has shown that there are very large resources of clay material with more than 70% smectite of montmorillonite type.

Figure 3-19 shows a geological map of Greece, which is a basic reference case of continent growth by geosyncline formation with subsequent folding, volcanism and sedimentation.

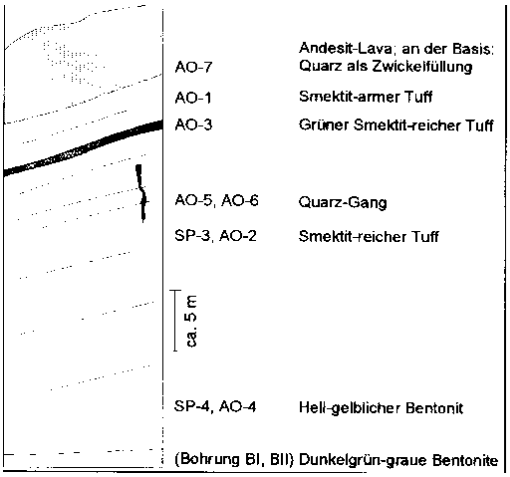

Figure 3-18. *Section at the Aspro Corio site /31/.*

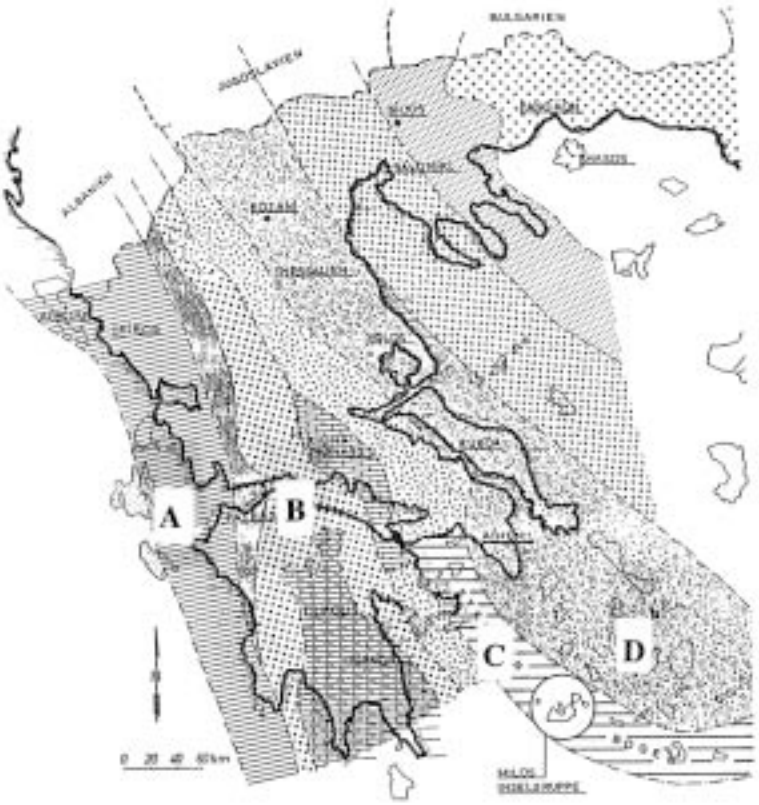

A Hellenides (folds, ridges)
B Pindos Ridge
C Cryst., sandst., shales (folds and active volcanism)
D Sedimentary basin

Figure 3-19. *The general geological build-up of Greece /31/. Major bentonite deposits are on the island Milos about 200 km southeast of Athens.*

Sweden

No bentonite deposit is presently being exploited in Sweden for extracting smectite, but attempts to mine the locally very extensive smectitic clay sources have been made both at Kinnekulle, Västergötland, where Ordovician "metabentonites" are exposed /26, 32/ and in Skåne, which is rich in sedimentary smectitic clays /26, 33/. In the latter county, a number of smectite clay bodies have been found, like the Vallåkra and Kågeröd zones. Also, there are several deposits of smectitic moraine clay originating from a number of smectitic sedimentary rocks.

Major smectite clay sources are represented by sediments formed in stable depositional environment such as lakes, sedimentary marine basins of nearshore origin or offshore marine environment, and by weathered rock. Sufficiently large clay masses for exploitation means that a number of natural processes must have combined to form deposits of potential interest:

- Transporting agents for accumulation of minute particles.
- Environment in which significant amounts of clay could be accumulated, e.g. flood plains, tidal flats, marine shelves, lakes etc.
- Constant conditions over significant periods of time to allow for development of thick deposits.

These conditions are fully or partly fulfilled by clays of Triassic and Jurassic age from Vallåkra and Kågeröd, as indicated in the map in Figure 3-20 and the stratigraphic column in Figure 3-21. This is valid also for certain Quaternary moraine clays, i.e. those in the Ängelholm and Lund regions.

Figure 3-20. *Generalized bedrock map of Skåne /33/.*

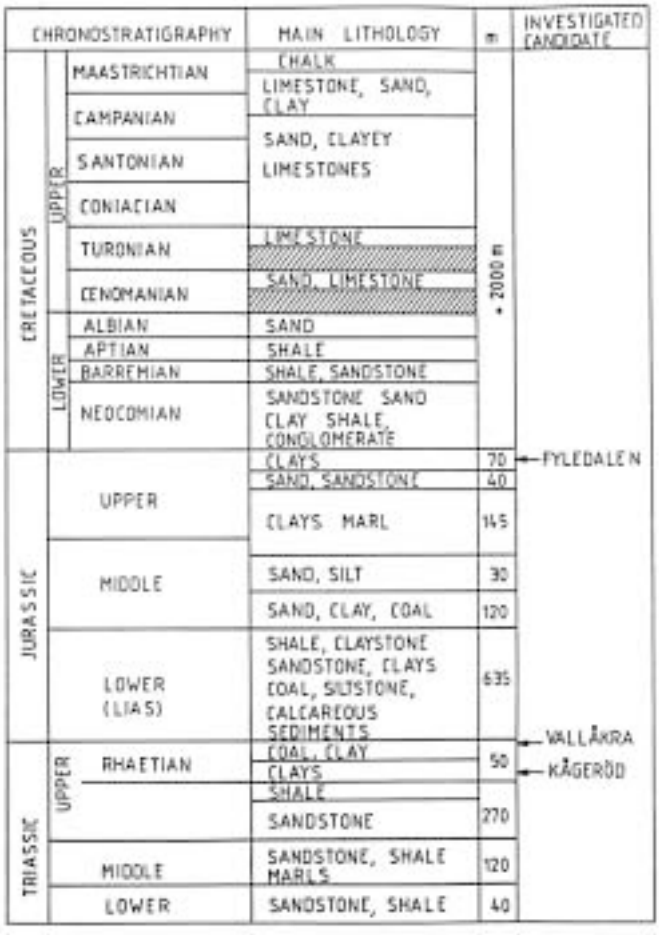

Figure 3-21. *Schematic stratigraphic column showing the Mesozoic strata in Skåne /33/. Fyledalen, Vallåkra and Kågeröd are potential smectite sources.*

Mesozoic clays

The lateral extension of the Vallåkra beds is huge as indicated by the map in Figure 3-22. A more detailed view is shown in Figure 3-23 and further detailing is exhibited in Figure 3-24. These beds represent very significant natural Swedish resources.

It is seen from the borehole data in Table 3-8 that the area where the clay is within reach for easy quarrying constitutes an approximately 2–3 km wide zone. An exact thickness of the clay beds is difficult to derive from borehole data and because of the fact that the area in NW Skåne is frequently faulted and tectonically disturbed. The thickness is, however, generally more than 5 m, which makes the deposit attractive for exploitation.

The approximately 15 m thick Keuper clay sediment layer in the Margreteberg area, which is the one that will be described in a later chapter with respect to the mineralogical and physical properties, was deposited about 200 M years ago on top of the clastic Kågeröd Formation /26, 33/. The clay was probably formed in saline shallow coastal water, its very high degree of homogeneity indicating constant conditions of deposition. On top of it an approximately 5 m thick rather complex sand/kaolinite series, termed Upper Vallåkra, was then formed, and later the sequence was covered by organic-rich sediments which include coal seams.

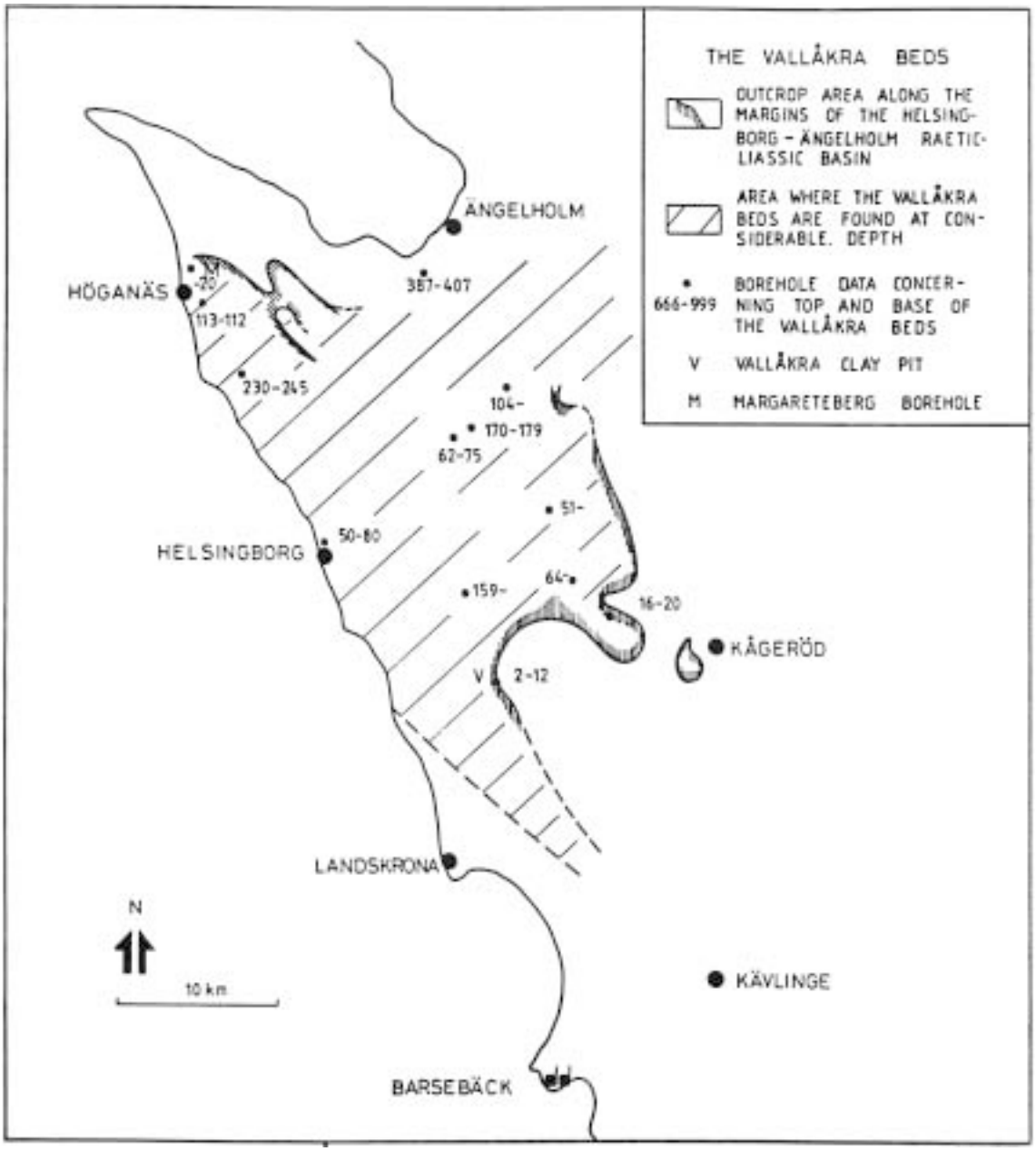

Figure 3-22. *Extension of the Vallåkra beds. The smectite-bearing area is about 500 km².*

The upper Jurassic clays in the Fyledalen area, which are mentioned in the diagram in Figure 3-20, have been extensively investigated but since they are rather poor in smectite they will not be further considered in the present context.

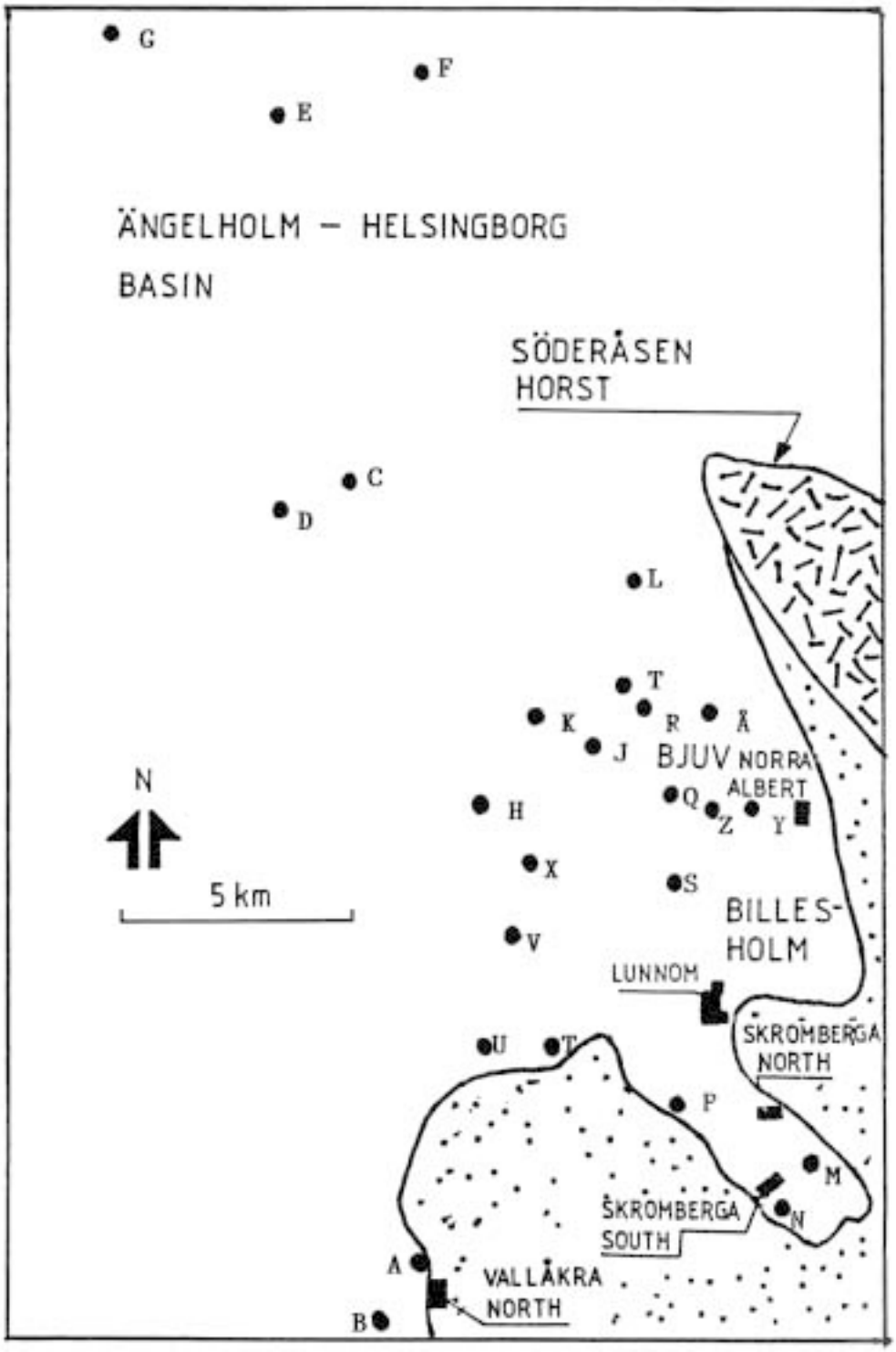

Figure 3-23. *Borehole positions in the Rhaetian and Jurassic areas (cf Table 3-8).*

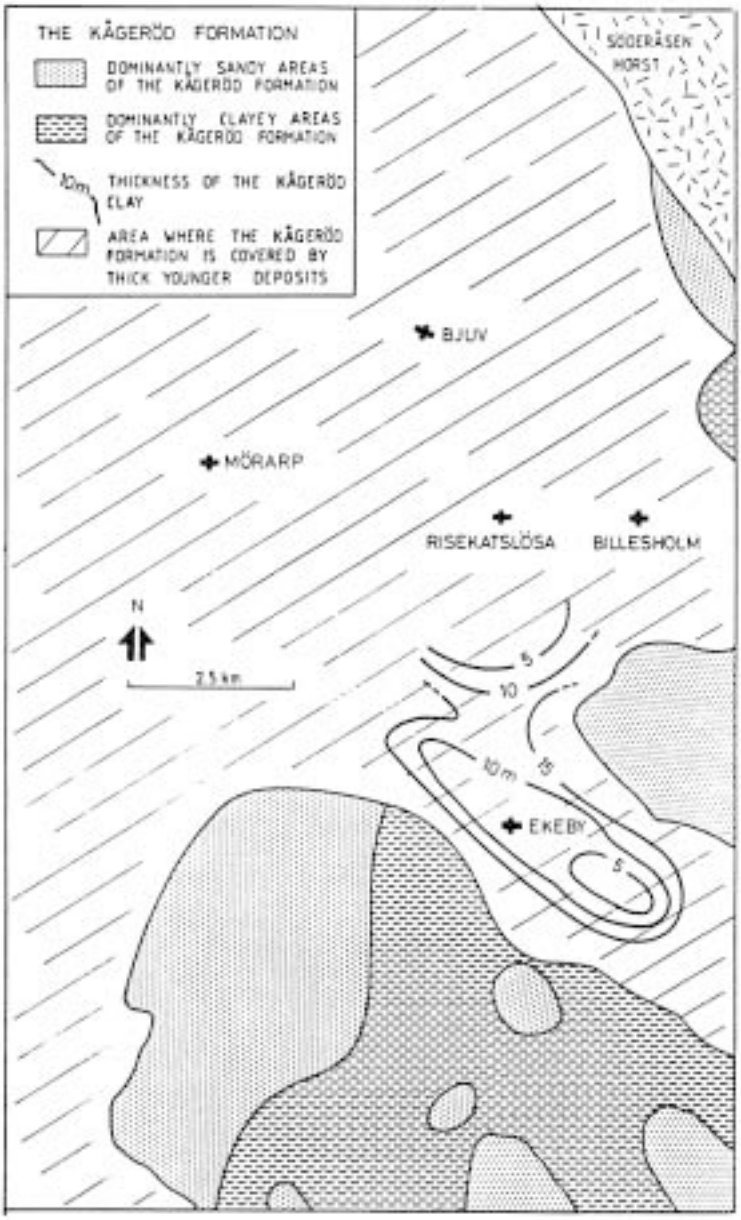

Figure 3-24. *Detailed plan view of the Kågeröd Formation.*

Table 3-8. The depth and thickness of the Vallåkra beds as derived from corings /33/.

Borehole	Depth, m	Thickness, m
A N Vallåkra 3	15–25	5
B Kvistofta 59	50	(150)
C Fleninge 266	170–179	9
D Fleninge 265	62–75	13
E Oregården	314	–
F Nya Wilhelmsfält	387–407	20
G Farhult 270	98–124	26
H Mörarp schact	53	–
I Bjuv schact III	51	–
J Bjuv 1	44–66	22
K Bjuv 2	35–48	13
L Gustav Tornerhjelms schact	96–104	8
M Schact consul	21–22	1
N Truedstorp 4	21	–
O Skromberga 273	16–20 20	4 20
P (Borehole without name)	42–57	15
Q Selleberga, concession 150	45	–
R Selleberga, concession 154	64	–
S Charlottenborg, concession 112	10	–
T Skromberga, concession 96	20	
U Skromberga, concession 4A	51	51
V Assarstorp 19A	56	56
X Mörarp, concession 8	103	–
Y Schact, Oscar II	39–39.2	0.2
Z Schact, Ljungsgård	55	55
Å Norra Vram, Concession 4		

3.8 Potential smectite clay resources

The formations described in the preceding chapter represent very large amounts of clay that can be used as raw material for enrichment of smectite minerals or for use as it is. Complete data of the quantity of smectitic clay are usually not available but approximate figures can be obtained from certain companies or derived from stratigraphic data. The total known resources on land of bentonitic materials in the countries specified earlier in the report is estimated at E11 to E12 m^3, but the actual figure may be much higher.

The outcropping Black Hill bentonites cover an area of at least 500 km^2 corresponding to at least E10 m^3 of bentonitic material. The bentonite deposits in the Gulf states probably represent about the same quantity /13/.

Japanese bentonites also represent very large volumes. Thus, in the Prefecture of Gumma the bentonite zone is about 25 km long and 2 km wide, corresponding to at least 10^8 m^3 bentonite-holding material. The total amount of exploitable bentonitic material in Japan can be estimated at E10 m^3 /22/.

The total European resources, excepting Russia, can be estimated at more than E10 m^3. In Italy the Sardinian resources of bentonitic clay represent no less than E9 m^3 and the entire amount of such clays in the whole of Italy probably also eceeds E9 m^3. The Greek and Spanish resources are estimated to be on the same order of magnitude.

As to Sweden, the clay materials belonging to the Kågeröd and Vallåkra formations can be estimated to represent at least E8 m^3 and the exploitable smectitic moraine clay in the Landskrona/Lund region about the same volume.

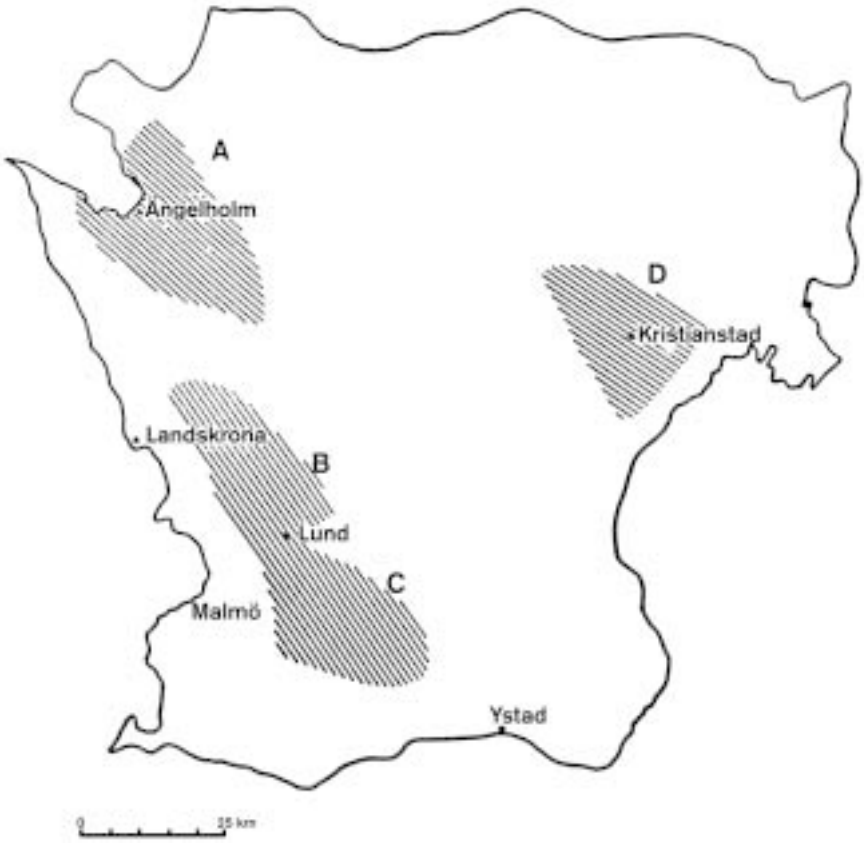

Figure 3-25. *Smectitic Quaternary deposits i Skåne of potential interest.*

3.9 Quality of natural smectite clay

The quality of smectitic clay deposits is determined by various criteria, like a minimum smectite content or a maximum content of certain accessory minerals or organic material. Most important factors are the type of smectite and the mineralogical and granulometrical homogeneities.

Autochtonic bentonites originating from ashfall are commonly relatively homogeneous, although thin layers of quartz sand and silt, gypsum, palygorskite and cristobalite often occur in the beds. Allochtonous bentonites like the Triassic bentonites in Argentina usually show much larger variations in composition because non-bentonitic material is carried to the area of accumulation together with ash and smectite.

In situ alteration of rock by hydrothermal effects or percolation of meteoric water has often yielded homogeneous reaction products but since percolation has usually taken place in a non-uniform pattern the altered mass often has an irregular shape and unaltered lenses are often noticed. Furthermore, the quartz and plagioclase components as well as biotite are commonly intact, meaning that the smectite content seldom exceeds about 50%.

In the present report we consider the following properties to be most important for exploiting a clay source for obtaining buffers and backfills:

- Amount of smectite-rich material.
- Smectite type.
- Degree of homogeneity with respect to the smectite content and the granulometry.
- Type and amount of accessory minerals.
- Organic content.

Quality designation must be made with reference to the intended use and one can therefore not apply simple scoring. Part 1 of this Handbook describes procedures for testing and assessing smectite clays /4/.

3.10 References

/1/ **Pusch R, 1977.** Required physical and mechanical properties of Buffer Masses. KBS Technical Report No.33, Swedish Nuclear Project (Svensk Kärnbränslehantering AB).

/2/ **Pusch R, 1979.** Highky compacted sodium bentonite for isolating rock-deposited radioactive waste products. Nuclear Technology, Vol 45, No 2 (pp 153–157).

/3/ **Pusch R**, **1999.** Is montmorillonite-rich clay of MX-80 type the ideal buffer for isolation of HLW? SKB TR-99-33. Svensk Kärnbränslehantering AB.

/4/ **Pusch R** et al, **1995.** The Buffer and Backfill Handbook, Part I. SKB Arbetsrapport AR 95-45. Svensk Kärnbränslehantering AB.

/5/ **Kehres A, 1983.** Isotherms de deshydratation des argiles. Energies d'hydratation – Diagrammes de pores surfaces internes et externes. Dr. Thesis, Université Paul Sabatier, Tolouse, France.

/6/ **Mooney R W, Keenan A G, Wood L A, 1987.** Adsorption of water vapor by montmorillonite. II. Effect of exchangeable ions and lattice swelling as measured by X-ray diffraction. Am. Chem. Soc. Journ., Vol 74 (pp 1371–1374).

/7/ **Sposito G, 1984.** The surface chemistry of soils. Oxford University Press, New York.

/8/ **Grim R E, 1967.** Clay Mineralogy. NcGraw-Hill, New York, London, Toronto.

/9/ **Pusch R, Muurinen A, Lehikoinen J, Bors J, Eriksen T**, **1999.** Microstructural and chemical parameters of bentonite as determinants of waste isolation efficiency. Final Report European Commission Contract No F14W-CT95-0012.

/10/ **Jasmund K, Lagaly G, 1993.** Tonminerale und Tone – Struktur, Eigenschaften, Anwendung und Einsatz in Industrie und Umwelt. Steinkopff Verlag, Darmstadt.

/11/ **Pusch R, 1962.** Clay particles. Nat. Swed. Build. Res. Council, Stockholm, Rep. No 40.

/12/ **Pusch R, 1970.** Clay Microstructure. Doc. D8:1970. Nat. Swed. Build. Res. Council, Stockholm.

/13/ **Allen B L, 1977.** Mineralogy and soil taxonomy. Minerals in Soil Environments, Soil Sci. Soc. of America, Madison, Wisconsin USA.

/14/ **Grindrod P, Takase H, Wood G P, 1999.** Modelling silicitation of a clay buffer subject to opposing temperature and hydration gradients. Eng. Geol., Vol 54 (pp 215–222).

/15/ **Pusch R, 1999.** Mobility and survival of sulphate-reducing bacteria in compacted and fully water saturated bentonite – microstructural aspects. SKB TR-99-30. Svensk Kärnbränslehantering AB.

/16/ **Jacobsson A, Pusch R, 1978.** Egenskaper hos bentonitbaserat buffertmaterial. KBS Teknisk Rapport 32 (Bilaga 7). Svensk Kärnbränslehantering AB.

/17/ **SKB, 1978.** Kärnbränslecykelns slutsteg. Slutförvaring av använt kärnbränsle. II Teknisk del.

/18/ **Roskill Information Services Ltd, 2001.** The economics of bentonite. 9th ed, Roskill Inform. Services, Clapham Road, London SW9 0JA, UK.

/19/ **Crawford A M, Radhakrina A S, Goutama M, Lau K C, 1984.** Engineering materials for waste isolation. Can. Soc. Civ. Engng, Montreal, Quebec.

/20/ **Grim R E, Güven N, 1978.** Bentonites. Developments in Sedimentology, 24. Elsevier Publ. Co.

/21/ **Pattersson S H, 1955.** Geology of the Northern Black Hills Bentonite Mining Districut. Ph. D. Thesis, Univ. Illinois.

/22/ **Iwa O S, 1969.** The clays of Japan. Proc. 1969 Int. clay conference in Tokyo, Part 1. Geological Survey of Japan.

/23/ **Karnland O, Pusch R, 1990.** Development of clay characterization methods for use in repository design with application to a natural Ca bentonite clay containing a redox front. SKB TR 90-42. Svensk Kärnbränslehantering AB.

/24/ **Svemar C, Pusch R, Lindgren A, 2001.** Interim report on WP1, Prototype Repository Project, European Commission Contract FIKW-2000-00055.

/25/ **Schomburg J, 1997.** Data and literature collection "Friedland clay". Int. Rep. DURTEC Co, Neubrandenburg, Germany.

/26/ **Pusch R, 1983.** Stability of deep-sited smectite minerals in crystalline rock – chemical aspects. SKBF/KBS TR 83-16. Svensk Kärnbränslehantering AB.

/27/ **Lombardi G, Mattia P, 1981.** Guidebook for the excursions in Sardinia and central Italy. 7th Int. Clay Conference, Bologna and Pavia, Italy.

/28/ **Linares J et al, 1989.** Investigacion de bentonitas como materiales de sellado. U.E.I. Fisicoquimica y Geoquimica Mineral Estacion Experimental del Zaridin (CSIC), Granada, Spain.

/29/ **Prikryl R, Ryndova T, Vejsada J, Jelinek E, Bohac J, Sebec O, 2001.** Tertiary montmorillonite-rich clays from the Cheb basin (Czech Republik): alternative backfill material in the nuclear waste disposal. Proc. Joint 6th biennial SGA-SEG meeting, Krakow, Poland 26–29 August 2001. Balkema Publ. Lisse/Abingdon/ Exton/Tokyo.

/30/ **Wetzenstein W, 1964.** Minerogeologisch bedingte Unterschiede der rheologischen Eigenschaften bei Bentoniten von der Insel Milos/ Griechenland. 117 Jahrgang, Heft 8, Berg- und Hüttenmännische Monathefte.

/31/ **Decher A, 1997.** Bentonite der Insel Milos/Griechenland. Aachener Geowissenschaftliche Beiträge. Band 23, ISBN 3-86073-602-7.

/32/ **Pusch R, Madsen F T, 1995.** Aspects of the illitization of the Kinnekulle bentonites. Clays and Clay Minerals, Vol 43, No 3 (pp 261–270).

/33/ **Erlström M, Pusch R, 1987.** Survey of Swedish buffer material candidates and methods for characterization. SKB TR 87-32. Svensk Kärnbränslehantering AB.

4 Ballast materials

This chapter deals with non-smectite mineral components, termed “ballast” here, for preparing mixtures with smectite clay like commercial bentonites for backfilling purposes. The chapter also describes major ballast sources, primarily glacial deposits and crushed rock.

4.1 Minerals

4.1.1 General

Ballast material of rock-forming minerals can either be of glacial origin or obtained by crushing rock. It can be used for preparing mixtures with smectitic clay for application in repositories where the hydraulic conductivity of the backfill does not need to be very low, but where its compressibility must be low as at the top of KBS-3 deposition holes. In order to achieve a high density, which is fundamental for obtaining both a low conductivity and a low compressibility, the grain size distribution must be suitable while the mineral composition is less important. Unweathered crystalline rock material is preferable since it sustains mixing and heavy compaction without undergoing mechanical degradation, while grains of weathered or sedimentary rock become crushed in an uncontrolled fashion. In certain contexts the mineral composition is of importance, for instance if a high thermal conductivity is required or if the longevity of the smectite component of the mixture has to be at maximum.

Figure 4-1 illustrates the importance of selecting a suitable grain size distribution of backfills; smaller grains fit in the voids between larger ones which makes the flow paths narrow and tortuous and the compressibility low because of effective lateral grain support.

Certain ballast minerals, i.a. sulphur-bearing minerals, can promote canister corrosion. This is particularly important for concepts that imply embedment of the canisters by mixtures of clay and ballast materials. The major difference between rock-forming and clay minerals is the low hydration potential and absence of cation exchange capacity of

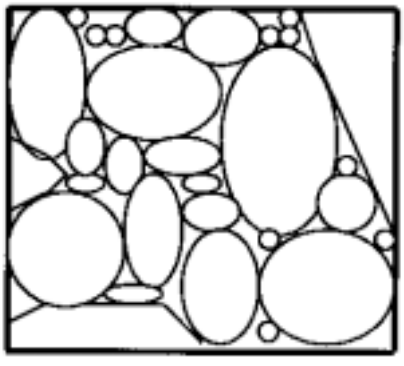

Figure 4-1. *Schematic picture of the microstructure of ballast grains in backfills.*

the rock-foming quartz, feldspars, carbonates, oxides and heavy minerals. The crystal structure of these minerals has a much lower content of lattice defects than clay crystallites, which means that their net electrical charge is low. The surfaces of these minerals are nearly as hydrophilic as the external surfaces of clay minerals but the much smaller specific surface means that the impact on the bulk properties by hydration, like swelling and softening, is small.

Special cases that are being considered as options for certain buffer concepts involve addition to the smectite bulk mass certain minerals in finely ground form like graphite, vivianite, quartz and illite. They are commercially available from certain mineral processing companies but for illite there is a cheaper way of obtaining sufficiently good material in nature. This mineral and its occurrence and availability is therefore included in the present document.

4.1.2 Hydration properties

Glacial material consisting of grains that have been exposed to abrasion, grinding and polishing in nature, represents a mineral phase with few defects and high compressive strength. When mixed with bentonite and compacted by use of high energies they stay stable and only the external grain surfaces become wetted. Crushing of rock, on the other hand, generates fissures, especially in mica grains, by which the surface area increases very significantly. Hydration of the fissure surfaces (cf Figure 3-8) makes them repell each other by which the fractures propagate and ultimately may break up the entire particle. By this the ballast grains soften, which promotes creep. This phenomenon explains, partly at least, the very pronounced settlement of fillings of freshly crushed rock if water has not been flooded over the surface before and during the compaction. Simple backfilling of tunnels, drifts and shafts with crushed rock and no water flushing will cause significant settlement and formation of gaps between the backfill and the roof.

4.1.3 Sorptive properties

The cation and anion exchange capacities of rock-forming minerals are very low and practically negligible with the exception of the micas. Thus, for muscovite screened through 100 mesh (d<0.149 mm) CEC is about 10 meq/100 g but for very finely ground material it can be 70–80 meq/100 g /2/. Biotite particles screened through 100 mesh has a CEC value of about 3 meq/100 g but fine-grinding brings the cation exchange capacity up to values that are similar to those of muscovite /2/.

4.1.4 Performance of mineral species in backfills

Quartz is a suitable ballast mineral in clay/ballast backfills for enhancing their thermal conductivity and for giving them a high mechanical strength and chemical resistance. Sulphur-bearing minerals are unsuitable since they have a potential to attack canisters of copper and iron and, if used for embedding canisters, they will undergo dissolution and yield precipitation of gypsum in the hottest part of the clay. Potassium-bearing minerals like K-feldspars will speed up illitization of the smectite. Carbonates dissolve and yield free calcium which replaces sodium in Na smectite clay.

The mineral composition is of importance in these respects and should be determined for any type of ballast intended for preparing repository backfills. Table 4-1 gives major data and assessments of minerals for use as ballast. For identification see Part 1 of this Handbook.

Table 4-1. Rock-forming minerals with respect to their usefulness as backfill components.

Group	Mineral	Species	Elements	Properties
Silicates (S)	Quartz (Q)		Si, O	Excellent (physically and chemically stable, high thermal conductivity)
	Feldspars (KF)	Microcline	Si, Al, K, O	Poor (provides potassium to smectite)
	(KF)	Orthoclase	Si, Al, K, O	Poor (provides potassium to smectite)
	(NaF, CaF)	Plagioclase	Si, Al, Na, Ca, O	Good (physically and chemically stable)
	Pyroxene (P)		Si, Fe, Mg, O	Good (physically and chemically stable)
	Amphibole (A)		Si, Al, Fe, Mg, O, OH	Acceptable (physically unstable, chemically stable)
	Mica (M)	Muscovite	Si, Al, K, O, OH	Poor (physically and chemically unstable)
		Biotite	Si, Al, K, Mg, Fe, O, OH	Poor (physically and chemically unstable)
	Epidote (E)		Si, Al, (Fe), Ca, O, OH	Good (physically and chemically stable)
	Chlorite (Ch)		Si, Al, Mg, Fe, O, OH	Poor (physically unstable)
Oxides (O)	Magnetite		Fe, O	Good (physically and chemically stable)
	Hematite		Fe, O	Good (physically and chemically stable)
Carbonates (C)	Calcite		Ca, O	Poor (physically and chemically unstable)
	Dolomite		Ca, Mg, O	Acceptable (chem. stability)
Sulphates (S)	Gypsum		Ca, S, O	Poor (Gives off sulphur)
	Barite		Ba, S, O	Poor (Gives off sulphur)
Chlorides (Cl)	Halite		Na, Cl	Poor (Dissolves and raises the porewater salinity)
Elements	Graphite		C	Poor (physically unstable)

4.1.5 Petrology

Fine-grained material commonly consists of individual crystals of silicates, oxides, carbonates and sulphates, the silicates usually being very dominant. Coarser grains often represent more than one mineral and the properties can then be anisotropic and varying within and among the grains. Rating of igneous or magmatic rock, is exemplified in Table 4-2, while metamorphic rock can be rated as in Table 4-3.

Table 4-2. Igneous or magmatic rock and its usefulness as a source for production of ballast for backfills. KF=K-feldspar, M=mica and Q=quartz.

Rock	Employment with respect to major requirements
Granite	Very good for low KF and M contents
Syenite	Acceptable but low heat conductivity since Q content is low
Diorite	Acceptable but low heat conductivity since Q content is low
Gabbro	Acceptable but low heat conductivity since Q is absent

Table 4-3. Metamorphic rock and its usefulness for ballast production.

Rock	Usefulness with respect to major requirements
Gneiss	Unweathered glacial material good, crushed rock unsuitable due to weak grains.
Mica schist	Unsuitable because of mechanical disintegration and elastic behavior at compaction and because of poor heat conductivity due to low quartz content.
Amphibolite	Unsuitable because of poor physical stability and low heat conductivity since the quartz content is low.
Quarzite	Very good because of high quartz content.

4.2 Glacial soil (sediments)

4.2.1 Sources

The properties of backfills consisting of mixtures of clay and ballast material are suitable if the latter has a suitable grain size distribution but this is usually not the case for natural sediments. It is therefore generally necessary to extract or add certain size fractions before mixing in the required amount of clay. Glacial material stems from moraine that was located below or in the glaciers where the ice rivers flew. The morain was eroded and abraded yielding grains with a size that varied from colloids to very big blocks. River-transported mineral particles and beach soils have undergone changes in mineral composition because of wearing and disintegration of mechanically weak grains. Soil material transported in rivers over long distances often contains much quartz and less feldspars because of their higher solubility.

Deposits of different origin have different size compositions and for practical and economical reasons it is important to select raw material that requires minimum sorting. Figure 4-2 illustrates the build-up of eskers, which represent the most common type of natural exploitable ballast sources in Scandinavia and Canada.

Various phenomena associated with deglaciation, like seasonal variation in flow rate of rivers and transgressive sea movements, have resulted in deposition of stratified sediments with strongly varying grain size, like varved clay. The organic content may be considerable in sediments formed under stagnant conditions. These factors combine to limit the possibility of finding larger amounts of granulometrically uniform material and sieving is necessary in practice for obtaining sand and gravel with a well defined grain size. Finer material than sand, i.e. silt, is usually required for obtaining a suitable gradation but the cost for separating it from ordinary glacial or postglacial material is so high that finely crushed rock is preferable.

4.2.2 Grain size distribution

Because of the frequent changes in the conditions for formation, there is almost always a significant variation in grain size distribution also in small volumes. Larger volumes show very significant variations due to the large-scale stratification exemplified in Figure 4-2.

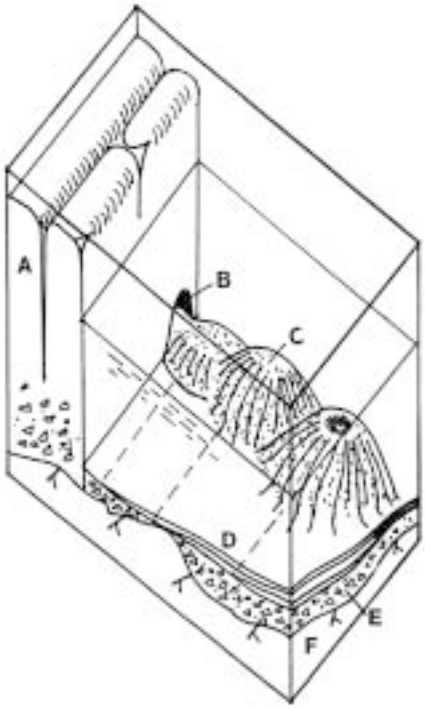

Block diagram showing the formation of an esker. A) Glacier, B) Melt-water exit, C) Esker unit ("hill"), D) Clay varves, E) Till, F) Bedrock.

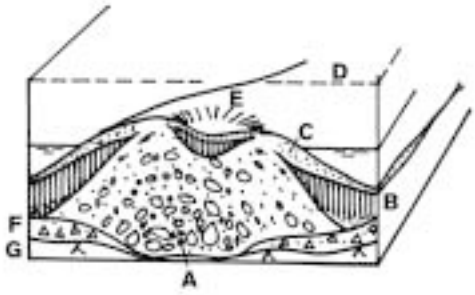

Cross section of esker exposed to wave erosion. A) Coarse-grained central part, B) Glacial clay, C) Eroded and redeposited coarser layer, D) Original sea level, E) Depression caused by embedded ice, F) Till, G) Bedrock.

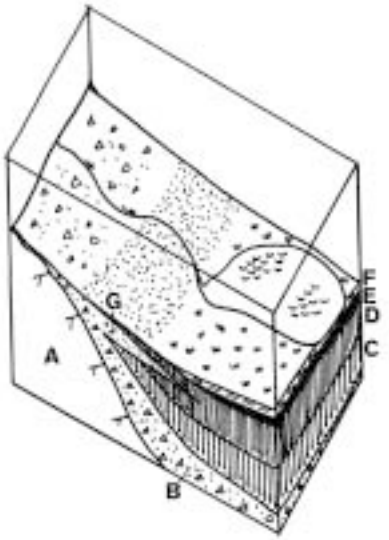

Block diagram showing the characteristic stratigraphy of hillside with eroded and redeposited coarse layer (G). A) Bedrock, B) Till, C) Glacial clay, D) Postglacial clay, E) Gyttja (mud), F) Peat.

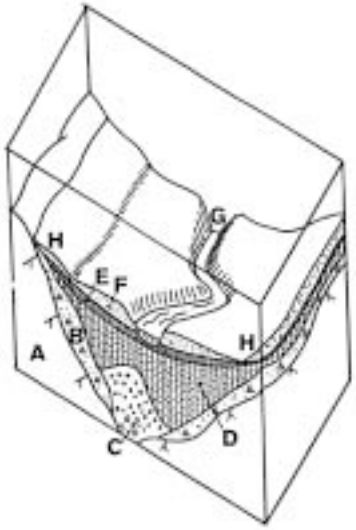

Block diagram showing the characteristic stratigraphy of river valleys in northern Sweden. A) Bedrock, B) Till, C) Esker nucleus, D) Glacial silt, E) Postglacial silty clay, F) Postglacial sand, G) River, H) Eroded and redeposited sand.

Figure 4-2. *Formation of eskers in valleys at glacier retreat /1/.*

Sediments often have grain size distributions of the type shown in Figure 4-3 i.e. the gradation curve is a straight line in a diagram with the logarithm of grain size plotted on one axis and the logarithm of the cumulative weight percentage on the other. In ordinary plottings sediment granulometry is as exemplified by Figure 4-4.

However, variations in gradation of the source material and in water flow has commonly given polymodal distributions, i.e. with more than one dominant grain size, as shown in Figure 4-5.

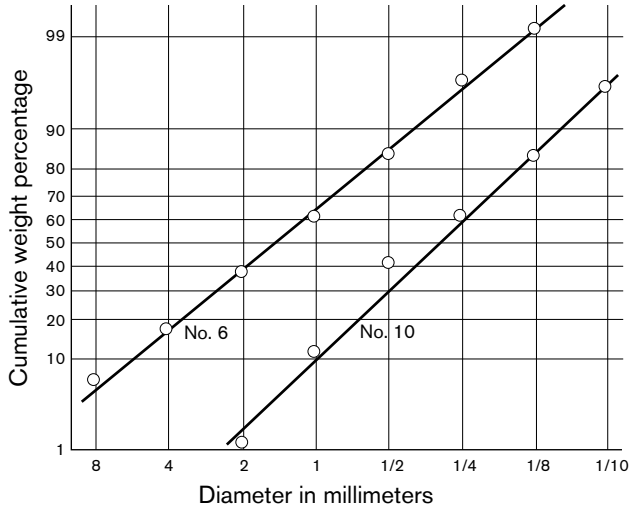

Figure 4-3. *Classical examples of particle size distributions in sediments /4/. The upper curve represents a coarse soil with a median grain diameter of about 1.3 mm. The lower curve is finer and has a median value of 0.35 mm.*

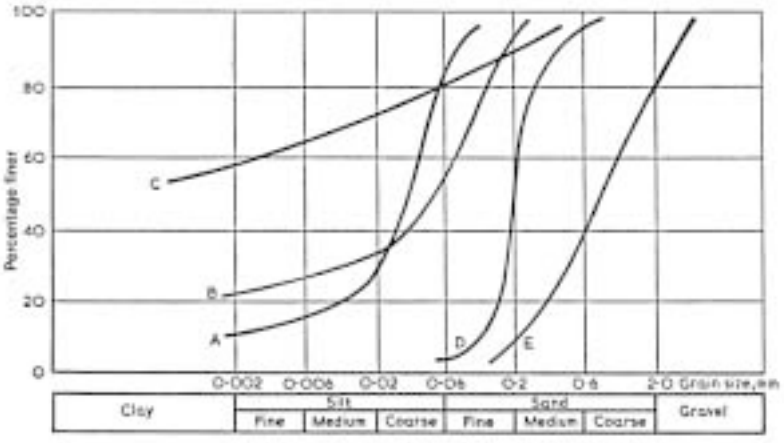

Figure 4-4. *Classical examples of granulometry of natural soils /4/. A) Silt with 10% clay and 15% sand. B) Sand with 22% clay, 35% silt and 43% fine sand. C) Weathered clayey sand. D) Fine sand. E) Sand suitable for concrete /4/.*

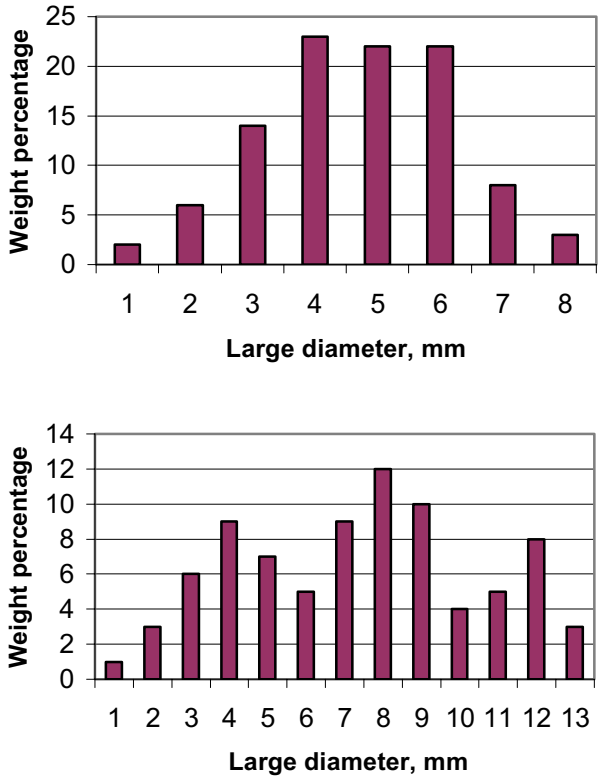

Figure 4-5. *Grain size in histogram form. Upper: Common shape (horizontal axis shows grain diameter in mm). Lower: Three-modal shape resulting from overlapping of three populations.*

4.2.3 Grain shape

The shape of ballast grains is of importance for the compactability of backfills. Glacial soils consist of grains that are commonly well rounded because of abrasion and wearing in the course of transportation and setting. This is obvious from Figure 4-6, which shows that roundness and sphericity (cf Part 1) are mutually related. The higher the sphericity (1.0 is the sphere), the less rough is the contour (angular 0–0.15, subangular 0.15–0.25, subrounded 0.25–0.40, rounded 0.40–0.60 and well rounded 0.60–1.00).

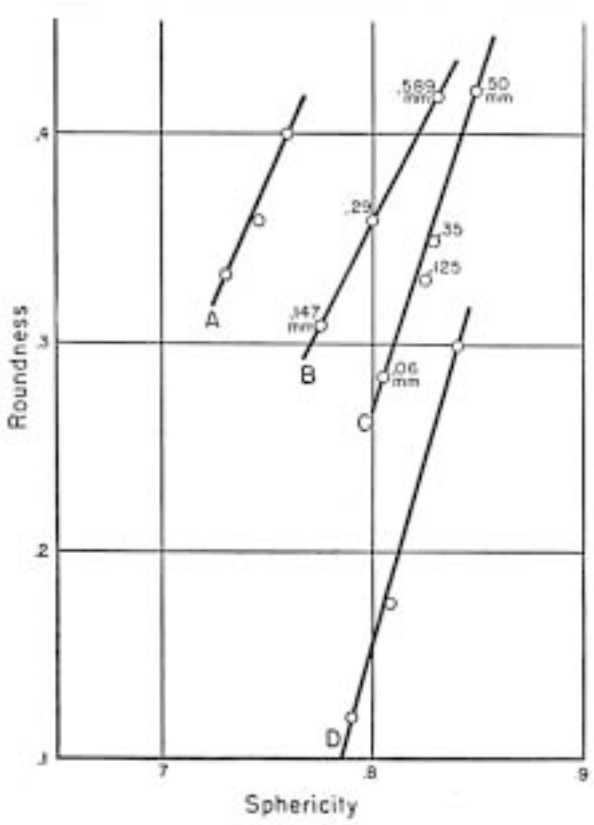

Figure 4-6. *Relation of sphericity and roundness (A=Fine beach sand, B=Coarse beach sand, C=Sandstone, D=River sand) /4/.*

4.2.4 Illite clay

Significant parts of countries that were glaciated in Quaternary time are covered with clayey sediments deposited in the sea, estuaries and lakes and they usually have illite as dominant clay mineral. Transgressions, regressions and seasonal variations in the rate of ice river flow caused concordant sediments with varved glacial clay as typical example. Especially the lower part of Quaternary clay deposits are relatively poor in clay-sized particles and the more finegrained, homogeneous and carbonate-poor overlying post-glacial clay is therefore the most suitable illite source. This is illustrated by Table 4-4 that gives data of typical soil profiles of clay sediments deposited in fresh water (Skå Edeby) and ocean water (Lilla Edet).

The table shows that the illite content is rather low even in the most fine-grained part of the profiles and processing in the form of enrichment by applying sedimentation for removal of coarser fractions is required if a high illite content is needed. This is an expensive process as is also the drying and grinding that is required for converting the rather wet clay (water contents 58 to 106%) into the air-dry form that is necessary for mixing the illite with smectite and ballast. An early pilot study performed by the Swedish Geological AB for SKB showed that commercial bentonite powder will be cheaper than illite powder prepared from Swedish postglacial clay in the county of Uppland using existing processing plants (Upsala-Ekeby ceramic industry).

Certain formations appear to be richer in illite in other glaciated areas, like in Canada and the US, but the amount of homogeneous material of such soils is commonly rather limited. It has been stated that illite dominates in post-glacial ocean sediments where it emanates from montmorillonite and kaolinite /2, 3/, as well as in lacustrine environment

Table 4-4. Geotechnical data for typical soil profiles in Sweden.

Site	Description	Depth, m	Density*, kg/m³	Clay content, %	Clay minerals**
Skå-Edeby	Green/grey muddy clay (post-glacial)	2	1430	59	I > K > Chl I=25%
(fresh-water)	Grey clay (post-glacial)	5	1490	77	I > K I=30%
	Brown/grey varved clay (glacial)	7	1590	52	I > K > Chl I=20%
	Brown/grey varved clay (glacial)	8	1610	63	I > K > Chl I=20%
	Brown/grey varved clay (glacial)	9	1620	56	I > K > Chl I=15%
	Brown/grey varved clay (glacial)	10	1610	54	I > K > Chl I=15%
Lilla Edet	Grey clay (post-glacial)	3	1480	70	I > K I=20%
(marine)	Grey clay (post-glacial)	6	1500	74	I > K I=20%
	Grey clay (glacial)	19	1610	55	I > K I=25%

*Density of natural water saturated soil. **I=Illite, K=Kaolinite, Chl=Chlorite

(Lake Erie) and recent Alluvium like in the Mississippi river, where it makes up 40 to 60% of the mineral content. In ancient ocean sediments illite dominates with increasing depth where time, temperature and access to potassium has led to conversion of smectites to this mineral /3/.

4.3 Till (moraine)

4.3.1 Sources

Till covers the bedrock in glaciated areas and is available in large quantities in Scandinavia, northern British Isles, Canada and Russia. It was formed by the scraping action of advancing glaciers and its lower parts have been compacted under effective pressures as high as 30 MPa (basal till). The mineral composition reflects that of the rock from which it stems. Where the bedrock consisted of granite and gneiss the till is usually rich in quartz, feldspars and heavy minerals, and where it was dominated by limestone and clay-bearing strata, the till is marly and clayey, respectively.

4.3.2 Grain size distribution

Using histograms one would expect a rather uniform height of the size fraction columns and this is also often the case (Figure 4-7), deviations partly being due to different rock types from which the material originated. Stones and blocks are contained in the till matrix, often oriented or arranged in a more or less regular fashion depending on the stress conditions generated by the advancing glaciers. The most typical property of till is the lognormal gradation as illustrated by Figure 4-9, which represents till material that is relatively rich in clay.

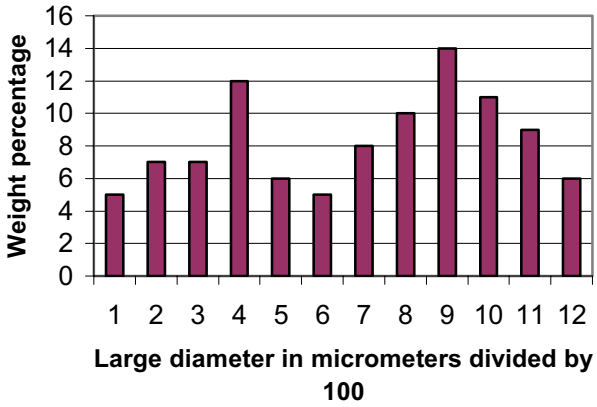

Figure 4-7. *Typical grain size distribution of fine-grained till. The vertical axis shows the percentage of the respective class.*

The presence of practically all size fractions make tills tight, especially if they are clayey and have smectite minerals in the clay fraction. They can then serve as good backfills without adding any clay to them and be excellent if a small amount of bentonite is added (cf Chapter 10). An example of clayey till from southern Sweden that is of potential use for backfilling of repositories is illustrated by Figures 4-8 and 4-9.

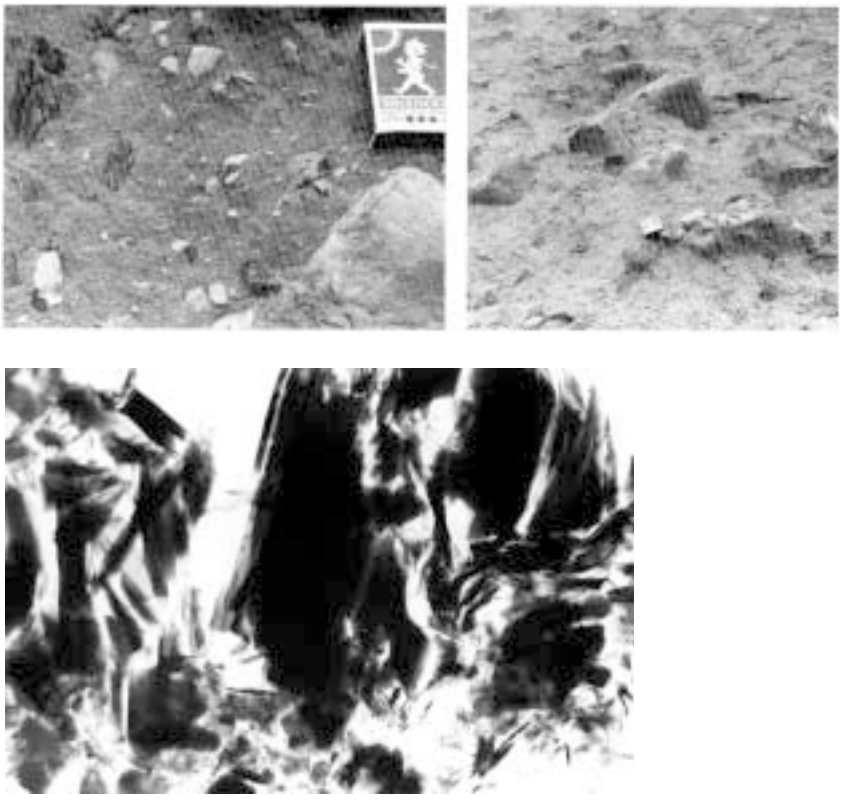

Figure 4-8. *Smectitic till from Skåne, Sweden. The dry density is about 2000 kg/m³. The clay content is about 15% by weight with smectite forming 5–10% of the total mass. Upper: Typical appearance of larger grains contained in the finer silt/clay matrix. Magnification 10 x. Lower: Transmission electron micrograph showing fine particles squeezed into a dense arrangement. Magnification 10 000 x.*

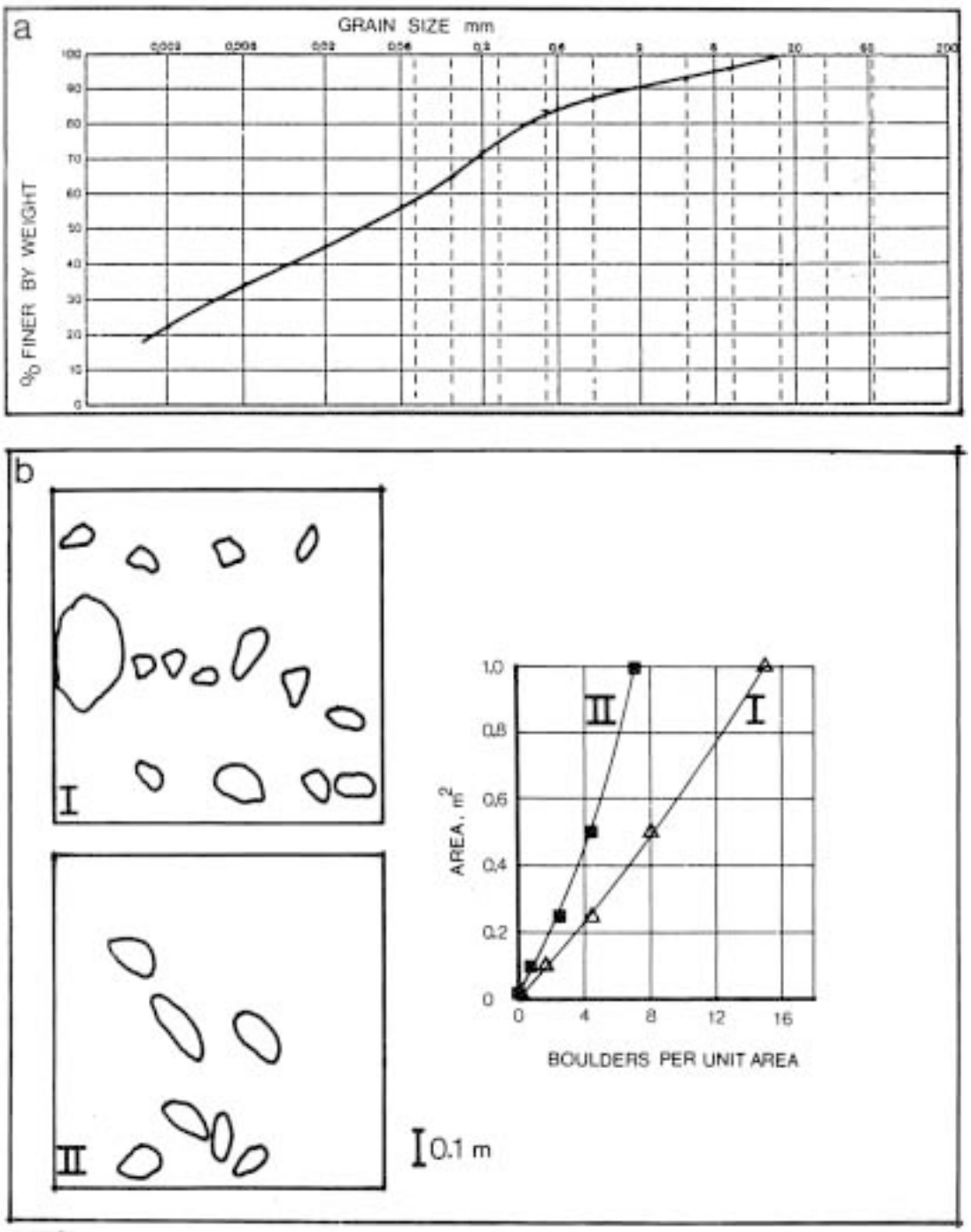

Figure 4-9. *Grain size distribution of clayey till ("boulder clay") from Hyllie (a). The lower part (b) shows the variation of frequency of boulders >60 mm in closely located plane vertical sections /5/.*

Experience tells that it is difficult to excavate clayey tills because of their density and high shear strength, which makes it more expensive to utilize them than sediments. Also, tills require considerable compaction energy to reach bulk densities of the required order of magnitude, i.e. about 2000 kg/m^3. However, their suitable grain size composition and limited need for adding fines to reach a low hydraulic conductivity still makes smectitic clayey till interesting as backfill materials.

Tills like coarse sediments have structures and grain size distributions that are strongly scale-dependent (Figure 4-9). Thus, the amount of material sampled for determination of the granulometry must be sufficently large to get reliable, representative data.

4.4 Crushed rock

4.4.1 Preparation techniques

Crushing of rock for production of ballast material can be made in one or two steps depending on the required gradation. Taking 20 mm as a common upper limit, crushing of all material is first made to reduce the grain size to this value for which gyratory crushers are suitable. A second crushing process can then be employed if the gradation needs to be changed.

4.4.2 Grain size and shape

The granulometry of crushed and ground rock is largely determined by the rock structure and by the sieving and crushing techniques. The grains formed by crushing crystalline rock naturally have a very low roundness while the sphericity parameter may vary from nearly unity for isotropic rock like granite to less than 0.5 for gneiss and amphibolite. The fragments are usually rich in fissures and fractures which give them an appreciable porosity and internal specific surface area. The low degree of roundness means that the particles have asperities that break under heavy compaction.

While the shape of glacial material – excepting coarse till – is usually characterized by a high degree of sphericity and roundness, the very obvious difference in shape of crushed rock makes it necessary to define it for which one can use the three "diameters" defined in Figure 4-10 (cf Part 1).

While a major principle for obtaining very dense layering of spherical grains and a minimum porosity is to select a gradation of Fuller's type, meaning that smaller grains fit in the voids between larger ones, there is no simple rule for composing backfills with oblate particles. The Fuller curve and a similar mathematically derived curve by Wentworth represent parabolic gradation of the type shown in Figure 4-11.

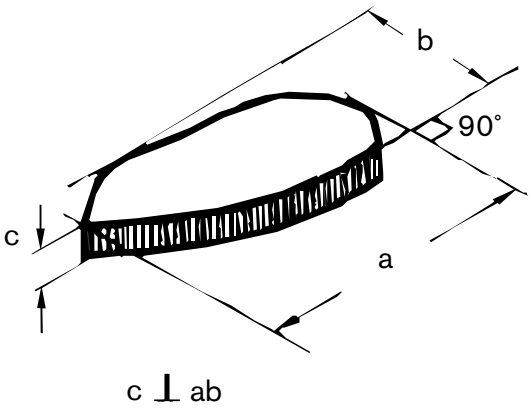

Figure 4-10. *Parameters for definition of grain size.*

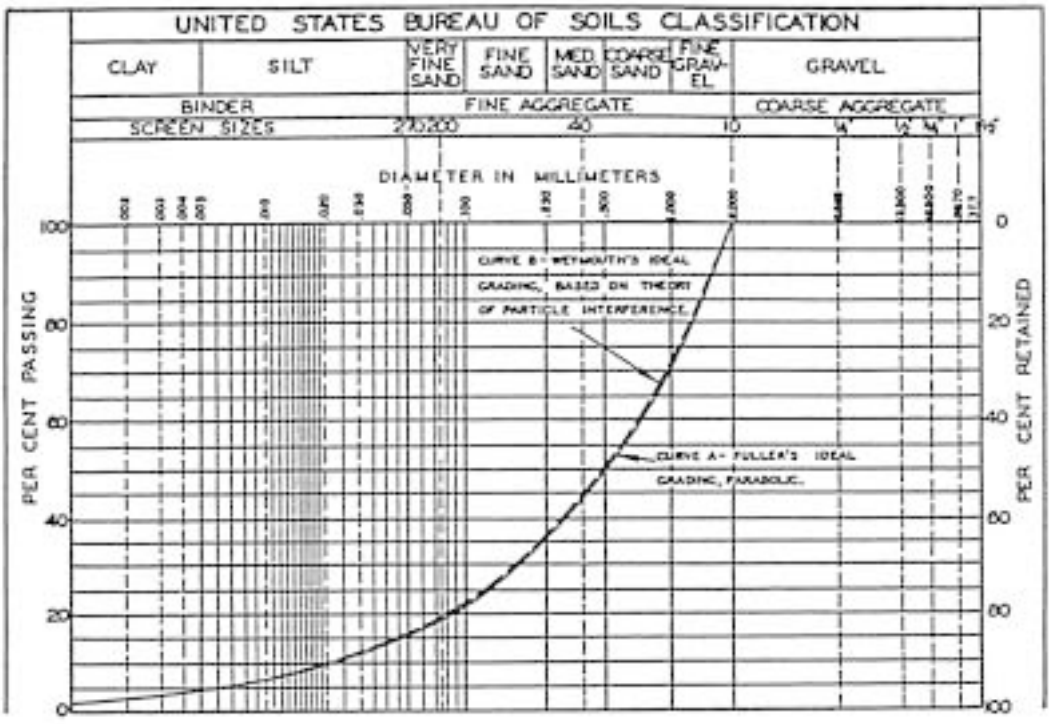

Figure 4-11. *Fuller's and Wentworth's curves in a classical diagram with weight percent passing the respective screen sizes plotted against particle diameter.*

Non-spherical grains and grains with a low degree of roundness, i.e. with rough surfaces, give lower bulk densities than spherical ones for any given grain size distribution and require stronger compaction, except when the grains break down due to abrasion. This has been illustrated by compression tests of four types of material with the grain size distribution shown in Figure 4-12.

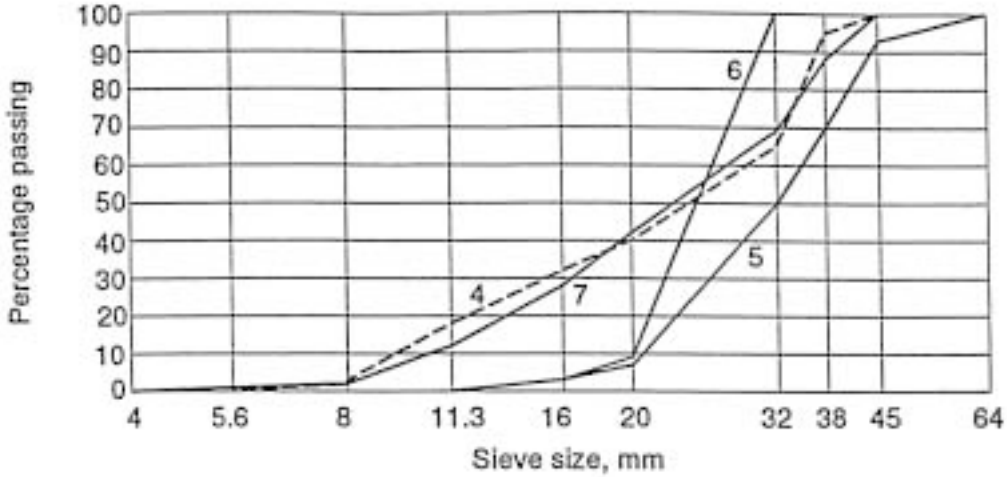

Figure 4-12. *Size distribution (b-diameter) of four coarse materials. 4 is a mixture of well-rounded glacial material, 5 is crushed fine-grained granite, 6 is crushed quartzite and 7 blasted gneiss rock /6/*
.

The major results from the tests are given in Table 4-5, from which one finds that the similarly sized grain assemblages of spherical and well rounded material (No 4) and blasted rock (No 7) had quite different densities and void ratios (e) in uncompacted form; e_{max}=0.70 and e_{max}=0.93, respectively, while they were equally dense after effective compaction, i.e. e_{min}=0.50. The high e-value of the blasted, angular material (No 6) is explained by the open network formed by the anisometric grains, which were broken and formed finer fragments under heavy compaction giving almost the same density as for the spherical, well rounded grains of glacial material.

A practically useful measure of the oblateness of crushed rock fragments is the splintery factor defined as $f=b/c$, where b and c are defined in Figure 4-10. They are determined by combination of square-mesh sieves and grating (rod) sieves (cf Part 1 of this Handbook). In road and earth dam construction, suitable crushed rock material commonly has $1.2<f<1.35$. This parameter is shown in Table 4-5 as well.

The table shows that the splintery factor is a better measure of the anisotropy of platy grains than the sphericity. Blasting and crushing of granite do not yield significantly anisotropic fragments and their size is therefore usually taken as the square-mesh size, i.e. a, b, and c are approximated to be equal.

Comprehensive testing has been made in conjunction with SKB's research on backfill materials prepared by blasting and crushing, using crystalline rock of various origin. Figures 4-13 and 4-14 illustrate typical grain size distributions of blasted and crushed granitic rock. They show that Fuller-type size distribution is obtained for both blasted and crushed rock of this type. For gneiss is would be required to use grating sieves as well for quantifying the deviation from spherical size.

Table 4-5. Granulometric data of coarse rock material with grain sizes according to Figure 4-12.

Material	D_{50} mm	$C_u=D_{60}/D_{10}$	Splintery factor, f	Spher-icity	Round-ness	e_{max}	e_{min}	ρ_d kg/m^3
Glacial (4)	25	3.1	1	0.71	0.38	0.70	0.50	2690
Crushed granite (5)	32	1.65	1.17	0.69	0.10	0.94	0.59	2680
Crushed quartzite (6)	25	1.30	1.33	0.64	0.22	0.97	0.53	2640
Blasted gneiss (7)	23	2.6	1.32	0.63	0.18	0.93	0.50	2690

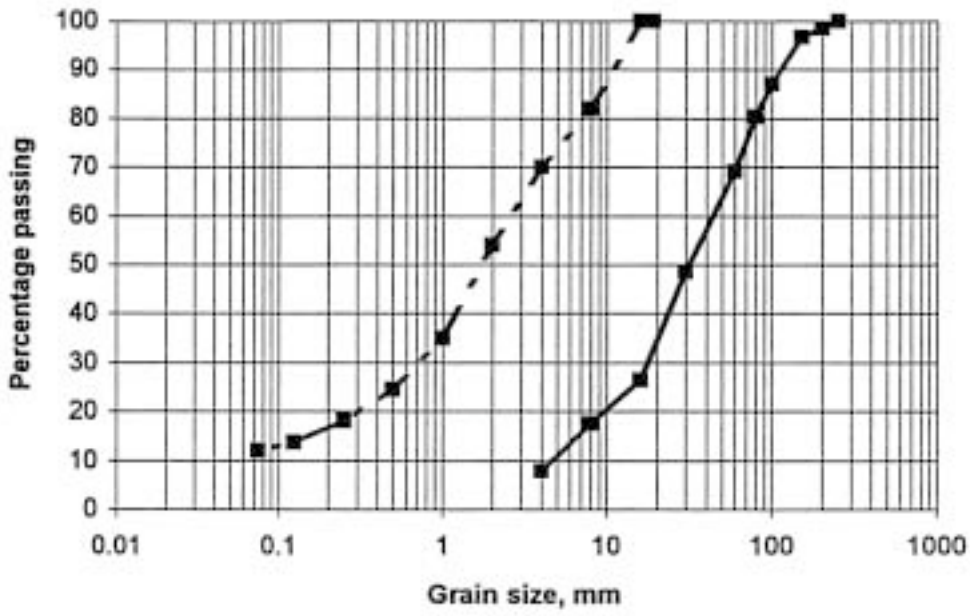

Figure 4-13. *Grain size distribution of blasted crystalline rock of granitic type (right curve, Boliden, Västerbotten) and crushed rock (left curve, Morgårdshammar, Dalarna).*

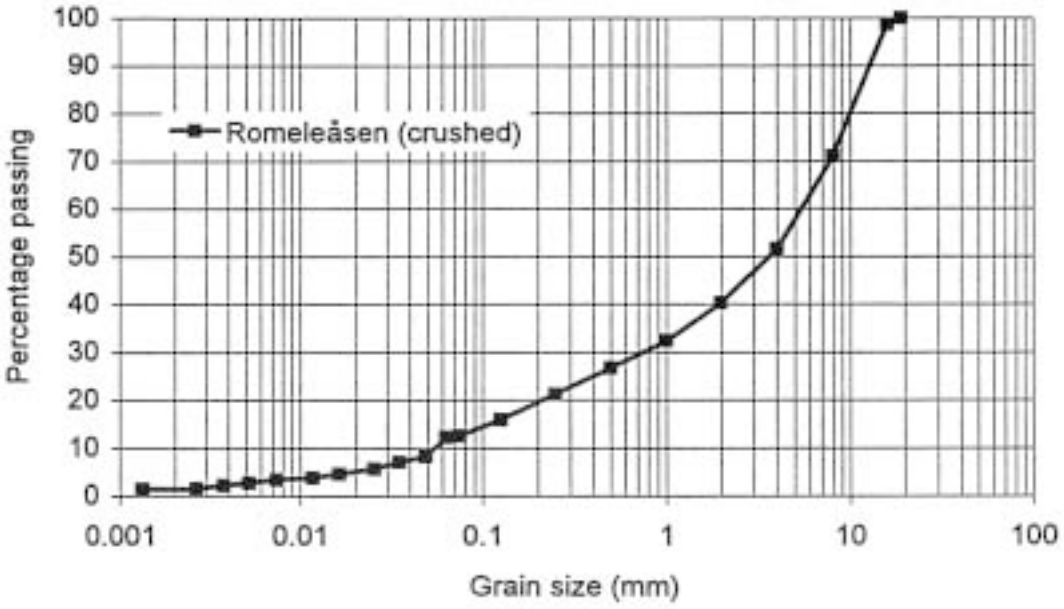

Figure 4-14. *Grain size distribution of crushed granitic rock from Romeleåsen (Skåne).*

4.5 TBM muck

4.5.1 Fragmentation

The cutting heads of tunnel boring (TBM) and raise-boring machines are equipped with buttons or sets of discs that are pressed against the rock for fragmentation. This yields breakage in the form of crushing below the cutters and production of small and large chips. TBM:s normally have discs and the large chips are platy because of the form of the plastic zone and the influence of tangential stresses. The impact on the rock and the fragmentation processes have been studied in detail in several contexts and the reason for the anisotropic shape explained, cf Figure 4-15 /7/.

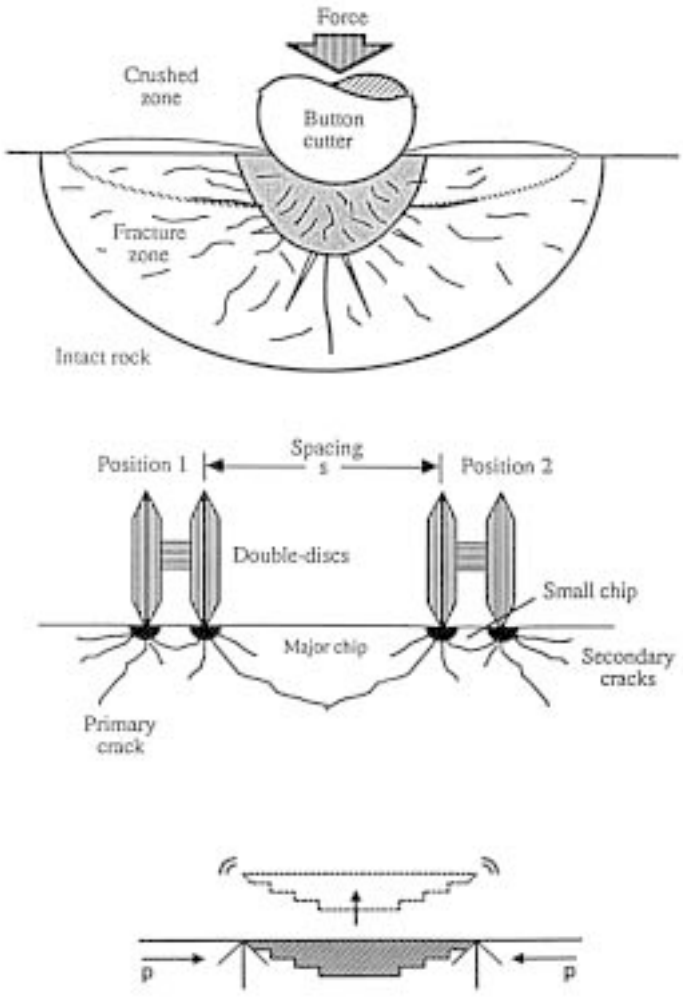

Figure 4-15. *Fracturing of brittle rock. Upper: Whittaker's and Frith's model of the impact of button cutters. Central: Guo's model of chip formation. Lower: High tangential stresses release chips /7/.*

4.5.2 Grain size and shape

The elongation and flatness of the chips from TBM-drilling makes it necessary to express the size in terms of the "diameters" *a*, *b* and *c* defined in Figure 4-10. As for blasted and crushed rock measurements for determining the size distributions are made by use of square mesh and grating (rod) sieves (cf Part 1). The former give the size in terms of the *b*-diameter while the latter yield the *c*-diameter. Typical size distributions of chips from TBM drilling are indicated in Figure 4-16. This figure also shows that TBM drilling may produce ideal (Fuller-type) distribution of the size expressed in terms of the *b*-diameter. Figure 4-17 shows examples of the appearance of chips and Figure 4-18 illustrates the effect of crushing of TBM muck in one and two steps, yielding nearly the desired ("wanted") distribution already after the first crushing process.

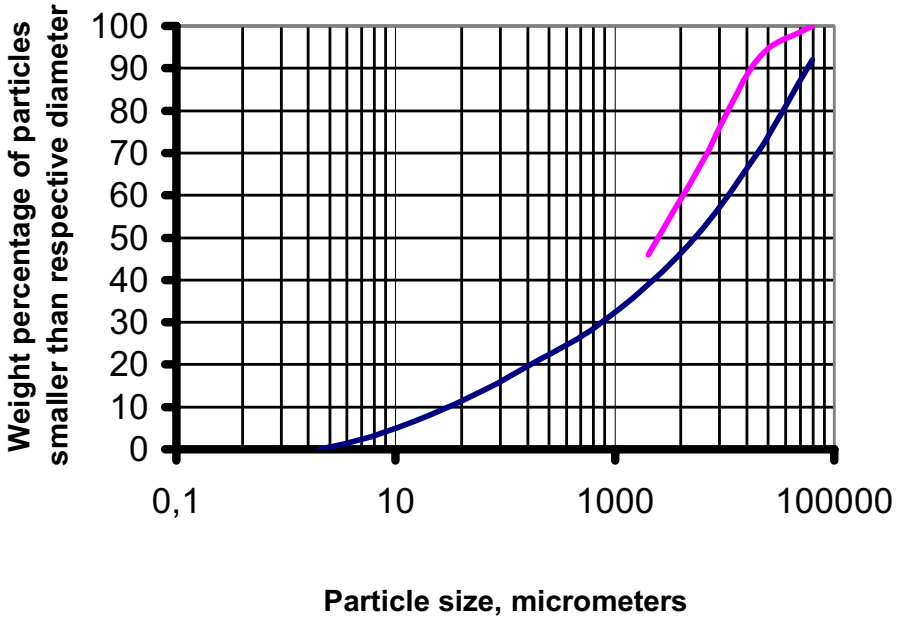

Figure 4-16. *Crushed TBM muck. Typical size distribution in terms of c and b diameters. The upper curve represents "c" and the lower "b".*

Figure 4-17. *TBM chips with typical platy shape. The large diameter a is 1.2 to 2.2 times the intermediate diameter b, which is 2-3 times the smallest diameter c.*

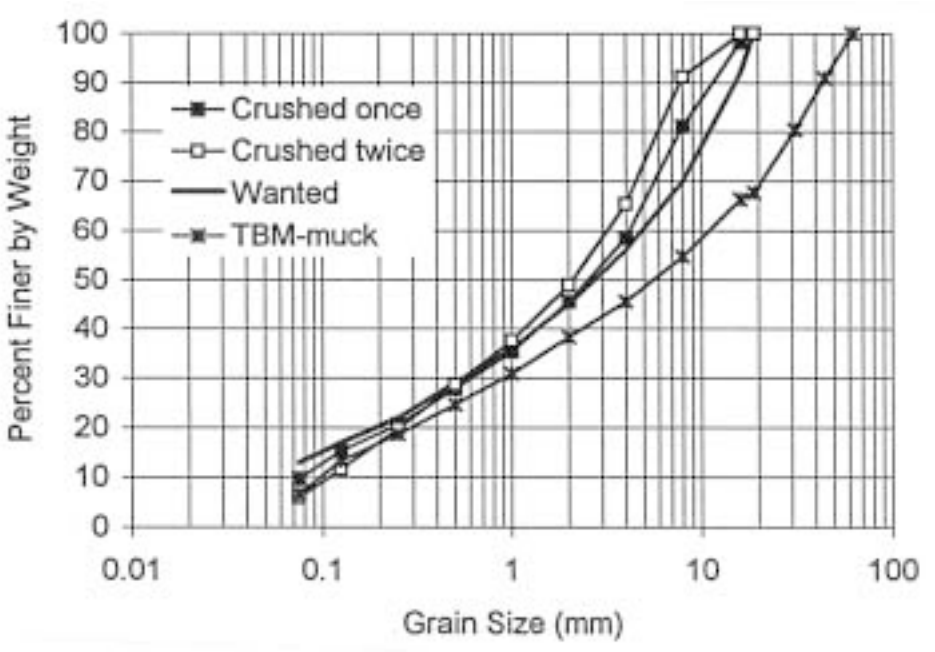

Figure 4-18. *Results of full scale tests of crushing TBM muck. The size represents the b diameter /6/.*

4.6 Commercially available ballast materials in Sweden

4.6.1 Glacial products and crushed rock

Gravel, sand and crushed rock are exploitable at more than 20 000 sites in Sweden, mostly eskers and deltas /7/.

About 400 of them are licensed pits for production of ballast (aggregates) which amounted to about 100 Mt per year in the early 90:s. About 400 of them were macadam-producing quarries in 1992 but the number had increased to about 1200 a year later /8/. In certain areas, like southwestern Sweden, the fraction of rock crushing plants was about 75% in 1993. Exploitation of sand and gravel from below the sea level is prohibited in Sweden for environmental reasons.

Figure 4-19 shows the distribution of natural gravel sources in Sweden from which it is obvious that quite large exploitable regions are found in the counties of Skåne, Småland, Södermanland and Dalarna. Figure 4-20 shows the distribution of crushing plants in Sweden.

4.6.2 Special sources

Pure quartz sand is occasionally found in certain geological formations, like cyclothemes and eroded sandstone beds /4/. Such material is found and exploited at a few sites in Sweden; the most important sources are located at Baskarp and Fyledalen in Skåne. Quartz particles for mixing with clay or ballast materials can be obtained by crushing quartzite, which is the technique applied by the Swedish company Forshammars Bergverk near Lindesberg.

4.6.3 Characterization (“Quality”)

A number of data for characterization of the soil material from various pits are available through the SGU Grusdataarkiv, which provides definitions of the parameters that are not included in Part 1 of this Handbook. The main ones are:

1. Grain shape
2. Brittleness of grains
3. Durability
4. Clay content
5. Humus content
6. Petrology
7. Mica content

Testing of material from natural sources or from crushed rock is made by the Swedish Geotechnical Institute, geological and geotechnical university departments and private companies. The matter is fully treated in geological literature /9, 10, 11/.

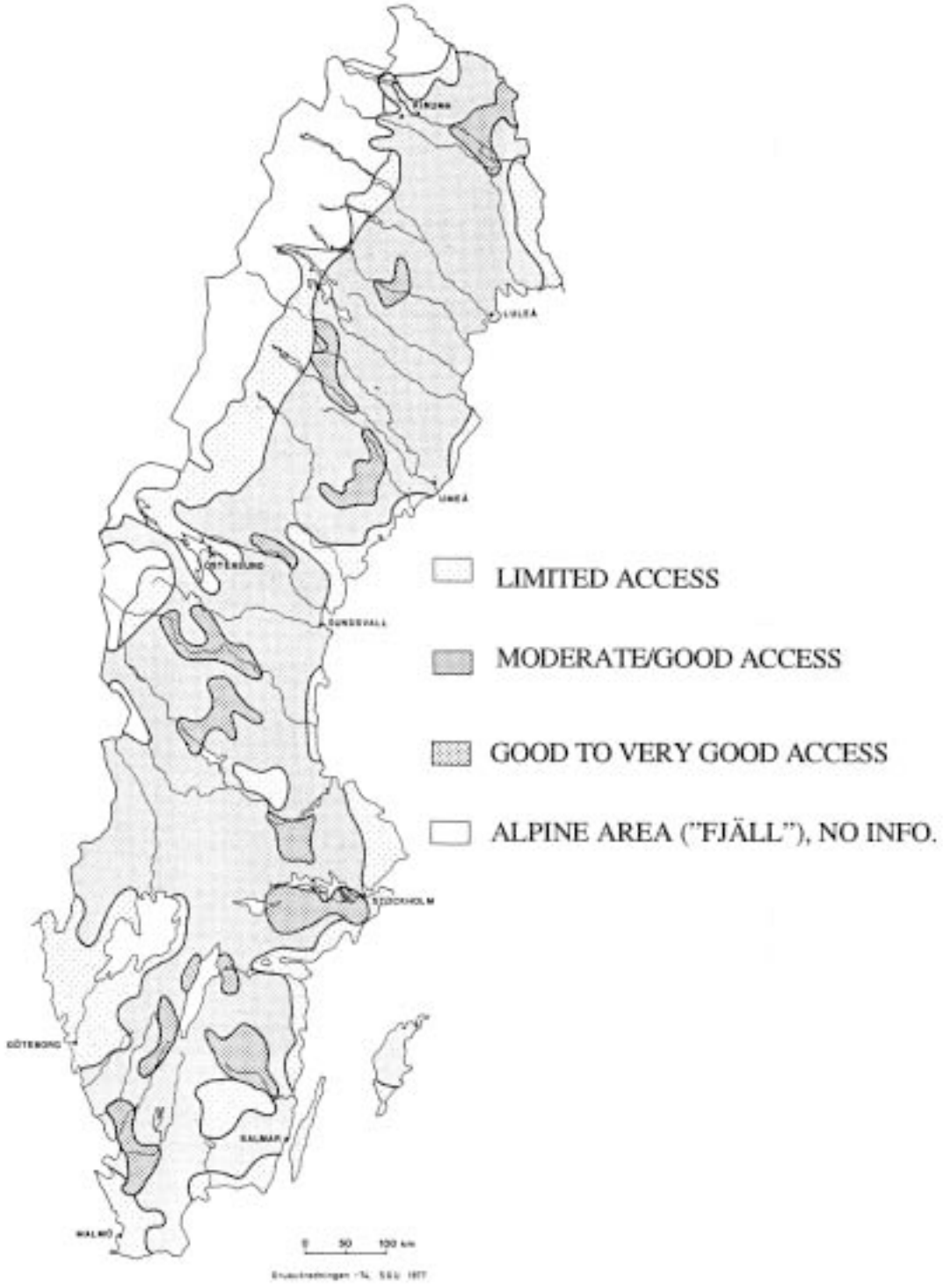

Figure 4-19. *Distribution of natural gravel in Sweden /7/.*

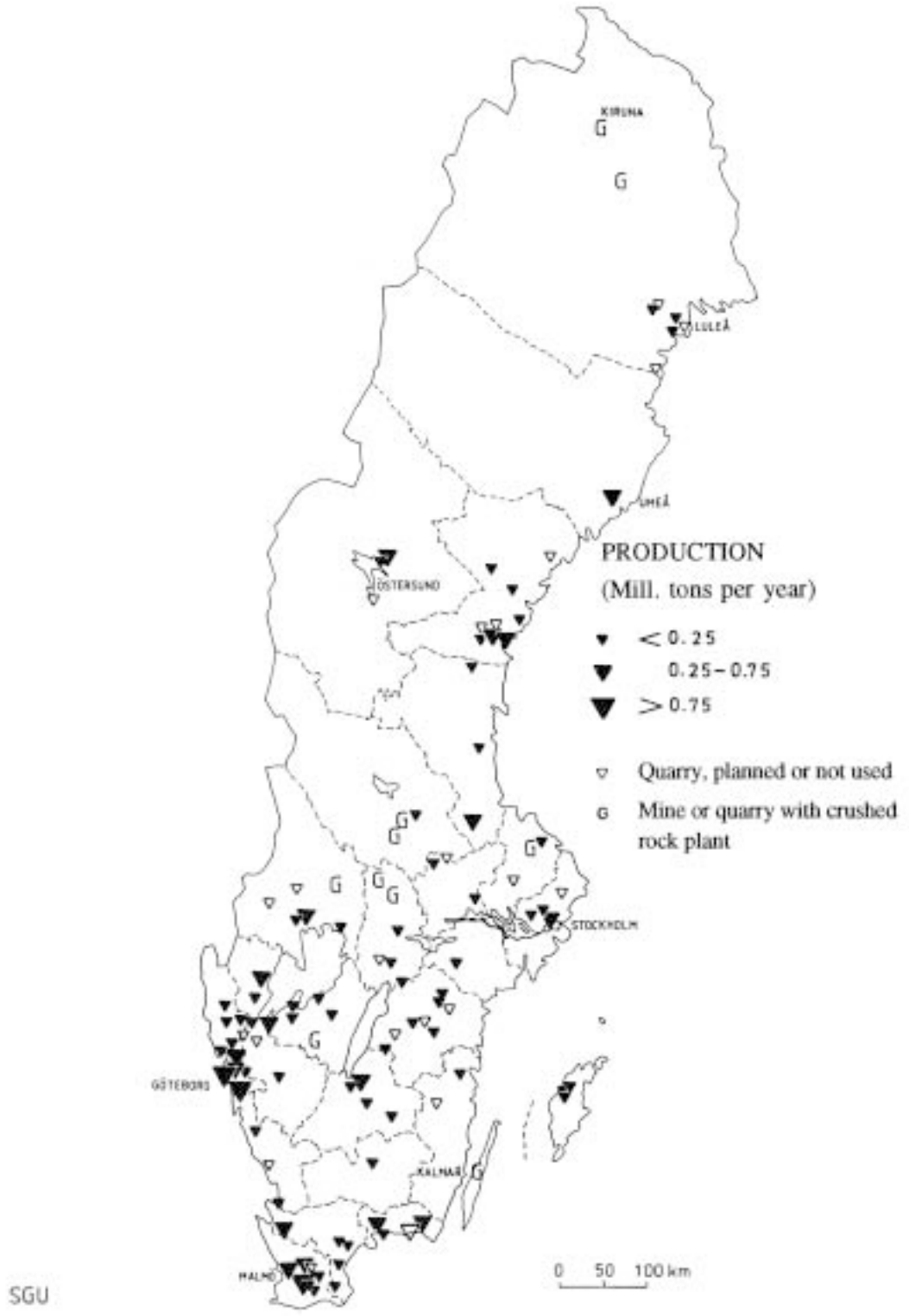

Figure 4-20. *Location of crushing plants in Sweden /7/. Open triangle means planned quarry. G means mine or stone quarry where rock crushing takes place.*

4.7 References

/1/ **Pusch R, 1981.** Scandinavian engineering geology – a glimpse. Lecture, Proc. 10th Int. Conf. Soil Mech. a. Found. Engng., Stockholm.

/2/ **Grim R E, 1967.** Clay Mineralogy. McGraw-Hill, New York.

/3/ **Pusch R, 1994.** Waste Disposal in Rock. Developments in Geotechnical Engineering, 76. Elsevier Publ. Co, ISBN:0-444-89449-7.

/4/ **Pettijohn F J, 1949.** Sedimentary Rocks. Harper's Geoscience Series, New York.

/5/ **Pusch R, 1973.** Structural variations in boulder clay. Proc. Int. Symp. Soil Structure, Chalmers Technical University, Gothenburg.

/6/ **Pusch R, 1995.** Consequences of using crushed crystalline rock as ballast in KBS-3 tunnels instead of rounded quartz particles. SKB TR 95-14. Svensk Kärnbränslehantering AB.

/7/ **Pusch R, 1995.** Rock Mechanics on a Geological Base. Developments in Geotechnical Engineering, 77. Elsevier Publ. Co.

/8/ **SGU, 1993.** Grus, sand och industrimineral. SGU P; 1994:7 (ISSN 0283-2038).

/9/ **Ericsson B, Grånäs K, 1983.** SGU:s Grusdataarkiv. Ett system för datalagring och presentation av grusinformation.

/10/ **Ed. Smith & Collis, 1993.** Aggregates, sand, gravel and crushed rock aggregate for construction purposes. Geol. Soc. London, The Geological Socl. Publ. House (339 p).

/11/ **Lagerblad B, Trägårdh S, 1996.** Ballast för betong. Cement- och Betonginstitutet, CBI-rapport 2-96.

5 Backfills

This chapter deals with artificially prepared soil material for backfilling of tunnels, drifts, and shafts in repositories. The backfills do not have to be as tight and expansive as buffer clay but must still be relatively impermeable and have low compressibility for minimizing compression under its own load and under the pressure provided by the contacting buffer in KBS-3 deposition holes. This requires a suitable composition of the mixtures granulometrically as well as mineralogically. The microstructural constitution is most important since it determines both the density of the clay component and thereby the hydraulic conductivity, expandability and compressibility of the mixture. In the present chapter mixtures of smectite-rich material and ballast, and natural clayey materials are in focus. For the firstmentioned type the gradation of the ballast and the relative amounts of ballast and clay are most important.

5.1 Options

While the buffer clay, i.e. the canister-embedment, should have an excellent isolating capacity implying a very low hydraulic conductivity and a high expandability, backfills in tunnels, drifts and shafts can be allowed to be more permeable and less expansive. Considering also cost aspects early proposed backfills were mixtures of bentonite and ballast and they have also been investigated in systematic laboratory experiments and in a comprehensive field experiment, the Stripa Buffer Material Test (BMT). Later, natural smectitic clays have been found to be an alternative and both options are considered in this chapter.

5.2 Clay/ballast mixtures

5.2.1 Principle of composition

Mixtures of clay and ballast with different compositions can be defined to meet the desired criteria, which, for fulfilling the demands of KBS-3 type concepts is a low hydraulic conductivity and a low compressibility. A basic priniciple for achieving this is to compose the mixture such that the space between non-clay ballast grains is small and occupied by clay minerals /1/. Thereby, the hydraulic conductivity of the mixture will be low, especially if the clay contains smectite minerals, while the compressibility is low since an applied pressure will be transferred via the densely spaced ballast grains.

This principle is demonstrated in Figure 5-1, which shows the difference between the basic case with only ballast material and the case with mixed-in smectite clay granules that absorb water, expand and form a low-permeable clay gel in most of the voids.

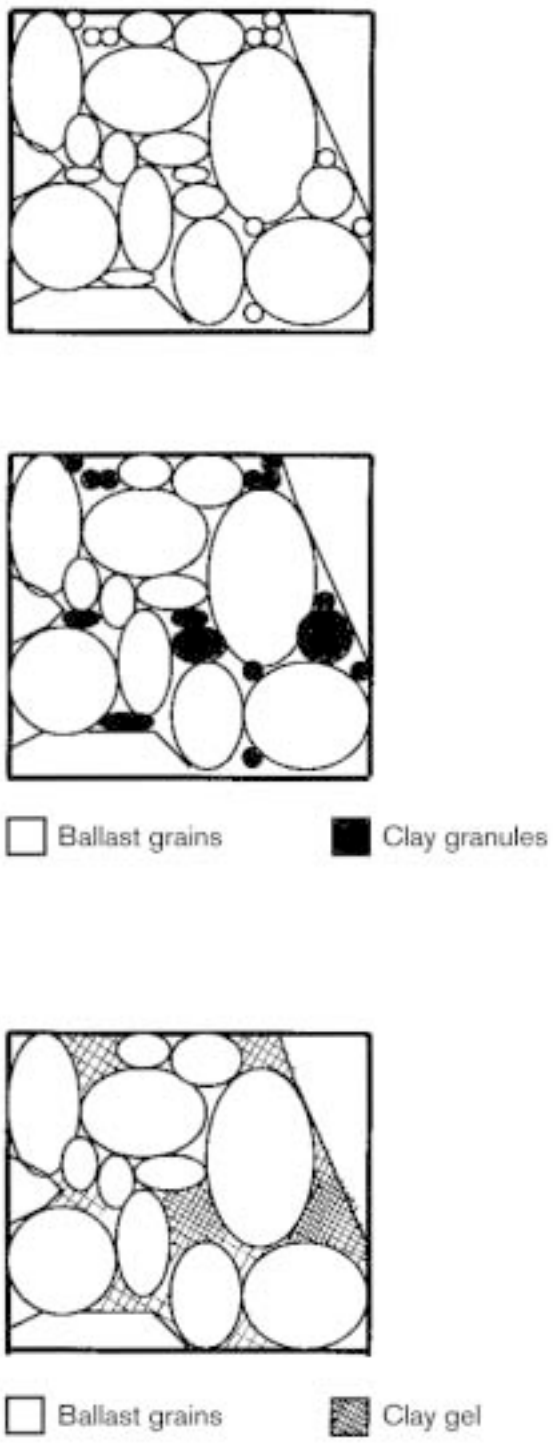

Figure 5-1. *Performance of backfill without and with clay component. Upper: Basic case with only ballast material (cf Figure 4-1). Center: Case with smectite clay granules in the voids between larger ballast grains. Lower: State with the clay hydrated and expanded to form a clay gel in the voids.*

As in other geotechnical contexts, a clay content exceeding about 15% means that the clay matrix becomes continuous with the ballast grains floating in it. Theoretically, optimum performance with respect to bulk hydraulic conductivity and compressibility is obtained by using a Fuller-type ballast grain size distribution and 5–10% expandable clay by weight. The clay is preferably commercial, finely ground smectite-rich Na bentonite with montmorillonite as major smectite species. In practice, the clay content should be somewhat higher and one commonly considers 10–15% as a practical minimum since the smectite content of good bentonites like MX-80 is commonly not higher than about 70%. For practical reasons one can take the weight of the clay to include the hygroscopic water, which is about 10% of the clay mass if it is stored at a relative humidity of 40–60%.

5.2.2 Theoretical considerations

Importance of fines in the ballast

Starting from Darcy's basic flow equation one can express the unit flux q in terms of mass of water flowing perpendicularly through a given area of an isotropic porous medium, as a function of seven characteristic parameters /2/:

$$q = f(i, \gamma, \mu, D_x, S, \eta, n) \tag{5-1}$$

where

i = hydraulic gradient
γ = density of fluid
μ = viscosity of fluid
D_x = representative grain size
S = gradation factor expressing the shape of the grain distribution curve
η = grain shape factor
n = porosity

By means of dimensional analysis the following expression can be derived /2/:

$$q = i(\gamma / \mu)k_0 \tag{5-2}$$

and:

$$K = (\gamma / \mu)k_0 \tag{5-3}$$

where

K = experimentally determined hydraulic conductivity
k_0 = "specific permeability" of dimension (length)^2 describing the geometry and size of the void network

k_0 can be expressed as:

$$k_0 = \beta_\alpha \cdot D_a^2 \tag{5-4}$$

where

β_a = dimensionless factor describing the geometry (but not the size) of the void network
D_α^2 = measure of the cross-sectional area of the average pore channel

Figure 5-2 shows plottings of *log* k_0 and *log* K versus *log* D_5, which is the percentage of particles representing the 5th percentile of the grain size curve. The diagram shows that the plottings form bands for C_u=1–3 and C_u >3n (C_u=D_{60}/D_{10}), the first one representing relative uniform grain size and the other, flatter grain size curves in ordinary grain size diagrams (cf Part 1).

The diagram in Figure 5-2 shows that C_u is not a determinant of the hydraulic conductivity but that D_5 is a key parameter, implying that the few weight percent of the finest material most significantly affect the hydraulic conductivity. By choosing different values for α in D_a, the bands in the diagram will change their relative positions. However, various investigations show that one can take α=5 and that D_5 is the conductivity-controlling grain size independently of the size distribution of the rest of the mineral assemblage, provided that the gradation curve is not discontinuous /2/. Taking for instance D_5=0.1 mm, the average conductivity obtained by using the diagram is about E-4 m/s, while for D_5 ~ 0.3 mm it is E-3 m/s. Extrapolation suggests that the conductivity may be as low as 10^{-5} m/s for D_5 ~ 0.05 mm. The conductivity calculated by use of the diagram in Figure 5-2 fits fairly well with Swedish investigations /3/ and with the Finnish investigations of materials with different granulometry referred to in Figure 5-3.

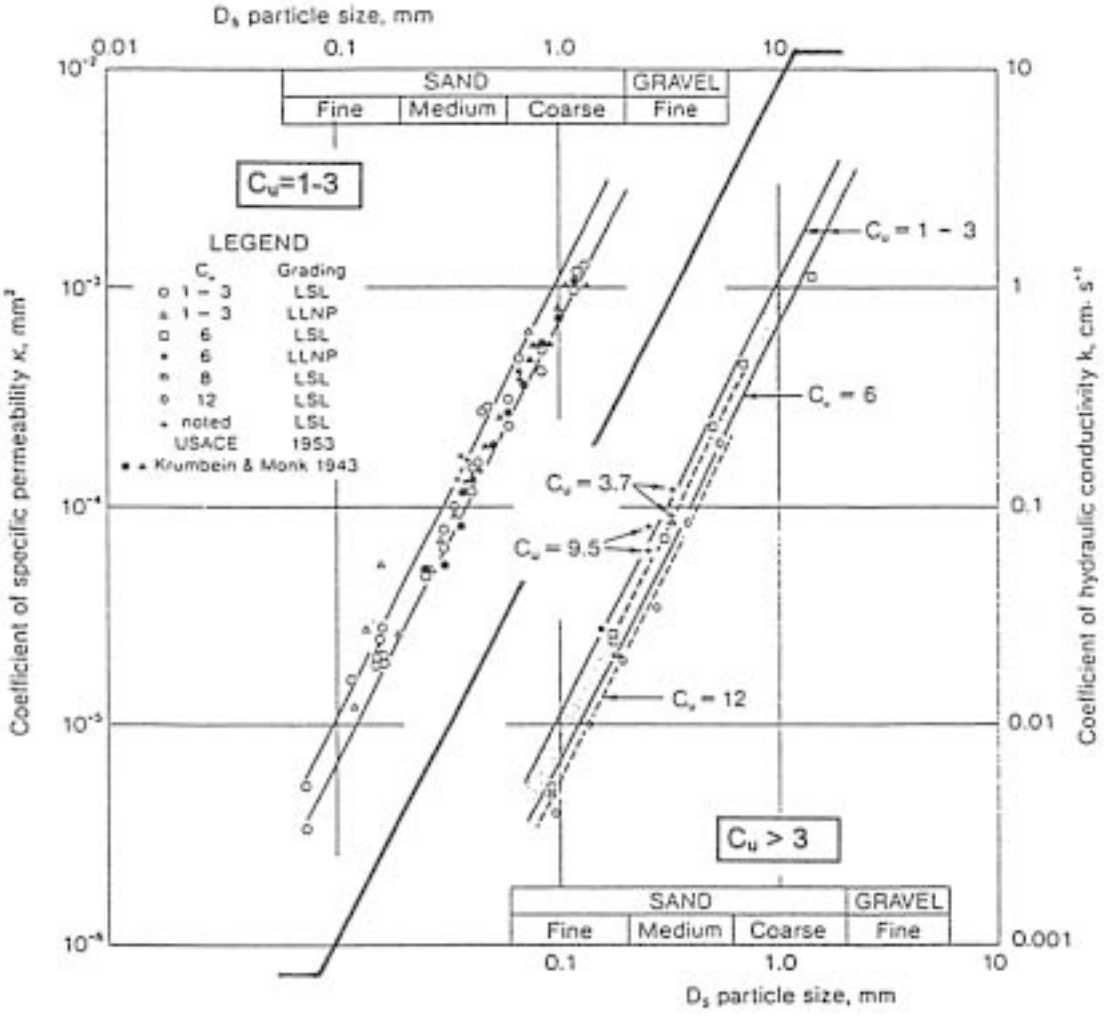

Figure 5-2. *Specific permeability in mm² versus D_5 grain size in mm /2/. The diagram is used in the following fashion: 1) Determine the gradation coefficient C_u. If C_u >3 use the right part of the diagram. 2) Determine D_5 by sieving. 3) Identify D_5 on the horizontal axis and find the corresponding hydraulic conductivity from the right, vertical axis. Example: C_u=12 and D_5=0.1 mm; K=0.006 cm/s=6 E-5 m/s.*

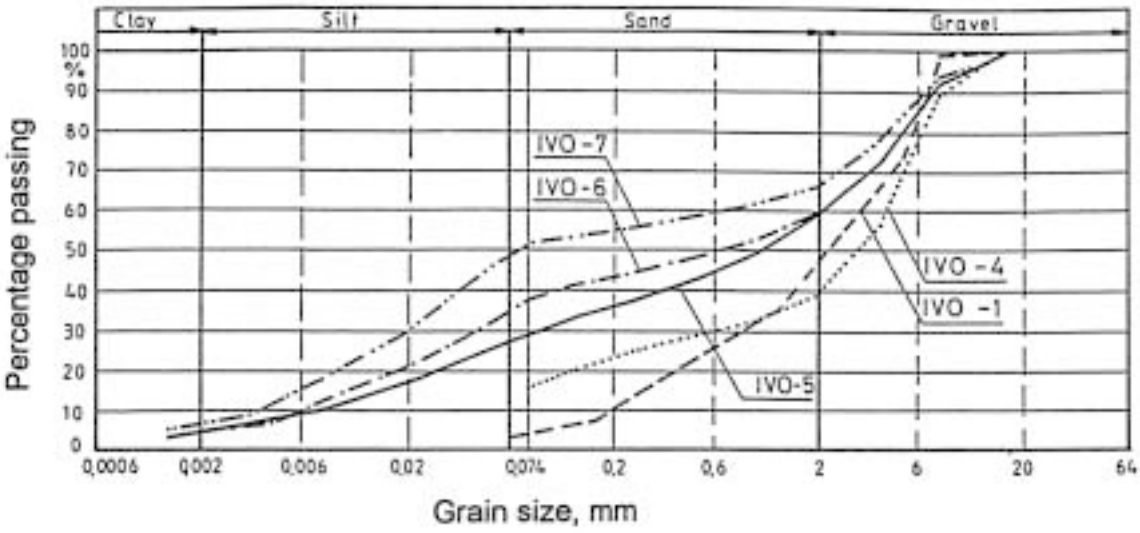

Figure 5-3. *Examples of granular composition of crushed and ground rock for possible use as ballast component in backfills. IVO-1 represents crushed rock with no admixture of ground rock /4/.*

From a theoretical point of view one realizes the significance of the fine material and the restrictions of flow imposed by it by applying Poiseuille's law (Equation 5-5). Hence, soils with very small particles also have small r-values, yielding low flow rates and fluxes:

$$v = \pi p \cdot r^4 / 8 l \eta \qquad (5\text{-}5)$$

where

v = flow rate
p = pressure
r = channel (void) diameter
l = channel length
η = viscosity of fluid

5.2.3 Ballast granulometry with clay added

Applying the principles outlined in the preceding section the granulometry of the ballast material may preferably be of the type IVO-5, IVO-6 or IVO-7 in Figure 5-3. They represent crushed rock with fines added to them and have turned out to have a relatively low hydraulic conductivity, i.e. E-7 m/s /4/. This serves to illustrate that conductivities of the order required for backfills in SKB repositories, i.e. about E-10 to E-11 m/s, can not be obtained without adding smectite clay to the ballast.

The importance of the tail of the distribution curve has been recognized in the composition of earth dam cores for many decades and it was also a major issue in the preparation of backfill of tunnels in the Stripa project /3/. The coarser fractions being rich in quartz were of glacial origin, while the "filler" consisted of crushed and finely ground feldspatic rock. Figure 5-4 shows the grain size distribution of the ballast, which is of Fuller-type with a tail that yields D_5=0.008 mm, and the composition after adding 10% and 20% MX-80 bentonite with the grain (granule) composition shown in Figure 5-5.

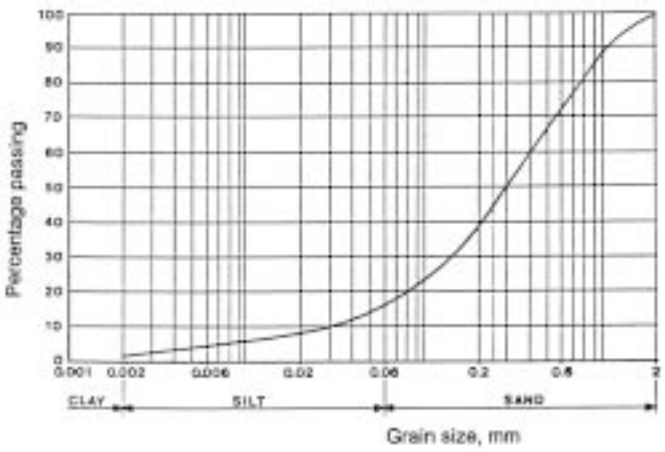

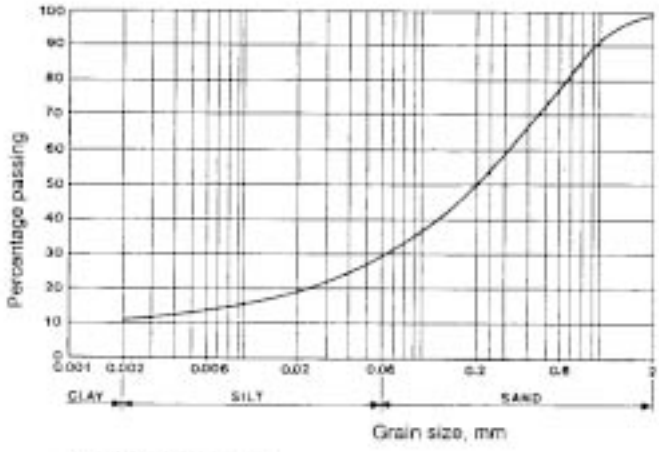

a) 10% bentonite mixture.

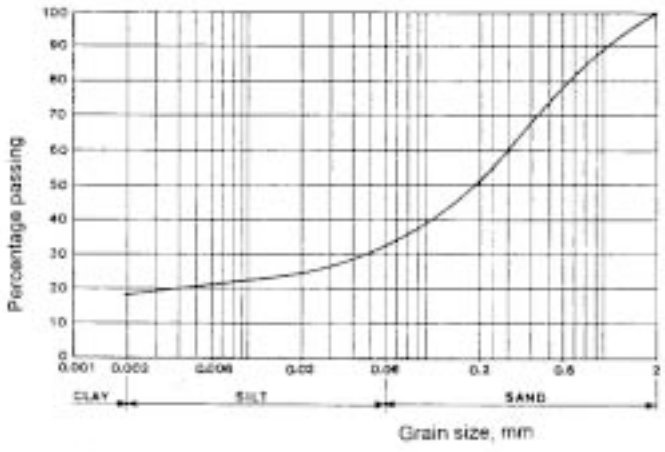

b) 20% bentonite mixture.

Figure 5-4. *Grain size distribution of the artificially composed ballast used for the Buffer Mass Test (BMT) experiment /3/. Upper: Ballast composed of glacial and crushed rock. Lower two figures show the granulometric composition after adding 10 and 20% MX-80 bentonite, respectively.*

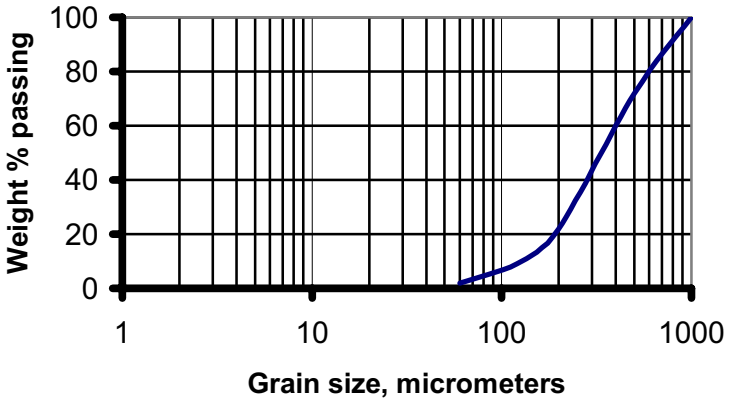

Figure 5-5. *Size distribution of MX-80 bentonite grains /5/.*

The BMT backfills represent the case of adding more than one fine-grained component to the ballast, i.e. finely ground rock and bentonite granules. The mixing sequence is important: the ballast is first prepared under dry conditions, i.e. the water content of the material must not exceed 1–2%, and the clay material then added in air-dry form (water content about 10%). If water is to be added it should be the last procedure (cf Chapter 10).

In general, the grain size characteristics of mixtures can be described in the way shown in Figure 5-6. Two- and three-modal distributions can easily be prepared but the time for preparation may be long for getting homogeneous distribution of the fines.

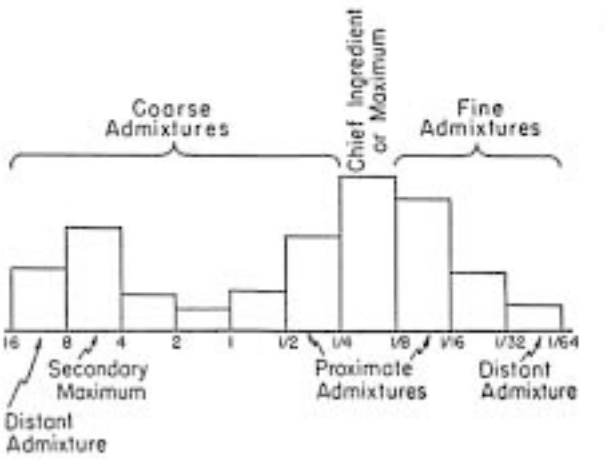

Figure 5-6. *Histogram specifying the grain size distribution of artificially composed soil /1/. The height of the columns represent the percentage of each class. The horizontal scale is in mm.*

5.2.4 Microstructural modelling

Numerical calculations

Attempts have been made to model the homogenization process of clay/ballast mixtures using a general material model /6/. The study, which was made in 2D and concerned mixtures with about 10% clay, was based on the assumption that the granules and ballast grains were rod-shaped and regularly arranged as shown in Figure 5-7. The ballast grains were assumed to have a diameter of 2.5 mm while the bentonite grains were taken to be 1 mm in diameter. The dry density of the granules was set at 1980 kg/m^3, while that of the ballast grains was taken to be 2650 kg/m^3. The dry density of the mixture was 1560 kg/m^3 (2000 kg/m^3 at saturation).

Figure 5-8 shows successive stages in the homogenization process, which ultimately yields a very significant variation in clay dry density, i.e. from 620 to 1450 kg/m^3 (1400 to 1930 kg/m^3 at saturation) /6/.

The study using the finite element method (FEM) indicates that the most narrow part of the voids between the ballast grains will not be filled by the clay phase. The resulting open space, which forms isolated ring-shaped zones around the contact points of adjacent ballast grains, has some effect on the overall hydraulic conductivity but the heterogeneity of the clay is even more important. Thus, the clay density will be low in the outer part of the expanded grains, which means that the net hydraulic conductivity will be high and the risk of piping and erosion of the softest parts considerable. Most important is that these softer parts will undergo coagulation and become very permeable if the groundwater is salt. This is concluded to be a major explanation of the discrepancy between the hydraulic conductivity data of backfills with coarse-grained clay components and of backfills with more fine-grained clay. The recommendation is therefore to use very fine-grained clay when the amount of clay added to the ballast is small.

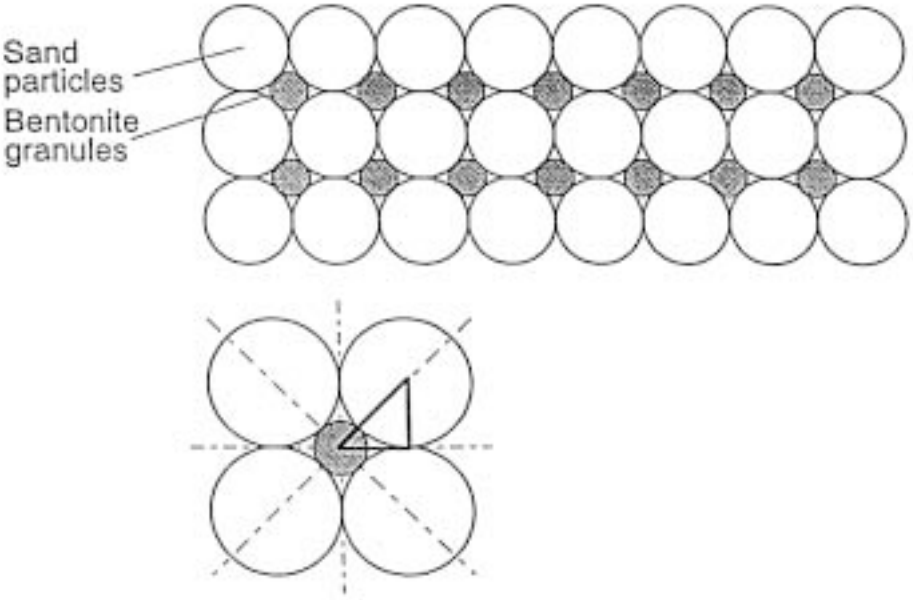

Figure 5-7. *Schematic picture of the initial microstructure of clay/sand mixtures /6/.*

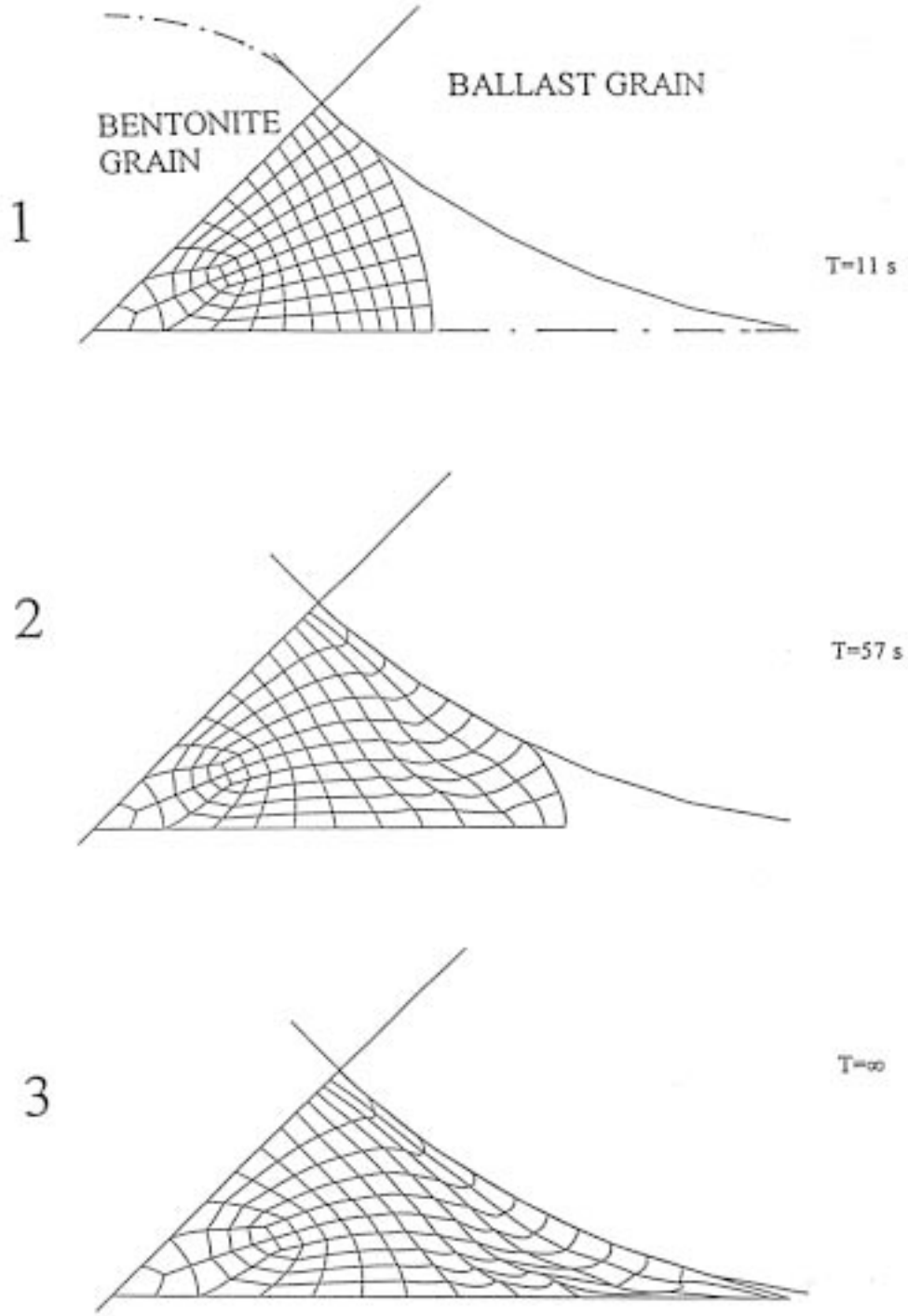

Figure 5-8. *Expansion of 0.5 mm bentonite grain with an initial dry density of 2290 kg/m³ in the voids. The outermost part of the gel in the final expansion stage has a dry density of 650 kg/m³ (ρ_{sat}=1420 kg/m³), while the densest left part has a dry density of about 1450 kg/m³ (ρ_{sat}=1930 kg/m³). Notice the quick expansion (T is time in seconds).*

Semi-empirical modelling

Using laboratory compaction data a relationship between the content and dry density of backfills with the BMT ballast and MX-80 clay (Figures 5-4 and 5-5) has been derived. It is shown in Figure 5-9 for backfill compacted to 100% Standard Proctor, which implies that the mixture can have a dry density as high as 2000 kg/m^3 for a bentonite content of less than about 20%.

Using fundamental soil physical relationships one can express the porosity n_s of the ballast as in Equation (5-6):

$$n_s = 1 - \rho_d/\rho_s(1-b) \qquad (5\text{-}6)$$

where

ρ_d = dry density of the mixture
ρ_s = density of the minerals
b = bentonite content (weight fraction)

A certain fraction of the ballast voids are filled with bentonite. If the density of the clay filling is ρ_{db} the degree of clay filling S_b will be as specified by Equation (5-7):

$$S_b = [\rho_s/\rho_{db}]/[(\rho_s/\rho_d)1/b - 1/b + 1)] \qquad (5\text{-}7)$$

Simplifying the issue by assuming uniform densities and equal compaction degrees of mixtures and clay fractions, as well as taking the maximum density at water saturation of the clay fraction to be 1600 kg/m^3, one can derive the relationships in Table 5-1 for different clay contents.

The density of the clay fraction determines the swelling pressure and good agreement between laboratory data and those predicted by use of the densities in the table is good. In practice, 100% Proctor density is difficult to obtain depending on the water content as discussed in Chapters 9 and 10.

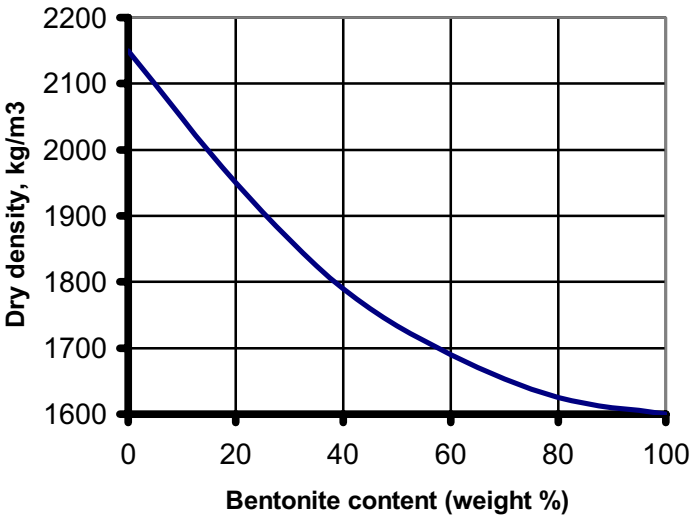

Figure 5-9. *Relationship between bentonite (MX-80) content and dry density of the mixture at 100% Proctor compaction. BMT ballast.*

Table 5-1. Semi-theoretical relationships between clay contents, compaction degrees and physical soil data.

Clay content, %	Degree of Proctor compaction, %	ρ_d, kg/m^3	ρ_{sat}, kg/m^3	S_b	n_s	ρ_b^*, kg/m^3
10	100	2050	2290	0.40	0.317	1600
10	87.5	1790	2130	0.32	0.403	1400
10	75	1540	1970	0.25	0.487	1200
20	100	1950	2230	0.57	0.42	1600
20	87.5	1710	2070	0.50	0.49	1400
20	75	1460	1920	0.43	0.57	1200
50	100	1750	2100	0.81	0.67	1600
50	87.5	1530	1960	0.76	0.72	1400
50	75	1310	1830	0.72	0.76	1200

* Density of clay content at complete water saturation.

Table 5-2. Hydraulic conductivity (K) and swelling pressure (p_s) of backfill mixtures of MX-80 clay and ballast material of BMT type /5, 7/. The highest conductivity and lowest swelling pressure refer to tests with salt water.

Clay content, weight percent	Density at water saturation kg/m^3	K, m/s	p_s, kPa
10	2100	E-8 to E-7	20 to 100
30	2100	E-10 to E-9	200 to 500
50	2100	E-12 to E-10	1000 to 2000

One would expect from the data in Table 5-1 that the hydraulic conductivity should be low and the swelling pressure high for effectively compacted mixtures and typical laboratory data confirm that this is the case for higher clay contents than 10% as shown in Table 5-2. Clay densities on the order of magnitude indicated in the table mean that such backfill mixtures are very sensitive to salt water. This is indicated by the range in data.

5.2.5 Special effects of crushed rock ballast

Microstructural investigations of bentonite/ballast mixtures resembling those intended for backfilling of repository tunnels, drifts and shafts have been performed for testing the various numerical and analytical models. These studies were made by saturating the mixtures with acrylate impregnation fluid, which is absorbed by dry clay like water, and preparing thin sections (10–30 μm) for light microscopy after polymerization. The density corresponded to about 2000 kg/m^3 in fluid-saturated state. The study demonstrated the validity of the modelling approach that rounded ballast grains of glacial origin as well as jagged grains of crushed TBM muck are homogeneously embedded in clay matrix for clay contents exceeding 10%. However, it was also found that crushed rock grains, which are rich in mechanically induced fissures, are coated with strongly attached fine-grained debris. These very small fragments of rock-forming minerals partly prevent the clay from adhering to the grains and can be assumed to provide flow paths in the backfill (Figure 5-10). The sealing potential of backfills with low clay contents and crushed rock as ballast is believed to be lower than mixtures made by use of glacial ballast.

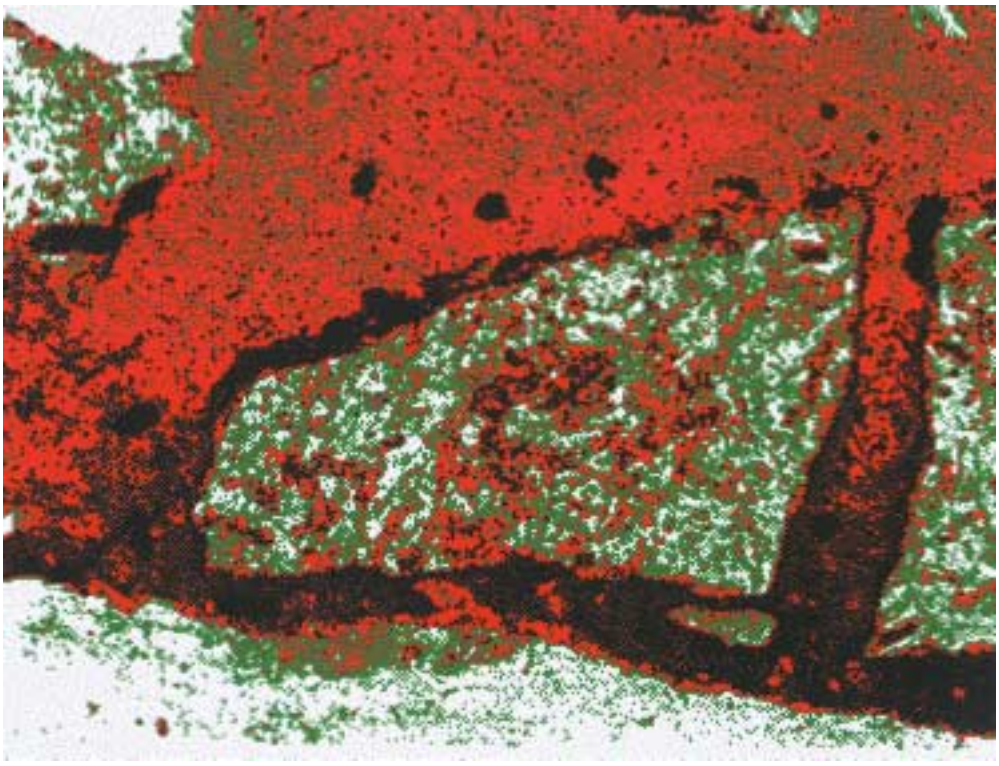

Figure 5-10. *Micrograph of thin section of acrylate-embedded mixture of 10% MX-80 bentonite and 90% crushed TBM muck. The micrograph, in which one identifies ballast grains that appear white/green, has been converted into to digital, colored form for making variations in clay density obvious. Red: medium-dense clay. Green: soft clay. Black: dense debris grain coatings. Magnification 100 x.*

5.3 Natural smectitic clays

5.3.1 General

It is evident that natural smectitic clays can be considered as backfill material candidates provided that the quality in terms of smectite content and cost for preparation, which includes drying, grinding and possibly wetting, are acceptable. A necessary criterion is that sufficiently large amounts of suitable material are available for getting access over long period of time to the same material for backfilling of the large space represented by underground repositories.

The survey of soil material resources given in Chapter 3 shows that smectitic soil in Sweden is believed to be present in sufficiently large quantities for Swedish purposes and similar conditions prevail in many other countries. The problem is that exploitation for large-scale testing in underground laboratories is expensive and requires establishment or use of mineral processing plants.

The same basic laws respecting hydraulic conductivity, swelling pressure, and compressibility apply to natural and artificially prepared backfill soils but there is a major difference in performance because all processed grains of the natural clay contain some smectite, while the ballast grains of artificially prepared mixtures do not. This difference is of course increasingly obvious when the smectite content rises.

5.3.2 Example of potentially useful natural clays – the German Friedland Ton

Occurrence

A very homogeneous clay body of Tertiary age with a volume of at least 200 milllion cubic meters, is located in the Friedland area close to Neubrandenburg in north-eastern Germany and it has been exploited for ceramic industries and for isolation of waste piles for a very long time. The clay contains at least 50% expandable minerals (montmorillonite in Na-form and mixed-layer mica/montmorillonite), and accessory minerals with very little sulphur and potassium contents. It is exploited by the company DURTEC, Neubrandenburg, Germany.

Different grain (granule) size distributions can be obtained by using different grinding equipments and the product can be wetted to an optimum water content with respect to the compactability. Comprehensive field tests by SKB in the underground laboratory at Äspö have shown that the size distribution in Table 5-3 is suitable for minimizing dusting. Compaction of this clay with special respect to achievable density in field experiments is discussed in Chapter 10. The content of clay-sized particles as determined by disintegration is on the order of 90% by weight.

Compactability

Compaction using modified Proctor technique with a 10 cm diameter tube and applying material in four layers, gave a density including the water content of 2120 kg/m^3, corresponding to a dry density of 1853 kg/m^3 and a density at saturation of about 2170 kg/m^3. The expected net dry density at field compaction is about 1600 kg/m^3, yielding a final density at saturation of about 2000 kg/m^3.

Physical properties compared to mixed ballasts

As demonstrated in the preceding text on mixed ballasts the clay component has a low density even at very effective compaction and this makes it sensitive to high electrolyte contents in the porewater; the hydraulic conductivity is high and the swelling pressure low (cf Table 5-2). Natural clay with a high content of clay-sized particles, like the Friedland Ton, is significantly less sensitive since all the grains contain about 50% of smectite, meaning that the smectite phase has about the same density as the clay in bulk. For a density of 2000 kg/m^3 the hydraulic conductivity is about 4E-12 m/s using low-electrolyte water and 7E-11 m/s at percolation with 10% $CaCl_2$ solution. The swelling pressure is 650 kPa for the salt solution and 850 kPa for distilled water. These values indicate that backfills of Friedland Ton type are much tighter than mixed backfills with the same density (cf Tables 5-2 and 5-3).

The obvious difference in tightness between the two backfill types is explained by the much more homogeneous microstructural constitution of the Friedland Ton as illustrated by Figure 5-11. It shows a transmission electron micrograph that represents a practically two-dimensional section through a sample with a density of 2000 kg/m^3 in fluid-saturated state, i.e. the same as the mixed clay in Figure 5-10. The micrograph of the Friedland Ton has a magnification that is 25 times higher than that of the mixed clay and hence demonstrates the better fineness and homogeneity on the microstructural scale.

Table 5-3. Grain (granule) size distribution of natural dried, ground and slightly moistened (14% water content) natural clay (Friedland Ton).

Size intervals, mm	Content in weight percent
2–8	25
1–2	25
0.1–1	30
<0.1	20

Table 5-4. Hydraulic conductivity and swelling pressure of Friedland Ton /5/.

Density at water saturation, kg/m^3	Hydraulic conductivity, m/s	Swelling pressure, kPa	Water for saturation
1800	5E-11	150	Distilled water
2000	4E-12	850	Distilled water
1800	E-10	150	3.5% $CaCl_2$
2000	2E-11	1000	3.5% $CaCl_2$

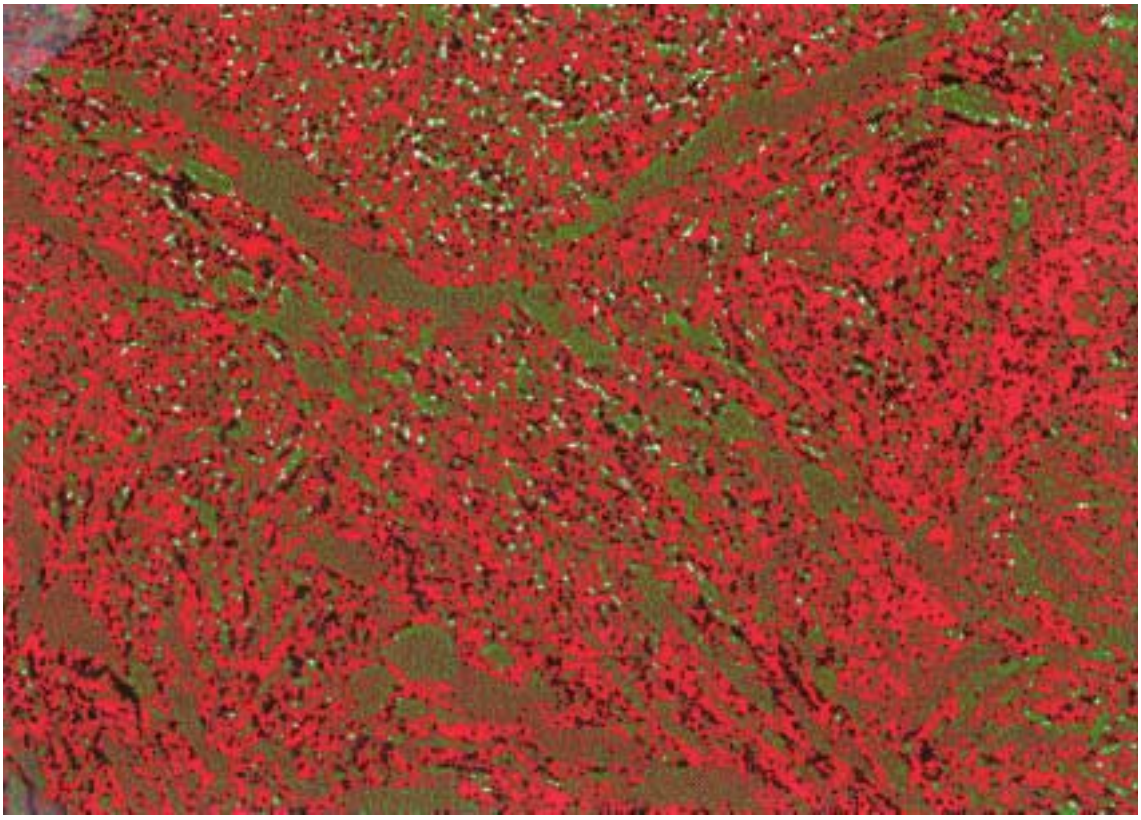

Figure 5-11. *Micrograph of thin section of acrylate-embedded Friedland Ton /5/. The micrograph has been converted into to digital, colored form for showing variations in clay density, which are small. Red: medium-dense smectitic clay. Green: smectite. Black: dense non-clay minerals. Magnification 2500 x.*

5.4 References

/1/ **Pettijohn F J, 1949.** Sedimentary Rocks. Harper's Geoscience Series, New York.

/2/ **Kenney T C, Lau D & Ofoegbu G I, 1984.** Permeability of compacted granular materials. Canadian Geotechnical Journal, No 4, Vol 21, 1984 (pp 726–729).

/3/ **Pusch R, Börgesson L, Nilsson J, 1982**. Buffer Mass Test – Buffer materials. Stripa Project Technical Report 82-06. Svensk Kärnbränslehantering AB.

/4/ **Holopainen P, Pirhonen V & Snellman M, 1984**. Crushed aggregate-bentonite mixtures as backfill material for the Finnish repositories low- and intermediate-level radioactive wastes. Nuclear Waste Commission of Finnish Power Companies, YJT-84-07.

/5/ **Pusch R, 1998.** Backfilling with mixtures of bentonite/ballast materials or natural smectitic clay? SKB TR-98-16. Svensk Kärnbränslehantering AB.

/6/ **Börgesson L, 1993**. Swelling and homogenisation of bentonite granules i buffer and backfill. SKB AR 95-22. Svensk Kärnbränslehantering AB.

/7/ **Pusch R, 1994.** Waste Disposal in Rock, Developments in Geotechnical Engineering, 75. Elsevier Publ. Co. ISBN:0-444-89449-7.

6 Chemical properties

This chapter deals with the chemical composition and properties of smectitic clays and ballast materials. It is a very comprehensive issue and the text is confined to give only major data on the chemical composition of clays considered or tested by SKB for reference purposes and for providing a basis for estimating the chemical stability and chemically affected physical performance of smectitic clays.

6.1 Buffer materials, raw and refined

6.1.1 General

This chapter gives examples of the chemical composition of raw materials for preparation of smectite-rich buffers and backfills and hence serves as reference in characterizing clays that are considered as engineered barriers. Porewater chemistry is treated briefly for giving a basis for explaining chemical processes that have an impact on the physical properties of buffers and backfills.

6.1.2 Chemical composition of smectitic clays

The chemical constitution of Wyoming-type montmorillonites from various parts of the world is exemplified in Table 6-1, which also gives the layer charge and the water contained in the interlamellar space after drying at 105°C following the ordinary geotechnical procedure. The data show a surprisingly small variation in chemical composition of these bentonites, which have very similar physical properties. The clays listed in Table 6-2 have been investigated in the current SKB research work with respect to their physical properties (cf Chapter 7).

The clays typically have a high aluminum content and a layer charge of 0.30 to 0.35. The aluminum content in octahedral positions is approximately the same for all the clays, and this is also the case for the tetrahedral positions except for one of the clays from Argenitina. The silica content in tetrahedral positions is high for all the clays, which hence represent rather pure montmorillonites. The iron content is low for the Japanese montmorillonite from the Hojun mine while it is appreciable for three of the clays from Argentina. The iron content may cause cementation effects under hydrothermal conditions, the risk being lowest for montmorillonites from Crook County and Hojun mine.

For NMR investigations a very low iron content is required and this is best fulfilled by the Japanese montmorillonite from the Hojun mine. Certain Texan montmorillonites have also been reported to be useful for such investigations.

Table 6-1. Composition of commercial montmorillonites of Wyoming type expressed as weight percentages of oxides [1].

1. Hojun Mine, Gumma, Japan
2. Tala, Heras, Mendoza, Argentina
3. Crook County, Wyo., USA
4. Rokkaku, Yamagata, Japan
5. Amory, Miss., USA
6. Santa Elena, Potrerillos, Mendoza, Argentina
7. San Gabriel, Potrerillos, Mendoza, Argentina
8. Emilia Calingasta, San Juan, Argentina
9. Sin Procedencia, Argentina

Oxide	Wyoming-type 1	2	3	4	5	6	7	8	9
SiO_2	64.80	62.00	62.30	62.70	59.73	60.22	60.76	59.91	58.67
Al_2O_2	24.54	23.42	23.50	22.20	24.30	23.67	23.08	21.97	27.34
TiO_2	–	–	–	–		0.34	0.38	0.33	–
Fe_2O_3	1.27	3.74	3.35	4.62	5.54	6.28	6.10	6.72	3.64
FeO	0.56	0.32	0.37	0.48	0.37	–	–	–	0.38
MgO	1.60	0.93	1.95	2.00	2.10	1.46	1.44	2.15	2.00
CaO	0.00	0.68	0.31	0.58	0.00	0.13	0.17	0.34	0.00
Na_2O	0.40	0.72	0.40	0.01	0.80	0.09	0.13	0.09	0.62
K_2O	0.60	2.63	0.03	0.12	0.22	0.19	0.21	0.11	0.18
H_2O^+	6.71	5.21	6.45	7.06	6.59	6.86	6.07	6.66	7.04
Total[1)]	100.48	99.65	98.66	99.77	99.65	99.24	98.34	98.28	99.87
H_2O^-	6.22	6.44	7.81	7.13	13.70	6.81	7.65	8.81	10.88
Al Tetrahedr.	0.04	0.08	0.10	0.08	0.24	0.20	0.16	0.17	0.34
Al Octahedr.	1.72	1.66	1.64	1.55	1.56	1.56	1.56	1.48	1.67
Si Tet.	3.96	3.92	3.90	3.92	3.76	3.80	3.84	3.83	3.66
Layer charge per formula unit	0.34	0.34	0.31	0.33	0.34	0.34	0.30	0.35	0.34

[1)] The deviation from 100% is caused by inevitable errors in the chemical analyses.

Table 6-2. Typical composition of buffer materials tested in the current research work for SKB. Weight percentages of oxides.

Clay	Smectite type	Elements								
		SiO_2	Al_2O_3	Fe_2O_3	MgO	CaO	K_2O	Na_2O	S*	LOI**
MX-80 bulk (US)	Na montm.	63.8	19.8	5.0	3.2	3.1	1.0	2.8	0.12	7.2
MX-80 clay fract.	Na montm.	63.7	21.6	4.6	3.8	1.8	0.6	1.9	–	8.3
Tixoton bulk (Germany)	Na montm.***	54.7	18.2	5.9	3.7	4.4	0.5	3.4	–	8.4
IBECO**** bulk (Germany)	Ca montm.	67.5	19.6	5.0	3.2	2.6	1.0	0.9	0.06	8.0
IBECO clay fract	Ca montm.	67.2	20.4	4.7	3.4	2.3	0.9	0.5	–	8.9
Los Trancos, bulk (Spain)	Beidellite	62.7	24.6	3.3	4.8	1.6	0.3	1.2	–	9.9
Los Trancos, clay fraction	Beidellite	63.7	24.7	2.9	5.4	1.4	0.1	0.8	–	11.2
Cerro del Aguila, bulk (Spain)	Saponite	61.6	9.8	3.0	20.0	1.1	2.0	0.9	–	8.5
Cerro del Aguila, clay fraction	Saponite	60.3	9.0	3.4	24.0	1.0	1.4	0.3	–	10.3
RMN) (Czech Rep.	Montm. Nontron.	53.7	19.5	13.9	2.8	3.4	1.2	0.9	–	–
Kunigel bulk (Japan)	Na montm.	73.8	14.4	2.4	2.1	2.4	0.4	2.8	–	4.7
Kunigel, clay frac.	Na montm.	67.6	21.2	3.0	3.0	0.8	0.2	2.9	–	7
Friedland bulk (Germany)	Mixed-lay montm/mica	57.2	18.0	5.5	2.0	–	3.1	0.9	0.3	7

* S in sulphides, total S is about 0.25.

** Ignition loss of clay predried at 105°C.

*** Converted to Na form by soda treatment.

****Now IKO-Minerals GmbH.

6.1.3 Accessory minerals

Natural smectite clays of sedimentary origin, like most true bentonites, contain various other minerals which were deposited together with the smectite minerals or with minerals that were later converted to smectite. Usually, quartz, feldspars, micas, chlorite, sulphides, sulphates, oxides and carbonates are therefore present in various amounts.

The content of organic material and amorphous inorganic material may be considerable. The amorphous material consists of SiO_2 and Al- and Fe-hydroxides and amounts to a few percent, while the organic content is commonly 0.2–0.7%. All the non-smectite constituents do not contribute to the sealing power of the clay. Some of them, primarily the feldspars and micas, do also further reduce this power by giving off potassium that is consumed in the conversion of smectite to illite, and by producing cementing agents as will be discussed in a later section. Table 6-3 illustrates the mineral composition of a number of bentonites that have been investigated in the current SKB research work with respect to their physical properties.

Quartz has been suggested as a suitable component of smectite buffers since it significantly increases the thermal conductivity. However, at pH>8, which may well be reached in mixtures of Na bentonite and quartz, the solubility of silica increases significantly (i.e. from 3 mMoles per liter to more than 6 mMoles per liter), and silica released from the buffer close to a hot canister will migrate towards the cold rock where it precipitates and causes cementation.

Table 6-4 gives examples of the mineral composition of a number of commercially available clays with different smectite contents. They have been investigated with respect to their performance (cf Chapter 7).

Table 6-3. Examples of the mineral composition of smectite-rich clays in weight percent (based on /1/).

Mineral	Hojun Japan	Chish. Miss. USA	Amory Miss. USA	Upton Wyo. USA	Belle F. S. Dak. USA	Clay sp. Wyo. USA	South-European (IBECO) Germany	Central European (RMN) Czech Rep.
Montmorillonite	83.9	97.3	89.3	79.5	91.9	87.7	88	90
Quartz	14.9	2.3	5.9	16.3	4.0	10.0	2	2
Muscovite	–	–	0.1	0.1	0.1	–	–	–
Chlorite	–	–	–	0.1	–	–	–	
Feldspars	–	–	4.7	2.3	4.0	2.3	2	<1
Mixed-layers	–	–	–	–	–	–	–	–
Others	1.0	0.3	–	1.8	–	0.3	8	7
Total	99.8	99.9	100.0	100.1	100.0	100.0	100	99.5
Trace minerals	Bio, Lim	Bio	Bio, Lim, org.	Bio, Lim, org.	Bio, Lim	Bio	Bio	Mica
Mafic minerals	Tu, Zi	Ru, Zi, Tu	Zi, Tu	Tu	Tu, Ru	Zi	Ru, Zi	–

Bio=Biotite, Lim=Limonite, org.=organics, Tu=Turmaline, Zi=Zirkon, Ru=Rutile

Table 6-4. Examples of the content of inorganic constituents of smectitic buffer materials tested by SKB.

Clay	Smectite	Quartz	Feldspar	Mica	Carbonates	Pyrite	Others
MX-80 (Amer. Coll.) (Suedchemie)	75	***	**	*	*	(*)	*
Tixoton Na bentonite	90	*	*	–	**	*	–
Moosburg Ca bentonite (Suedchemie)	65	**	**	***	**	–	**
Na bentonite (IBECO)	70	**	**	*	*	*	–
Ca bentonite (IBECO)	80	**	**	*	*	*	–
RMN (Obrnice)	90	*	*	*	**	–	–
Saponite (Greek expl.)	70	**	**	**	–	–	–
Beidellite (Span. expl.)	35	**	*	*	–	–	–
Kunigel (Kunimine)	50	***	*	–	*	*	–
Friedland (Frieton)	45[1)]	***	**	**	*	*	–

*** Abundant (>10%)

** Moderately abundant (3–10%)

* Traces (<3%)

[1)] Montmorillonite/mixed layer

6.1.4 Adsorbed cations

The type of adsorbed cations of smectite determines the degree of hydration and the rheological properties. Maximum expandability is obtained for Li and Na as adsorbed cations, while it is at minimum for Ca and polyvalent cations. Buffer clay for use in repositories is therefore suitably smectite clay of natural Na type or Ca smectite treated with Na carbonate on an industrial scale for bringing it to Na form. The cations in natural smectite clays can be exchanged and reflect the conditions under which they were formed and the changes that they have undergone.

Table 6-5 gives typical examples of the dominant adsorbed cations and of the cation exchange capacity of a number of bentonites /1/. The table shows that Wyoming bentonite may have a significant fraction of the exchange sites occupied by magnesium and calcium although sodium dominates.

Table 6-5. Adsorbed cations and cation exchange capacity in meq/100g of natural bentonites (based on /1/).

Material	Na^+	Ca^{2+}	K^+	Mg^{2+}	Fe	Al^{3+}	CEC meq/100 g
Bel Fourche	18.99	36.96	4.92	20.70	0.38	traces	81.97
Wyoming (blue)*	41.64	29.94	8.09	30.00	0.29	traces	109.67
Wyoming (yellow)*	32.71	22.30	8.65	24.54	0.21	traces	88.20
Greek (Milos)	–	52.05	3.90	27.47	–	–	81.35
German (Erbslöh)	–	105.76	3.55	66.41	–	–	71.07
Hungarian bentonite	–	37.15	4.50	7.88	–	–	34.46
Friedland	11.0	4.0	34.0	2.0	0.5	–	40.0
Czech bentonite (RMN)	–	46.45	11.53	47.26	0.21	–	62.34

* MX-80 type

6.1.5 Phosphorous and nitrogen

Phosphorous and nitrogen are nutrients to bacteria, which can form organic colloids with a possible ability to transport radionuclides, and can therefore be of importance. Colorimetric determination has shown that Wyoming bentonite contains about 100 ppm phosphorous and 200 ppm nitrogen /1/. Commercial bentonites stockpiled for drying on the ground surface may be contaminated by various sources, like cow feces.

6.1.6 Sulphur

Sulphur-bearing minerals are nearly always present in bentonites mostly in the form of sulphides, primarily FeS_2. Table 6-6 shows the content of S (total) and of sulphides in a number of bentonites. Heating to 425°C of air-dry material for 15 h significantly reduces the sulphide content /1/.

6.1.7 Organic content

Like phosphorous and nitrogen the organic content of buffers may serve as nutrient to bacteria and produce organic colloids. For common commercial bentonites it has been determined using a number of techniques and it has been concluded that the CO_2-gas method recommended in Part 1 yields results that are similar to those of more sophisticated techniques like IR and spectrophotometric analyses. For MX-80 it has been found that the organic content of untreated material ranges between 475 and 750 ppm while heating to 425°C for 15 h reduces it to 150–250 ppm /1/. Analyses of organic substance extracted from MX-80 have shown that some form of kerogene dominates but that fulvic and humic acids are also present /1/. This distinction may have an impact on potential bacterial activity.

6.1.8 High-quality smectite clays

Certain smectite clays have been used and proposed for special applications in repositories as for grouting and pelletization.

For effective penetration of smectite grouts /2/ the particle size should be less than 1 μm, which requires that the diameter of coherent smectite aggregates and accessory minerals is less than this measure. This can be achieved by grinding bentonite like MX-80.

Pellets in the form of highly compacted pills with a size of 5–20 mm have been proposed and used for filling of the space between large compacted blocks and the rock in deposition holes and tunnels /3/. In order to make effective use of the pellet filling the ben-

Table 6-6. Total sulphur content and content of sulphide in some commercial bentonites (based on /1/).

Material	Total S, ppm	Sulphide (untreated mtrl), ppm	Heated mtrl, ppm
MX-80 (Bel Fourche)	2700–3200	1000	150
Wyoming (Sheppard)	300–1700	700	0
Erbslöh (Na-treated	80–130	–	–
Friedland	650	10000	–
Milos (Ca-form)	5600–6600*	–	–

* Lower sulphur content can be found.

tonite should be particularly smectite-rich, either by selecting such brands, like American Colloid's SWY-1, or by refining MX-80 through centrifugation. The pellets need to be prepared by tablet machines with high pressures.

6.1.9 Porewater chemistry of smectitic clays

Experimental

The chemical composition of the porewater in smectite-rich buffer clay is determined by the interaction of groundwater in the host rock and the minerals. Ion exchange processes play a major role and also dissolution of accessory minerals like carbonates, particularly calcite, and sulphur-bearing minerals. A typical reaction is when Na montmorillonite is dispersed in distilled water; Na is given off to the porewater and protons replacing them in the exchange positions, which raises pH of the porewater to as much as 10 and makes Eh drop (Figure 6-1). If the clay is dispersed in Na-rich water Na is absorbed and protons released, which means that pH of the porewater drops to values that can be as low as 3. Dispersion in water rich in Ca and Mg causes absorption of these cations and release of initially absorbed Na. pH will thereby also be changed.

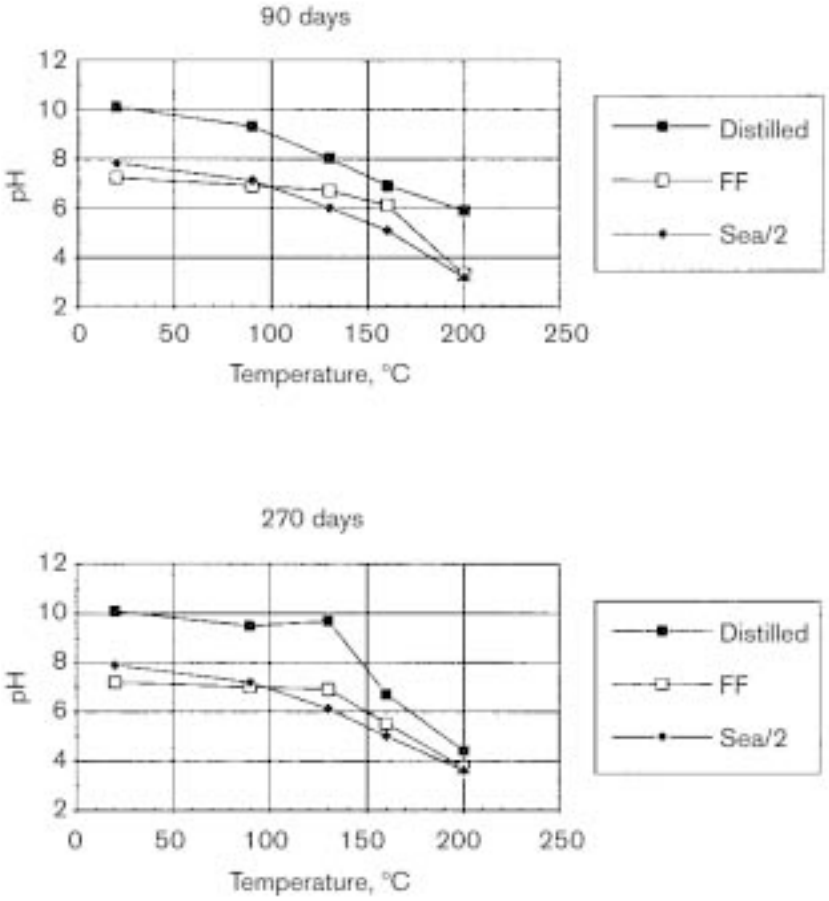

Figure 6-1. *Change in pH in hydrothermal testing of MX-80. The clay was confined in teflon-coated cells that were placed in larger vessels with initially distilled water, Ca-rich strongly brackish water (FF), and artificial seawater with 50% of the TDS in ocean water. The difference between the tests using different waters dropped with temperature and time /4/.*

Porewater analysis

Determination of the porewater composition through chemical analysis is not a straightforward matter since the ions are not uniformly distributed in the clay-water mass (Figure 6-2). Thus, the interlamellar porewater, which is free from anions, can not be distinguished from the free porewater and any chemical analysis only gives the average composition. Expulsion of porewater under successively increased pressure shows a change in composition since low pressures expel water contained in large voids while high pressures cause water from small voids and from the interlamellar space to be released.

Experiments with expulsion of porewater has given data that were successfully compared with predictions using the code HYDRAQL/CE /5/. The tests were made so that the clay samples were kept in a teflon cell connected to a vessel with initially pure water through a filter. Ions from the porewater of the initially fluid-saturated clay diffused into the "external water" where the electrolyte content increased on expense of that of the porewater. Figure 6-3 shows the change in total dissolved salt (TDS) content as a function of the successively increased density of the clay from which porewater was expelled. One observes that the TDS increased with increasing density of the clay both for the porewater and for the "external water". It was concluded that the water chemistry was largely determined by the dissolution of accessory minerals like calcite.

Such experiments have also been made for investigating the electrolyte composition of the porewater of MX-80. Figure 6-4 shows the strong dissolution and diffusion of silica from the clay to the surrounding "external water" when the temperature is raised, while Figure 6-5 shows that aluminum tends to stay in the clay where it forms various hydrated complexes /4/.

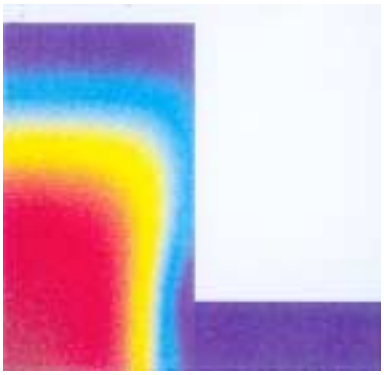

Figure 6-2. *Relative monovalent anion concentration (%) in a REV for equilibrating 0.1 M monovalent electrolyte in MX-80 clay with the density 2130 kg/m^3. The picture shows that anions (red and yellow) are confined in the center of the wide part of the widest channels (50 μm) and that cations (blue) are close to the mineral surfaces and in the channels /5/.*

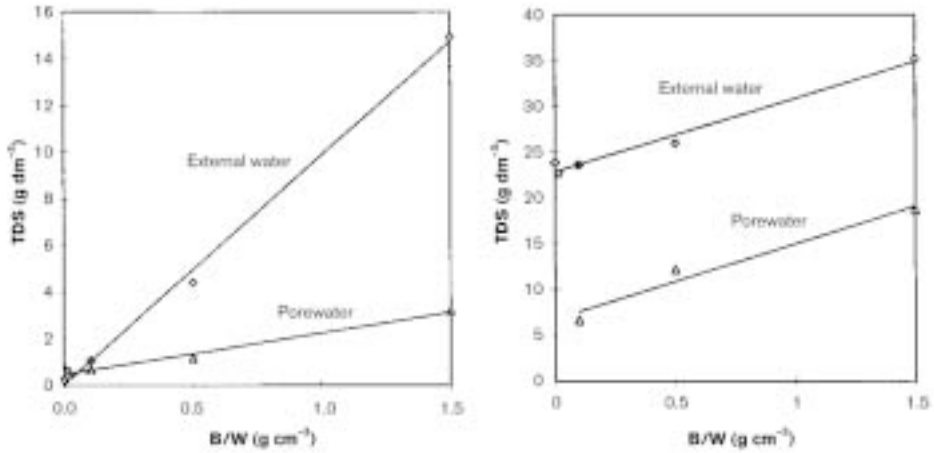

Figure 6-3. *TDS in porewater for different densities. The initial clay density and corresponding bentonite/water contents are given in the legend /5/. B/W is the inverse of the water content and represents the ratio of mass of solids to that of water water (i.e. B/W=1 means w=100%, B/W=1.5 means w=0.67, which corresponds to a density of kg/m³ at fluid saturation). Left: MX-80 clay saturated with distilled water. Right: MX-80 clay saturated with ocean-type water.*

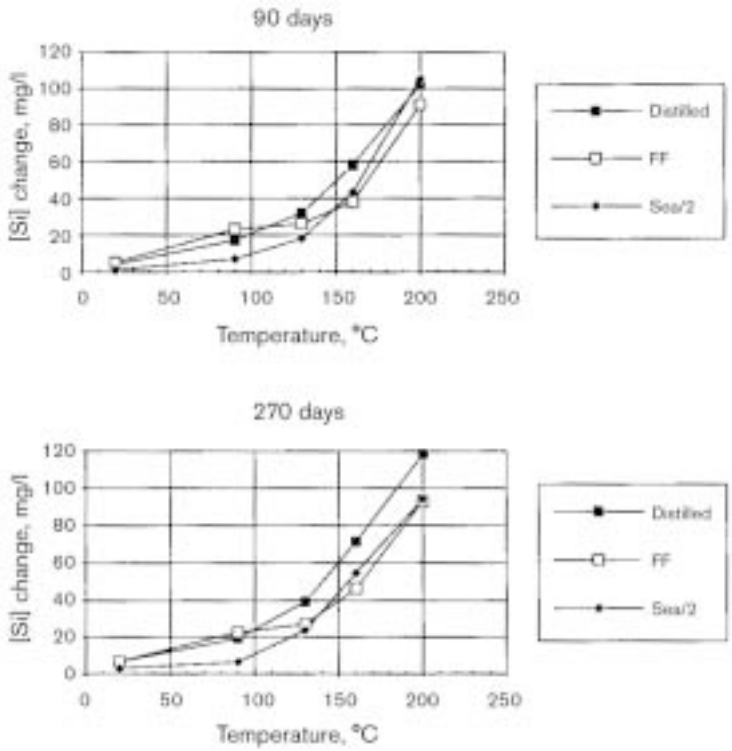

Figure 6-4. *Change in Si concentration at hydrothermal testing of MX-80. The clay was confined in teflon-coated cells that were placed in larger vessels with initially distilled water, Ca-rich strongly brackish water (FF), and artificial seawater with 50% of the TDS in ocean water. The porewater and surrounding "external water" became saturated with Si well below 100°C. The difference between the tests with different waters was small /4/.*

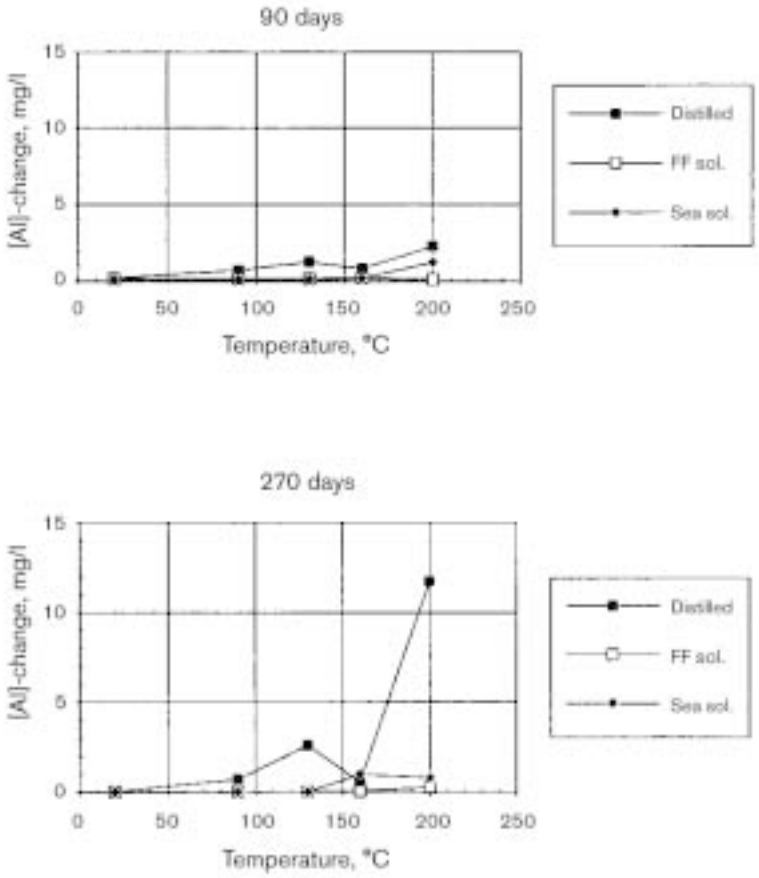

Figure 6-5. *Change in Al concentration at hydrothermal testing of MX-80 cf Figure 6-1. The concentration of Al was very low except for the 200°C test with distilled water when the clay underwent significant dissolution /4/.*

Theoretical – role of calcite

Dissolution/precipitation is dealt with in Part 3 of this Handbook. However, some basic concepts that have to do with the performance of the very important clay component calcite will be mentioned here.

Calcite has a significant impact on the porewater chemistry, particularly on pH.
In principle, one can write the reaction of Na smectite and calcite ($CaCO_3$) as /6/:

$$2NaX + CaCO_3 + H^+ \rightarrow CaX_2 + 2Na^+ + HCO_3^- \qquad (6\text{-}1)$$

where X represents the smectite phase.

Theoretical – redox reactions

Redox reactions can be explained by dissolution of pyrite (FeS_2), yielding magnetite (Fe_3O_4) and sulphate ions [$(SO_4)^{2-}$]. Under oxidizing conditions pyrite can react with hematite (Fe_2O_3) which also produces [$(SO_4)^{2-}$] ions /6/.

6.1.10 Crystal constitution of smectitic clays

Identification and characterization of buffer clays for general purposes and quality designation is made by use of the various methods described in Part 1 of this Handbook. The chemical and mineralogical compositions of which Tables 6-1 to 6-5 give examples are determined by chemical analysis and so is the ion exchange capacities. XRD analysis with and without glycol treatment gives characteristic fingerprints of smectites as illustrated by the spectra in Figure 6-6 and 6-7, which can be used as references in characterization of such clays. The methodology is described in Part 1.

For the examination the MX-80 material was suspended and disaggregated in 0.01 N NH_4OH-solution overnight by overhead rotation and the 2 µm fraction of the clay separated by sedimentation. This sub-fraction was dropped on a Si-holder to orient the clay particles. Spectra were taken after air drying and ethylene glycol saturation, respectively. The corresponding diagrams of the material containing the coarser fractions, mostly silt, shows several other peaks representing quartz, feldspars, calcite and other minerals. The spectrum in Figure 6-6 shows the following:

- The investigated MX-80 clay is composed of ~70% smectite with minor amounts of mixed-layer illite/smectite.
- Ethylene-glycol saturation shows the characteristic swelling of montmorillonite: The distance between the positions of the (002)- and (003)-interference is typical.
- This MX-80 clay contains also a minor amount of illite/smectite with 15–30% smectitic layers.

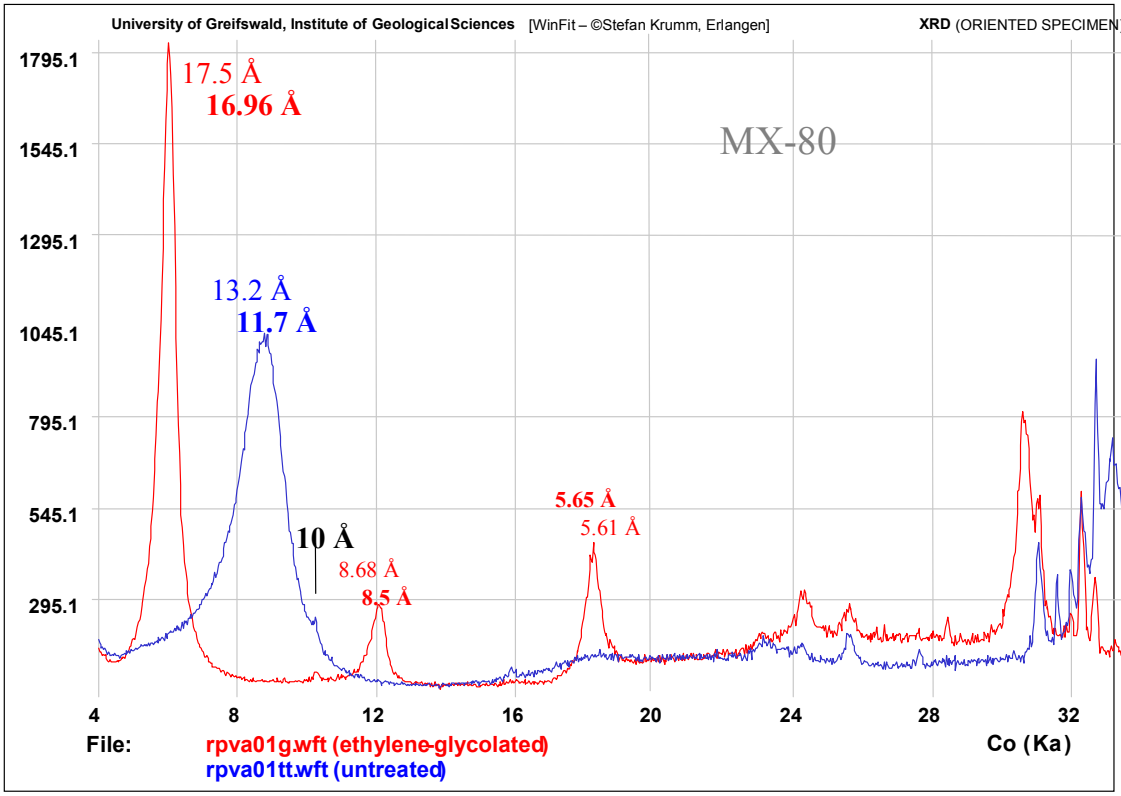

Figure 6-6. *Typical XRD spectrum of MX-80 (oriented specimen, horizontal axis is 2Θ). Freiberg Präzitronik diffractometer HZG 4A with Seifert RDAL300 (Fe-filtered Co-Kα-radiation, solid slits 1° and proportional detector; step size 0.03 °2θ á 2s). This diffracrogram and its peak characteristics were analysed by the deconvolution procedure of the WinFit-software.*

The spectrum in Figure 6-7 represents Friedland Ton and shows the predominance of mixed-layers minerals of muscovite/montmorillonite type and the presence of muscovite and kaolinite. Some montmorillonite is present as well. The diagram represents all the soil material including the clay and silt fractions. The clay may represent a meta-stable product of exposure of a richer montmorillonite clay to hydrothermal conditions. As for MX-80 there is a clear displacement of the major (001) peak by ethylene-glycol treatment. The swelling of this clay is smaller than that of MX-80 because of the lower content of expandable minerals.

Further examples of the crystal structure expressed in terms of XRD spectra are represented by Figure 6-8, which shows the typical peak pattern of smectite-rich clay in random particle orientation ("random powder") with and without glycolation, and of illite-rich clay. The smectite spectrum, which shows the same obvious displacement of the (001) peak as oriented specimens, shows that rather much smectite/illite mixed-layer minerals, quartz and feldspars are present. The illite spectrum also demonstrates the presence of a significant amount of quartz and chlorite while there are almost no feldspars.

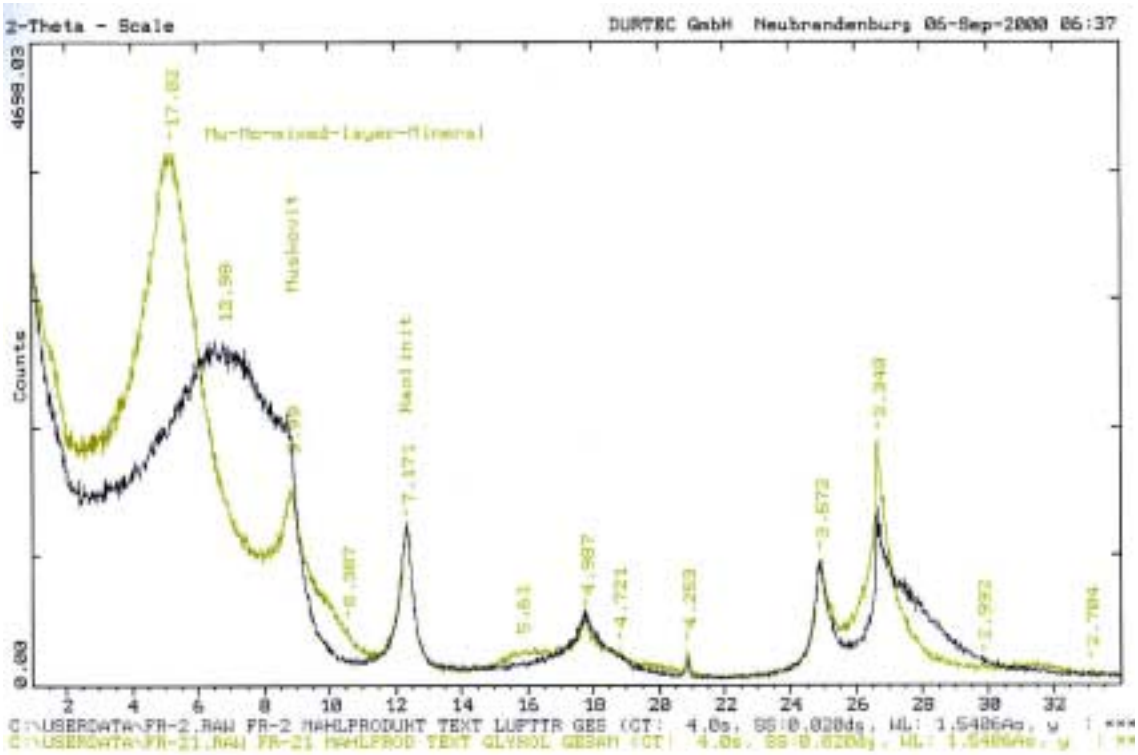

Figure 6-7. *Typical XRD spectrum of Friedland clay (oriented specimen, horizontal axis is 2Θ). The light greenish spectrum represents the condition after ethylene glycol treatment. This diffracrogram and its peak characteristics were analysed by the German company DURTEC.*

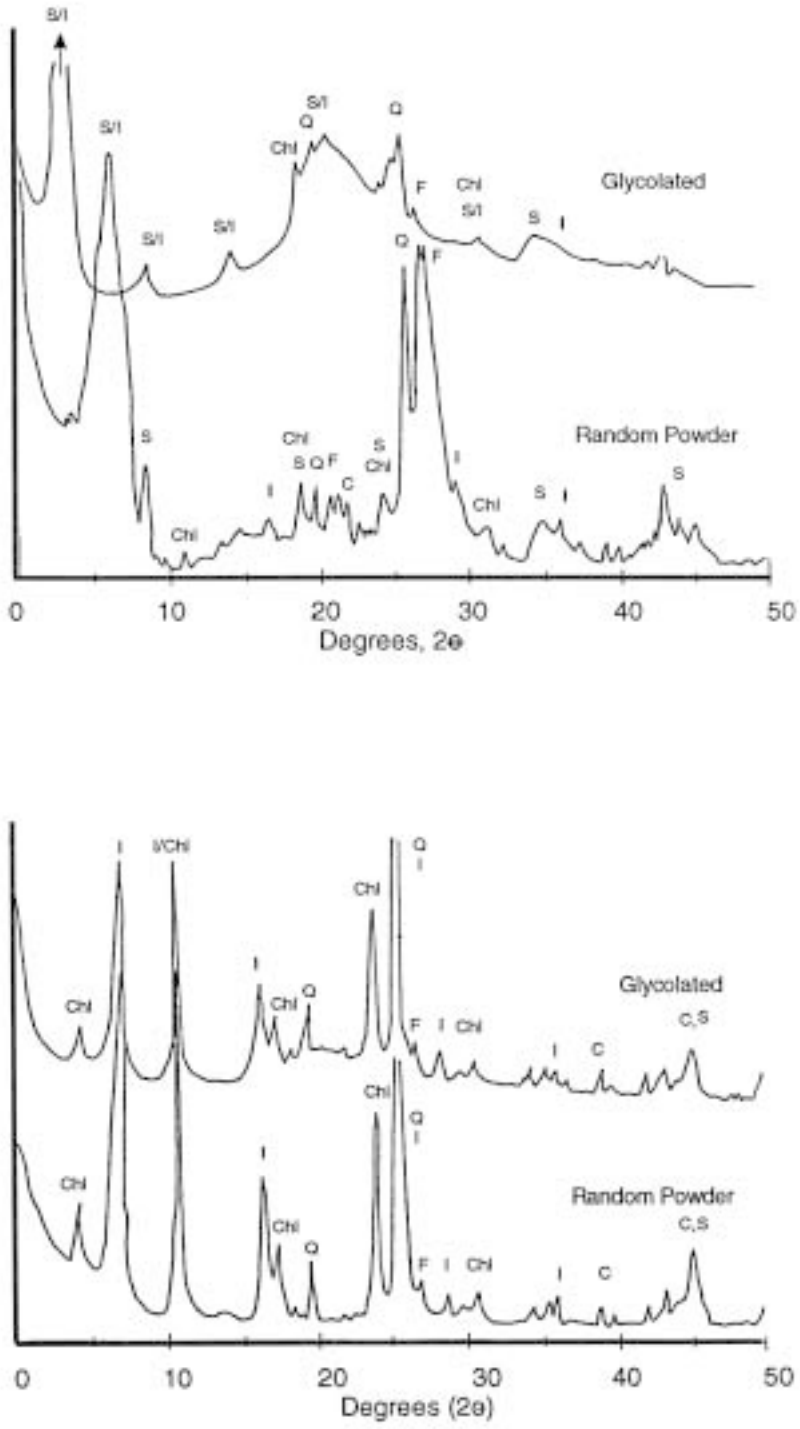

Figure 6-8. *XRD spectra for Saskachewan (Canada) bentonite (upper) and Canadian illitic clay /7/. S=Smectite, S/I=Mixed-layer minerals, I=Illite, Q=Quartz, Chl=Chlorite, F=Feldspar, C=Calcite /7/.*

6.2 Ballast material

6.2.1 Basis of selection of suitable ballast materials

General

From a chemical point of view it is essential that the ballast used for preparing mixtures with clay does not contain minerals or other components that can affect the integrity of the clay in the mixture, the buffer and the waste canisters. Table 6-7 gives an overview of the various ways in which the ballast can have negative chemical impact on the buffer and canisters.

Certain minerals contribute to the longevity of canisters if mixed with the buffer and backfill materials like vivianite [$Fe_3(PO_4)_2 \cdot 8H_2O$)], which consumes oxygen and hence reduces canister corrosion. However, dissolution of this mineral produces phosphate which serves as nutrient to bacteria and may therefore not be suitable.

6.2.2 Mineral composition

The mineral composition of natural soils of glacial origin, sediments and tills reflects that of the rock from which they originate. Usually, the content of weathered minerals is higher than that of the rock that is presently found below the soil cover. Coarser fractions of glacial soils, i.e. silt, sand and gravel have a mineral composition that is usually typical of that of the local bedrock.

Backfilling of tunnels in KBS-3 type repositories is planned to be made by use of the rock material excavated in the construction phase, which makes the composition and properties of the parent rock particularly important. For granites the composition ranges from acid to intermediate silica content, i.e. from granite via syenite, diorite to monzonite, which are all suitable raw materials for ballast production, especially the fine-crystalline, feldspar-poor types, since they have a higher strength and hence give better mechanical properties (less fracturing at compaction, lower compressibility, higher shear strength) than feldspar- and mica-rich material /8/. The main advantage of a low content of feldspars, particularly of those containing potassium, is, however, that hydrothermally induced cementation and impact on the conversion of buffer smectite to illite by giving off potassium will be smaller. Backfills in a KBS-3 repository will be exposed to lower temperatures than the buffer but there is still a desire to use as chemically stable ballast material as possible.

Table 6-7. Chemical impact of ballast on a KBS-3 repository.

Component	Impact on buffer	Impact on canister	Unsuitable minerals
Oxygen	–	Corrosion	Hematite Carbonates
Potassium	Illitization	–	K-Feldspars Muscovite
Sulphur	–	Corrosion	Pyrite
Calcium	Cementation	–	Calcite
Silica	Cementation	–	Feldspars
Aluminum	Cementation	–	Feldspars
Microbes	–	Corrosion	Organics

Table 6-8. Example of mineral composition of granitic rock in Sweden in volume percent.

Site	Rock type	Quartz (orthoclase and microcline)	K-feldspars feldspars	Other minerals	Mafic	Micas
Stripa	Monzonite	44	12	39	3	2
		35	24	35	<3	<2
Fjällbacka	Granite	30	27	36	1	6
		25	37	28	1	9

The quartz content of granitic rock can vary much and is not directly related to the silica content. It is usually highest for granite among the igneous rocks – commonly 10–30% by volume – and since this mineral is more chemically and mechanically stable than feldspars, this rock type is most suitable for preparation of backfills.

Granite commonly contains 10–50% feldspars, 10–30% mafic minerals and 1–5% mica. The chemical composition of the feldspars is of importance since the potassic ones can yield free potassium which alters smectite to illite. Table 6-8 shows examples of typical granitic rocks. One concludes from these data that K-feldspars may represent up to 40% by volume of igneous rock of granitic type /9/. The content of carbonates and sulphur-bearing minerals is usually negligible except for fracture fillings.

6.2.3 Organic content

While igneous rock excavated at several hundred meters depth in the construction of an underground repository almost never contains more than negligible organic material, natural soils of glacial origin, particularly sediments, can contain organic residues, humus etc to an extent that may disqualify them since these constituents serve as nutrients to microbes. Sediments with a grain size that make them suitable for preparing ballast material, i.e. sand and gravel, usually have a content of organic matter of less than 5000 to 10 000 ppm. However, where organic soil like peat covers sand it may be enriched in humus and have an organic content of more than 20 000 ppm /10/. Sand and gravel in delta and river sediments may be particularly rich in organic contaminants. For preparing tunnel backfills with a minimum of bacterial nutrients, crushed rock is preferable to natural sand and gravel.

6.3 Chemical stability

6.3.1 General

The chemical integrity of buffers and backfills is determined by thermodynamically controlled reactions. Thus, mineral transformations take place that depend on the stability conditions of interacting minerals and porewater under the prevailing temperature and temperature gradient conditions. The matter is very complex and not yet fully understood. In this report some basic facts are given that refer to the buffer according to the KBS-3 concept, i.e. highly compacted sodium bentonite.

6.3.2 Chemical processes

Short-term heating of dry bentonite powder

Heating of air-dry bentonite powder for more than a few hours at a temperature exceeding about 450°C causes dehydroxylation and permanent breakdown of the crystal structure /1/. Heating to 400–425°C for 15 hours hour does not alter the structure and can be made for reduction of the content of organic matter and iron sulphide.

Long-term exposure to heat of partly and fully water saturated buffer clay

Two major types of processes take place in the water-saturated buffer: 1) Dissolution/ precipitation and 2) Conversion of the smectite to non-expansive mineral forms /11/.

Cementation

The temperature gradient that is initially high (1 centigrade per centimeter distance from the canister surface) and then drops to a few hundredths of this value after several hundred years has the following effects on the buffer, which is initially not fully water saturated but reaches saturation in a few decades:

1. Dissolution of buffer silicates with concomitant diffusion of released elements, primarily silicon, into the colder part, where precipitation takes place in the form of amorphous silica, cristobalite or quartz according to the generalized model expressed in Equation (6-2):

   $$\text{Smectite} + K^{+} + Al^{3+} \longrightarrow \text{Illite} + Si^{4+} \qquad (6\text{-}2)$$

   This yields cementation of smectite stacks resulting in brittleness and reduced expandability. It is clear from the text on the influence of hydrothermal processes on the porewater composition that significant amounts of silica are released from the minerals and diffuse out into the surroundings driven by concentration gradients at higher temperatures. This is obvious from actual observations in nature as illustrated by the Swedish Kinnekulle case /12/. Here, the sediments adjacent to a 2 m thick Ordovician bentonite bed have been very significantly cemented by silica precipitation (cf Figure 6-9) to at least 5 m distance from the bed and this is also the calculated effect using Grindrod/Takase's geochemical model /12/.

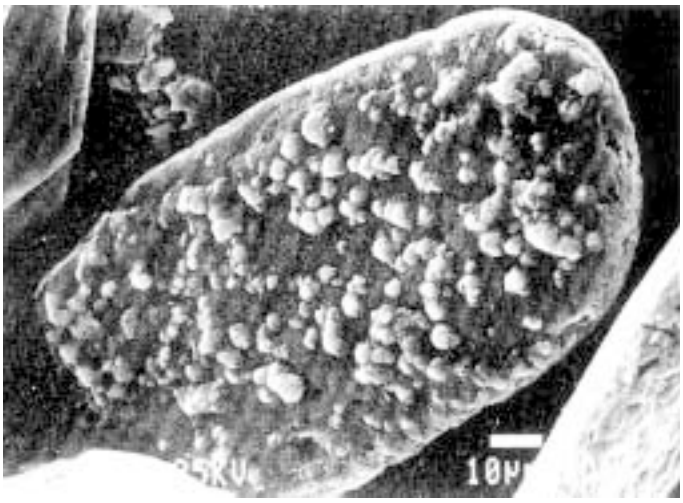

Figure 6-9. *Silica precipitated on a silt particle in Kinnekulle bentonite /13/.*

2. Dissolution of sulphur-bearing minerals and carbonates in the clay and migration in ionic form of released sulphur, calcium and magnesium or iron towards the hot part where precipitation takes place of compounds with a solubility that drops with reduced temperature like carbonates. This mechanism also yields cementation (Figure 6-10).

3. Sodium, calcium, magnesium and potassium in the groundwater and clay porewater, moving in with the water that is taken up in the water saturation process, will precipitate and accumulate as cement in the incompletely water saturated transition zone – the wetting front – due to the cyclic water migration in the evaporation/condensation process that takes place in the buffer /2/. The controlling parameters of the rate and extent of the salt accumulation process are the thermal gradient, groundwater composition, rate of groundwater flow to and along the canister holes, and the salt diffusion rate in both groundwater and clay porewater. In the post-heating period it is probable that precipitated salt will dissolve and become less abundant in the buffer.

4. Iron released from iron-bearing minerals and canisters may form hydroxides and oxyhydroxides, serving as cementing agents.

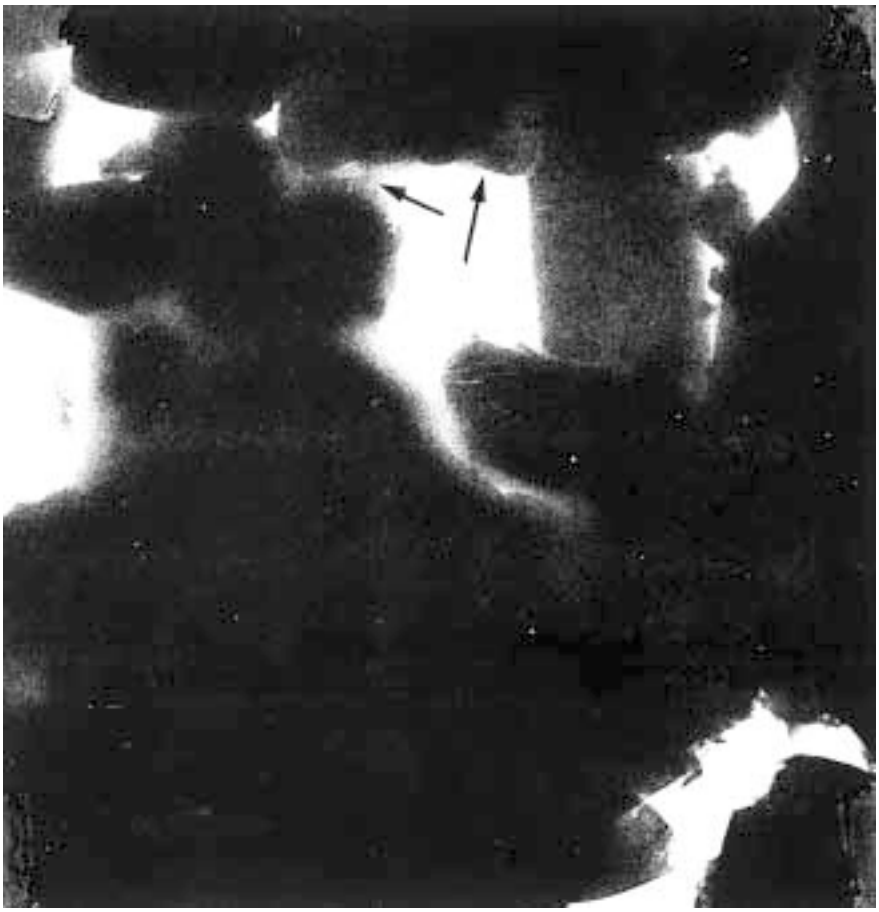

Figure 6-10. *Transmission electron micrograph of carbonate-cemented moraine clay from Skåne, southern Sweden. The arrows indicate carbonate precipitations that weld particled together. The edge length of the micrograph is 10 μm.*

The buffer smectite can be attacked by hot vapor in the drier part of the transition zone and by hot water in the wetter part. The impact is insignificant at temperatures below 80–90°C but hydrothermal tests in which such clay was exposed to vapor in a heating/cooling sequence reaching higher temperatures than 100°C have shown that a significant part of the swelling potential may be lost due to cementation through precipitation of dissolved silica and aluminum /14/. At temperatures well below 100°C the net effect of dissolution of the smectite minerals may be insignificant in the "dry" zone close to the hot canister but of some importance in the transition zone between the dry zone and the saturated clay closer to the rock in KBS-3 deposition holes. The extent of vapor-induced cementation is believed to be controlled by the temperature gradient and rate of wetting of the buffer. It may be that the processes leading to precipitation are at least partly reversible in the post-heating phase.

Conversion of smectite

The long-term chemical stability of montmorillonite depends on the temperature and groundwater composition in a very complex way. Under commonly prevailing pH conditions the most probable mechanism in alteration of smectite (S) is conversion to non-expanding hydrous mica, i.e. "illite" (I). Illite has a crystal structure that is similar to that of montmorillonite but with a higher lattice charge due to partial replacement of tetrahedral silica by aluminum, and with the interlamellar space collapsed through replacement of the hydrated cations by non-hydrated potassium /11, 15, 16, 17, 18/. Such conversion is assumed to take place in two ways: 1) replacement of tetrahedral silica by aluminum and uptake of external potassium, leading to mixed-layer (I/S) minerals with successively dominating I, and 2) neoformation of hydrous mica in the voids of the smectite clay that supplies silica and aluminum or magnesium, while potassium enters from outside and triggers crystallization of hydrous mica as indicated in Figure 6-11.

The rate of conversion of smectite to illite is assumed to be controlled by the access to potassium irrespective of the conversion mechanism. In KBS-3 buffer some of the silica and aluminum will migrate to the colder parts of the buffer where they precipitate and cause cementation while some is accessible for neoformation of illite.

Neoformation of illite is expected to take place at certain concentrations of silica (H_4SiO_4), aluminum and potassium, yielding crystal nuclei in the form of laths. When precipitation takes place the potassium concentration drops locally and the concentration gradient thus formed brings in more potassium by which the process continues. Geochemical codes tend to indicate that illite should be formed from smectites in a certain "window" of phase diagrams of silica, aluminum and potassium /17, 18/, but they do not seem to be able to indicate whether the conversion takes place via mixed-layer mineral stages or by dissolution/neoformation.

Natural analogs provide examples of the extent and rate of conversion from smectite to non-expandable minerals. Detailed descriptions of the Ordovician Kinnekulle bentonite, which still contains about 25% smectite after a heating sequence much like the one expected in a KBS-3 repository, and of the Silurian Hamra bentonite with about the same smectite content after 10 million years exposure to more than 100°C /11/, seem to validate the working model that is presently used in the Swedish R&D work on smectite conversion. It is based on the hypothesis that smectite alteration can take place either by

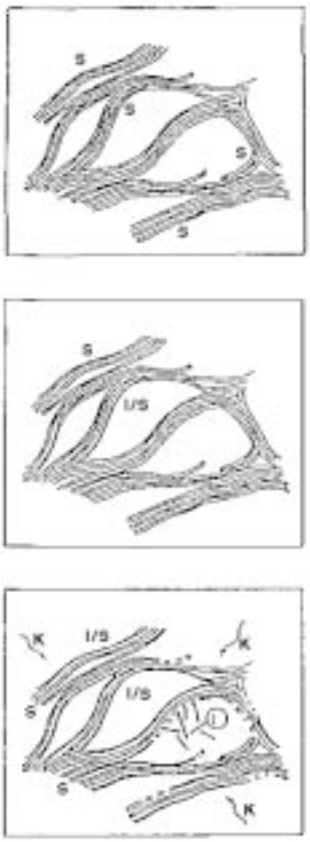

Figure 6-11. *Schematic picture of conversion of smectite to illite via mixed-layer mineral formation or dissolution/neoformation. Upper: Initial state. Central: Layer-wise collapse of smectite layers takes place due to fixation of potassium in smectite that undergoes lattice charge change. Lower: Neoformation of illite laths with Si and Al from dissolved silicates and K^+ entering from the groundwater /2/.*

successive transformation to mixed smectite/illite and further to pure illite, or by dissolution of smectite and neofirmation of illite. Both require sufficient energy and access to potassium. The model is based on Pytte's theory /11/:

$$-dS/dt = [Ae^{-U/RT(t)}] [(K^+/Na^+)mS^n] \quad (6\text{-}3)$$

where:

S = mole fraction of smectite in I/S assemblages
R = universal gas constant
T = absolute temperature
t = time
m, n = coefficients

The problem with this and similar theories is that the activation energy is not known with great certainty. It is assumed to be in the range of 26 to 28 kcal/mole for which calculations give reasonable results. The potassium content is the most important parameter for higher temperatures as demonstrated by application of the theory to

actual conversion cases in nature. Thus, the S-to-I conversion in the bentonite layers at Kinnekulle in Sweden cannot be explained by use of Pytte's theory unless it is assumed that the potassium content was maintained high by strong groundwater convection in the region /19, 20/. Figure 6-12 shows the temperature dependence of illitization for an activation energy of 27 kcal/mole and a potassium concentration of 0.01 moles/liter in the water. It implies that a 100% smectite clay element exposed to 200°C may contain only 20% smectite after about 10 years and that almost complete conversion to illite would take about 1000 years. For 100°C temperature 90% of the smectite would remain after 1000 years and 50% after 10 000 years.

The I/S conversion, which is commonly assumed to take place stepwise, yielding irregular or regular mixed-layer stratification as well as neoformed illite, is believed to reach a final state with around 80–90% S and 10–20% I and other non-expandables in the buffer of a KBS-3 repository after 100 000 years. This rather insignificant conversion is because of stagnation of the conversion by the very moderate temperatures that prevail already after a few hundred years and the return to the low ambient temperature after a few thousand years.

Recent and ongoing investigations of the North Sea sediments in conjunction with oil prospection tends to show that the Pytte-based model may be too conservative /21/. Thus, for a 50 million years old clay from 1670 m depth below sea bottom in the Oseberg Field, where the temperature has been 60 to 80°C, the content of smectite and mixed layer (S/I) is reported to be 66% while the diagram in Figure 6-12 would give about 30%. A typical XRD spectrum for this clay in natural form with and without glycolation and after heating to 350 and 550°C in the laboratory is shown in Figure 6-13. However, the access to potassium may have been a limiting factor, which underlines the importance of avoiding e.g. potassic ballast in backfills in the repository. It is important to notice that the clay, which is termed claystone, has undergone slight cementation, associated with the illitization.

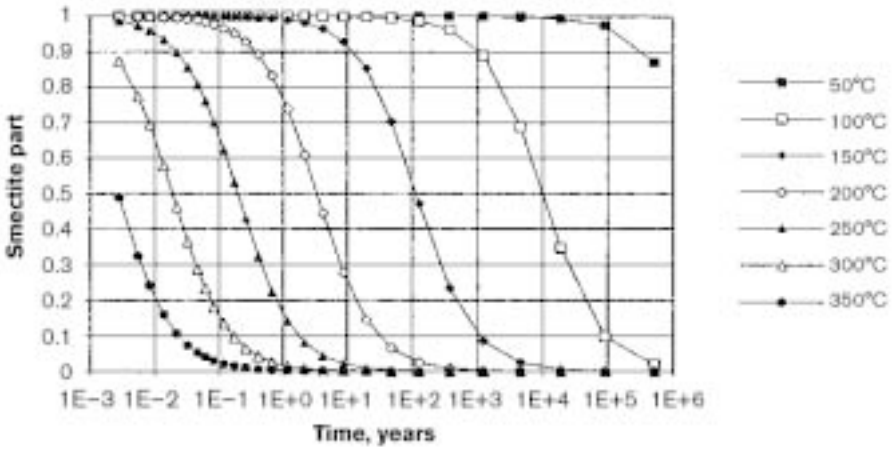

Figure 6-12. *Rate of conversion of smectite to illite according to the Pytte-based model for 27 kcal/moles activation energy and a potassium concentration of 0.01 moles per liter /19/. The initial smectite content (smectite part) that is taken as 100% (unity) drops successively with time.*

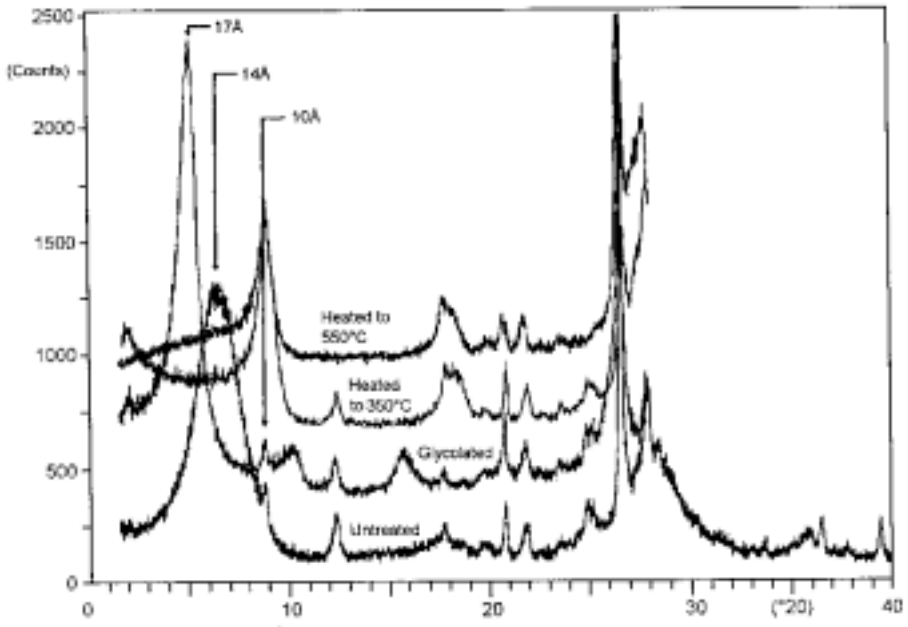

Figure 6-13. *Typical XRD spectrum for a North Sea Lower Tertiary bentonite-type claystone with high content of smectite and high expandability. In most analyses of the minus 2 μm fraction a broad 10–14 Å (001) peak was recorded for natural material and this peak changed to 16.9 to 17 Å on glycolation. It collapsed to 10 Å upon heating to 350°C and higher temperatures /21/.*

There are in fact two more conversion mechanisms that are at least theoretically involved in the degradation of smectite, namely formation of chlorite /15, 18/ and sodium illite, i.e. brammalite /22/. The firstmentioned reaction is not a major one and the second, which has been investigated through hydrothermal treatment of MX-80 using very strong NaCl solutions, has shown that, as predicted by thermodynamics /23/, brammalite can be formed. It is concluded that MX-80 clay saturated with or exposed to concentrated NaCl solutions at 110°C, i.e. conditions that are not too far from those of the buffer clay close to the hot canisters, underwent only slight mineralogical changes in the 30 days long hydrothermal period. They had the form of collapse of montmorillonite stacks, conversion to beidellite, and formation of stable aggregates that are larger than in untreated MX-80. The aggregation is believed to be partly caused by neoformation of sodium illite. The mechanical stability of the aggregates was probably due to cementation by precipitation of silicious matter that was set free by the beidellitization or by dissolution of smectite stack edges. In experiments with air-dry clay contacting NaCl solutions cementation may have been related to vapor attack.

Since the temperature was higher than in a KBS-3 repository and the salt content appreciably higher than what is normally found at 500 m depth in Swedish crystalline rock, these processes may not be significant in the buffer clay. It should be added that brammalite has been identified in nature /24, 25/.

Influence of radiation

A number of laboratory experiments have indicated that γ radiation has two major effects, 1) radiolysis of the porewater, by which the radical OH and various other products like negatively charged O_2 are produced, and 2) breakdown of the crystal lattice of clay minerals /1/. The first process yields decomposition of the porewater that can result in gas accumulation at the surface of HLW canisters, while the second mechanism yields mechanical disintegration of the crystallites by which the average particle size is reduced and the crystal lattice fragmented. The impact of strong radiation has been investigated by 1-year long experiments with MX-80 saturated with low-electrolyte water and exposed to a total dose of 3E7 Gy and a temperature gradient of 90 to 130°C /2, 26/. This study showed that thermally induced mineral transformations like dissolution of feldspars and neoformation of chlorite and quartz occurred but that the large majority of the smectite remained unchanged.

Porewater from the canister-embedding smectite clay will enter leaking canisters and cause dissolution of radioactive waste and released radionuclides will diffuse through the water into the clay. Positively charged elements will migrate into the clay yielding cation exchange, which means that they get adsorbed and expose the crystal lattice to α radiation /27/. Plutonium and americium are radionuclides that can be of concern and laboratory tests have shown that montmorillonite that has been saturated with either of these elements, yielding around $5x10^{18}$ alpha doses per gram of clay, is completely destroyed and converted to an amorphous, silicious mass. Using a relevant value of the number of alphas per mass unit of waste and considering a single hole representing a manufacturing defect or resulting from "pitting" corrosion of a KBS-3 type canister, one finds that such degradation may take place in a cone-shaped zone all the way through the clay to the rock in about 10 000 years. The amount of buffer that can be altered is very small, however, and the net effect on its physical performance is concluded to be insignificant.

6.4 References

/1/ **Jacobsson A, Pusch R, 1978**. Egenskaper hos bentonitbaserat buffertmaterial. KBS Teknisk Rapport 32. Svensk Kärnbränslehantering AB.

/2/ **Pusch R, 1994.** Waste Disposal in Rock. Developments in Geotechnical Engineering, 76. Elsevier Publ. Co.

/3/ **Gloth H, 1997.** GTS:s Investigation of the swelling behaviour of sodium bentonite pellets (MX-80) with a Friedland clay-based drilling mud in a borehole. NAGRA Interner Bericht 97-56, NAGRA, Wettingen.

/4/ **Pusch R, Karnland O, Hökmark H, Sandén T, Börgesson L, 1991**. Final Report of the Rock Sealing Project – Sealing properties and longevity of smectitic clay grouts. Stripa Project Technical Report 91-30. Svensk Kärnbränslehantering AB.

/5/ **Pusch R, Muurinen A, Lehikoinen J, Bors J, Eriksen T, 1999.** Microstructural and chemical parameters of bentonite as determinants of waste isolation efficiency. Final Report European Commission, Contract No F14W-CT95-0012. European Commission, Brussels.

/6/ **Ohe T, Tsukamoto M**, 1997. Geochemical properties of bentonite porewater in high-level repository condition. Nuclear Technology, Vol 118 (pp 49–57).

/7/ **Dixon D A, Chandler N A, Wan A W-L, Stroes-Gascoyne S, Graham J, Oscarson D W, 1997**. Pre- and post-test properties of the buffer, backfill, sand and rock components of the buffer/container experiment. AECL-11786 COG-97-287-1. Whiteshell Laboratories, Pinawa, Manitoba ROE 1LO.

/8/ **Pusch R, 1995.** Consequences of using crushed crystalline rock as ballast in KBS-3 tunnels instead of rounded quartz particles. SKB TR 95-14. Svensk Kärnbränslehantering AB.

/9/ **Williams H, Turner F J, Gilbert C M, 1954.** Petrography. W H Freeman & Co, San Francisco.

/10/ **Pusch R, 1973.** Influence of organic matter on the geotechnical properties of clays. Document D11:1973. National Swedish Building Research Council, Stockholm.

/11/ **Pusch R, 1993.** Evolution of models for conversion of smectite to non-expandable minerals. SKB TR 93-33. Svensk Kärnbränslehantering AB.

/12/ **Pusch R, Takase H, Benbow S, 1998.** Chemical processes causing cementation in heat-affected smectite – the Kinnnekulle bentonite. SKB TR-98-25. Svensk Kärnbränslehantering AB.

/13/ **Mueller-Vonmoos M, Kahr G, Bucher F, Madsen F T, 1990.** Investigation of Kinnekulle K-bentonite aimed at assessing the long-term stability of bentonites under repository conditions. Engineering Geology, Vol 27 (pp 269–280).

/14/ **Pusch R, 2000.** On the effect of hot water vapor on MX-80 clay. SKB TR-00-16. Svensk Kärnbränslehantering AB.

/15/ **Grauer R, 1986.** Bentonite as a backfill material in the high-level waste repository: chemical aspects. NAGRA Technical Report 86-12E.

/16/ **Nadeau P H, Wilson M J, McHardy W J, Tait J M, 1985.** The conversion of smectite to illite during diagenesis: Evidence from some illitic clays from bentonites and sandstones. Mineral Mag., Vol 49 (pp 393–400).

/17/ **Fritz B, 1981.** Etude thermodynamique et modélisation des réactions hydrothermales et diagénétiques. Sciences Géologiques, Mem. No 65, Université Louis Pasteur de Strasbourg. ISSN 0302-2684.

/18/ **Jahren J S, Aagard P, 1989.** Competitional variations in diagenetic chlorites and illites, and relationships with formation-water chemistry. Clays and Clay Minerals, Vol 24 (pp 157–170).

/19/ **Pusch R, 1998.** Transport of radionuclides in smectite clay. Environmental Interactions of Clays, Eds A Parker & J E Rae, Springer (ISBN 3-540-58738-1), (pp 7–35).

/20/ **Pusch R, Madsen F T, 1995**. Aspects on the illitization of the Kinnekulle bentonites. Clays and Clay Minerals, Vol 43, No 3 (pp 261–270).

/21/ **Roaldset E, Bjaanes E, Mjöen K, 1995.** Stability of smectite – environmental aspects of petroleum geological observations. Contribution to the Intern. Workshop on Microstructural Modelling with Special Emphasis on the Use of Clays for Waste Isolation, Lund October 1998. Norwegian Technical University at Trondheim.

/22/ **Pusch R, 2002.** Alteration of MX-80 by hydrothermal treatment under high salt content conditions. SKB Technical Report (In print).

/23/ **Tardy Y, Touret O, 1986.** Hydration energies of smectites. A model for glauconite, illite anf correncite formation. Instit. De Geologie, Univ. Louis Pasteur and Centre de Sedimentologie, Strasbourg.

/24/ **Frey A A, 1969.** A mixed-layer paragonite-phengite of low-grade metamorphic origin. Contribution of Mineral Petrology, Vol 24 (pp 63–65).

/25/ **Bannister R A, 1943.** Brammalite (Sodium Illite) a new mineral from Llandebie, South Wales. Mineralogical Magazine, Vol 26 (pp 304–307).

/26/ **Pusch R, Karnland O, Lajudie A, Lechelle J, Decarreau A, 1993.** MX-80 clay exposed to high temperatures and gamma radiation. SKB TR-93-03. Svensk Kärnbränslehantering AB.

/27/ **Bell G W, 1984.** The implications of alpha radiation damage for bentonites utilized in high-level waste disposal. Smectite Alteration. SKB TR 84-11. Svensk Kärnbränslehantering AB.

7 Physical properties

This chapter gives the basis of selection of suitable buffers and clay/ballast mixtures with respect to their desired performance in a repository. Major physical properties of common commercial smectite-rich clays and clay/ballast mixtures are described in detail and can serve as reference in designing buffers and backfills.

7.1 Most important properties

The most important properties of clay as waste embedment are:

1. Hydraulic conductivity
2. Gas conductivity
3. Ion diffusion capacity
4. Swelling potential (expressed in terms of swelling pressure)
5. Rheological properties
6. Thermal behavior
7. Colloid filtering
8. Microbiological filtering

All these properties depend on the type and content of the smectite component and of the density. Also, the type of adsorbed cation in interlamellar positions and on external surfaces of the stacks of lamellae is of significance as it controls the initially formed microstructure of the applied buffer and backfill. In a longer perspective, the cations can be exchanged by others that are brought about by the groundwater or by canister corrosion and this may alter their physical properties.

This chapter gives data obtained from a large number of systematic laboratory investigations, most of them carried out in the research work performed for SKB. Processes that can change the physical properties are briefly discussed.

7.2 Physico/chemical background

7.2.1 General

The electrical charge and colloidal size of clay particles make them hydrate and interact such that their hydraulic conductivity and stress/strain properties are quite different from friction soils. This is particularly important for smectites because their net charge is higher than any of the other clay mineral types and because the particles are pseudo-crystalline and absorb water within the crystallites. The very fine tortuous pore systems offers considerable resistance to water and gas flow, especially at higher densities and

such clays exert suction of water and have soil-water potentials that are of fundamental importance to engineered clay barriers. The introductory part of the present chapter summarizes some basic facts that are of importance to the understanding of their performance.

7.2.2 Clay/water systems

The energy status of the clay-water system governs the development of "matric" and "osmotic" forces that are responsible for hydration and dehydration. In general one can explain clay water suction that is measured by tensiometers etc as the net effect of the thermodynamic terms /1/:

Ψ_m = matric potential,
Ψ_s = osmotic, i.e. solution, potential (referring to the interaction between solute and water molecules); Ψ_s=nRTc, where n=number of molecules per mole of salt, R=universal gas constant, T=abs. temperature and c=concentration of solutes,
Ψ_g = gravitational potential,
Ψ_a = pneumatic air pressure,
Ψ_p = external pressure transmitted to the particles through the fluid phase.

Considering first the clay as a soil-water continuum one can calculate the spacing between the particles and the well fitting results between such calculations and high-pressure consolidation tests on Na-montmorillonite saturated with 0.003 molar NaCl solution are shown in Figure 7-1. Since there is good agreement between theories and experiments it may be imagined that the compression/swelling performance is governed by the Ψ_s potential and that, at complete fluid saturation, the matric potential Ψ_m=0. These potentials are averages only and particle spacing and density variations on the microstructural scale need to be considered for defining the true thermodynamic conditions in the clay matrix /1/.

It is generally accepted that no more than 3 interlamellar hydrate layers can be established, which means that the curve in Figure 7-1 does not give true information on the interlamellar distance beyond about 10 Å. While the stacking of lamellae at this and smaller distances, which correspond to high bulk densities, can be approximately taken as a plane-parallel arrangement of particles it is quite different at lower swelling pressures and the energy state of the porewater is consequently not the same. For lower bulk

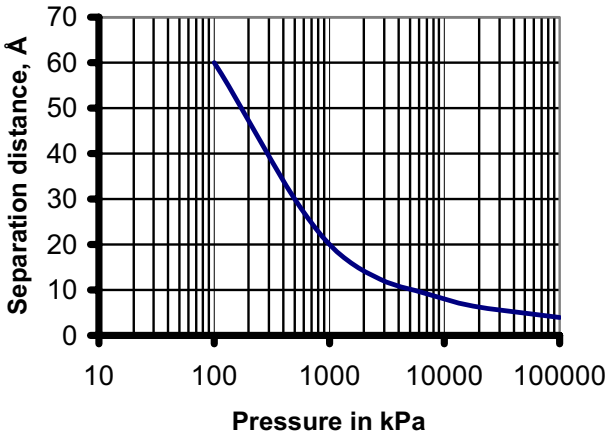

Figure 7-1. *Swelling pressure versus interparticle separation for 0.003 molar NaCl montmorillonite (after Yong).*

densities a large part of the porewater volume is “free” and located in voids between particle stacks and aggregates, which is the term for closely located cohering stacks of lamellae. The particle spacing then represents some average of the intra-aggregate lamellar distance and the distance between stacks of lamellae.

The type of absorbed cations is important in this respect since bi- and polyvalent cations cause growth in stack thickness and size, which means that the voids between the stacks of lamellae are bigger in Ca than in Na montmorillonite. The number of lamellae forming a stack is 3–5 for Na^+ in exchange positions, while it is around 10 for Ca^{2+}, implying thicker stacks.

The difference in relative amounts of interlamellar and total porewater is illustrated by Figure 7-2 /2/ and it is obvious that the bigger stacks and voids in Ca montmorillonite clay gives it a higher hydraulic conductivity. However, the diagram demonstrates that in both clay types the fraction of interlamellar water is large at higher densities and since this fraction is immobile at normal hydraulic gradients it is clear that the hydraulic conductivity of dense buffer is very low irrespective of the type of adsorbed cation. This is manifested by numerous examples later in this chapter.

Swelling beyond about 20 Å is thought to be associated with double-layer interaction between external surfaces of stacks of lamellae and hence an osmotic phenomenon. This is related to the electrical double-layers in Figure 7-3, which illustrates the constitution and extension of the double-layers at the basal planes of stacks of lamellae under marine and fresh-water conditions, respectively. Figure 7-4 describes the charge distribution in the narrow space between two adjacent parallel montorillonite particles with a spacing that allows development of complete electrical double-layers. This matter is basic to the understanding of ion diffusion, which is discussed later in this report.

As indicated by Figure 7-3 the electrical double-layers extend to a larger distance from the mineral surface at low porewater electrolyte concentrations than at high ones, which means that the clay expands to a larger volume in the firstmentioned case.

The implication of Figure 7-4 is that the space between clay aggregates is smaller at higher densities and that the equally charged units repell each other and hence contribute to the swelling pressure.

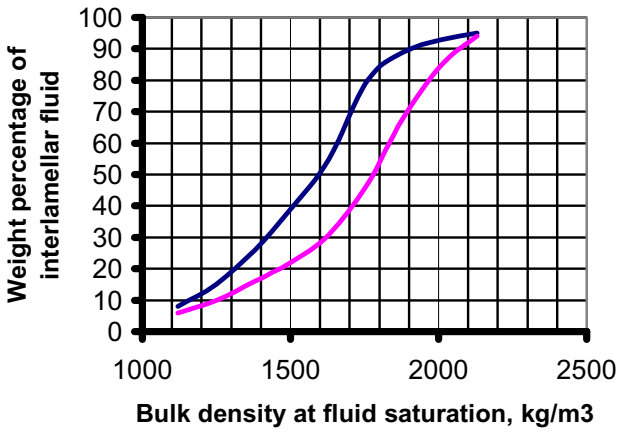

Figure 7-2. *Theoretical fraction of total porewater in montmorillonite that is in interlamellar positions. Upper curve represents Na clay and the lower curve Ca clay.*

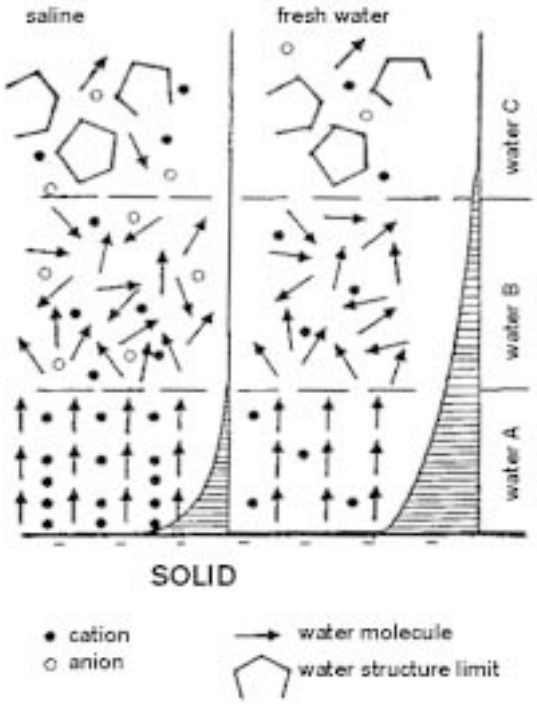

Figure 7-3. *Possible constitution of electrical double-layers and water structure at mineral surfaces in saline (marine) and fresh water, respectively. Water A is largely immobile, while Water B is assumed to have a low viscosity. Water C has the same properties as normal, free water.*

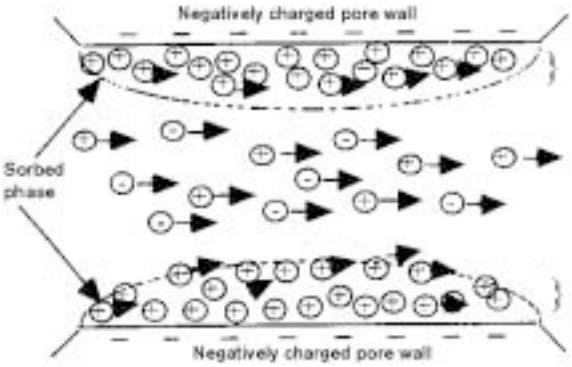

Figure 7-4. *Schematic picture of interacting electrical double-layers (after Neretnieks).*

The electrolyte concentration has a substantial influence on the interparticle distance at low and moderate densities because the stacks of lamellae that form a network with rather much space will coagulate at high electrolyte concentration. The effect of changes in porewater composition on the microstructural constitution is obvious: If the clay initially has Na^+ in the exchange positions and the porewater becomes rich in Ca^{2+}, partial interlamellar dehydration takes place because the stacks of lamellae contract and the voids between them become larger and more continuous, which leads to a drop in shear strength and swelling pressure under constant bulk volume conditions, and to an increased hydraulic conductivity.

The net effect of porewater salinity and bulk density on the microstructure is illustrated by Figure 7-5, in which reference to the swelling pressure is also made. For Ca smectite the much fewer contacts between stacks, i.e. the lower frequency of interacting external double-layers, means that the influence of the salt content on the swelling pressure is appreciably smaller than for the Na case at low and intermediate bulk densities. Hence, there is a difference between Na and Ca smectites concerning their swelling behavior, which is explained by microstructural differences.

Naturally, there is a corresponding effect on the hydraulic conductivity in the sense that a high density and a low electrolyte content in the porewater give Na-smectite a very low conductivity, while that of dense Ca-smectite is only somewhat higher because of the dense particle arrangement. For low densities the difference between the two states becomes obvious, however, and for densities lower than 1600–1800 kg/m^3 Ca-smectite becomes very conductive because of the lack of microstructural continuity and coherence.

In contrast to clays sedimented in nature, artificially prepared ones maintain a certain degree of microstructural heterogeneity since the compacted clay grains do not expand enough to fill the voids. The softer parts of the clay matrix, i.e. the gels in the voids between expanded grains, are sensitive to the porewater chemistry. They make up a very small fraction of dense clays but a considerable part of soft ones. The impact, which is illustrated in Figure 7-6, is a further explanation of the high hydraulic conductivity of Ca-smectite of low and moderate densities.

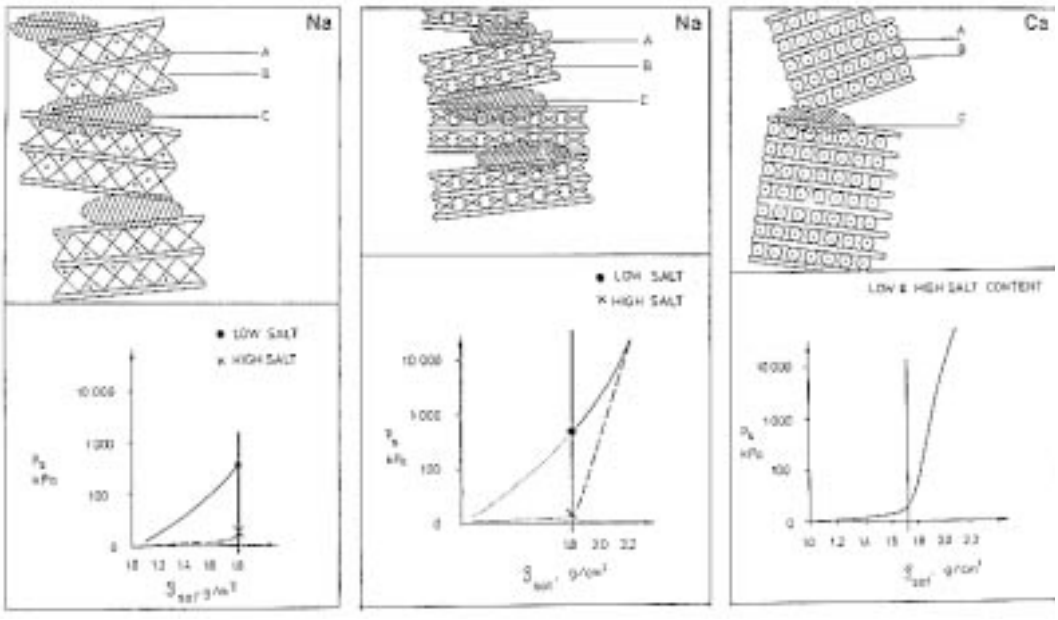

Figure 7-5. *Schematic pictures of stack assemblages and influence of density (at water saturation, expressed in g/cm^3 (1 g/cm^3 equals 1000 kg/m^3) and salinity for Na and Ca montmorillonite clay. A) Lamella, B) Interlamellar space, C) Stack contact region with interacting electrical double-layers /2/.*

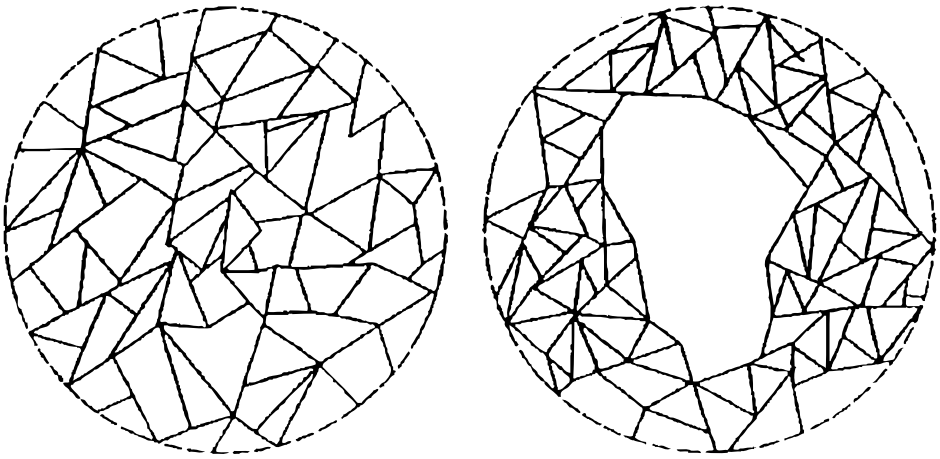

Figure 7-6. *Schematic picture of coagulation of clay particles. Left: Structurally homogeneous clay network. Right: Coagulation by increased electrolyte concentration in the porewater.*

7.2.3 Water tension

It is clear from the preceding text that "intracrystalline" swelling takes place through the matric potential Ψ_m and the osmotic potential Ψ_s. The presence of air/water interfaces is not required for water uptake caused by the matric potential. Hence, fully water saturated smectite clay will absorb water and expand until the hydration capacity for any given density is fully used up. Negative pressure of significance can not be measured using ordinary stress gauges but they can be determined from the relative humidity measured by suitably constructed probes that are inserted in clays. Still, a special type of stress meter, John Burland's probe /3/ seems to work down to –1.8 MPa.

7.3 Buffer materials

7.3.1 General

The clay materials investigated and similar ones that can be obtained from many of the natural resources and manufacturers are listed in Chapters 3 and 6. Their chemical and mineralogical compositions are specified in Tables 6-3 and 6-4, Chapter 6. Table 7-1 shows the buffer clay candidates tested in SKB's research work and the various properties that were determined.

7.3.2 Physical form of buffers

Clay materials like bentonite are usually treated in various ways before being packed and delivered. In a few cases the raw material is so uniform and rich in smectite that only simple drying in the sun of the excavated material with subsequent grinding has to be made at the quarries and plants. However, in most cases it is required to dry the material by use of a rotating kiln of the type used in the cement industry, and to transform the clay to Na form, which is asked for by most customers. The ion exchange, which is required because most of the bentonites in nature have calcium and magnesium as major

Table 7-1. Physical properties of certain buffer clay candidates investigated in SKB's R&D work. The first column indicates the major smectite mineral.

Clay	Manufacturing company	Smectite content	Properties[1)] K	D	p_s	λ	[ϕ,a,b]
Montm. MX-80	American Colloid (USA)	75	*	*	*	*	*
Montm. Tixoton	Süd-Chemie (Germany)	90	*	–	*	–	–
Montm. Moosburg	Süd-Chemie (Germany)	65	*	–	*	–	*
Montm. IBECO Na	Silver & Baryte (Greece)	80	*	–	*	*	*
Montm. IBECO Ca	Silver & Baryte (Greece)	80	*	–	*	*	*
Saponite S	(Through Enresa, Spain)	70	*	–	*	–	–
Beidellite	(Through Enresa, Spain)	35	*	–	*	–	–
Kunigel	Kunimine Ind., Japan	50	*	–	*	–	–
Montm. RMN	Obrnice (Czech Republic)	90	*	–	*	*	–
Mixed-layer, Friedland	DURTEC (Germany)	45	*	–	*	–	–

[1)] *K*=Hydraulic conductivity, *D*=Diffusivity, p_s=Swelling pressure, λ=heat conductivity and capacity, *[ϕ, a, b]*=Rheological parameters.

adsorbed cations, is made by mixing sodium carbonate in powder form into the moist clay. The processing is made stepwise with grinding to the required granule size as the last operation. The time given for the diffusion of ions and the ion exchange is very short and the process is far from complete, which means that carbonate powder grains remain in the mixture and that calcium and magnesium are released and form calcium carbonate precipitates once the clay is wetted.

The processed clay is commonly stored in silos or in stock piles protected from rain and is packed in 25–50 kg paper bags or 1000 kg big-bags for delivery. Bulk transport is often used but it is important to realize that this usually increases the water content, which may reach values as high as 18%. The customer then pays for the water adsorbed by the clay.

7.3.3 Granular composition

Refined clay like commercial bentonite can be obtained from the manufacturers with a range of size distributions of the grains. For preparing highly compacted blocks, the size distribution of the grains should be in a suitable rather coarse interval, while other and usually finer distributions are needed for preparing mixtures with ballast for backfilling purposes. Too fine-grained clay powder is difficult to compress since air will be entrapped and make the material behave elastically, and too large powder grains may result in microstructural heterogeneity. Figure 7-7 gives examples of size distributions that can be obtained from manufacturing companies and that are acceptable for preparing compacted blocks. For preparation of blocks with an initially high degree of water saturation the powder must be wetted, for which there are several techniques.

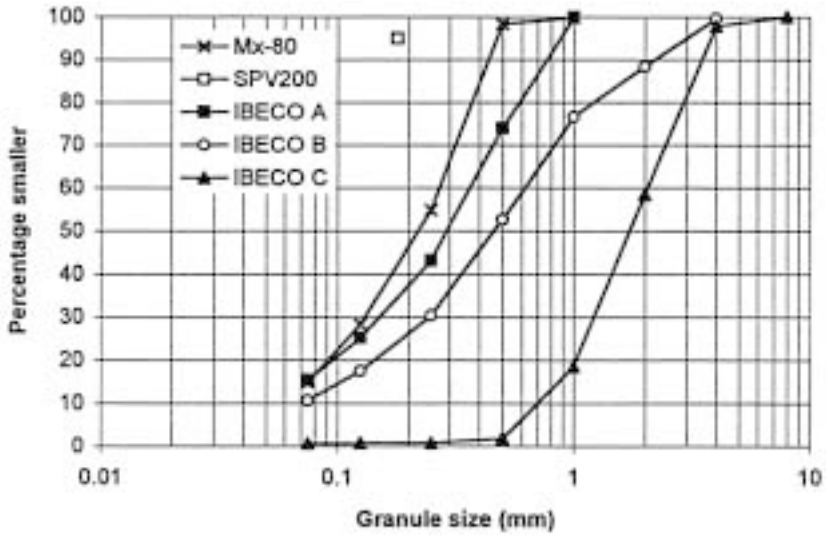

Figure **7-7.** *Block compaction. Upper: Available gradation of bentonite materials. They can all be used for preparing highly compacted blocks but the size distribution of the IBECO materials may be preferable. The lower picture shows a block compacted under 100 MPa pressure using the IBECO C material where one can identify the presence of large compressed grains. After wetting the materials becomes virtually homogeneous. The density including 10% water content is 2200 kg/m³.*

7.3.4 Hydraulic conductivity

General

A general picture of the importance of the mineralogical composition of clays with respect to the hydraulic conductivity is given by the diagrams in Figure 7-8, which illustrates the dependence of the hydraulic conductivity on density at saturation for differently composed clays.

Figure 7-9 shows the approximate relationship between the smectite content and the hydraulic conductivity for mechanically undisturbed clay with a high percentage of clay-sized particles, low-electrolyte porewater and a bulk density at saturation of about 2000 kg/m³. The conductivity is very low even when the smectite content drops to a few percent.

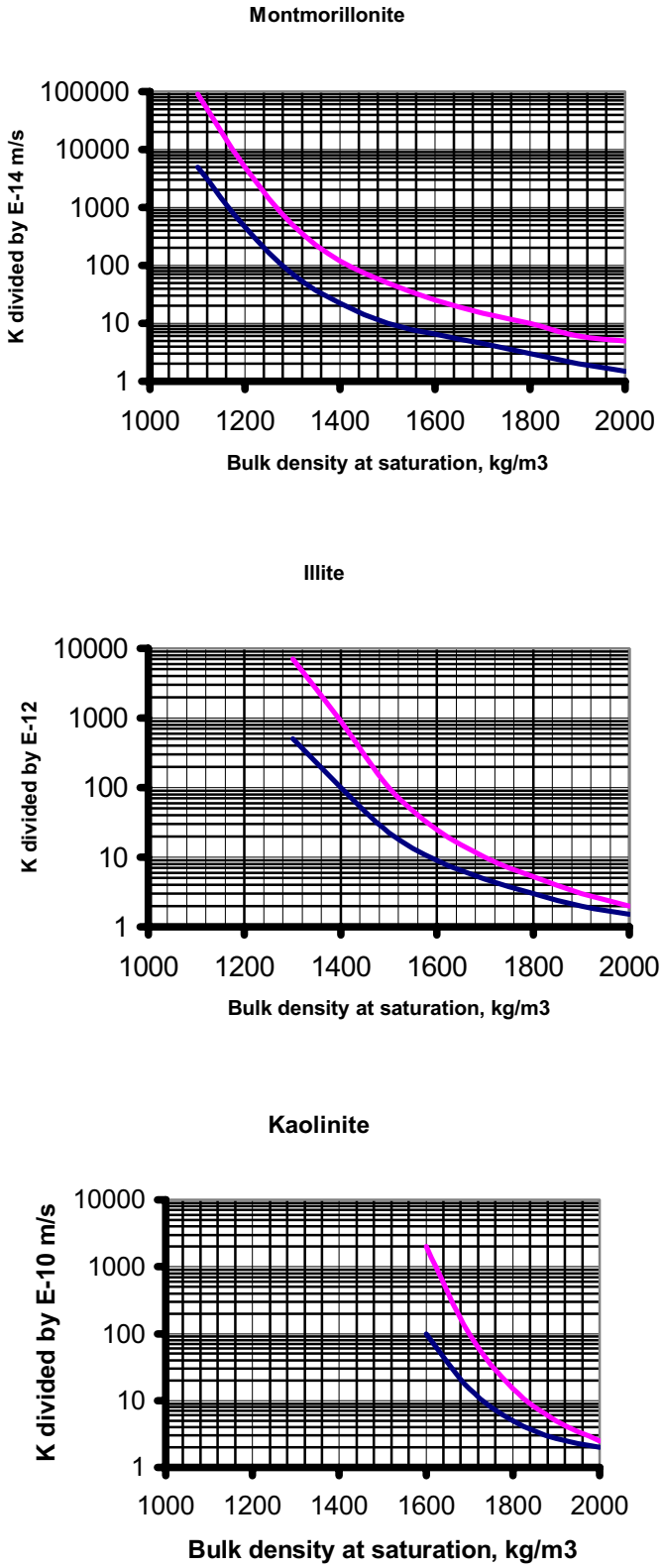

Figure 7-8. *Hydraulic conductivity K of artificially prepared mono-mineral clays as a function of density at fluid saturation (literature survey). The upper curve in each diagram represents saline (ocean-type) porewater while the lower represents saturation and percolation with distilled water. One sees that the hydraulic conductivity of montmorillonite with a bulk density of 1600 kg/m³ is around 100 times lower than that of illite and as much as 100 000 times lower than the conductivity of kaolinite. For the density 2000 kg/m³ the difference is smaller but still significant /2/.*

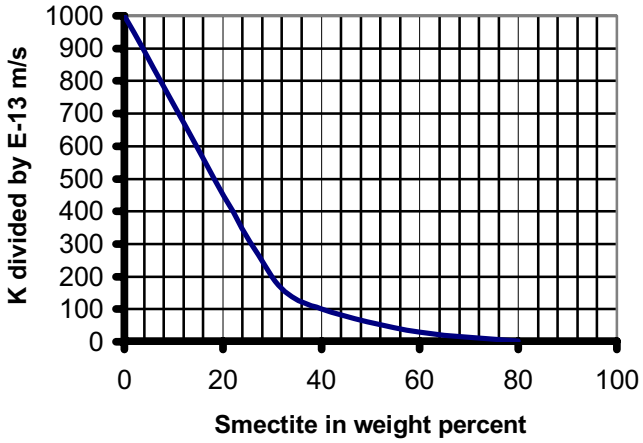

Figure 7-9. *Approximate relationship between the content in weight percent of smectite minerals and the hydraulic conductivity K for natural, mechanically undisturbed clay with a high percentage of clay-sized particles, mostly illite and chlorite, and saturated and permeated by low-electrolyte porewater. The bulk density at saturation is about 2000 kg/m³. The conductivity is very low even when the smectite content drops to a few percent /4/.*

The diagram in Figure 7-9 indicates that the conductivity for undisturbed clay with 70% smectite is about E-14 m/s, which agrees with the value given by the upper diagram in Figure 7-8. For a natural, mechanically undisturbed clay with a content of smectite of about 40%, the diagram in Figure 7-9 gives a *K*-value of about E-11 m/s, which is about the same as for artificially prepared clay with this smectite content as exemplified by the Friedland Ton.

One concludes from the diagrams in Figures 7-9 that dense clays that are rather poor in smectite but rich in illite and chlorite still have a very low conductivity. This is because the entire clay matrix has a high density. For mixtures of clay and ballast grains this is not so because the clay component usually has a varying and rather low density as described in Chapter 5.

The initial heterogeneity of clay materials prepared by compacting more or less dry bentonite grains is not evened out even in a very long perspective, which means that the hydraulic conductivity of equally smectite-rich natural, undisturbed clays is always lower, especially for low clay contents /5/.

Comparing the hydraulic data in Figure 7-9 and typical conductivity data of mixed clay/ballasts given in Table 7-2 one finds that the latter are much more conductive for any smectite content although the difference logically decreases with increasing smectite content. The swelling pressure is also significantly lower for the mixed clay/ballast materials.

Typical hydraulic conductivity data of tested buffer material candidates

Tables 7-3 and 7-4 give evaluated conductivity data of samples prepared from highly compacted powder of commercial bentonite clays with moderate and high bulk densities, and with very low densities, respectively. The latter data have been determined by use of three clay types only.

Table 7-2. Examples of hydraulic conductivity (*K*) of mixtures of MX-80 bentonite and granitic ballast (distilled water).

Smectite content, weight percent	Density at water saturation kg/m³	*K*, m/s
7	2100	E-8 to E-7
20	2100	E-10 to E-9
35	2100	E-11 to E-10

Table 7-3. Hydraulic conductivity in m/s of SKB-tested potential buffer materials saturated and percolated with distilled water. Bulk densities 1800–2100 kg/m³ /5, 6/.

Density, kg/m³	1800	1900	2000	2100
MX-80	4E-13	2E-13	8E-14	3E-14
IBECO, Na	9E-13	–	4E-13	–
IBECO, Ca	2E-11	–	2E-13	–
RMN	–	4E-13	–	8E-12*
Kunigel	3E-12	–	E-12	–
Beidellite	5E-12	–	5E-13	–
Saponite	E-12	–	5E-13	–

* With 5% graphite and 10% quartz powder.

Table 7-4. Hydraulic conductivity in m/s of tested buffer materials saturated and percolated with distilled water. Bulk densities 1100–1700 kg/m³ /2, 6/.

Density, kg/m³	1100	1200	1500	1700
MX-80	–	E-10	8E-12	E-12
Tixoton	3E-9	5E-10	–	–
RMN	–	–	–	3E-11

The data collected in Tables 7-2 and 7-3 deviate from those in Figure 7-8; they are about one order of magnitude higher than the diagram data. The reason for this is that the buffer clays have a smectite content of 70–90% while the montmorillonite diagram in Figure 7-8 represents very pure clay. Experience tells that samples compacted and allowed to rest in oedometers for a long period of time, i.e. several months, get a somewhat reduced hydraulic conductivity due to partial microstructural homogenization. The data given in the diagrams represent samples that were left to homogenize in the oedometers for a rather short time only.

The explanation in Section 7.2.2 why Ca smectites should have a higher hydraulic conductivity than Na smectites is verified by comparing the data of the two IBECO clays.

Influence of temperature

The effect of heating is three-fold /5/:

1. The viscosity of the porewater drops and the hydraulic conductivity is increased proportionally (cf Table 7-5).
2. In clays prepared from highly compacted bentonite powder, the powder grains (granules) disintegrate by which the microstructural homogeneity is improved and the hydraulic conductivity reduced.
3. At temperatures exceeding around 100°C and effective pressures corresponding to the swelling pressure, the average number of interlamellar hydrates appears to drop.

Influence of porewater salinity

Percolation of smectite clays with salt solutions gives a higher hydraulic conductivity than when electrolyte-poor solutions are used as explained in the preceding text. The difference is very obvious at low densities and it is significant even when the density at fluid saturation is as high as 1800 kg/m^3 as documented by the data in Table 7-6. For densities lower than about 1600 kg/m^3 Ca-smectite does not form a stable microstructural network when percolated by solutions with a high electrolyte content. Table 7-6 also provides examples of the conductivity of a less smectite-rich (45%) clay (Friedland Ton).

For higher densities the Friedland Ton appears to be less affected by high porewater salinity than MX-80, which is explained by a higher microstructural stability of mixed-layer clays than of pure smectite. An overview of the influence of porewater electrolytes on the hydraulic conductivity of the Friedland Ton is given in Figure 7-10, which also gives typical conductivity data of this clay for the case of saturation and percolation with distilled water.

This diagram demonstrates that the conductivity is remarkably low even for extreme concentrations of sodium and calcium in the porewater when the density exceeds about 2000 kg/m^3. This demonstrates that microstructural collapse due to coagulation (cf Figure 7-6) is limited in clays that contain much mixed-layer minerals, which have less capacity of forming homogeneous clay gels than e.g. montmorillonite.

Table 7-5. Example of the influence of temperature cycling of clay prepared from MX-80 powder. Data represent equilibrium after dissipation of generated porewater pressures. The higher conductivity at higher temperature is due to a drop in porewater viscosity.

Density at saturation, kg/m^3	Temperature, °C	Hydraulic conductivity, m/s
1660	22	3.4E-12
	75	1.2E-11
	22	2E-12
1930	65	E-12
	22	5E-13

Table 7-6. Hydraulic conductivity in m/s of MX-80 and Friedland Ton at high salinity of the percolate /7/.

Percolate	Density at saturation, kg/m³			
%	1600	1800	2000	2050
MX-80				
0.5 NaCl	7E-12	2E-12	2E-13	6E-14
3.5 NaCl	–	E-11	E-12	E-13
0.5 $CaCl_2$	E-10	2E-12	2E-13	9E-14
3.5 $CaCl_2$	E-9	3E-12	3E-13	9E-14
Friedland Ton				
2 NaCl	2E-8	–	–	–
10 NaCl	5E-8	E-9	5E-11	2E-11
3.5 $CaCl_2$	E-9	6E-10	2E-11	–
10 $CaCl_2$	–	5E-9	3E-11	2E-11

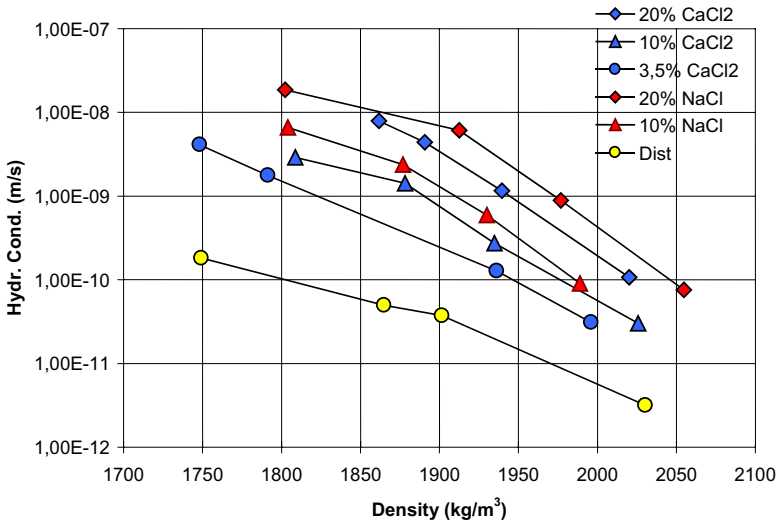

Figure 7-10. *Hydraulic conductivity tests on saturated samples of Friedland Ton /7/.*

Figure 7-11 illustrates that saturation and percolation of clay with strong $CaCl_2$ solution causes an initially very high flow rate. This is a general phenomenon illustrated here by an experiment with Friedland Ton. The figure shows that the evaluated hydraulic conductivity dropped to about E-8 m/s after two days and further to about 5E-10 m/s after 6 days. The drop in conductivity is believed to be due to successive microstructural homogenization of the system of compacted powder grains, and to clogging of voids by migration of particle aggregates set free and transported by flowing porewater /5/.

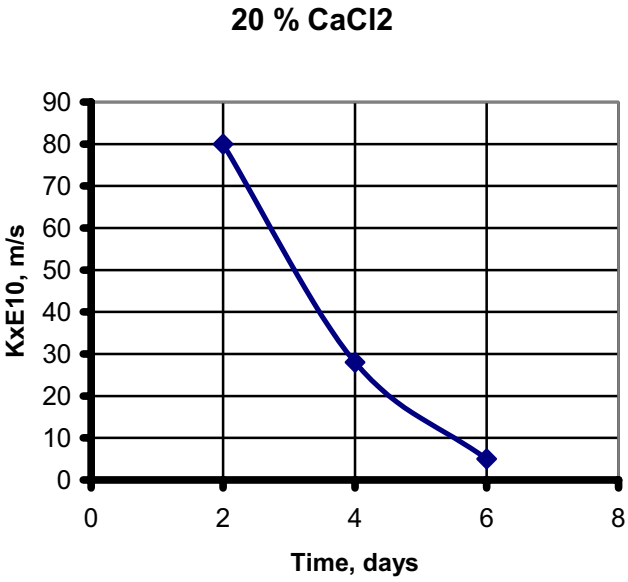

Figure 7-11. *Recorded hydraulic conductivity in the course of saturation and percolation of clay prepared by air-dry compacted Friedland Ton powder. The solution was 20% $CaCl_2$ and the clay density 2000 kg/m³ /7/.*

Influence of hydraulic gradient

The gradient-dependence of buffer clay with a density of more than 1600–1800 kg/m³ is insignificant under the hydraulic gradients that will prevail in a repository but the very high gradients that are commonly applied in laboratory experiments in order to get measurable quantities through clay samples in reasonable time can produce compression and increased tightness of the clay (see Part 1 of this Handbook).

7.3.5 Gas penetrability

Gas penetration

Permeation of gas through clay is a not yet fully understood phenomenon but in practice one can assume that the gas conductivity is about a thousand times higher than that of water. This means that once gas has made its way through buffer clay and further out through even more permeable geological units it will flow at a rate that is more dependent on the gas production rate than on the gas conductivity. The most important issue is therefore the gas pressure that yields penetration of gas through the buffer clay, i.e. *the critical gas pressure*. For stagnant gas penetration the solubility of the gas in question – air and hydrogen gas are the most important species – is an important matter.

Critical gas pressure

According to one of the current hypotheses the microstructural heterogeneity has a decisive influence on the critical gas pressure: gas makes its way where it finds least resistance, which is along continuous channels of neighboring larger voids where the capillary retention is at minimum /2/. However, there is an alternative approach assuming that fluid-saturated smectite clay is a porous, homogeneous medium and that gas passages are formed by separation of neighboring particles by overcoming their bond strength /8/. Both models imply that the critical gas pressure is on the same order of

magnitude as the swelling pressure, which is in turn closely related to the capillary pressure. This is natural since a pressure of this order is required to displace clay particle aggregates.

In Part 3 of this Handbook we will describe gas transport by use of a mathematical model that is based on the concept of critical pressure. Once this pressure has been reached or exceeded, the gas flow is quick and the corresponding gas conductivity about one thousand times higher than the hydraulic conductivity. However, no definite figures can be defined since the matter is very complex. Thus, a number of physical processes will occur that change the constitution of the clay, like particle transport, consolidation/expansion of the clay matrix adjacent to the transport channels at peristaltic gas movement, as well as local drying and associated time-dependent changes of channel dimensions.

7.3.6 Ion diffusivity

The "apparent" diffusivity does not give complete information on the various mechanisms involved in diffusive transport or of the diffusion transport capacity. The latter is expressed by the "effective" diffusion coefficient, which refers to the actual "effective" porosity and is of great practical use. It also gives some information on the ion transport on the microstructural level in contrast to the "apparent" diffusion coefficient. Thus, the importance of referring to the porosity is realized by the fact that cation diffusion takes place in several ways, i.e. in continuous water-filled voids, along exposed stack surfaces with electrical double-layers, and through the interlamellar space. The latter two mechanisms involve ion-exchange mechanisms for which a sorption parameter, K_d, is introduced (cf Part 3).

In practice, the ion transport capacity can be evaluated by applying Fick's law and relevant values of the coefficient of "effective" diffusion, D_e, for any density. Table 7-7 gives typical literature-derived data on this parameter for montmorillonite-rich bentonite with a density at saturation of 2000 kg/m^3, which represents the approximate density of canister-embedding clay buffer according to the KBS-3 concept. Theoretical models and calculations are examplified in Part 3.

The density of the clay plays a rather important role except for monovalent cations as illustrated by Figure 7-12. It demonstrates that the D_e of the anion chlorine becomes one order of magnitude lower if the dry density is increased from 500 to 1500 kg/m^3 (1950 kg/m^3 at fluid saturation) for which D_e is E-11 m^2/s. The curve for neutral molecules is approximately valid also for water.

Table 7-7. Effective diffusion coefficient D_e for elements migrating in MX-80 bentonite with a density at saturation of about 2000 kg/m^3 /9/.

Species	D_e, m^2/s
C-14	E-10
I-129	2E-12
Sr-90	2E-8
Cs-137	2E-9
Na-22	E-9
Pu-238	E-10
Am-243	E-10

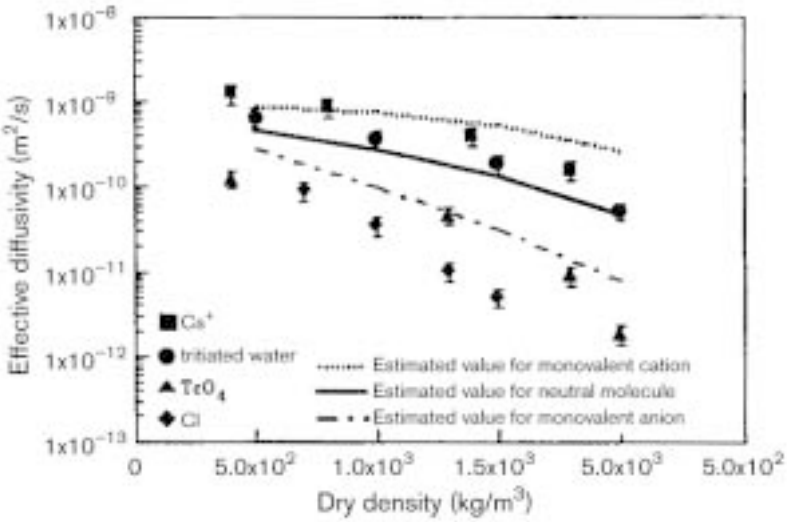

Figure 7-12. *Measured and calculated effective diffusivities for smectie-rich clay /10/.*

The diffusive anion transport capacity is proportional to the pore space of the voids between the stacks of smectite lamellae since they are excluded by the Donnan effect from the interlamellar space. With increasing density there is a strong reduction of the available space for migration and the diffusion coefficient of anions therefore drops significantly. Many cations move both by pore diffusion and surface diffusion including both the interlamellar space and the close vicinity of the stacks of lamellae where electrical double-layers with dominant cationic population exist /11/. Hence, the retarding effect of raising the density on the diffusion capacity of cations is very limited, especially for monovalent ions.

Various criteria relevant to the selection of data for practical application have been proposed /9/. The influence of porewater composition and type and amount of initially adsorbed cations has not been systematically investigated. The effect of heating on diffusive transport is not known well.

7.3.7 Colloid transport

The issue of colloid transport through buffers has not been examined in detail but some general conditions have been defined, as for minute smectite particles, which, through their ability to sorb positively charged radionuclides and other cations, can play a role in bringing contaminants to the biosphere. Such particles, like many other constituents of colloidal size, carry different electrical charges on different parts of their surfaces and hence form aggregates, gels and particle networks that easily couple to the dense buffer clay /12/. Release of smectite aggregates can take place if the porewater flow is sufficiently high but this is estimated to be impossible under the regional hydraulic gradients that prevail in the rock after closing the repository.

However, soon after emplacement of the buffer clay it will tend to enter fractures in the rock and the front of fracture-penetrating clay may be very soft so that groundwater flowing in the fractures may tear off small aggregates and transport them if the flow rate exceeds a few millimeters per second. Experiments as well as experience demonstrate that their size may be up to 2–50 μm. Their surface charge makes them interact with and become fixed to the common fracture minerals chlorite and micas and it is therefore believed that the transport of smectite aggregates will be insignificant over long distances /12/.

7.3.8 Swelling properties

General

The expandability of smectitic clay is a most important property for use as buffers and backfills since it provides a self-sealing potential and tight contact with surrounding rock and embedded canisters. The major influencing factors are the density, porewater salinity and type of adsorbed cation.

Influence of density and porewater salinity

The swelling pressure is strongly dependent on the density, salinity and major type of adsorbed cation at low densities. The density is the major factor as illustrated by Figure 7-13, which refers to MX-80 and a German commercial bentonite (Sued-Chemie) termed Moosburg. The latter is a calcium bentonite while MX-80 has sodium as major adsorbed ion.

The difference in swelling pressure between the two clays in the diagram, which is due to different microstructural constitutions as described earlier in this chapter, is negligible at higher densities than about 1900 kg/m^3, i.e. when the stacks of lamellae have been forced together so much that the microstructural patterns are similar.

Influence of smectite content

Figure 7-14 shows the approximate relationship between the smectite content and swelling pressure of clays with different amounts of smectite, representing mechanically undisturbed clay with a high percentage of clay-sized particles, low-electrolyte porewater and a bulk density at saturation of about 2000 kg/m^3. The corresponding values for artificially prepared mixtures of MX-80 clay and ballast are lower as discussed later in this chapter.

The diagram in Figure 7-14 indicates that the swelling pressure for 70–80% smectite is about 2–2.5 MPa, i.e. around 50% of the value of MX-80 clay with the same smectite content. The discrepancy may partly be due to slight cementation of the natural clays.

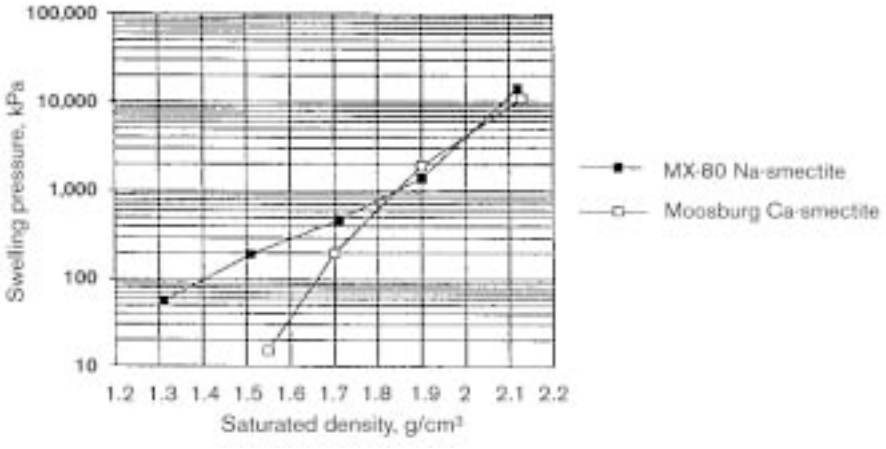

Figure 7-13. *Generalized diagram showing swelling pressure versus density at saturation with distilled water of a Na bentonite (MX-80) and a Ca bentonite with similar smectite content (Moosburg) /2/.*

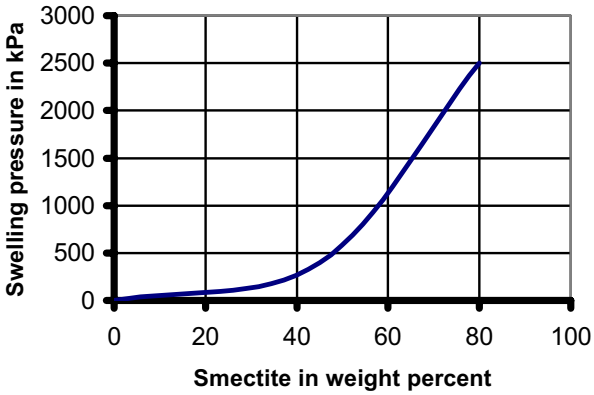

Figure 7-14. *Approximate relationship between the content in weight percent of smectite minerals and the swelling pressure for natural, mechanically undisturbed clay with a high percentage of clay-sized particles, mostly illite and chlorite, and saturated and permeated by distilled water. The bulk density at saturation is about 2000 kg/m³ /4/.*

Typical swelling pressure data of tested buffer material candidates

Typical data of a number of SKB-tested buffer materials are collected in Table 7-8. It demonstrates that while montmorillonite with sodium in exchange positions has a swelling potential even at very low densities, it almost vanishes when calcium occupies these positions and the bulk density at water saturation is below about 1800 kg/m³. The low values of Kunigel and Friedland clay is explained by their relatively low smectite contents. For high densities saponite and beidellite behave as montmorillonite, while they give somewhat higher swelling pressures at lower densities.

The data in Table 7-8 imply that the swelling pressure of smectite-rich clays in sodium form (MX-80, IBECO Na, and RMN) are somewhat different but interpolation of the data for the RMN clay to the nearest hundreths of kg/m³ means that the variations are small. In principle, the data for MX-80 can be taken as representative of clays with a content of montmorillonite in sodium form of 70–90%.

Table 7-8. Swelling pressure (p_s) in MPa of a number of tested buffer materials saturated with distilled water /3, 4/.

Density at saturation, kg/m³	1300	1500	1700	1800	1900	2000	2100
MX-80	0.06	0.2	0.4	0.8–0.9	1.4	4–5	10–12
IBECO, Na	–	–	–	0.6–1	–	4–5	–
IBECO, Ca	–	–	–	0.2	–	5	–
RMN	–	–	0.45	1.9*	2.5**	3.9**	–
Beidellite	–	–	–	1.5	–	4.2	–
Saponite	–	–	–	2.5	–	8.8	–
Kunigel	–	–	–	0.2	–	0.9	–
Friedland	–	–	0.05	0.1	0.3	0.8–1	2–2.5

* Density at saturation 1850 kg/m³.

** Mixture with 5% graphite and 10% quartz powder. Density at saturation 1950 kg/m³.

Influence of temperature

Early testing of bentonites indicated that a temperature rise makes the swelling pressure drop except for low densitites /13/. Since then the opposite has been reported for Na but not for Ca smectite with the explanation that the osmotic pressure rises with temperature and that the number of contacts between the stacks of lamellae in Na than in Ca smectite is higher. However, recent investigations in which great care was taken to allow heat-generated porewater pressures to dissipate have demonstrated that an increase in temperature causes a drop in swelling pressure also of MX-80 clay in Na form. This is demonstrated by the diagrams in Figures 7-15 and 7-16, which represent tests with clay prepared by use of strongly compacted MX-80 clay pellets. The study comprised temperature cycling in the interval 22 to 75°C.

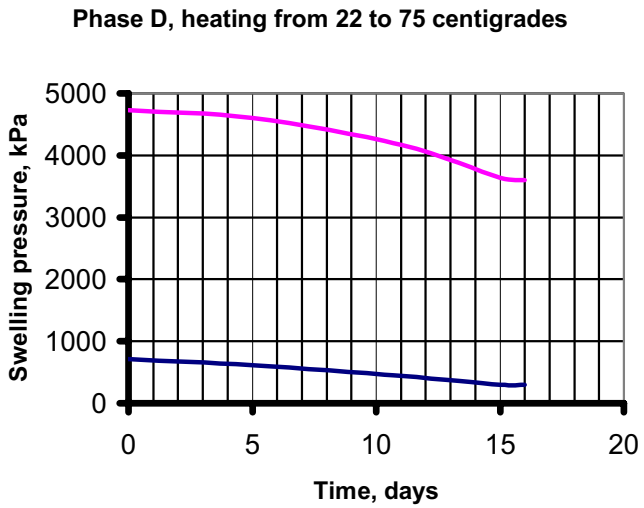

Figure 7-15. *Time-dependent change in swelling pressure of clay prepared from very strongly compacted MX-80 pellets percolated with distilled water in a heating period (Phase D). The upper curve represents a sample with 1930 kg/m³ density at saturation. The lower curve shows the pressure evolution for one with 1660 kg/m³ density at saturation.*

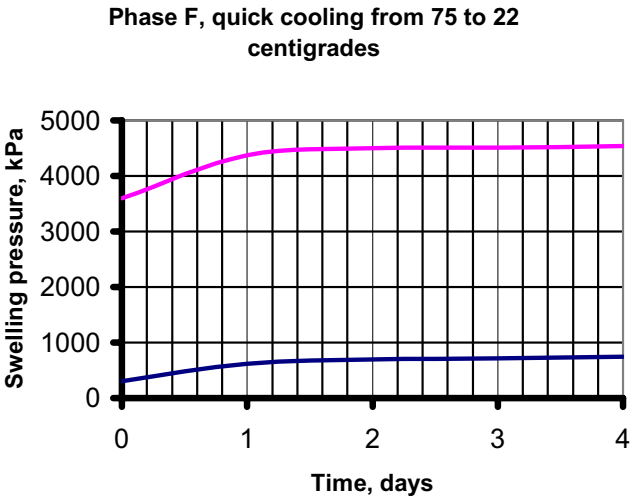

Figure 7-16. *Time-dependent change in swelling pressure of clay prepared from very strongly compacted MX-80 pellets percolated with distilled water in cooling period (Phase F). The upper curve represents a sample with 1930 kg/m³ density at saturation. The lower curve shows the pressure evolution for clay with 1660 kg/m³ density at saturation.*

Influence of porewater salinity

The influence of salinity on the swelling pressure is obvious for low densities (cf Figure 7-5) but when the density at saturation is higher than around 2000 kg/m^3 the swelling pressure is not significantly affected by the porewater chemistry /2/. This means that dense bentonite saturated with electrolyte-poor water has its tightness and swelling potential largely preserved even if the porewater is replaced by ocean water.

The Friedland Ton with about 45% expandables represented in Table 7-8 can be used as an example of the behavior of less smectite-rich clays with respect to porewater salinity as illustrated by the diagram in Figure 7-17. This clay is remarkably insensitive even to very high salt contents at densities exceeding about 2000 kg/m^3 and it has a swelling pressure of about 100 kPa at any salt content if the density at saturation is about 1900 kg/m^3.

Influence of time

The swelling pressure of a confined dry sample of expandable clay starts to develop as soon as it hydrates or is changed when a fully hydrated sample is exposed to water and is able to expand and take up more water. The behavior depends on the temperature conditions and on the water pressure. Tests have shown that the hydration rate of a smectite-rich clay sample compacted to a dry density of 1800 kg/m^3 is controlled by the suction potential but that it can be increased by applying a high water pressure (500–1000 kPa). However, the penetration depth is rather small, i.e. a few centimeters, since the channels through which water is pressed in quickly self-heal /14/.

Hydration of clay powder in the oedometer often gives a maximum value even before all parts of the sample are completely fluid-saturated. For very dense powder grains and high densities of the compacted powder the swelling pressure reaches a maximum in the course of the hydration and then drops somewhat before it rises again and reaches a second maximum. For less densely compacted clay powders the swelling pressure increases successively as illustrated in Figure 7-18.

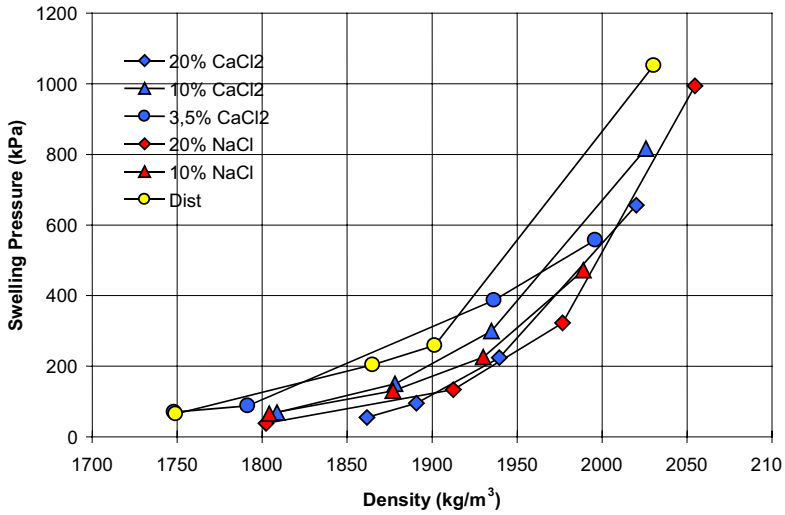

Figure 7-17. *Swelling pressure tests on saturated samples of Friedland Ton /7/.*

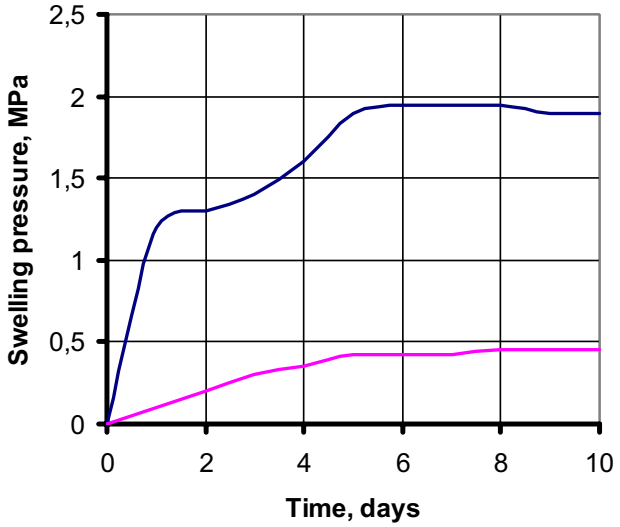

Figure 7-18. *Typical time-dependent evolution of swelling pressure on wetting of compacted bentonite powder with distilled water. Tests with RMN clay; upper curve: Density 1850 kg/m³ at complete saturation (dry density 1350 kg/m³); lower: Density 1700 kg/m³ at saturation (dry density 1110 kg/m³).*

The swelling pressure is known to be largely constant after a few weeks but for clays prepared from very strongly compacted pellets it may take several weeks or months before equilibrium is reached. If hydration takes place at some tens of centigrades above room temperature the thermally induced stresses tend to disintegrate the pellets, which exposes their interior to water and breaks cementation bonds, hence speeding up the fluid saturation.

7.3.9 Suction

Suction

The implication of the "matric" and "osmotic" forces that operate in clay/water systems is that suction in the porewater phase prevails when the degree of saturation is below 100%. The suction, which is largely independent of the density, is insignificant when the degree of water saturation is higher than 95%.

Table 7-9. Example of suction as a function of dry density and degree of water saturation (S_r) of MX-80 clay /17/.

S_r, %	Suction, MPa MX-80
30	100
40	70
50	50
70	20
90	10
95	8
99	1

7.3.10 Rheological properties

General

The rheological properties are expressed in the form of stress- and time-dependent strain as defined by the general material model described in Part 1. In practice, the rheology of buffer clays is of importance with respect to the strength of blocks of compacted clay powder and for the behavior of buffer and backfills on site during and after fluid saturation. In the present section strength data of compacted MX-80 clay blocks are given and also typical parameter data for saturated MX-80 clay. The block strength represents shearing under undrained conditions while the stress/strain behavior of the buffer on site represents drained conditions.

Compacted blocks of air-dry bentonite powder

The strength and deformation properties of blocks of compacted bentonite powder can be expressed in terms of the unconfined compressive strength and the tensile strength. The firstmentioned properties are determined in the laboratory using ordinary laboratory compression devices, like the triaxial test equipment or a simple uniaxial compression machine. The compression rate can be taken as for ordinary soft sedimentary rock or strong soil samples (cf Part 1). A typical picture of the stress/strain behavior of natural dense bentonite clay, which is somewhat stronger than artificially prepared clay because of slight cementation, is shown in Figure 7-19. Failure occurred at an axial strain of about 3% for a compressive stress of 2.5 MPa, which demonstrates ductile behavior.

The tensile strength can be determined by performing beam loading experiments for which a standard procedure has been developed, which will be described here /15/. Table 7-10 gives typical data of strength data evaluated from load testing of small blocks.

Samples with 50 mm diameter and 20 mm height are compacted under 100 MPa pressure and test specimens cut to yield beams with the dimensions 45x10x20 mm (a is 20 mm) by sawing. They are supported at the ends, and loaded with a gradually increasing force applied at the center of the sample. (Figure 7-20). Typical results of tests on MX-80 are summarized in Table 7-10.

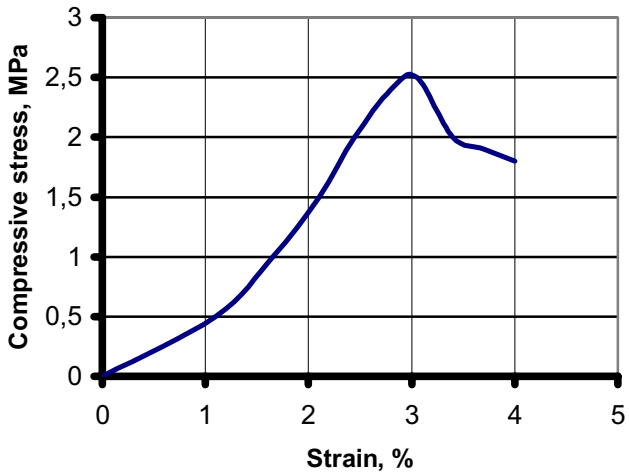

Figure 7-19. *Example of uniaxial testing of natural bentonite clay from Burgsvik, Sweden. The density of the saturated clay was about 2100 kg/m³.*

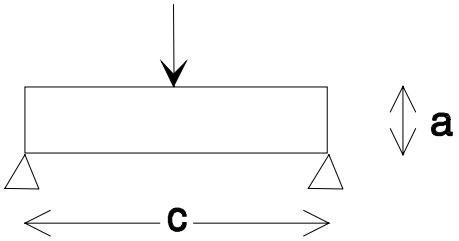

Figure 7-20. *Test arrangement for determination of the tensile strength.*

Table 7-10. Tensile strength of MX-80 bentonite blocks, compacted under 100 MPa pressure.

Water content, (%) Initial	Final	Void ratio, e	Degree of water saturation S_r, %	Tensile strength, MPa
10	10	0.51	55	2.8
18	17	0.60	79	1.9
26	24	0.76	88	1.3

The corresponding stress/strain curves are shown in Figure 7-21, from which one finds that blocks with high water contents give the lowest strength values. This may be explained by the capillary pressure providing additional strength to the dryer samples. Blocks with lower water content than about 8–10% are expected to break at lower stresses because of fine desiccation fissures.

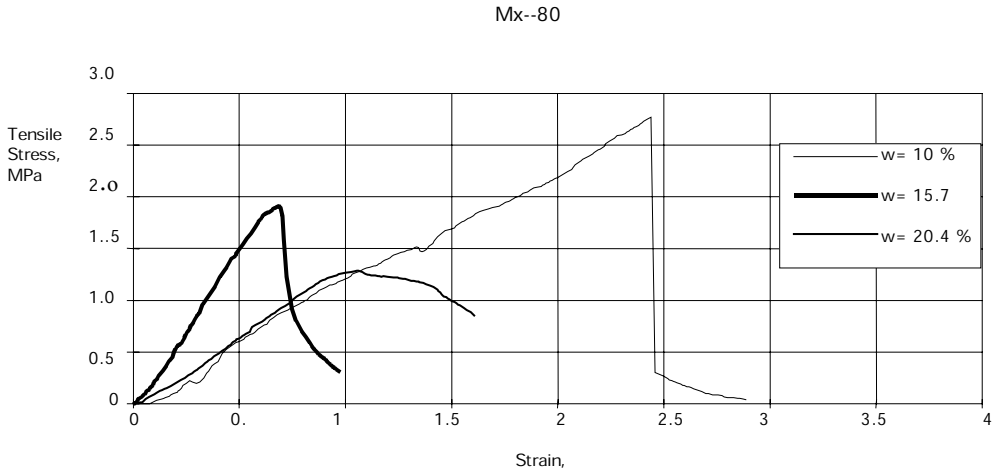

Figure 7-21. *Stress/strain behavior of MX-80 beams. Vertical axis gives the stress in MPa. The lowest and highest water contents gave the most ductile behavior, while the intermediate one gave a higher strain modulus and the smallest strain at failure /15/.*

Unsaturated and water saturated buffer – basic material model

Several material models for stress/strain analysis are being proposed for buffer clays, the one presently used for predicting the performance of MX-80 buffer being a coupled THM (Thermal/Hydro/Mechanical) finite element model that is adapted to the numerical code "ABAQUS" /16/, and for which a simplified expression of the stress conditions has been defined:

$$\bar{\sigma} = \sigma + \chi\, u_w \mathbf{I}. \qquad (7\text{-}1)$$

wher $\bar{\sigma}$ is the effective stress, σ the total stress, u_w the porewater pressure, χ a function of the degree of saturation (usual assumption χ=S_r), and I the unitary matrix.

For the *solids* a basic constitutive equation is expressed as:

$$d\tau^c = \mathbf{H} : d\varepsilon + \mathbf{g} \qquad (7\text{-}2)$$

where $d\boldsymbol{\tau}^c$ is the stress increment, **H** the material stiffness, $d\boldsymbol{\varepsilon}$ the strain increment and **g** is any strain-independent contribution (e.g. thermal expansion). **H** and **g** are defined in terms of the current state, strain direction, etc, and of the kinematic assumptions used to form the generalised strains.

For the pore fluid the constitutive equation is expressed as:

$$\frac{\rho_w}{\rho_w^0} \approx 1 + \frac{u_w}{K_w} - \varepsilon_w^{th}, \qquad (7\text{-}3)$$

where ρ_w is the density of the fluid, ρ_w^0 the density in the reference configuration, K_w the liquid's bulk modulus, and the ε-term temperature-induced strain.

The constitutive behaviour of the pore fluid follows Darcy's law, while vapour flow is modelled as a diffusion process driven by temperature gradients.

Heat conduction is assumed to be governed by the Fourier law. The conductivity can be completely anisotropic, orthotropic, or isotropic. The negative pore pressure u_w of unsaturated buffer material is a function of the degree of saturation S_r, independently of the void ratio.

$$u_w = f(S_r) \qquad (7\text{-}4)$$

The yield function is the relation between Mises' stress q and the plastic deviatoric strain ε_p^d for a specified stress path. The dilation angle determines the volume change during shear.

The mechanical behaviour is modelled by use of a non-linear Porous Elastic Model and Drucker-Prager Plasticity model. The effective stress theory as defined by Bishop is adapted to unsaturated conditions, introducing also a "moisture swelling" term.

The Porous Elastic Model implies a logarithmic relation between the void ratio e and the average effective stress p according to Equation (7-5).

$$\Delta e = \kappa \Delta \ln p \qquad (7\text{-}5)$$

where κ = porous bulk modulus
Poisson's ratio ν is also required.

The Drucker Prager Plasticity model makes use of the following parameters:

β = friction angle in the p-q plane
d = cohesion in the p-q plane
ψ = dilation angle
$q = f(\varepsilon^{d}_{pl})$ = yield function

Unsaturated and water saturated buffer – material parameters

1. The thermal flux is derived using the thermal conductivity (λ) and the specific heat c. Thermal data as function of void ratio e and degree of saturation S_r are obtained from the literature.

2. Porewater flux is taken to be in accordance with Darcy's law with the water pressure gradient as driving force both for unsaturated and saturated clay. The magnitude of the hydraulic conductivity K_p of partly saturated clay is a function of the void ratio, the degree of saturation S_r and the temperature:

$$K_p = (S_r)^{\delta} K \qquad (7\text{-}6)$$

where:

K_p = hydraulic conductivity of partly saturated soil (m/s)
K = hydraulic conductivity of completely saturated soil (m/s)
δ = exponent (usually between 3 and 10)

Data are obtained from the literature or by using examples in this chapter for:

- The hydraulic conductivity of water saturated material K as function of void ratio e and temperature T.
- Influence of degree of saturation S_r on the hydraulic conductivity K_p by the factor δ.
- Table of the matric suction u_w as a function of the degree of saturation S_r.

Water saturated buffer strength under undrained conditions

Equation (7-7) gives a generalized expression of the shear strength q as a function of the mean effective stress p:

$$q = ap^{b} \qquad (7\text{-}7)$$

where:

a = q for p = 1 kPa
b = inclination of curve in *logp/logq* diagrams

The number of data from experiments is limited but there seems to be an obvious difference between different clay types with respect to the key parameter a while b appears to be the same for all the materials (b=0.77). Table 7-11 illustrates the difference, which should be interpreted such that the shear resistance of Ca clay is twice as high as that of Na clay and that strengthening is induced by salt water. The difference between the two Na montmorillonite clays MX-80 and IBECO Na is insignificant as implied by the similar mineral contents. Figure 7-22 shows results from triaxial tests of a number of bentonite clays.

Table 7-11. The strength parameter a interpreted from triaxial tests /16/.

Clay	*a* (dimensionless)	Porewater
MX-80 (Na)	2.8	Distilled
IBECO (Na)	2.9	Distilled
MX-80 (Na)	3.5	3.5% NaCl
Moosburg (Ca)	5.5	Distilled

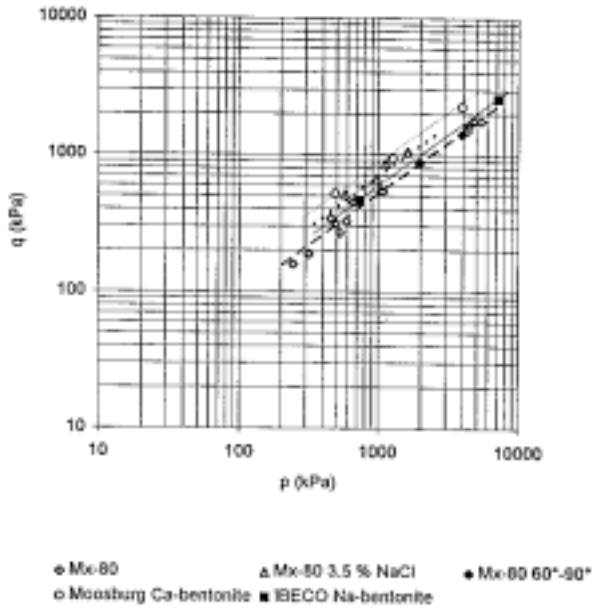

Figure 7-22. *Triaxial tests on bentonite buffer candidate materials /16/.*

Friction between bentonite and concrete or rock

A number of shear-box experiments with highly compacted MX-80 bentonite in contact with concrete and – in separate experiments – with sawed granite specimens – have shown that the shear strength of the contact can be expressed as in Equation (7-8):

$$t_{cont} = \sigma' tan\phi' \qquad (7\text{-}8)$$

where

t_{cont} = shear strength of the contact
σ' = effective normal stress, which is equal to the swelling pressure
ϕ' = friction angle of the contact zone

Experiments with the sodium-dominated MX-80 clay have shown that ϕ' is on the order of 15–20°, while tests on calcium-dominated smectite-rich clay have given friction angles of 8–12° /17/.

Water saturated buffer – long term creep

Purely empirical model

Different material models have been proposed for predicting creep strain of saturated MX-80 clay. A general material model is represented by the relationship in Equation (7-9), /16, 17/. It describes time-dependent strain as a function of the principal stress state and stress conditions at failure:

$$\dot{\gamma} = \dot{\gamma}_o e^{\alpha \frac{(\sigma_1-\sigma_3)}{(\sigma_1-\sigma_3)_{fe}}(-\alpha)\frac{(\sigma_1-\sigma_3)_0}{(\sigma_1-\sigma_3)_f}} \left(\frac{t}{t_r}\right)^n \quad (7\text{-}9)$$

where

t = time after stress change
t_r = reference time (10^5 s)
$(\sigma_1-\sigma_3)_0$ = reference deviator stress $[0.5\ (\sigma_1-\sigma_3)]$
$(\sigma_1-\sigma_3)_f$ = deviator stress at failure
$\dot{\gamma}$ = creep rate
$\dot{\gamma}_o$ = creep rate at time t_r
n and α = parameters derived from laboratory tests

Thermodynamically based model

A different approach based on thermodynamics and stochastic mechanics /18/, implies time dependence of the shear strain as in Equation (7-10):

$$d\gamma/dt = A\ T^a\ D^b\ (t+t_0) \quad (7\text{-}10)$$

where:

γ = angular shear strain
D = deviator (shear) stress
T = absolute temperature
a,b = exponents
t_o = term related to creep rate and evaluated as in Figure 7-23

A general expression for long term axial strain of a clay element assuming log time creep can be derived from Equation (7-11):

$$d\gamma/dt = \beta\ T\ D\ ln(t) \quad (7\text{-}11)$$

where:

γ = angular strain
β = strain parameter evaluated from undrained triaxial tests (3E-10 to 2E-8 K^{-1} kPa^{-1} for the density interval 1900 to 2100 kg/m^3 for MX-80)
D = deviator stress ($\sigma_1-\sigma_3$), kPa
T = temperature in K

This model is in principle of Eyring's type characterized by a time-dependent viscosity component and an elastic component, and yields creep curves of the commonly observed types as shown in Figure 7-24 /19/.

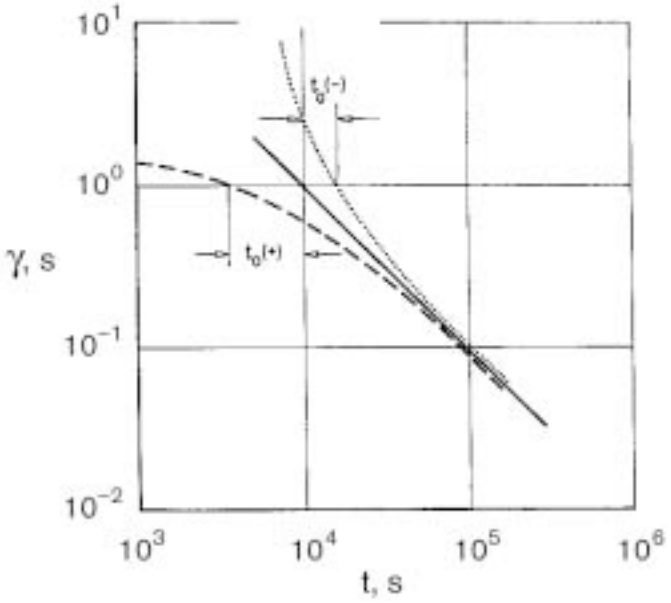

Figure 7-23. *Implication of the term t_o being a mathematical form for describing the form of the creep onset, i.e. the initial part of the creep strain rate at stress application assuming that it is ultimately proportional to log time /18/.*

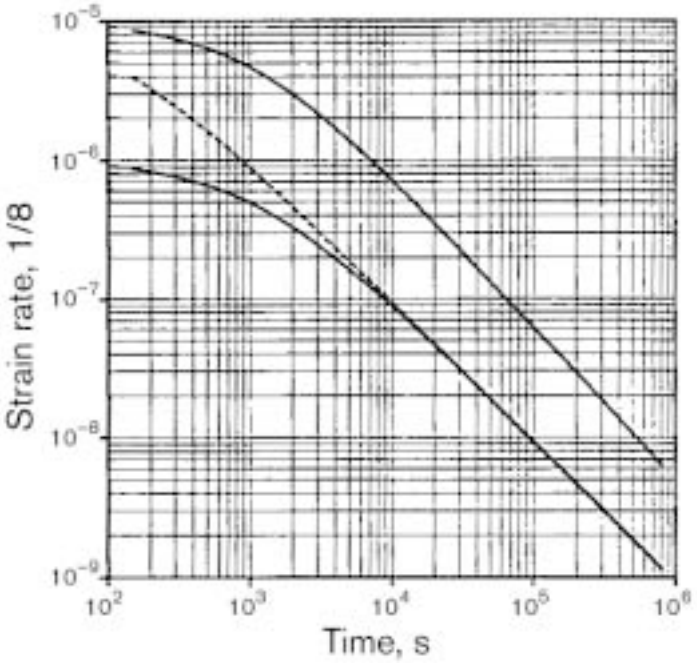

Figure 7-24. *Examples of theoretical creep curves derived from the Eyring-type rheological model /19/. The three curves are characterized by the following data sets (E=modulus of elasticity):*
Upper: E=10 MPa, η_o=E11 Pas, to=E3 s
Central: E=10 MPa, η_o=E11 Pas, to=E2 s
Lower: E=10 MPa, η_o=E12 Pas, to=E3 s

7.3.11 Thermal properties

Influence of water content

The heat conductivity depends on the amount of water in the clay. Commercially available bentonite like MX-80 is delivered with a water content (ratio of mass of water and solid matter) of 10–15%, which corresponds to 1 to 2 interlamellar hydrate layers, and compaction of such material to a dry density of 1500 kg/m^3 gives a heat conductivity of about 0.75 W/m,K /20/. Various tests have shown that an increase in the degree of water saturation from 50 to 100% raises the heat conductivity by around 100%.

Table 7-12 gives values illustrating the influence of the degree of water saturation of MX-80 clay /20/ and of the Czech RMN clay as reported by the Czech Technical University in Prague (CEG).

The reported data show that the RMN clay has a somewhat higher heat conductivity than MX-80 at incomplete fluid saturation while the difference is insignificant at a high degree of fluid saturation. Differences may be due to different particle organization, with respect to the thickness and interaction of stacks of lamellae, and to the distribution of porewater, which is not the same for equally smectite-rich clays in sodium and calcium form.

Influence of smectite content

A number of bentonites have been investigated with respect to their thermal properties and the investigations have led to some understanding of the importance of the mineral composition. Thus, addition of quartz powder and graphite have been shown to significally increase the heat conductivity but these additives will not be discussed here.

As to pure clays other than MX-80 there is information from comprehensive tests on a French candidate clay FoCa7 and from ongoing tests of the Czech candidate clay RMN as exemplified by Table 7-12. The FoCa7 clay contains about 90% mixed-layer kaolinite/smectite, 5% kaolinite and 5% smectite in beidellite form and is reported to have a thermal conductivity of about 1.6 W/m,K at 50–70% degree of water saturation /21/. Its microstructural constitution is similar to that of Ca-smectite.

Influence of stress and temperature

The effective stress and temperature are known to have a certain, rather small effect on the heat conductivity. A high effective stress implies a high density which has an increasing effect on the thermal conductivity. Increased temperature causes a reduction in swelling pressure, which has the opposite effect except if there is an external pressure, which would cause consolidation and an increase in density. Under a thermal gradient heat transfer will be aided by convection, which is most important at low degrees of fluid saturation.

Table 7-12. Thermal data of RMN and MX-80 clays.

Clay type	Dry density, kg/m^3	Degree of water saturation, Sr, %	Heat conductivity, λ W/m,K
RMN	1475	65	1.07
RMN	1597	99	1.22
MX-80	1570	70	0.90
MX-80	1700	98	1.14

7.3.12 Colloid filtering

Colloidal particles like minute smectite particles, organic objects, and various crystalline and amorphous precipitates can be moved by water flowing through interconnected voids if the density of the clay is very low, i.e. less than 1500 kg/m^3 at saturation, provided that high hydraulic gradients prevail. For the high density of canister-embedding buffer such transport is possible only at the initiation of the water saturation process but can be important in this phase (cf Figure 7-11). After complete saturation colloid filtering is assumed to be very effective but this remains to be validated experimentally /22/.

A study of diffusive transport of large organic molecules in the form of lignosulfonate and humic acid with special respect to their capacity of transporting cationic cations like Sr^+ has shown that such species in colloidal form do diffuse through very soft smectite clay. Their negative surface charge means that they do not sorb on the clay minerals and their diffusive transport capacity is estimated to be similar to that of the ions Cl^- and I^- at low ionic strength /23/.

7.3.13 Microbiological filtering

Bacteria, of which sulphate-reducing ones are of particular importance to engineered barriers of SKB-type, may stay alive and develop in soft smectite clay. They usually carry a negative surface charge and can therefore move through clay as large organic molecules like humus colloids. However, there are limitations because of the hydration conditions and of the very limited void space in dense buffer clay /24, 25/. At higher density than 1800 kg/m^3 of clay of MX-80 type the small size of interconnected voids and the limited access to free water prevent bacteria from moving and staying alive. Only spores are therefore believed to be operative but the working hypothesis is that there will ultimately be eradication of all life forms in the buffer /25/.

7.4 Clay/ballast mixtures

7.4.1 General

Backfilling of drifts, tunnels and shafts in a repository will be made by use of materials with required properties: 1) low hydraulic conductivity and 2) low compressibility. For simple blocking of certain passages like adits and transport ramps in order to make unwanted access to the repository difficult after sealing, muck from blasting or muck from TBM operations in the construction phase may be sufficient. However, material with low hydraulic conductivity and an ability to expand and support rock will be needed for most other purposes, like backfilling of deposition tunnels of KBS-3 type /2/. For this repository concept it is necessary to use backfills with a low compressibility since the upward pressure of buffer clay can otherwise make it expand upwards rather much on the expence of the backfill by which the density of the upper part of the buffer will drop.

This chapter deals with the properties of backfill materials that consist of clay/ballast mixtures. Natural clays with no processing except crushing, sieving and drying represent an option for backfilling and clays like the Friedland Ton that has been described earlier in this chapter may well be considered as candidate materials.

7.4.2 Processing

Preparation of backfills for achieving effective sealing capacity requires that the various components are thoroughly mixed, applied without separation, and compacted to get a sufficiently homogeneous and dense fill. These matters are described and discussed in Chapter 10, while typical physical properties of mixtures of bentonite and ballast are given in this section. Such backfills are suitably applied by pushing the material into the space forming inclined layers which are compacted before the next layer is applied etc. This is a rather time-consuming process and the use of precompacted blocks of natural clay is hence an option.

7.4.3 Granular composition

The principles for composing and preparing backfills have been outlined in Chapter 5. For validating the theoretically derived expressions for the hydraulic conductivity, which are based on the assumption of a uniform density of the clay component, it is required that the grain size distribution of clay/ballast mixtures be such that the clay grains fill up the voids between the differently sized ballast grains (Figure 7-25). The overall aim is to select a size distribution of the clay powder that makes the grains fit into and occupy all the differently sized ballast voids

The bentonite component of backfills of KBS-3 type must be in sufficiently fine-grained form to fit into the voids between the ballast grains. This can be achieved by using very finely ground powder, which offers some practical difficulties like dusting in the mixing process and also the formation of a clay coating of the ballast grains when the finely dispersed smectite material comes into contact with the hydrated surface of the ballast grains. The latter process means that part of the clay component is used up as a coating of the ballast grain surfaces and may leave too little for filling voids.

Using a microstructural model (GMM) developed for bentonite /24/ and taking the clay in the ballast voids to be uniformly distributed with a density that is controlled by the void size of the ballast materials one obtains diagrams of the form shown in Figures 7-26 and 7-27. This sort of microstructural analysis can be made for any ballast material for estimating the required minimum clay content for 100% filling of the ballast voids /25/.

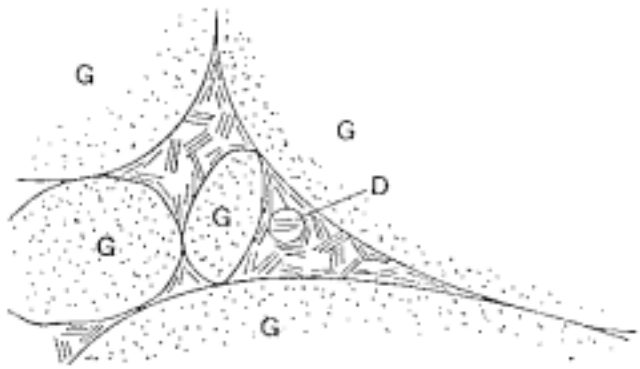

Figure 7-25. *Schematic picture of the microstructure of bentonite-poor mixtures. G=ballast grains, D=clay powder grains /2/.*

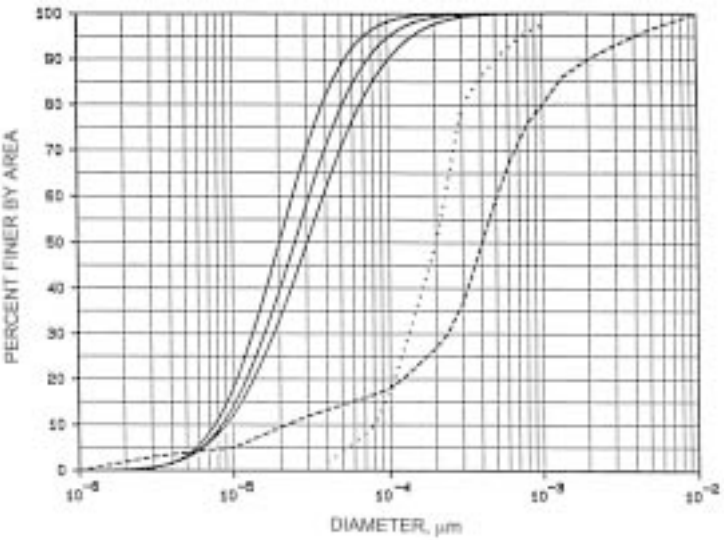

Figure 7-26. *Void size distributions assumed for the Stripa Buffer Mass Test (BMT) ballast mixed with 10% granulated MX-80 bentonite at 100% (solid left), 87.5% and 75% (solid right) compaction expressed in terms of modified Proctor density. Also the grain size distribution of the ballast material (dashed line) and of the granulated bentonite material (dotted line) are shown in this plot.*

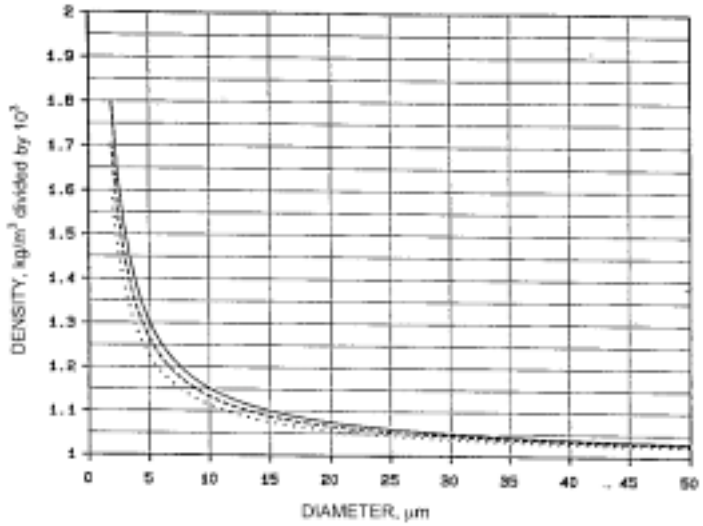

Figure 7-27. *Relationship between the diameter of the gel-filled voids of the ballast grain system, and the density of the gel filling. The curves refer to 10% bentonite content and from right to left 100%, 87.5% and 75% compaction.*

7.4.4 Hydraulic conductivity

Predictions

Applying the theoretical expressions in Chapter 5 for the net hydraulic conductivity of backfills consisting of mixed clay and ballast one can predict the hydraulic conductivity of any mixture of ballast and bentonite by using the relationships between the size of the ballast voids and the density of the clay confined in these voids as given by the diagrams in Figures 7-26 and 27. They refer to different degrees of compaction, which is a simple measure of the compaction effort and achievable density. Such calculations have led to the relationships in Figure 7-28 for the ballast in Figure 7-26 and different bentonite contents assuming 100% Standard Proctor compaction. The diagrams show the factor by which the hydraulic conductivity exceeds E-11 m/s, i.e. 2 to 20 times for MX-80 and 100 to 5 million times for Ca bentonite, assuming electrolyte-poor water. Na backfill with as little as 5% sodium bentonite of MX-80 type will not have a higher hydraulic conductivity than about 2E-10 m/s, while Ca bentonite backfills can have a conductivity of up to 5E-5 m/s for the same clay content. The minimum values are 2E-11 m/s and E-9 m/s, respectively.

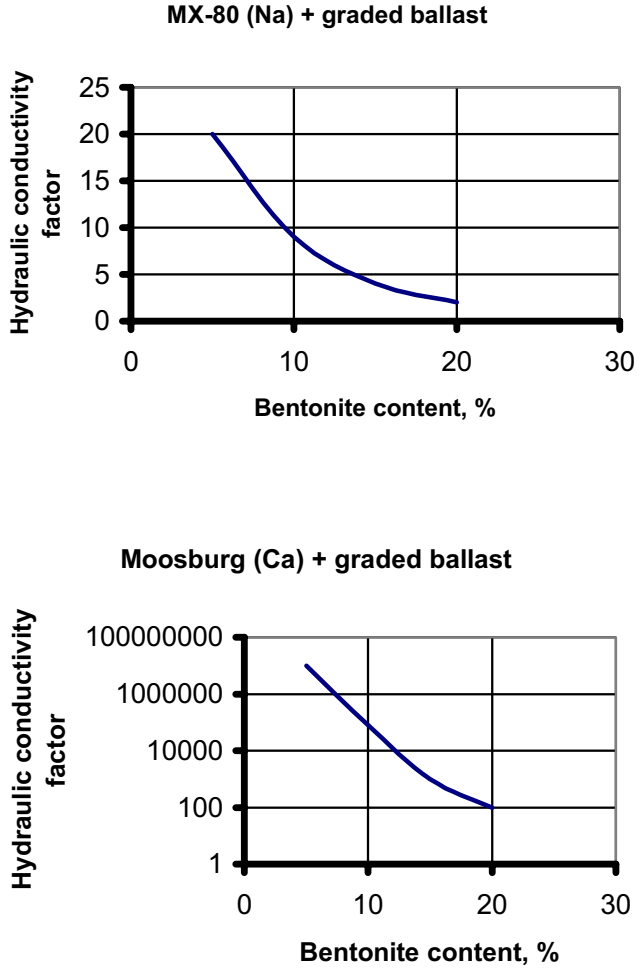

Figure 7-28. *Calculated deviation from the reference conductivity E-11 m/s of mixtures of ballast (cf Figure 7-26) and Na and Ca bentonite for different bentonite contents. The hydraulic factor multiplied by E-11 m/s gives the theoretically derived conductivity. (100% Proctor compaction, electrolyte-poor water).*

Experimental

Materials

A number of experiments that have shed light on the performance of clay/ballast mixtures and indicate the importance of various granulometric factors have been made. One study of particular interest concerned mixtures of GEKO/QI bentonite, which is very similar to IKO bentonites, and two ballast types with different grain shape characteristics. The ballasts had the compositions shown in Figure 7-29. Ballast 1 represented commercially available "Silver sand" and Ballast 2 sieved crushed granitic rock.

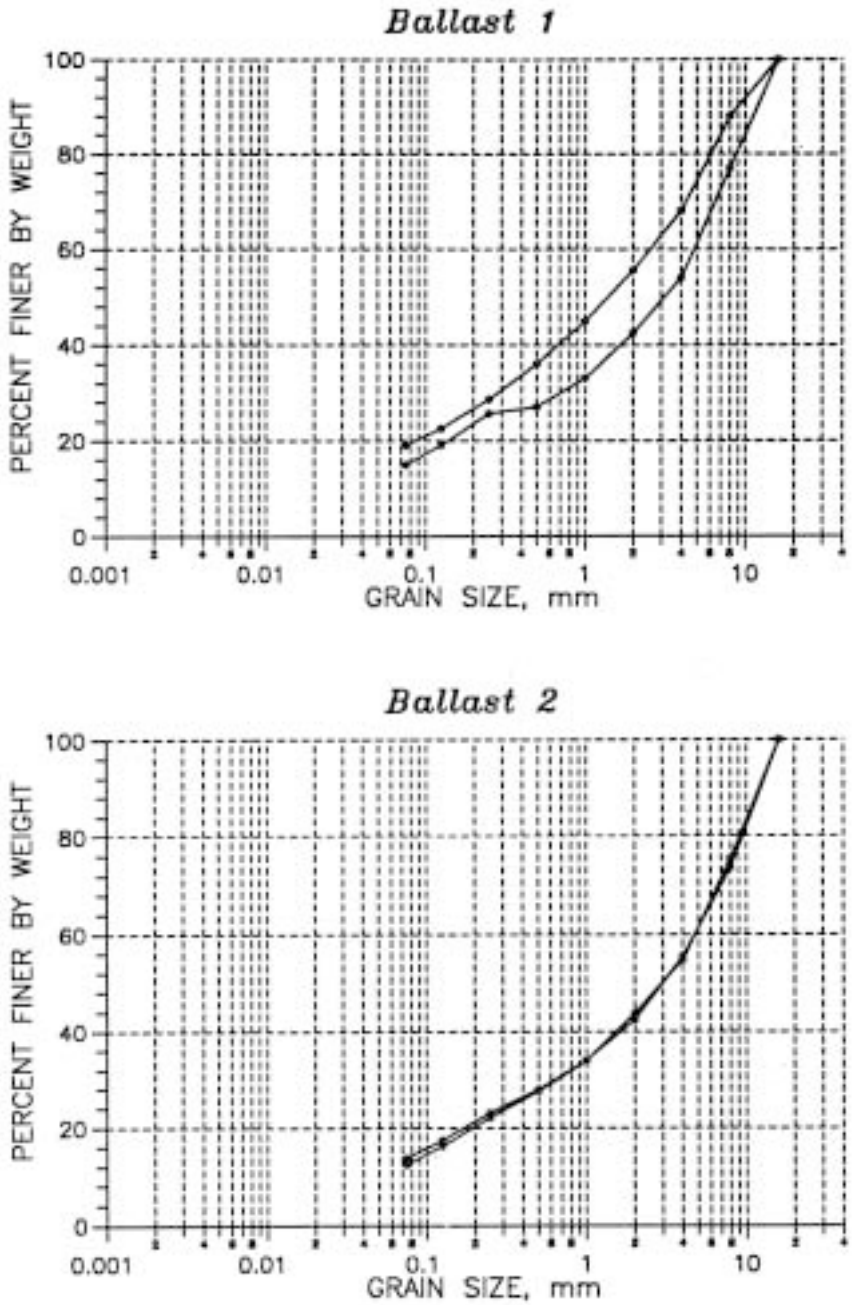

***Figure* 7-29.** *Grain size distributions of Ballast 1 and Ballast 2. Two samples of each material were analyzed (after Pusch and Hökmark).*

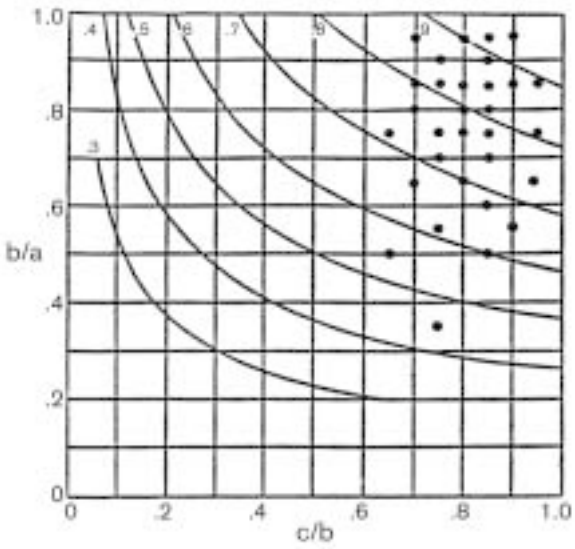

Figure 7-30. *Graph showing the sphericity of Ballast 1 grains. The curves represent sphericity values from 0.3 to 0.9.*

The grain shape of Ballast 1, which had practically no water content, was estimated by use of light microscopy and expressed in terms of *sphericity* and *roundness* (cf Chapter 6, Part 1 of the Handbook). Figure 7-30 shows plots of the ratios *b/a* and *c/b* of an arbitrarily selected grain assemblage. As expected, the sphericity of the coastal sediment from which "Silver sand" is manufactured, is found to be high.

The surface smoothness, of which the roundness is a measure, is of importance as well for the possibility of clay grains to move into the most narrow space between ballast grains. Ballast 1 grains have a very profound roundness and they can be termed "rounded or well rounded without sharp edges and corners" using common terminology. Microscopical analyses showed that quartz formed at least 95% of all the "Silver sand" grains.

The examination of the grain shape of Ballast 2 types showed that the grains deviated considerably from spherical form and that the finest fraction had a good deal of particles that were "bladed" and "rod like". For the crushed rock the majority of the grains plotted in diagrams with *b/a* and *c/b* on the axes gave sphericity data in the interval 0.3 to 0.7.

As to roundness, the particles belonging to the Ballast 2 had a very irregular surface shape with sharp edges and corners, hence belonging to classes A and B (angular or subangular), cf Part 1 of the Handbook.

The mineral composition of Ballast 2 was estimated in conjunction with the microscopy and it turned out that all fractions contained quartz, feldspars and heavy minerals in approximately the same proportions as in granite, which was the source material.

Preparation

Mixtures consisting of the two ballast types and bentonite with approximately the same grain size distribution as MX-80 and a water content of 13% were prepared by use of a mixer in the laboratory. The solids were mixed in air-dry condition and the mixtures compacted in oedometers with 10 cm diameter. The bulk densities, which were a few percent higher than the dry densities, are given in Table 7-13 together with the evaluated hydraulic conductivity at percolation with distilled water.

Table 7-13. Composition and compaction data and evaluated hydraulic conductivity (K).

Ballast type	Bentonite content, %	Dry density, kg/m³	Density at saturation, kg/m³	K m/s	Estimated degree of Proctor compaction, %
1	10	1750	2100	E-9	90
1	10	1900	2200	4E-11	100
1	20	1770	2100	E-10	90
1	20	2010	2270	E-11	100
2	10	1970	2240	9E-10	90
2	10	2180	2370	2E-11	100
2	20	1760	2110	E-11	95
2	20	1880	2180	E-11	100

The data in Table 7-13 show that all materials compacted to 100% Proctor density had approximately the same conductivity for the respective bentonite content. The densities are higher for most of the mixtures with crushed rock (Ballast 2), which should have led to lower conductivities but the finest debris is concluded to have been enriched along the surfaces of the ballast grains and to have created coatings with a higher conductivity than of ordinary clay matrix (cf Chapter 5). The conductivities are on the same order of magnitude as the predictions represented by MX-80 with graded ballast shown in Figure 7-28.

General aspects of the composition of clay/ballast mixtures

The examples of the hydraulic conductivity in this chapter show that it is possible to achieve a low hydraulic conductivity applying the principle of composing clay/ballast mixtures in such a fashion that the size and frequency of voids that are not clay-filled are minimized. Particularly good results have been obtained in the laboratory by selecting properly graded air-dry components and compacting them effectively.

As outlined in Chapter 5, the basic principle of proper composition of soil for bringing down the hydraulic conductivity is to try to get a grain size distribution with a very fine "tail", i.e. the D_5 should be very low and this is also what crushed rock provides when using it as ballast material but the finest debris appears to attach to the larger ballast grains with the abovementioned negative effect on the hydraulic conductivity. However, there are natural soils that have much fines in them and till (moraine) can be very suitable as demonstrated by large scale experiments conducted by the Swedish State Power Board /2/. Figure 7-31 shows the grain size distribution of the silty till that was used and to which 3 and 5% very fine-grained Na bentonite was added in separated tests. For the 3% bentonite mixture the density after water saturation was 2230 kg/m³ and the hydraulic conductivity 5E-11 m/s, while for the 5% bentonite mixture the corresponding values were 2290 kg/m³ and 5E-12 m/s, respectively. D_5 of the till was about 0.006 mm, which implies effective filling of voids between larger ballast grains by smaller ones and hence a minimum of clay required to occupy the remaining very small voids in the ballast.

It is also possible to prepare mixtures at optimum water content, which means that water must be added to reach the maximum density (cf Part 1 of the Handbook). This technique is used in ordinary road- and dam construction and may well be applied also in the

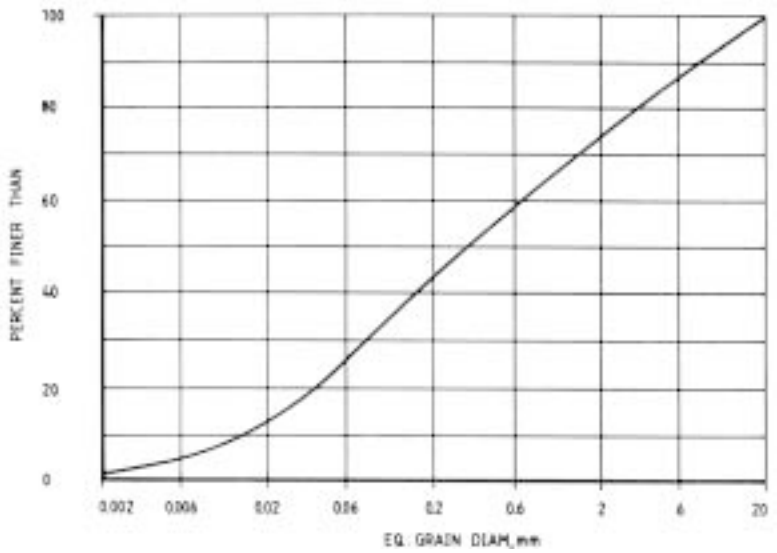

Figure 7-31. *Till used for ballast in field preparation of bentonite mixtures from which samples were taken for laboratory testing (after Pusch and Alsterlind).*

preparation of backfills for repositories, but the addition of water is a complicating and time-consuming operation that may also have a negative effect on the microstructural homogeneity.

Influence of porewater salinity

The fact that the density of the clay fillings in the voids between ballast grains is rather low, i.e. 1300–1600 kg/m^3, even if the average density of the clay/ballast mixture is high, makes the mixtures sensitive to high electrolyte contents of percolates as concerns the hydraulic conductivity. In general the hydraulic conductivity is raised by one to two orders of magnitude when the percolate is changed from distilled water to sea water because of the widening of the voids in the clay component caused by coagulation (cf Section 7.2.2 in this Chapter).

A similar effect appears if Ca smectite is used for preparing clay/ballast mixtures or – although to a limited extent – by percolating mixtures with Na-saturated smectite with Ca-rich solutions. The hydraulic conductivity can be as drastically increased as illustrated in the lower diagram in Figure 7-28, which means that the content of Ca bentonite should be at least 30–40% to reach conductivities lower than E-10 m/s for 100% Proctor compaction.

Influence of hydraulic gradient and heating

Parts of the clay fillings of the voids between the ballast grains are soft, which causes erosion and transport of fine particles at high hydraulic gradients. Clogging of flow paths and thixotropic reformation of clay particle networks will be caused, by which the net conductivity is reduced and temporary changes in flow rate take place (Figure 7-32).

Heating by a few tens of centigrades is expected to have the same effect as on pure buffer clay, i.e. to make the clay component more homogeneous. Hence, also the entire mixture is believed to become more homogeneous but the effect is probably not very significant.

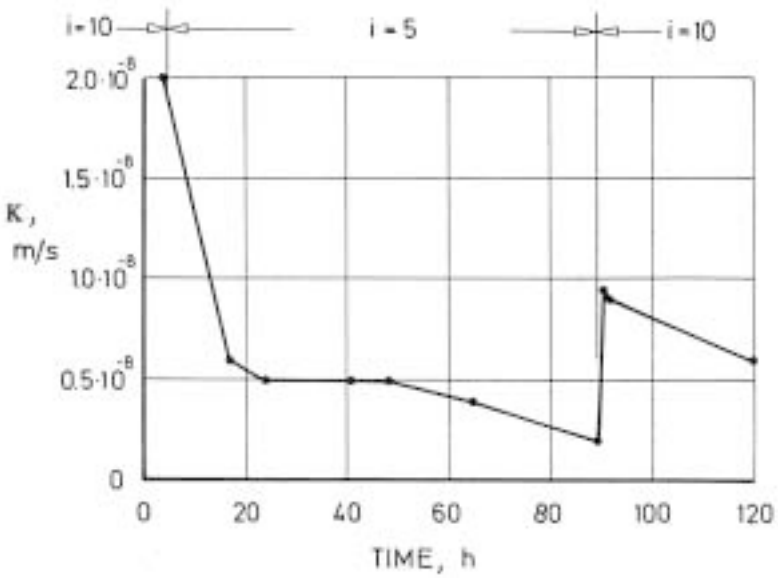

Figure 7-32. *Change in evaluated conductivity of clay-poor backfill material resulting primarily from particle transport. The hydraulic gradient is termed i.*

7.4.5 Gas conductivity

Experiments as part of SKB's research program included gas penetration tests and they consistently showed very low critical gas pressure values and very quick gas flow once gas had penetrated the material /2/. The critical pressure for backfills with 10–30% bentonite was up to a few tens of kilopascals, which approximately corresponds to the swelling pressure.

7.4.6 Ion diffusivity

Very little systematic work has been made on diffusive ion transport through clay/ballast mixtures. For very low contents of smectite clay, i.e. less than 10–20%, the diffusivity of both cations and anions is expected to be determined primarily by the porosity of the system of ballast particles with insignificant retardation due to sorption and tortuosity, while a higher clay content than 20–30% causes additional reduction in diffusivity due to the clay content. The diffusive transport capacity is believed to be roughly proportional to the clay content.

7.4.7 Swelling properties

Low-electrolyte porewater

The swelling properties are determined by the clay content and the density, or void ratio, of the clay fillings of the ballast voids. Typical data for material saturated with distilled water are given in Table 7-14, which refers to the same type of materials as in Table 7-13, i.e. MX-80 bentonite mixed with rounded and angular ballast materials. The same aspects apply as on the hydraulic conductivity, i.e. that the effective component – the clay – has a very low density when the bulk density of the mixture is low. It is in fact fully expanded and does not exert a significant pressure when its density is less than about 1600 kg/m^3, which is nearly always the case when the bulk density of the water saturated mixture is below 2100 kg/m^3.

Table 7-14. Swelling pressure p_s of saturated backfill materials /26/.

Ballast type	Bentonite content, %	Dry density, kg/m³	Density at saturation with distilled water, kg/m³	p_s kPa
1	10	1420	1890	20
1	10	1750	2110	150
1	10	2150	2350	400
1	20	1270	1800	50
1	20	1420	1890	100
1	20	1580	1995	200
2	10	2180	2375	575

The expandability of 10% MX-80 bentonite mixtures at 100% Proctor compaction has been found to be about 3% for a dry density of 2150 kg/m³, while for lower dry densities than 1900 kg/m³, the expansion potential is negligible. For mixtures with 20% bentonite content the swelling is expected to be at least twice as high as that of the 10% mixture for the same dry density. Even at much lower densities, mixtures with 20% bentonite have an appreciable expandability, which explains why backfills with only 20% Na bentonite backfilled in tunnels maintain contact with the tunnel roof even when the average dry density is not higher than about 800 kg/m³ provided that the groundwater is poor in electrolytes /27, 28/.

High-electrolyte porewater

While the swelling pressure for ordinary backfill densities, i.e. 2000 to 2100 kg/m³ after saturation with low-electrolyte groundwater, can be sufficiently high to support the roof of tunnels etc, salt water makes it drop significantly. Thus, for seawater the swelling pressure is markedly reduced especially if the density is low, and it totally disappears in mixtures with 10–15% Na bentonite at bulk dry densities of less than 2000 kg/m³. The impact of salt water on the swelling pressure of natural clays with a moderate content of expandables like the Friedland Ton is much smaller as discussed earlier in this chapter.

7.4.8 Rheological properties

The compressibility of the backfill, which, together with the hydraulic conductivity, is the major physical parameter because it determines the upward expansion of the buffer in the deposition holes and the displacement of the rock surrounding it. It depends on the porosity (void ratio) as expressed by the empirical compression parameters m and β (cf Part 1 of the Handbook). In principle, uniaxial compression of an element Δh with thickness h is expressed as:

$$\Delta h = \frac{h}{m\beta}\left[\left(\frac{\sigma'}{\sigma' j}\right)^{\beta} - \left(\frac{\sigma_0{}'}{\sigma_j{}'}\right)^{\beta}\right] \qquad (7\text{-}12)$$

where

m,β = strain parameters
σ' = pressure increment
σ_0' = effective pressure prior to compression
σ_j' = reference stress (100 kPa)

The diagram in Figure 7-33 illustrates the compression of backfill with 10% MX-80 clay and 90% ballast of Ballast 1 type as evaluated from laboratory compression tests using a 0.25 m diameter Rowe oedometer. The curves demonstrate that poorly compacted backfill exposed to a swelling pressure of a few MPa exerted by contacting MX-80 buffer can be several decimeters. The data emerge from tests with freshly prepared "dry" backfills, i.e. before hydration in tunnels and shafts has taken place since this is the state in which they are most sensitive to external pressure. After complete saturation compression is very slow and proceeds only until the effective (grain) pressure is equal to the swelling pressure of the contacting buffer, which may be saturated before the backfill.

Table 7-15 gives values of the compression parameters m and β as evaluated from oedometer tests with bentonite/ballast mixtures with different bentonite contents and ballast types.

7.4.9 Thermal properties

As for buffer materials the heat conductivity strongly depends on the water content but the thermal properties of the ballast material also play an important role. Thus, pure quartz serves as a much more effective heat conductor than feldspar-rich material like most crushed rock and was the ballast type initially proposed for the KBS-3 concept. Table 7-16 illustrates that the thermal conductivity of largely water saturated mixtures of fine-grained Na bentonite (SPV) mixed with quartz sand is considerably higher than for pure bentonite. This is the case also for lower degrees of saturation.

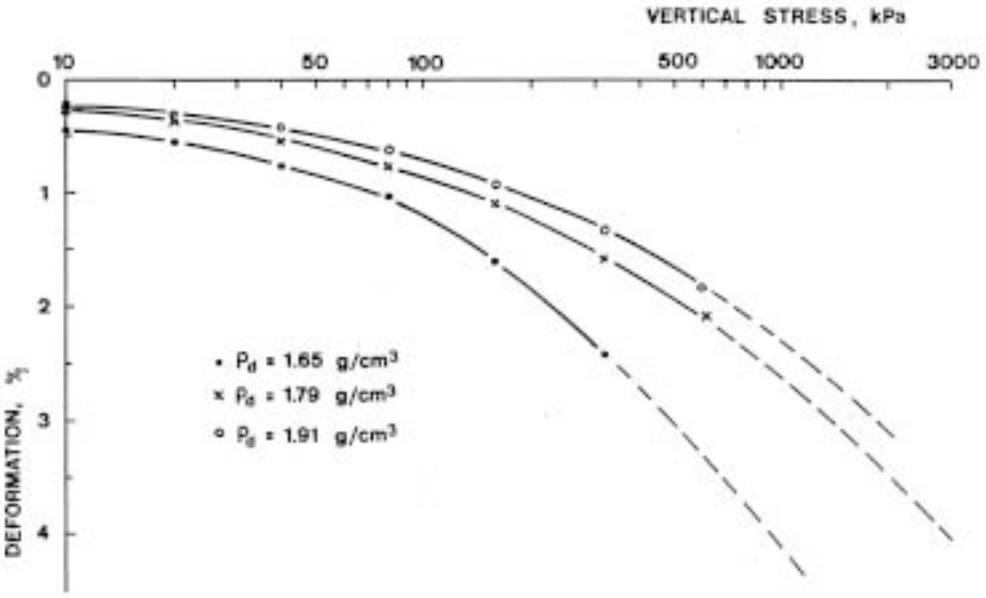

Figure 7-33. *Uniaxial compression of mixture of MX-80 clay and well graded ballast /29/.*

Table 7-15. Compressibility of unsaturated backfill materials /29/.

Ballast type	Bentonite content, %	Dry density, kg/m³	Water content, %	m MPa	β
1	10	2150	4	200	0.75
1	10	1650	10	105	0.73
1	10	1790	10	167	0.73
1	10	1910	10	199	0.67
2	15	1300	14.8	20	0.73
2	15	1600	14.5	60	–
2	15	1900	13–15	160	0.74

Table 7-16. Thermal conductivity (λ) as a function of the void ratio (e) and the degree of water saturation (S_r) of mixtures of SPV200 and quartz sand /20/.

Mixture	e	S_r %	λ W/m,K
SPV/Sand (Ratio 50/50)	0.45	95	1.78
SPV/Sand (Ratio 30/70	0.39	93	2.51

7.5 Physical stability

7.5.1 General

Physical stability has two meanings in the context of preparation of buffer and backfill materials: the coherence and strength of compacted blocks, and the piping and erosion resistance of soft clays like clay-based grouts and the bentonite/ballast mixtures. Clays with a density at complete fluid saturation exceeding 1600–1700 kg/m³ are usually not sensitive to piping and erosion.

7.5.2 Clay/ballast mixtures

Dispersion of expansive clays is known to be affected by the so-called sodium adsorption ratio (*SAR*), which is defined as:

$$SAR = Na/[(Ca + Mg)/2]^{1/2} \quad (7\text{-}13)$$

where the chemical symbols represent the respective amount of adsorbed cation /25/. The dispersibility of such clays is also related to the parameter *ESP*:

$$ESP = (Na/\text{total exchange capacity}) \times 100 \quad (7\text{-}14)$$

where the exchange capacity is expressed in milliequivalents per 100 g dry clay. Very low *SAR* and *ESP* values (<5) are typical of non-dispersive clays, while higher values than 15 characteristically point to strong slaking. Experience from pinhole tests shows that clays tested with sodium ions occupying more than about 10% of the exchange complex exhibit dispersion provided that the electrolyte concentration of the fluid is lower than 10^{-3} N.

Piping and erosion may be of importance for the homogeneity of smectitic backfills since high hydraulic gradients that prevail in the peripheral parts of the backfill at and shortly after the application in the tunnels may cause dispersion and washing out of fine particles, particularly from smectite aggregates if the flow rate of water exceeds a critical value /30/.

Considering first ballasts, ordinary filter criteria imply that migration of smaller grains into the voids between larger ones is largely eliminated if the network of larger grains does not contain voids that let smaller ones through. This requires Fuller- or till-type size distributions with no discontinuities of the part of the curves that represent D<0.1 mm.

For bentonite/ballast mixtures the situation is different because the clay gel in the voids between ballast grains can be disrupted and release a large number of small stacks under high hydraulic gradients. They can be transported in the direction of percolating water from the rock in conjunction with the saturation of the backfill. This process may be critical because the hydraulic gradient will initially be very high.

Experimental investigations using microscopy and special equipment for determination of the resistance to piping and erosion have demonstrated that there is a critical gradient for "hydraulic fracturing" of soft clay gels, like those located in the voids between ballast grains /31, 32/. Typical data are given in Table 7-17. The tests demonstrate that the critical gradient is in the range of 30–50 (pressure difference in meters per meter) for very soft Na bentonite and that it increases very significantly with increasing density. For Ca clay of low density the critical gradient is even lower and for values on the order of 35–40 it is required that the density is raised to about 1400 kg/m^3.

For very effectively compacted clay/ballast mixtures with a high clay content the density of the clay filling of the ballast voids can be sufficiently high to eliminate the risk of piping and erosion but for low bulk densities and clay contents the density of the clay phase may be in a critical range as illustrated by the fact that the clay density may be as low as 700 kg/m^3 in moderately compacted clay/ballast mixtures with a clay content of 10%.

Table 7-17. Critical hydraulic gradients yielding piping of water saturated clay. w=water content, ρ_s=density, F=pressure fluid /31/.

ρ_s, kg/m^3 (saturated)	Fluid*	Critical gradient
Na-dominated		
1080	Dist	30–40
1080	FF	50–55
1080	Sea	50
1140	Dist.	40
1140	FF	35
1140	Sea	40
Ca-dominated		
1380	Sea	35
1380	FF	40

* Dist=Distilled water, FF=Strongly brackish (11 000 ppm), Ca-dominated solution, Sea=Seawater (36 000 ppm).

7.6 References

/1/ **Yong R N, Mohamed A M O, 1992.** A study of particle interaction energies in wetting of unsaturated expansive clays. Can. Geot. Jour., Vol 29 (pp 1060–1070).

/2/ **Pusch R, 1994**. Waste Disposal in Rock. Developments in Geotechnical Engineering, 76. Elsevier Publ. Co.

/3/ **Yong R N, 2002.** Personal communication.

/4/ **Pusch R, Börgesson L, Erlström M, 1987.** Alteration of isolating properties of dense smectite clay in repository environment as examplified by seven pre-Quaternary clays. SKB TR 87-29. Svensk Kärnbränslehantering AB.

/5/ **Pusch R, 2001.** The microstructure of MX-80 clay with respect to its bulk physical properties under different environmental conditions. SKB TR-01-08. Svensk Kärnbränslehantering AB.

/6/ **Pusch R, 2002.** Physical properties of Czech buffer candidate RMN. SKB Technical Report (in print).

/7/ **Pusch R, 2001.** Experimental study of the effect of high porewater salinity on the physical properties of a natural smectitic clay. SKB TR-01-07. Svensk Kärnbränslehantering AB.

/8/ **Horseman S T, Harrington J F, 1997.** Study of gas migration in MX-80 buffer bentonite. Nat. Envir. Research Council, British Geol. Survey. Report WE/97/7.

/9/ **Brandberg F, Skagius K, 1991**. Porosity, sorption and diffusivity data compiled for the SKB 91 study. SKB TR 91-16. Svensk Kärnbränslehantering AB.

/10/ **Kato H, Muroi M, Yamada N, Ishida H, Sato H, 1995.** Estimation of effective diffusivity in compacted bentonite. In: Murakami T, Ewing R C (Ed). Scientific Basis for Nuclear Waste Management XVIII. Mat. Res. Soc. Symp. Proc., Vol 353, MRS Pittsburgh (pp 277–284).

/11/ **Muurinen A, Lehikoinen U, 1995.** Evaluation of phenomena affecting diffusion of cations in compacted bentonite. Report YJT-95-05. Voimayhtiöiden Ydinjätetoimikunta, Helsinki.

/12/ **Pusch R, 1999.** Clay colloid formation and release from MX-80 buffer. SKB TR-99-31. Svensk Kärnbränslehantering AB.

/13/ **Pusch R, 1982.** Mineral-water interactions and their influence on the physical behavior of highly compacted Na bentonite. Can. Geot. Jour., Vol 19 (pp 381–387).

/14/ **Pusch R, 2001.** Can the water content of highly compacted bentonite be increased by applying a high water pressure? SKB TR-01-33. Svensk Kärnbränslehantering AB.

/15/ **Johannesson L-E, Börgesson L, Sandén T, 1995.** Compaction of bentonite blocks. SKB TR 95-19. Svensk Kärnbränslehantering AB.

/16/ **Börgesson L, Johannesson L-E, Sandén T, Hernelind J, 1995**. Modelling of the physical behaviour of water saturated clay barriers. Laboratory tests, material models and finite element application. SKB TR 95-20. Svensk Kärnbränslehantering AB.

/17/ **Börgesson L, Hernelind J, 1999.** Coupled thermo-hydro-mechanical calculations of the water saturation phase of a KBS-3 deposition hole. SKB TR-99-41. Svensk Kärnbränslehantering AB.

/18/ **Pusch R, Adey R, 1999.** Creep in buffer clay. SKB TR-99-32. Svensk Kärnbränslehantering AB.

/19/ **Pusch R, Börgesson L, Erlström M, 1987.** Alteration of isolating properties of dense smectite clay in repository environment as exemplified by seven pre-Quaternary clays. SKB TR-87-29. Svensk Kärnbränslehantering AB.

/20/ **Börgesson L, Fredrikson A, Johannesson L-E, 1994**. Heat conductivity of buffer materials. SKB TR 94-29. Svensk Kärnbränslehantering AB.

/21/ **Pusch R, Karnland O, Lajudie A, Lechelle J, Bouchet A, 1993.** Hydrothermal field test with French candidate clay embedding steel heater in the Stripa mine. SKB TR-93-02. Svensk Kärnbränslehantering AB.

/22/ **Cheung S C H, Yu R, 2001.** The effects ofdensity and hydraulic gradient on clay permeability. Proc. Int. Symp. on Suction, Swelling, Permeability and Structure of Clays. Clay Science for Engineering, Adachi K, Fukue M (Ed), Shizuoka, Japan. A A Balkema/Rotterdam/Brookfield.

/23/ **Wold S, Eriksen T, 2000.** Diffusion of organic colloids in compacted bentonite. SKB TR-00-19. Svensk Kärnbränslehantering AB.

/24/ **Pusch R, Karnland O, Hökmark H, 1990.** GMM – A general microstructural model for qualitative and quantitative studies of smectite clays. SKB TR-90-43. Svensk Kärnbränslehantering AB.

/25/ **Pedersen K, 2000.** Microbial processes in radioactive waste disposal. SKB TR-00-04. Svensk Kärnbränslehantering AB.

/26/ **Pusch R, 1995.** Consequences of using crushed crystalline rock as ballast in KBS-3 tunnels instead of rounded quartz particles. SKB TR-95-14. Svensk Kärnbränslehantering AB.

/27/ **Pusch R, Börgesson L, Nilsson J, 1982**. Buffer Mass Test – Buffer Materials. Stripa Project Internal Report 82-06. Svensk Kärnbränslehantering AB.

/28/ **Pusch R, Börgesson L, Ramqvist G, 1985**. Final Report of the Buffer Mass Test – Volume II: test results. Stripa Project Technical Report 85-12. Svensk Kärnbränslehantering AB.

/29/ **Börgesson L, Johannesson L-E, Fredrikson A, 1993.** Laboratory investigation of highly compacted bentonite blocks for buffer material. Compaction technique and material composition. SKB Djupförvar Projekt Rapport PR 44-93-009. Svensk Kärnbränslehantering AB.

/30/ **Pusch R, 1983.** Stability of bentonite gels in crystalline rock – Physical aspects. SKBF/KBS Technical Report 83-04. Svensk Kärnbränslehantering AB.

/31/ **Pusch R, Erlström M, Börgesson L, 1987**. Piping and erosion phenomena in soft clay gels. SKB TR 87-09. Svensk Kärnbränslehantering AB.

/32/ **Pusch R, Karnland O, Hökmark H, Sandén T, Börgesson L, 1991**. Final Report of the Rock Sealing Project – Sealing properties and longevity of smectitic clay grouts. Stripa Project Technical Report TR 91-30. Svensk Kärnbränslehantering AB.

8 Techniques for preparation of buffers

This chapter deals with methods for preparing buffer materials, primarily blocks of highly compacted smectite-rich clay materials. Also, major physical properties of compacted blocks are given as a basis of determining the performance of the system of blocks applied in deposition holes before hydration, swelling and homogenisation has started.

8.1 Clay material

8.1.1 General

Homogeneous smectitic clay can be prepared by consolidation of a bentonite slurry, which is a technique that can be used in tunnels where masonries of compacted clay blocks expand and provide the pressure for consolidation of gap-filling clay slurry (Figure 8-1). This technique has been proposed in ongoing studies of backfilling and for preparing samples for laboratory investigations /1/, but the process is extremely slow because of the very low hydraulic conductivity of the consolidating mass.

The basic technique of block compaction was first tried by the author in the late seventies utilizing a method worked out by ASEA Atom (now ABB) for very strong cold isostatic compression of powders. It was used for preparing large cylindrical blocks for the Stripa project.

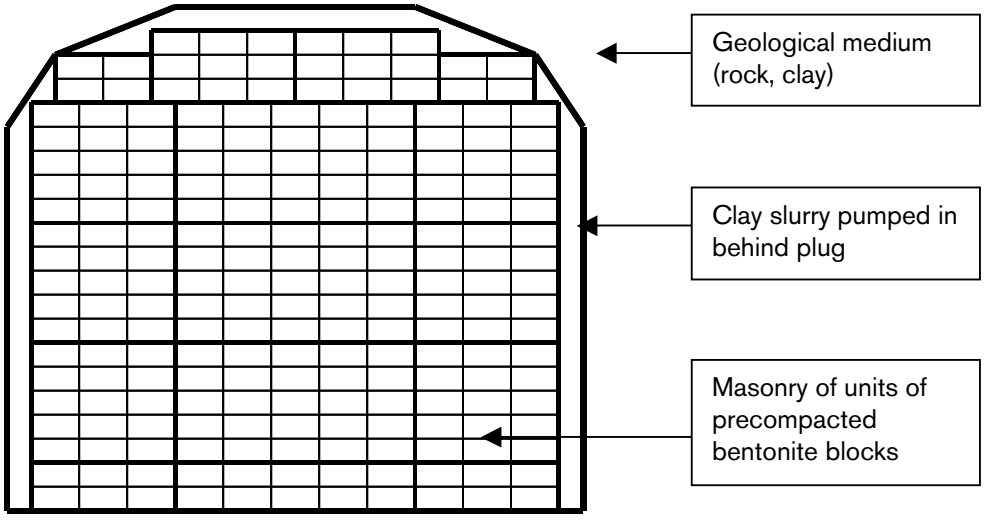

Figure 8-1. *Clay block masonry with clay slurry filling gap to surroundings.*

8.1.2 Principles for preparing blocks of highly compacted bentonite

Two techniques can be used for preparing blocks of compacted bentonite: "isostatic" compression and "uniaxial" compression. In Sweden the firstmentioned technique has been applied by IFÖ Co, Bromölla (now IFÖ Ceramics), which is ordinarily using their ABB Quintus Press units for "cold isostatic compaction" of mineral powder for the electrical industry. The powder is poured into a cylindrical space and compacted radially by use of a rubber membrane that is pressurized by oil. The pressure can be up to 150 MPa and heat can be added, which was not the case when this technique was utilized for the preparation of bentonite blocks.

The "uniaxial" technique, which is currently applied for preparation of large blocks for the Prototype Repository project at Äspö involves layer-wise pouring of bentonite powder in a rigid steel form and compressing it stepwise by use of a piston in much the same way as at laboratory compaction (Figure 8-2, see also Part 1 of the Handbook).

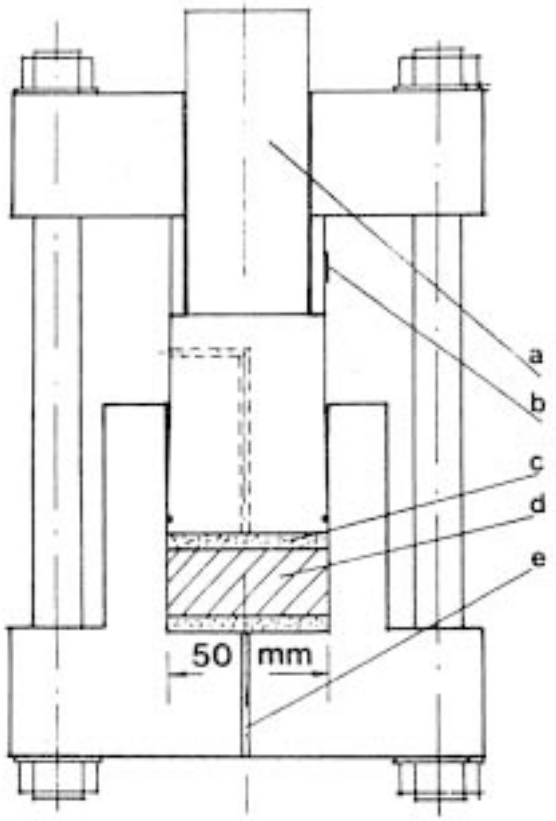

Figure 8-2. *The first device for compaction and water saturation of powdered clay for SKB's R&D on buffers and backfills. The compressed powder sample was fluid-saturated with simultaneous recording of the swelling pressure. Subsequent percolation gave the hydraulic conductivity. a) Piston for loading the sample; when the ring (b) is stress-free the applied load balances the swelling pressure. c) Filter. d) Sample. e) Lower water inlet.*

For larger blocks special respect must be paid to the selection of a suitable shape of the form for minimizing stress accumulation and fracturing of the compacted blocks, which can have a diameter of about 1.7 meter and a height of 0.3–0.4 meter. Full cylinders as well as blocks of annular shape can be produced. Uniaxial compaction can be made to manufacture blocks of any size provided that the compressive force is sufficiently high to yield the desired density. If it is about 2000 kg/m^3 blocks with 0.3 m diameter can be prepared by use of ordinary hydraulically operated loading units with a capacity of a few hundred tons. However, a number of practical aspects must be considered, like the impact of entrapped air and granulometry. They are listed and discussed in this chapter.

8.2 General relationships between the clay powder consistency, compaction pressure and net density

8.2.1 General

Comprehensive pilot studies of the required pressure to yield a certain required density of powdered bentonite were made in the late seventies in Sweden by SKB /2/ and systematic investigations on the same issue were made a few years later by Bucher et al in Switzerland /3/. These investigations confirmed that a pressure of about 100 MPa is required to give a dry density of 1900–2000 kg/m^3 and that the density is insignificantly increased beyond ρ_d =2100 kg/m^3 even if pressures up to 200 MPa are applied. As indicated by the diagram in Figure 8-3 different bentonite materials with the same water content were found to give different relationships between pressure and density. Variation of the water content was early found to have a significant effect on the compaction curve (Figure 8-4). According to /3/ a water content of about 5% would yield the highest density of MX-80. Very dry material is known to require high pressures to yield even moderate densities.

Pellets can be prepared by using ordinary tablet machines and densities of up to about 2200 kg/m^3 have been achieved. The shape can be ellipsoidal or almost spherical and as for block preparation the size depends on the pressure. For maximum density of a pellet fill two or more sizes are suitable.

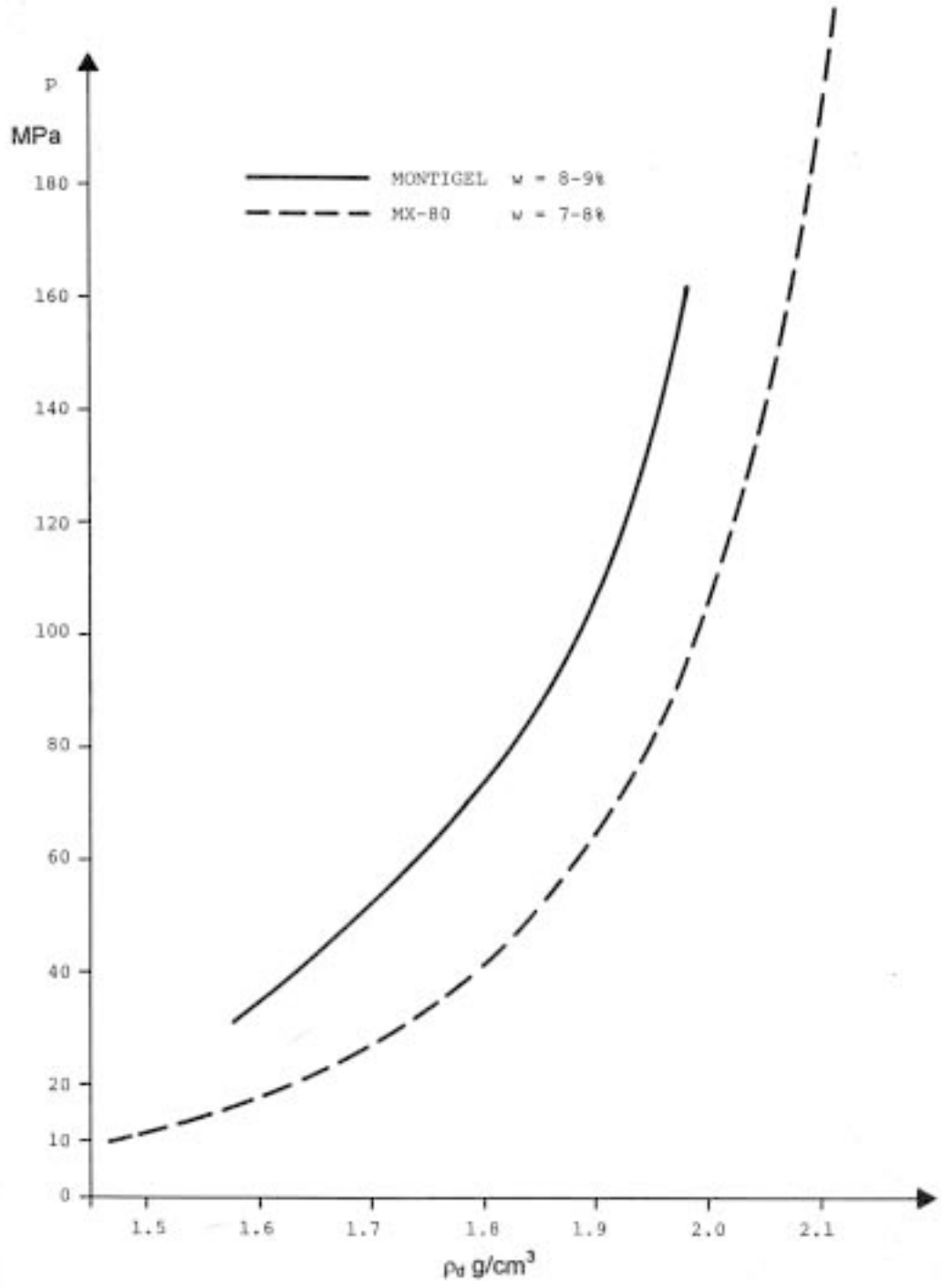

Figure 8-3. *Compaction pressure p related to the dry density ρ_d of two bentonite materials. Montigel is a commercial bentonite with Ca as dominant cation /3/. MX-80 is SKB's reference clay material.*

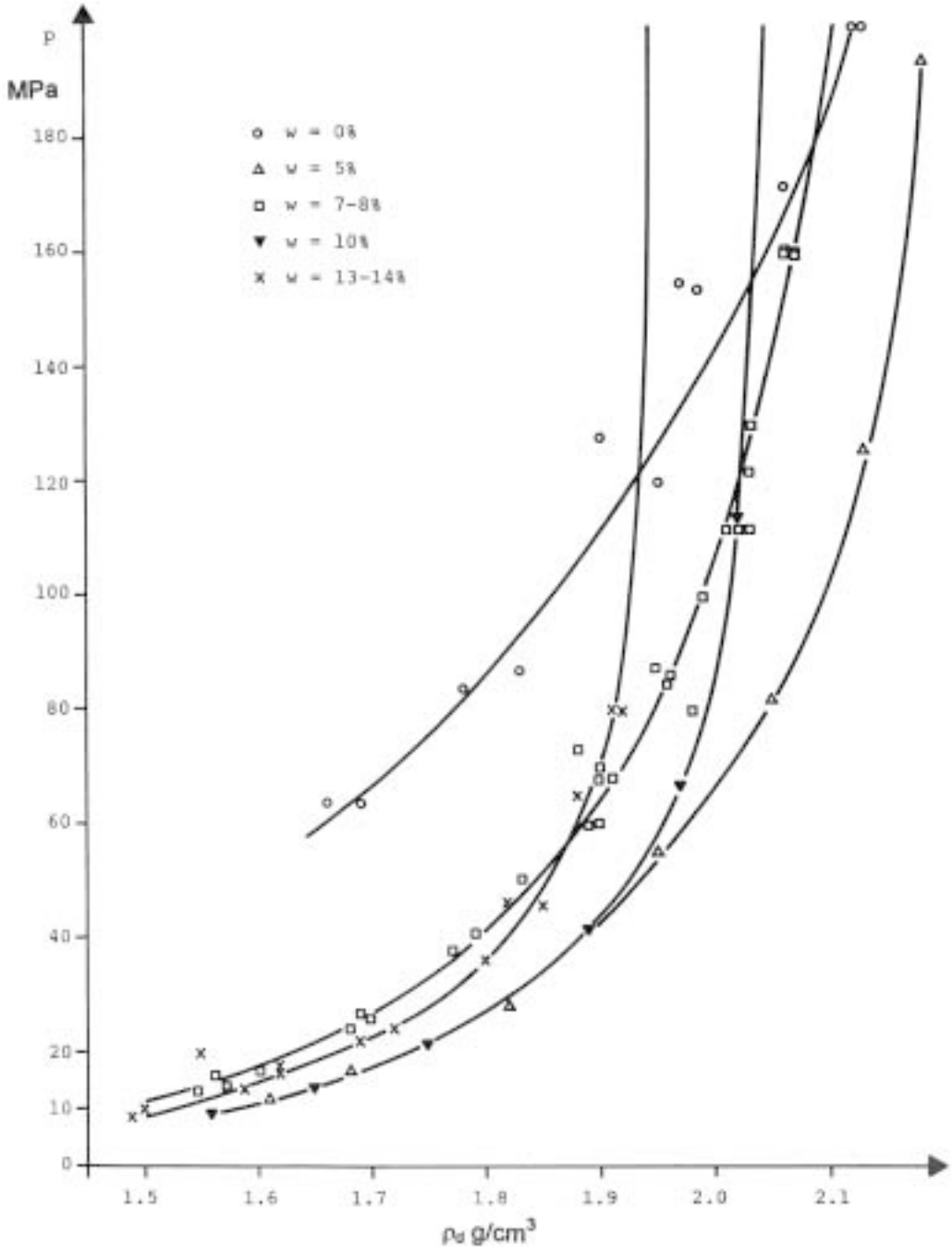

Figure 8-4. *Compaction pressure p related to the dry density ρ_d of MX-80 bentonite /3/. The different curves refer to different water contents.*

8.2.2 Influence of various factors on the compactibility of bentonite materials

A detailed, systematic investigation of the influence of various factors on the compactibility using laboratory equipment was performed in Sweden in 1993 /4/. The outcome of this investigation is summarized here.

Test program

The intention of the study was to investigate the importance of various factors on the density, homogeneity and physical properties of uniaxially compacted big blocks. These factors were:

- Water content.
- Compaction pressure.
- Form geometry.
- Compaction rate.
- Creep during compaction.
- Bentonite type and granulometry.

Materials

Two bentonite materials were used: a sodium-converted Ca-bentonite from Greece (IBECO-Na) and a naturally occurring bentonite with Na as major adsorbed cation from Wyoming USA (MX-80), cf Table 7-1. Two different forms of the natural Na-bentonite were used. One of them was granulated (MX-80) and the other one consisting of a finely ground powder (SPV200).

The mineralogical and chemical differences between the bentonites were small, as exemplified also by the fact that the liquid limit was the interval 400–518% for all of them.

The grain size distributions of the three bentonite materials are shown in Figures 8-5 to 8-7. The diagrams show that more than 80% of the dispersed clay particles are smaller than 0.002 mm and thus belong to the clay fraction. The size distributions of the powder grains of the dry bulk materials (according to technical data sheets from the supplier) of the two types of natural Na-bentonite are also shown in the diagrams. In the granulated bentonite (MX-80) more than 60% of the grains in the bulk material were larger than 0.2 mm, while in the powder (SPV 200) only approximately 5% of the grains in the bulk material exceeded this measure.

The bentonite materials were mixed with distilled water to water contents up to 35% and compacted uniaxially to different densities. After compaction the bulk density (ρ) and the water content (w) of the samples were determined and the void ratio (e) calculated.

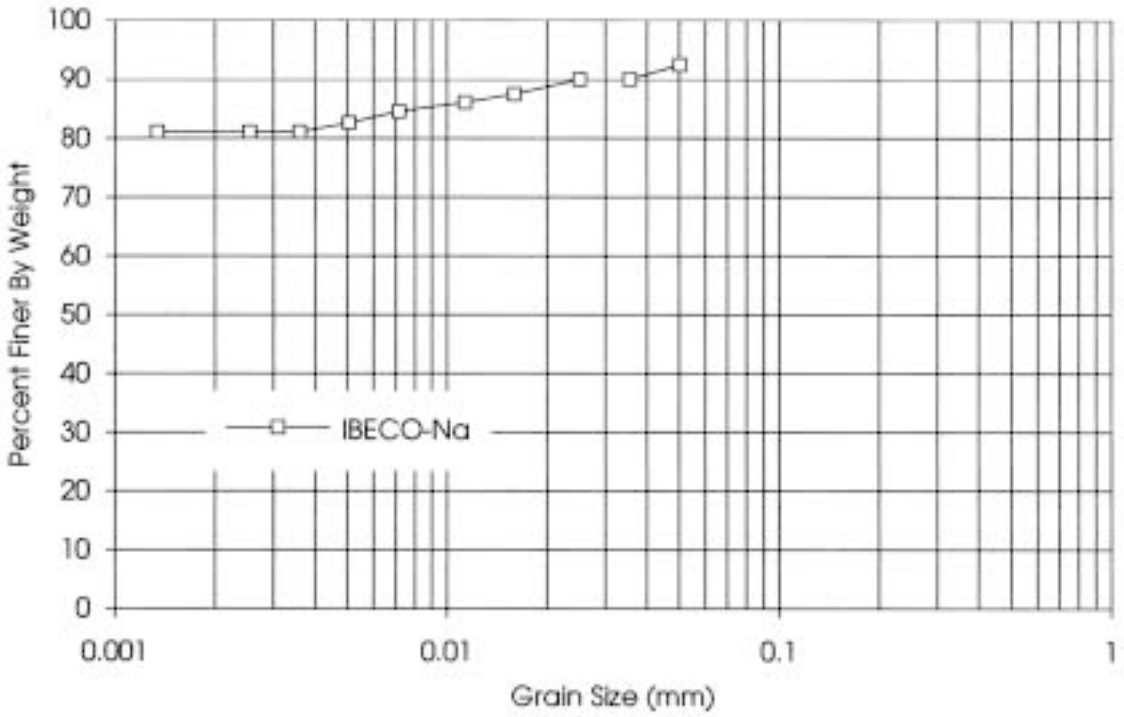

Figure 8-5. *Grain size distribution for dispersed IBECO-Na bentonite.*

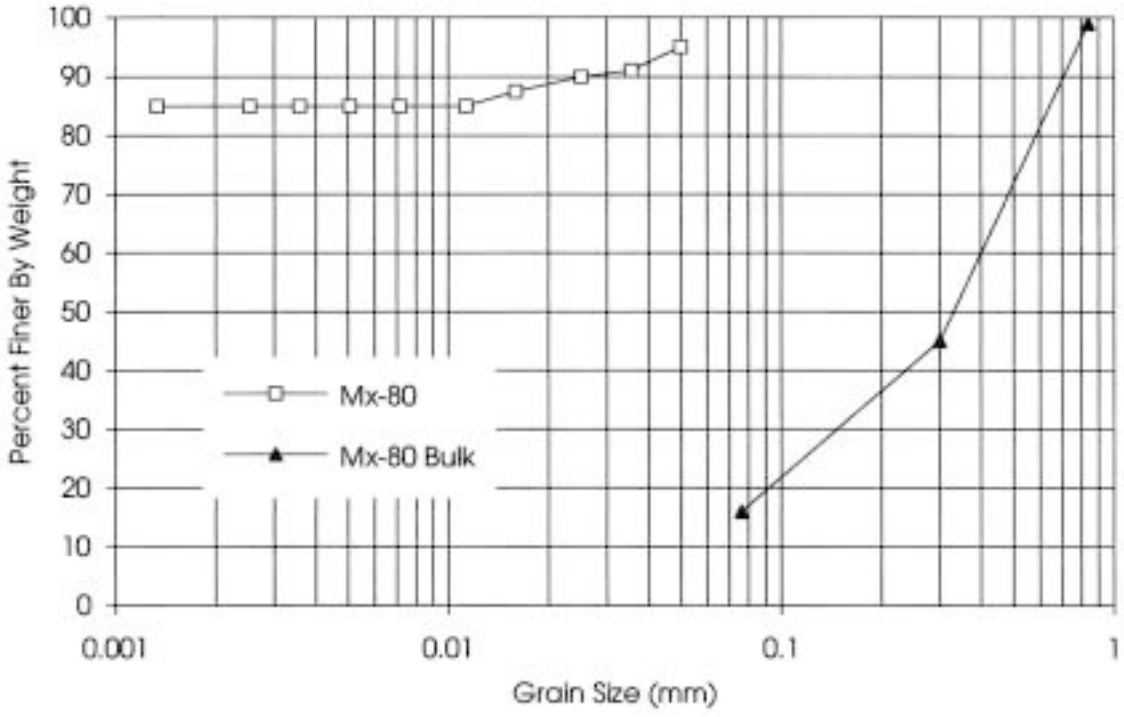

Figure 8-6. *Grain size distribution for MX-80 bentonite in dispersed as well as in dry powder form.*

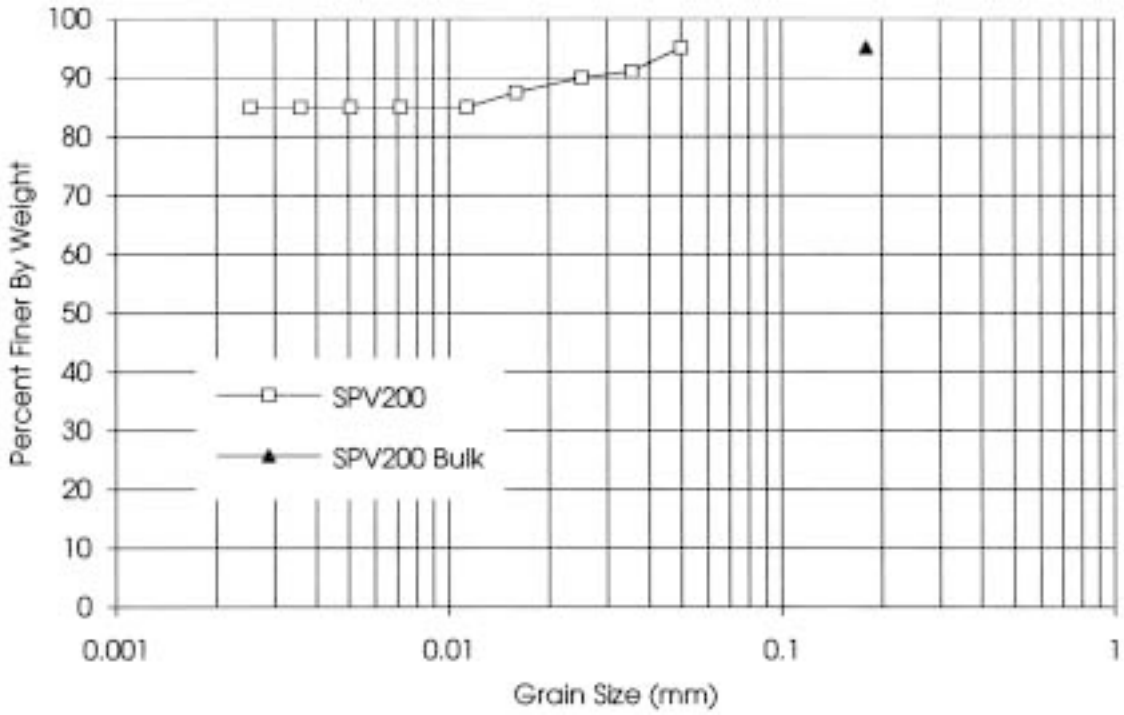

Figure 8-7. *Grain size distribution for SPV200 bentonite in dispersed form. One plot is given for the clay in the bulk form /4/.*

The grain size distribution is not a unique material property. It is in fact dependent on a number conditions of which the major ones are:

Air-dry material

1. Abrasion in the course of sample preparation and sieving can change the original granule size dristribution very significantly.
2. Higher relative humidities than 70% cause aggregation and expansion of aggregates.

Material dispersed in water

1. Intense agitation causes more dispersion than mild treatment /5/. The actual size of smectite particles can range from separate stacks of lamellae with a thickness of down to 30 Å to aggregates of stacks with a thickness of a few micrometers.
2. The strong deviation from the Stoke sphere shape of stacks of smectite lamellae and interparticle forces between particles of colloidal size make the determination of size uncertain.

Main results

In Figure 8-8 the dry density is plotted as a function of the water content. The maximum dry density for a certain water content corresponding to complete water saturation is also plotted. The figure shows that the dry density decreases with increasing water content and approaches the curve for maximum dry density almost asymptotically. The corresponding relationship for a less smectite-rich clay (Friedland Ton) is also shown in the figure. One finds that the void ratio is lower at lower smectite content and the degree of water saturation higher. This finding of substantial importance since it demonstrates:

1. The compactability of smectitic clays drops with increasing smectite content. This phenomenon is obvious also at dynamic compaction using rollers.
2. A higher degree of water saturation can be achieved by using clay materials with a lower smectite content than smectite-rich clay for the same pressure. Thus, for a water content of Friedland Ton clay powder of 15–20% blocks with more than 90% degree of water saturation can be produced. provided that the compaction. This is of great importance for reaching a high heat conductivity.

The results are plotted in Figure 8-9, with the void content as a function of the water content. It increases with increasing water content by the increment $\Delta e \approx 0.12$ when the water ratio increased from 10% to 20%. When the water content is changed from 20% to 30% the void ratio increased by the amount $\Delta e \approx 0.20$.

The lower diagram in Figure 8-9 shows the degree of saturation plotted as a function of the water content. The figure shows that the degree of saturation increases rapidly with increasing water content for water contents between 10% and 22%. At water contents above 22% the degree of saturation is only slightly affected by the water content. The maximum degree of saturation appeared to be 96–98%.

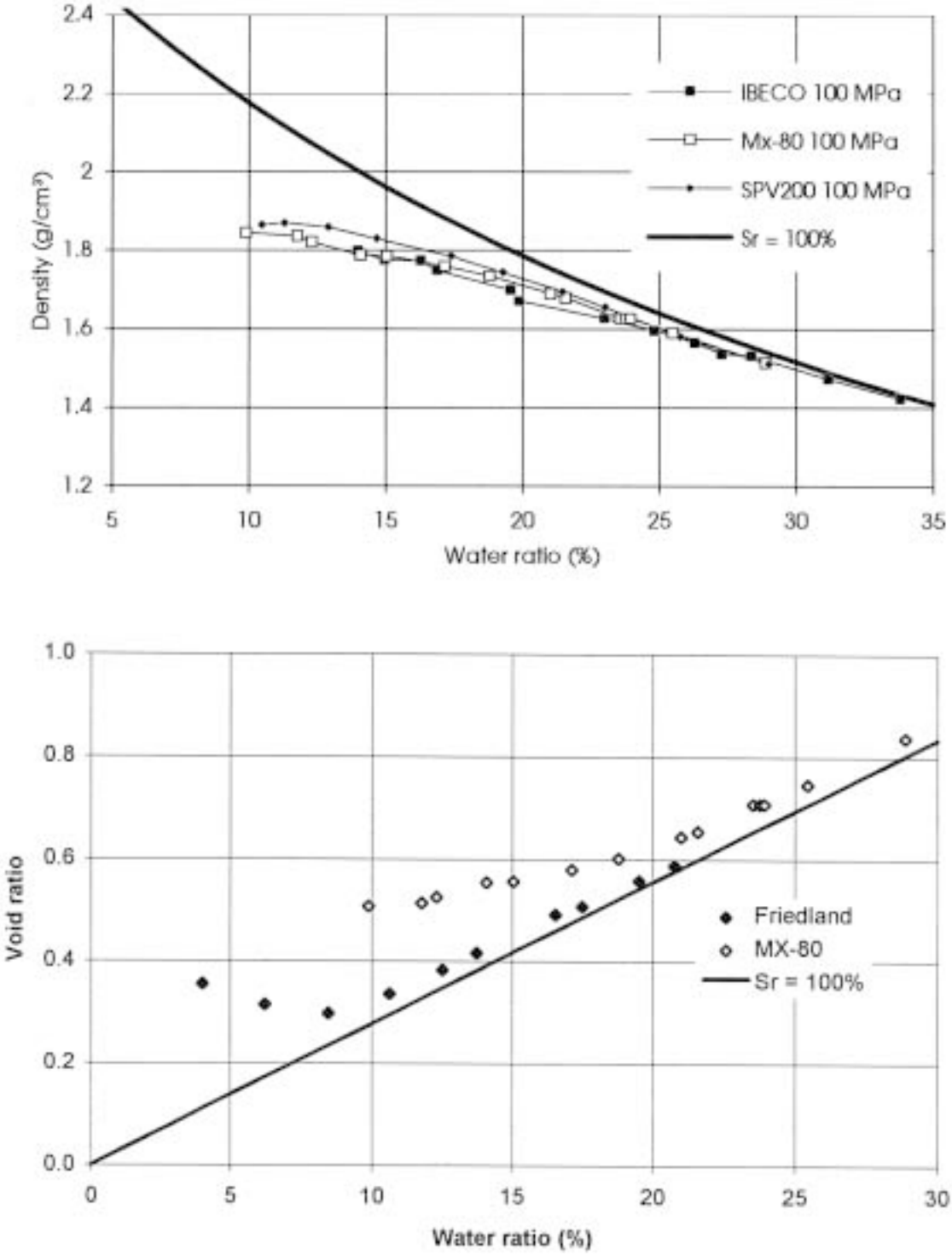

Figure 8-8. *The dry density as a function of water ratio. Upper: behavior of three bentonites prepared by use of a compaction pressure = 100 MPa. The solid line represents the theoretical relationship between water content and dry density at 100% degree of water saturation (S_r=100%). Lower: Comparison of Friedland clay (45% smectite) and MX-80 (75% smectite) /4/.*

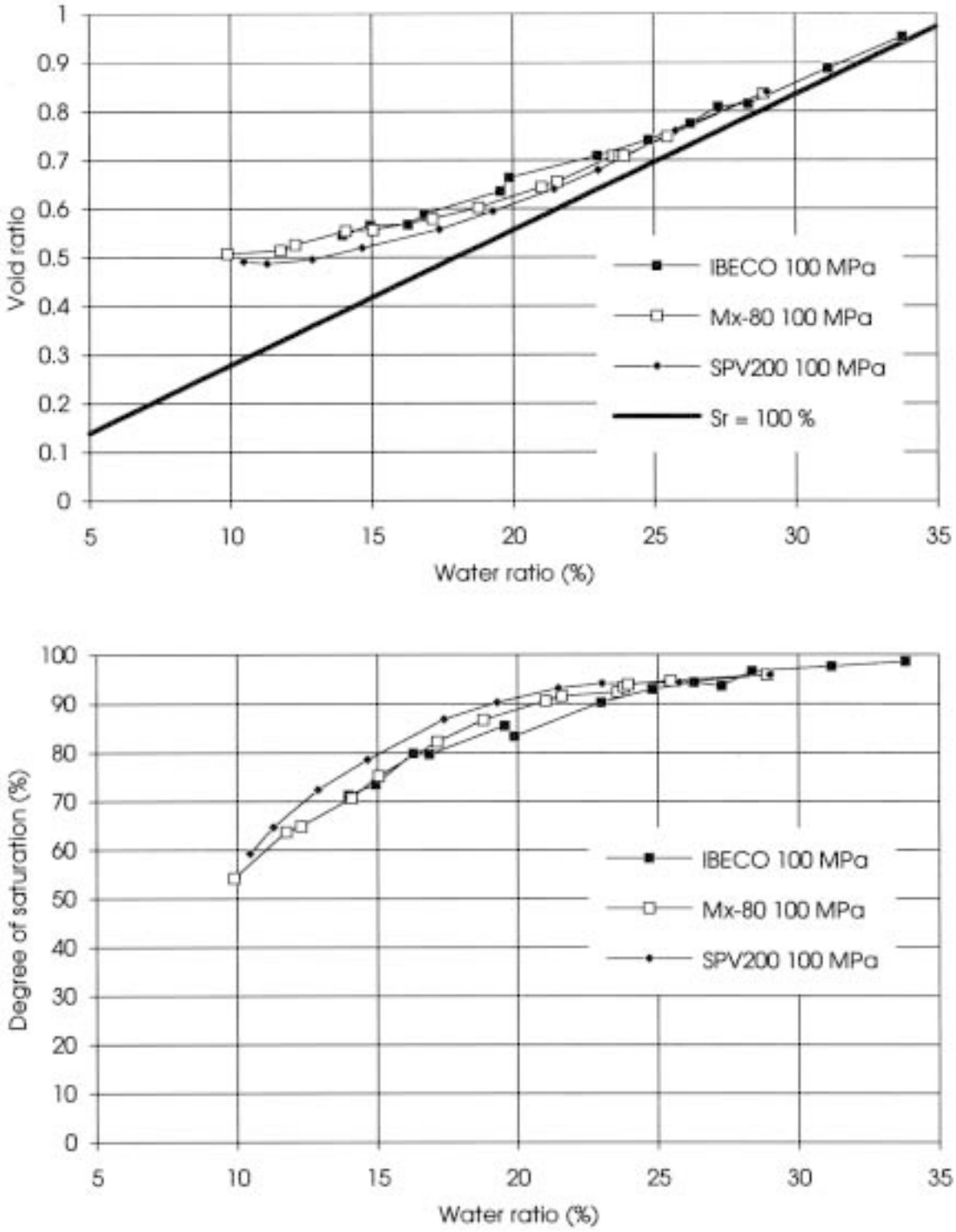

Figure 8-9. *Void ratio (a) and degree of saturation (b) plotted as a function of the water content for the bentonites. Compaction pressure = 100 MPa /4/.*

Influence of form geometry

The ratio of the diameter and height of a form affects the homogeneity of the compacted sample due to the friction between the sample and the form /4/. In order to investigate this effect samples were compacted in a cylinder with a diameter of 49 mm and a height of 240 mm. Samples with the heights 100 mm, 70 mm, 40 mm, 20 mm, 10 mm, and 5 mm were compacted at four different water contents 10%, 15%, 18% and 22%. The compaction pressure was 100 MPa. The results are given in Figures 8-10 and 8-11 and they are interpreted as follows:

- Samples with a lower water content than about 18% showed a significant increase in void ratio over the sample length, illustrating the strong effect of form friction.
- At a water content of 22%, there was almost no difference in void ratio between the bottom and the upper parts of the samples and the degree of water saturation was up to about 92%.
- At a water content of 22% the applied pressure 100 MPa is concluded to have given almost complete water saturation and a liquid state. At unloading it expanded and gave incomplete but uniform saturation.

Tests were made with the compaction pressures 100 and 300 MPa using the two bentonites MX-80 and IBECO-Na. The results from the tests on MX-80 are shown in Figure 8-12, which demonstrates that for a compaction pressure of 150 MPa the sample reached 100% degree of saturation if the water content of the sample exceeded 17%, and that the samples reached 100% degree of saturation also for the compaction loads 50, 75 and 100 MPa if the water content of the samples exceeded 21%. The strong effect of unloading and release of the samples from the form on the degree of water saturation is clearly demonstrated by the lower diagram in the figure.

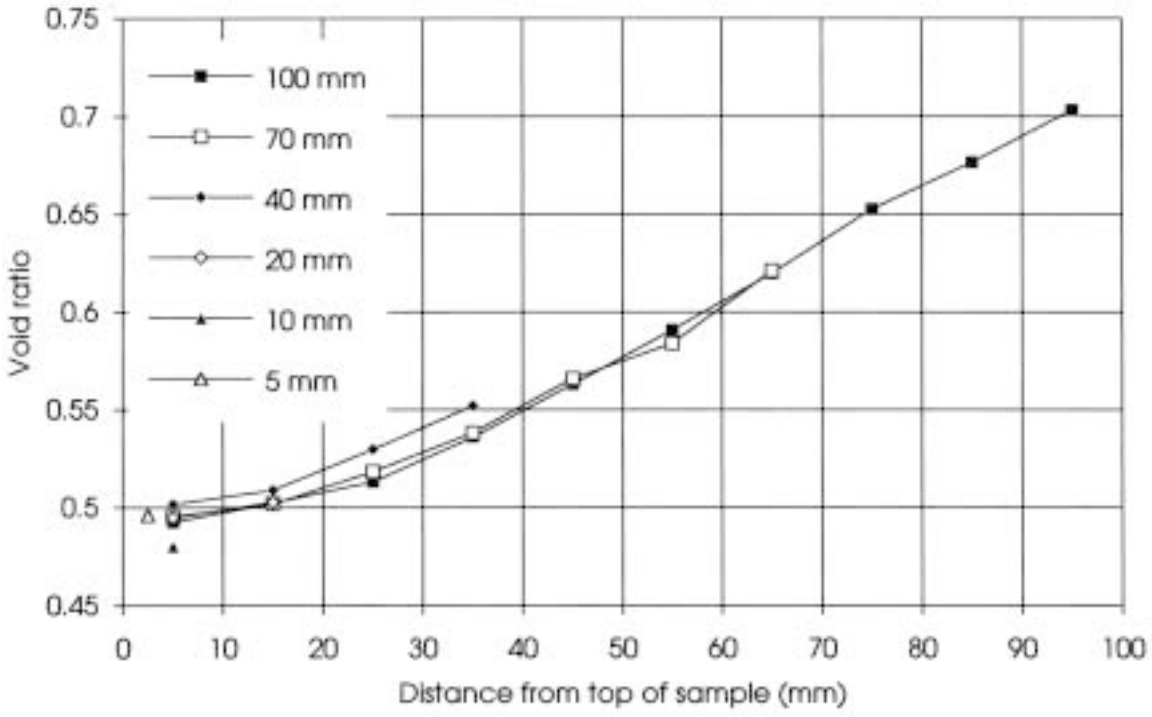

Figure 8-10. *The void ratio as a function of the distance from the top surface on which the piston rested. The symbols represent the various initial sample heights. All samples had a water content of 10% /4/.*

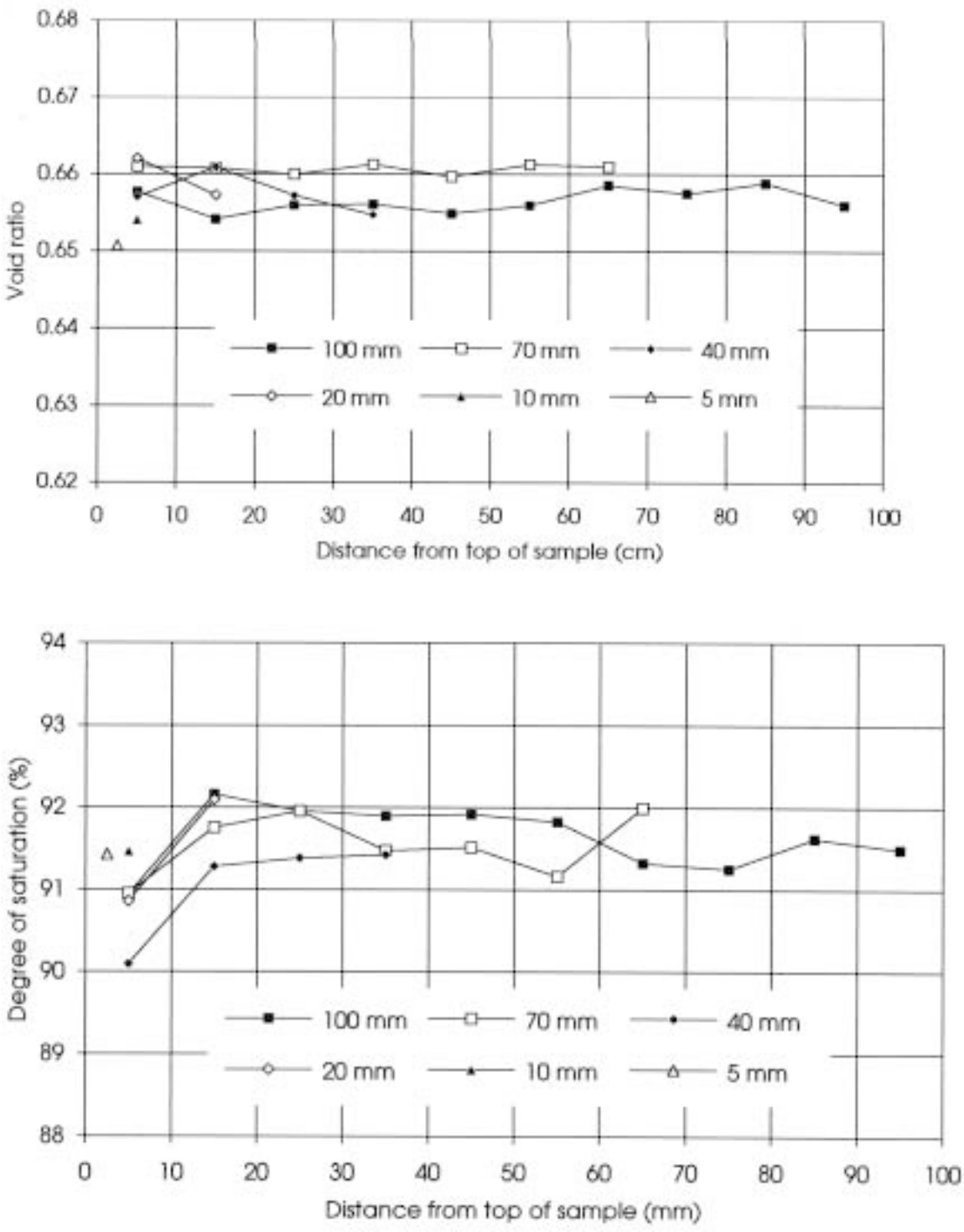

Figure 8-11. *The void ratio (upper) and the degree of saturation (lower) for a water content of 22% /4/.*

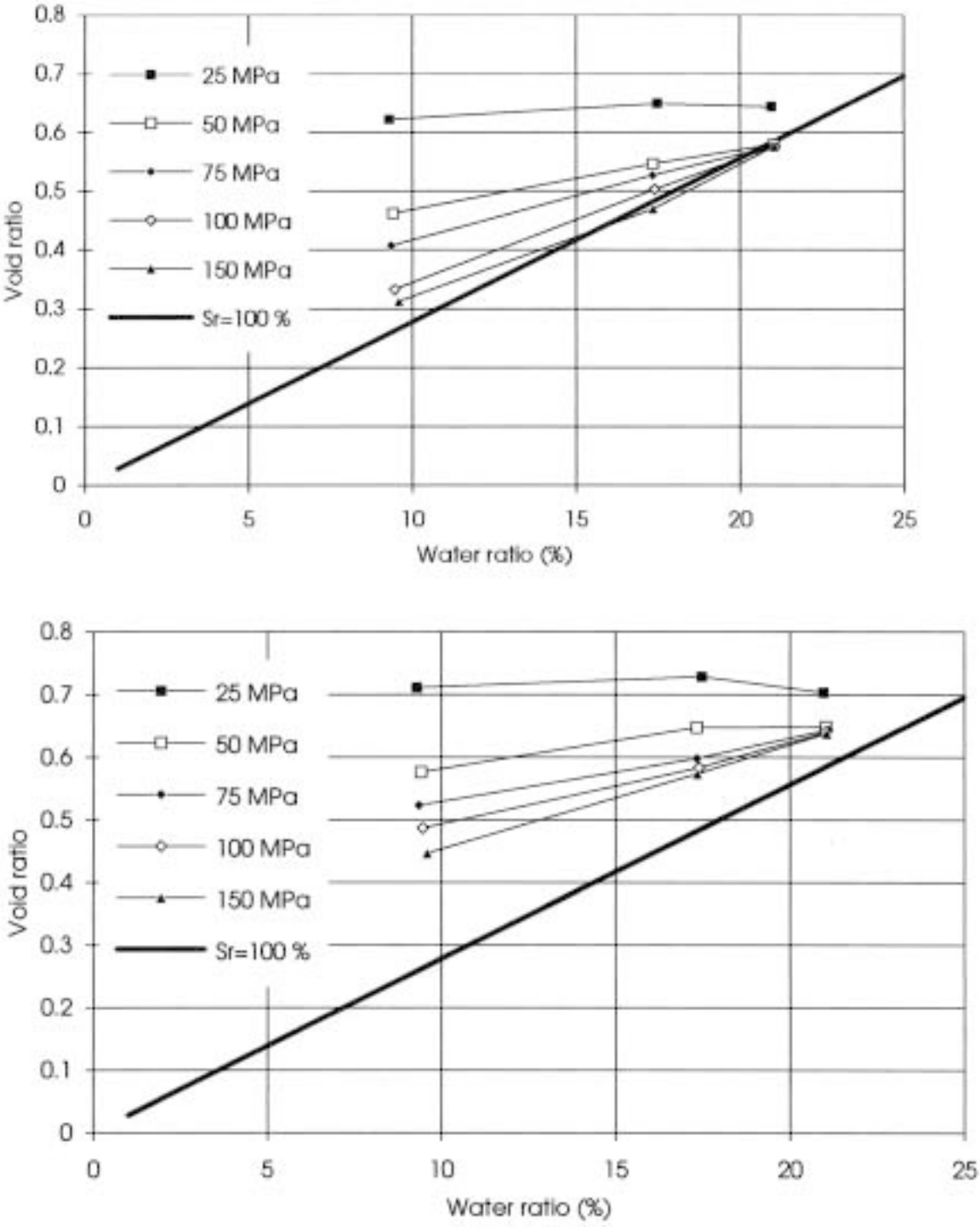

Figure 8-12. *The void ratio plotted as a function of water content. Upper: during the compaction. Lower: after removal from the form. Compaction pressure 25–150 MPa /4/.*

Influence of compression rate

Compaction of manually manageable blocks on an industrial scale is expected to require higher compression rates, which made it important to study if the rate has any significant influence on the block properties /4/. Tests on MX-80 were made with the compression rates specified in Table 8-1, which also gives the void ratio and degree of saturation for two water contents. All the samples had an initial height of 20 mm. The conclusion is that the rate of compression had an insignificant effect for the small sizes tested as is obvious from the similar e and S_r data determined after compaction.

Influence of creep curing compaction

Time-dependent compression under constant load has been investigated by maintaining a constant pressure of 100 MPa on 20 mm thick compacted MX-80 samples with 10 and 21% water content for various time periods, i.e. 1 s, 25 s, and 500 s /4/. The sample heights were measured at compression, creep and unloading. After removal of the pressure the water content and density were measured and the blocks weighed. Three tests were made on samples with 10 and 21% water content and the data obtained were used to calculate the change in void ratio and degree of water saturation during the entire operation. Three tests were made at each water content. The compression rate was 0.04 mm/s. The results of the laboratory measurements are shown in Table 8-2, which demonstrates that there was a very small but measurable effect of creep in the sample with the lowest water content.

Table 8-1. Summary of results from tests with different compression rates /4/.

Press Velocity, mm/s	w, %	e	S_r, %
0.04	10	0.49	61
0.3	10	0.48	60
1.8	10	0.48	59
0.04	21	0.63	92
0.3	21	0.63	91
1.8	21	0.63	91

Table 8-2. Block properties measured after removal of the 100 MPa pressure /4/.

w, %	Resting time, s	e	S_r, %
10	1	0.49	61
10	25	0.48	58
10	500	0.46	62
21	1	0.63	92
21	25	0.63	92
21	500	0.62	92

Influence of bentonite type and powder granulometry

The type of granulometry of the bentonite may affect the result of the compression at block preparation as can be concluded by comparing the compression curves of the three bentonites MX-80, IBECO, and SPV200 /4/. Figure 8-13 shows the behavior of MX-80 at loading and unloading. The following conclusions were drawn:

- IBECO and MX-80 have almost identical compression properties.
- SPV200, which is much more fine-grained than MX-80, gave somewhat lower *e*-values and higher S_r-values than the other two materials.

In recent time additional bentonites have been investigated including the Czech RMN clay and the present understanding is that the grain size distribution and major adsorbed cation type, which determines the size of air-dry clay aggregates, do not have a very significant influence on the compressibility. Referring to the earlier mentioned tests on Friedland Ton, it is concluded that a moderate smectite content yields the best compression properties.

Expansion after compaction

Figure 8-14 shows the expansion ratio (increase in volume divided by initial volume) as a function of the compaction pressure for three different water contents /4/. The figure shows that the expansion rate was about 4% and almost independent of the compaction pressure at a water content of 21%. At the water content 9.4% the ratio increased strongly with increasing compaction pressure and reached values as high as 11%. This expansion was associated with the formation of numerous fissures.

The major conclusions from these observations are:

- The expansion was about 4% when the samples were compacted to yield complete water saturation.
- The expansion increased with increasing compressive pressure when the samples were unsaturated.
- The expansion increased with decreasing degree of saturation.

Scale effects

The size of isostatically compacted samples does not have any influence on the homogeneity of the products as concluded from IFÖ Ceramics experience while uniaxially compressed samples exhibit various defects like fissures depending on nonuniform expansion on stress release in the form /4/. Fractures appeared frequently at the upper edge of many blocks as can also be explained by FEM calculation using relevant material data, Figure 8-15 /6/.

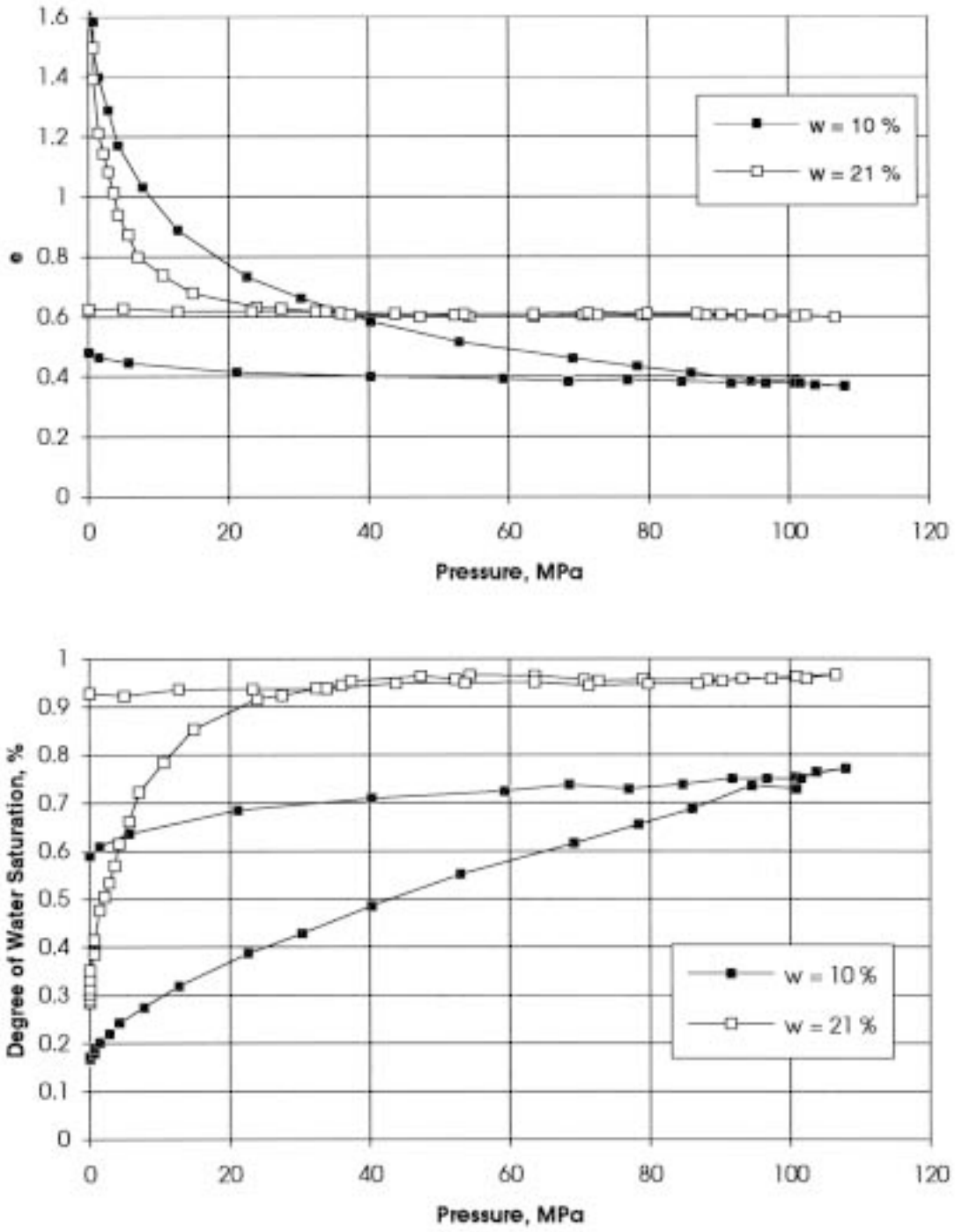

Figure 8-13. *Void ratio and degree of water saturation during load increase and unloading of MX-80 at w=10% and w=21%. Loading causes reduction from initially e=1.6 and S_r=0.9 and 0.6, respectively, to low e-values and a rather high degree of water saturation irrespective of the degree of unloading /4/.*

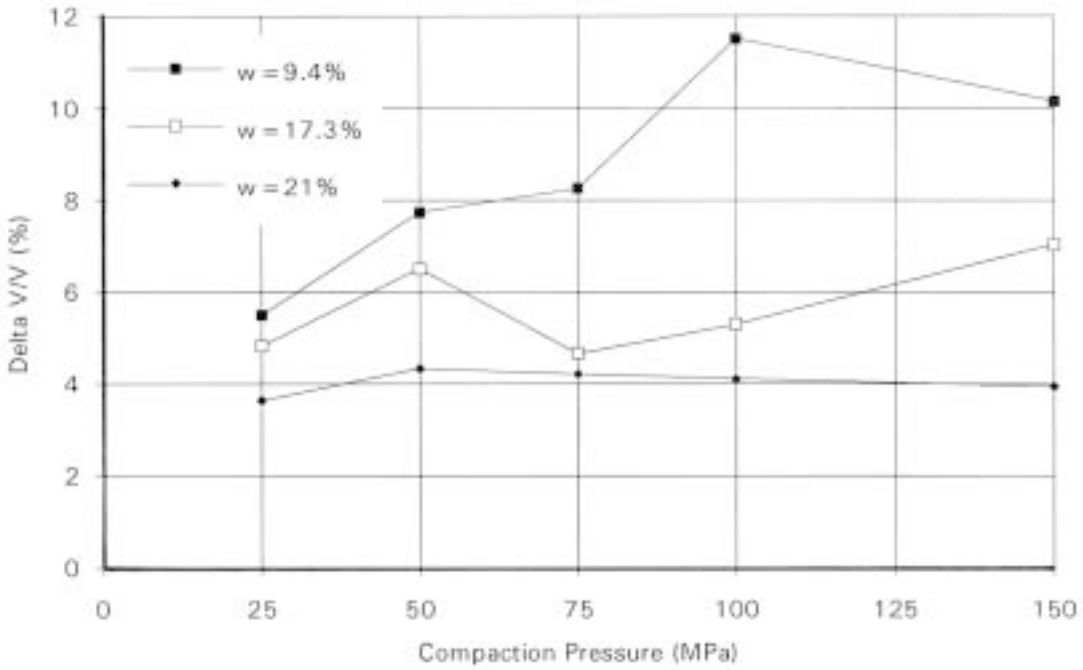

Figure 8-14. *The expansion ratio δ_e, termed V/V in the figure, as a function of the compaction pressure for differently wetted MX-80 samples /4/.*

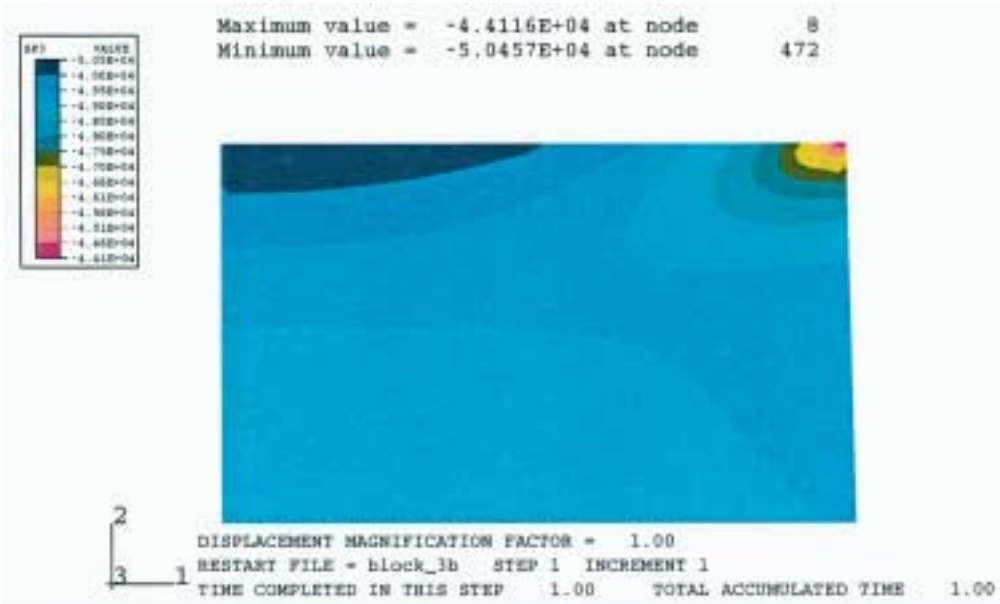

Figure 8-15. *FEM-derived stress focus at upper edge of compacted block /6/.*

8.3 Production of large blocks

8.3.1 General

In practice, significantly larger blocks than the ones investigated in the laboratory are required for field tests and for use in a repository and this presents a number of challenges, such as means of letting air out of the compressed powder mass, reduction of form friction, and development of techniques for quick compression and handling of the blocks. This section summarizes experience from two projects.

8.3.2 The Stripa blocks prepared by isostatic compaction

Preparation

At the time when the Stripa Project was launched no data from systematic investigations on the properties of highly compacted powdered materials were at hand, except for small-scale laboratory tests, and since rather big blocks were required, the experience from other users of powder technology had to be relied on, which led to co-operation with the IFÖ factory at Bromölla mentioned earlier. The products, obtained by compacting MX-80 powder had the form of cylinders with a height of about 1.5 m and an average radius of 0.42 m (Figure 8-16) /7, 8/.

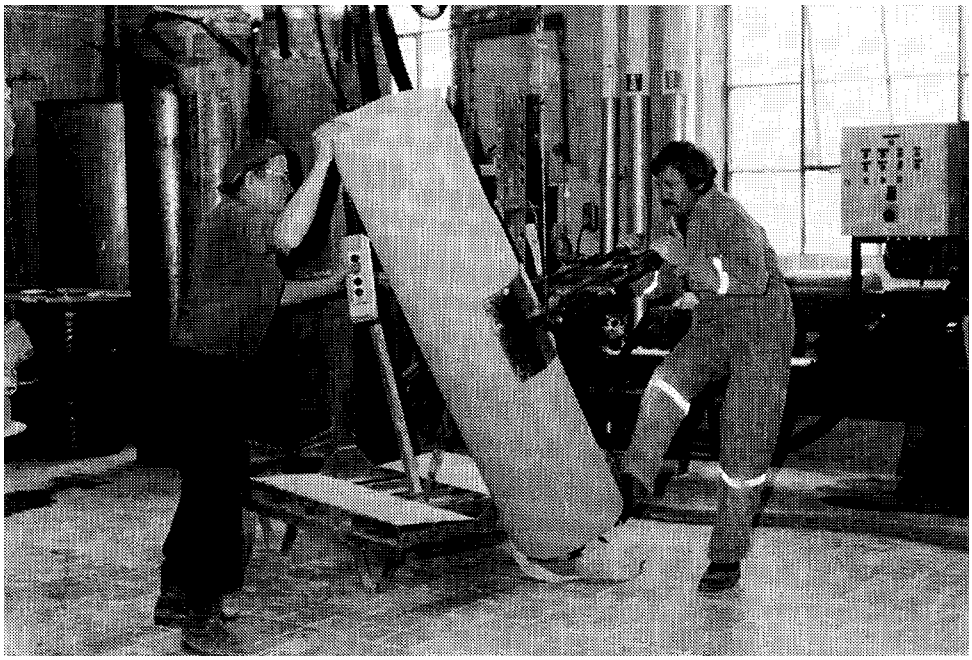

Figure 8-16. *Highly compacted bentonite cylinder in the IFÖ factory. Notice the rather regular shape, the diameter being approximately 0.4 m.*

The process involved filling of the powder in a cylindrically shaped rubber sleeve with rigid base plates, and compressing it radially by applying an outer pressure of approximately 100 MPa to obtain the desired dry density, i.e. about 2000 kg/m^3. The pressure was held constant for a few minutes before releasing and removing the bentonite core. The required compression pressure and time were found to depend on the water content and some preliminary tests had to be made before the operation ran properly.

Two series of blocks were made using powder with somewhat different water contents. This gave a bulk density of 2090–2140 kg/m^3 for powder with the water content 13% and 2070–2110 kg/m^3 for powder with about 10% water content.

Manufacturing of blocks designed for use in field experiments

The cylinders were cut into disc- and rod-shaped blocks by using a machine saw. This operation gave blocks of various predetermined shapes for the build-up of block columns in which the heaters for the field experiments should fit and which had to fit the deposition holes with specified tolerance (Figures 8-17 and 8-18). After sawing, the blocks were wrapped in tightly fitting "welded" 0.15 mm plastic cover to preserve the original water content. They were then placed in strong plastic boxes for transportation to the test site. Unwrapping for drilling of holes for application of temperature gauges and moisture sensors was made shortly before insertion in the 0.76 m diameter holes that had been bored in the rock.

All the blocks were perfectly homogeneous with no cracks or other defects as could be concluded after careful examination both immediately after compaction and manufacturing and at the insertion in the holes several months and even up to a year later.

Effect of storage in humid air

A few blocks with a volume of a few cubic decimeters were saved for testing the sensitivity to moist air in the Stripa underground laboratory and they behaved according to the predictions with respect to the hydration potential of smectite-rich clay. Thus, the blocks took up water from the air and their shallow parts expanded and disintegrated already after a few days in RH=80–100%. The degradation went on successively and the blocks entirely broke up into fragments after a number of weeks. This points to the necessity of effectively shielding bentonite material, blocks as well as powder, from moist air.

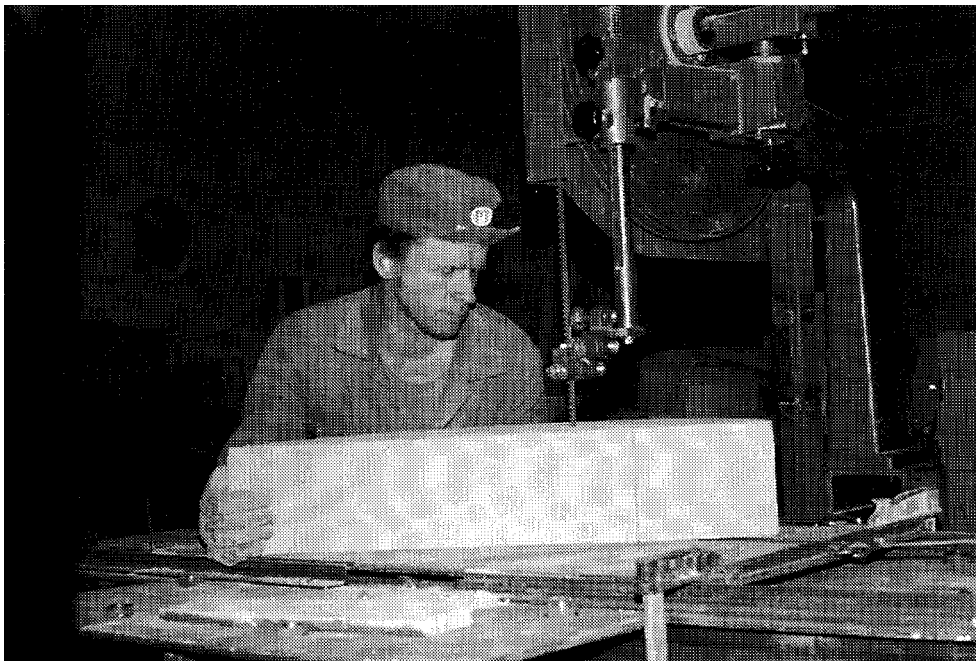

Figure 8-17. *Sawing of blocks from the big clay cores for emplacement around heaters in the Stripa BMT test /7/.*

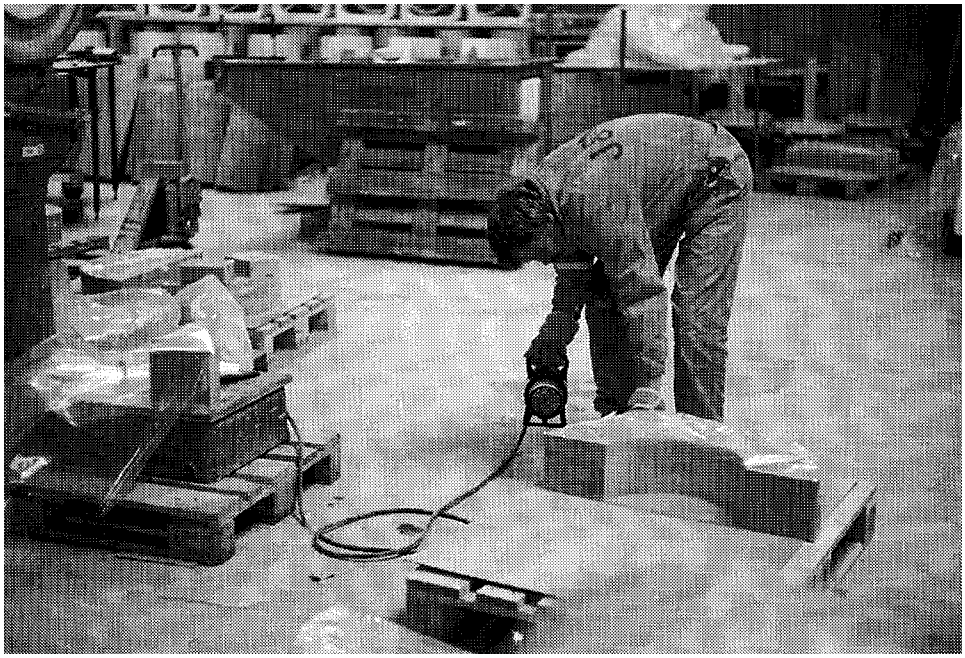

Figure 8-18. *Trimming of blocks for for emplacement around heaters in the Stripa BMT test /7/.*

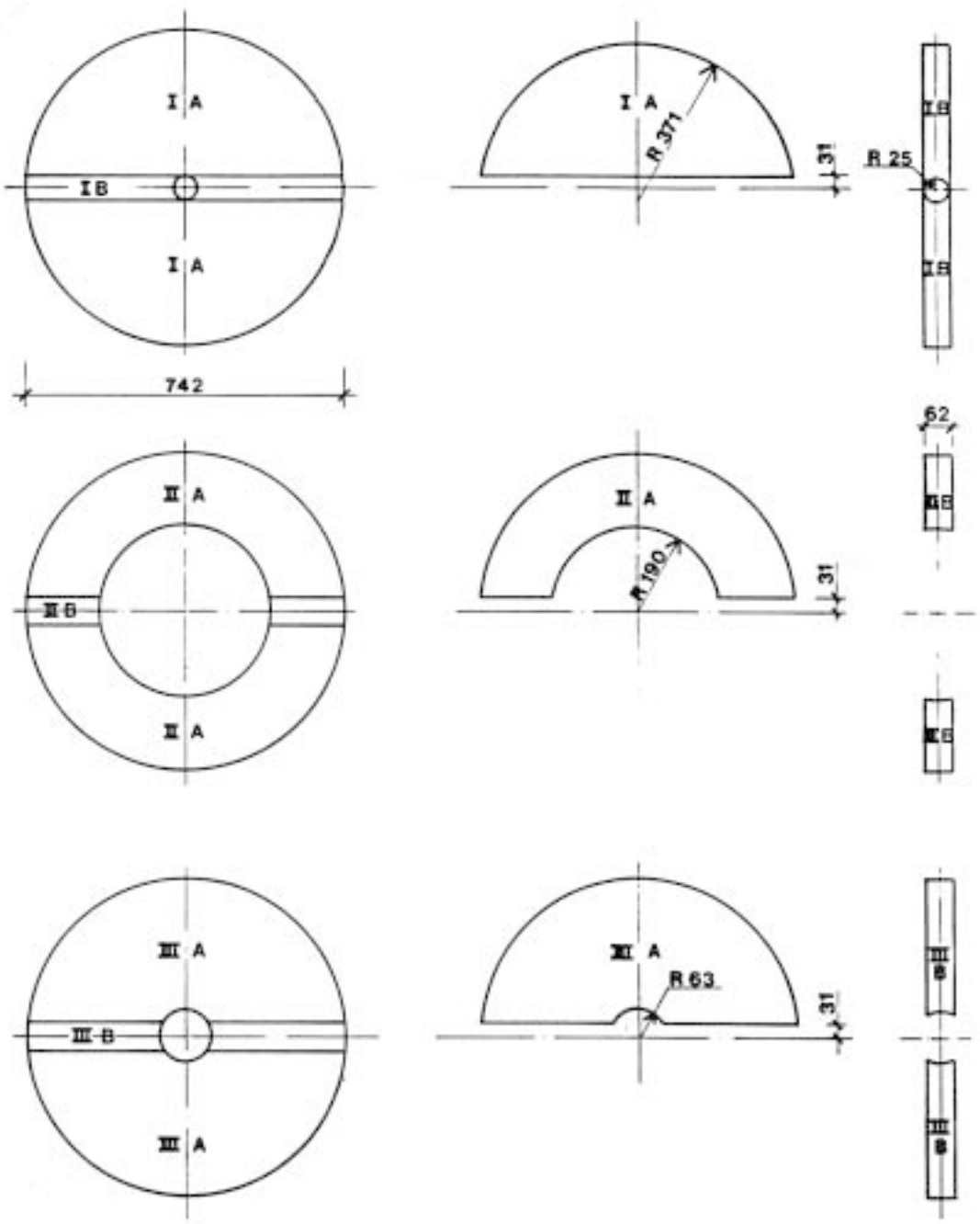

Figure 8-19. *Example of layout of block shapes (dimensions in mm). The thickness of the blocks was 150 mm /8/.*

8.3.3 Recent R&D work for production of uniaxially compacted, larger blocks

General

Comprehensive work for development of a feasible block preparation technique has been made utilizing one of the production lines at the Höganäs Bjuf AB at Bjuv, Skåne. This industry normally produces refractory bricks and plates and the machinery and other facilities were estimated to be suitable also for the preparation of highly compacted bentonite blocks /7/. They were intended to be manageable by one man and therefore needed to have a weight of no more than 10–15 kg. This was achieved by using a box-shaped form with the edges 200x240 mm. The height after compaction under 100 MPa pressure, using a compaction rate of 200 mm/s, was 80 mm and the weight about 10 kg (cf Figure 8-20). The time for manufacturing 100 blocks could be brought down to about 10–15 minutes.

Form friction

The variation in void ratio along the height of a block must naturally be very small and special precautions have to be taken. A preferable way of minimizing heterogeneity turns out to be lubrication of the form, using ordinary form oil. Most of the oil, which is sprayed in the form of very fine drops, evaporates after the compaction and detailed microscopic studies and chemical analyses have not shown any signs of it.

Figure 8-20. *Block produced by uniaxial compression.*

Enclosed air

One of the problems with uniaxial compaction of blocks with a height of more than a few tens of millimeters is that the expansion after release of the samples from the form yields cracks that are perpendicular to the direction of compaction. Some of them are concluded to result from stress concentrations induced at the expulsion of the samples from the form, while others are related to the presence of compressed air in the samples. The possibility of applying vacuum in order to avoid the latter type of defects has been investigated in the laboratory using small samples and it is presently applied in the preparation of very large blocks (several hundred kilograms). Figure 8-21 illustrates that vacuum yields a higher degree of water saturation of compressed blocks by expelling air from the voids in the compression phase /9/.

Special problems are caused when compacting bentonite with a high water content. Liquefaction and edge distortion are common phenomena and require specially designed forms. Sticking to the form is another problem, which can be avoided by using geotextile of suitable sort. Form oil helps to reduce also this problem.

Storage

Examples of problems that may cause problems during storage in stockpiles are:

- desiccation of the blocks despite the plastic wrapping,
- sticking of the blocks to each other if many blocks are stored together on a pallet,
- development of mould on the blocks.

The firstmentioned effect can probably be eliminated by using special plastic foil. The sticking of blocks may take place at higher water ratio and individual wrapping is then a necessary step to be taken.

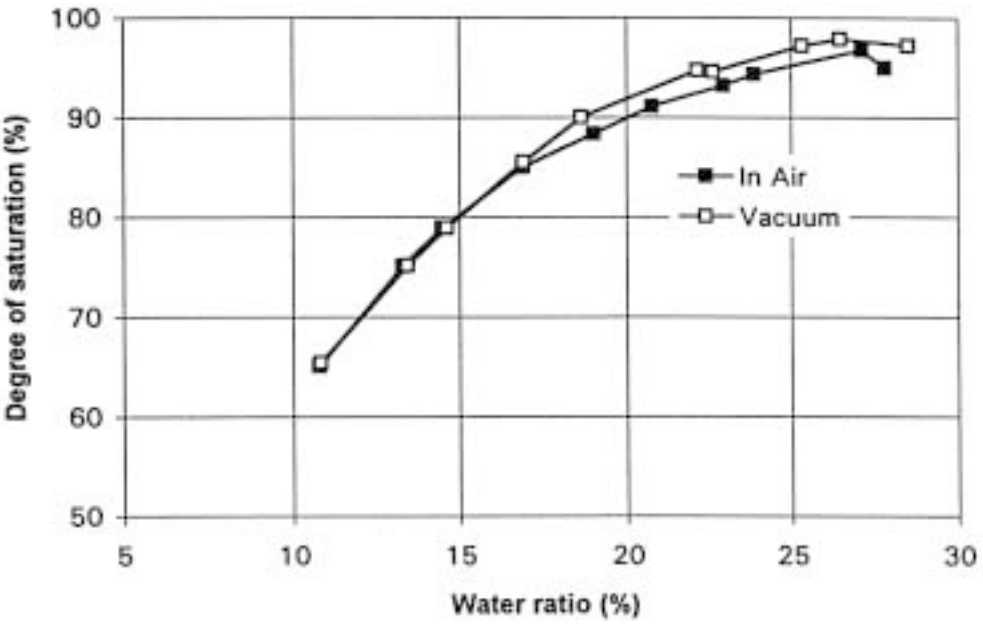

Figure 8-21. *Degree of saturation as a function of water ratio for samples compacted in air and during vacuum /9/.*

As to the formation of mould, experience shows that this is a common phenomenon if the water content exceeds about 15%. This speaks in favor of compacting blocks at the natural water content, i.e. 8–12% of the bentonite material. Such blocks can be stored for years without being wrapped in plastic as long as the relative humidity in the storage room is maintained in the interval 30–70%.

8.4 General aspects on big block production

Production of big cylindrical blocks by use of isostatic compaction seems to give more homogeneous block material than the uniaxial technique. However, the time and cost for preparing blocks with required geometry by sawing makes the latter technique more attractive, especially if very large blocks are asked for. An example of production and handling of large blocks by uniaxial compression is shown in Figure 8-22. Lifting is shown to be made by use of vacuum technique.

The press had a capacity of 30 000 tons and was capable of producing blocks with a weight of about 2 tons. The form employed for the production can be equipped with an arrangement for preparing large annular blocks as well. It is hardly practical to make bigger blocks by using this technique while isostatic compacting may well be used for producing big cylindrical blocks and cup-shaped blocks, which would make it possible to prepare two halves for a canister.

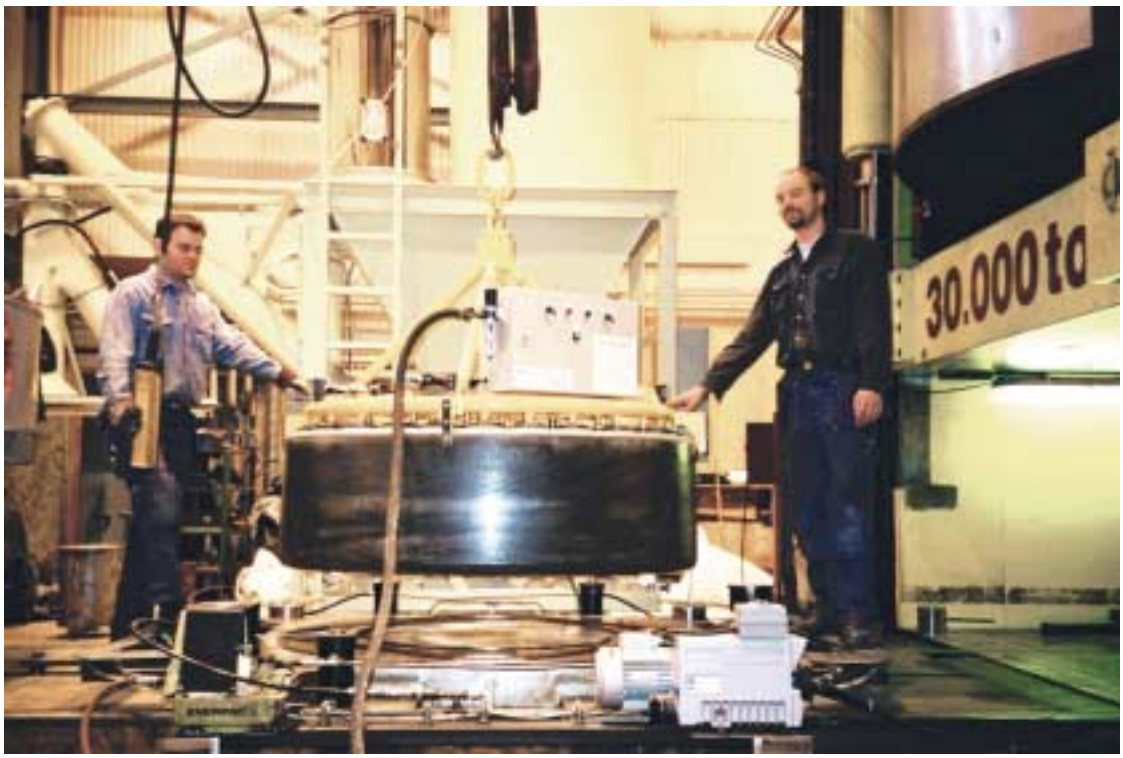

Figure 8-22. *A uniaxially compressed 2 t block of MX-80 clay is handled by vacuum technique. The black color of the block is the lubrication (photo by Clay Technology AB).*

8.5 References

/1/ **Touret O, 1988**. Structure des argiles hydratees thermodynamique de la deshydration et de la compaction des smectites. Ph.D. thesis, at the Dept. of Geology, Universite Louis Pasteur.

/2/ **Jacobsson A, Pusch R, 1978**. Egenskaper hos bentonitbaserat buffertmaterial. KBS Teknisk Rapport 32.

/3/ **Bucher F, Jeger P, Kahr G, Lehner J, 1982**. Herstellung und Homogenität hochverdichteter Bentonitproben. NAGRA Technischer Bericht 82-05.

/4/ **Börgesson L, Johannesson L-E, Fredrikson A, 1993**. Laboratory investigations of highly compacted bentonite blocks for buffer material – Compaction technique and material composition. SKB Djupförvar, Projekt Rapport PR 44-93-009. Svensk Kärnbränslehantering AB.

/5/ **Pusch R, 1962.** Clay particles. Nat. Swed. Build. Res. Council, Stockholm.

/6/ **Börgesson L, 2002.** Personal comm.

/7/ **Pusch R, Börgesson L, Nilsson J, 1982**. Buffer Mass Test – Buffer Materials. Stripa Project Internal Report 82-06. Svensk Kärnbränslehantering AB.

/8/ **Pusch R, Nilsson J, Ramqvist G, 1985**. Final Report of the Buffer Mass Test – Volume I: scope, preparative field work, and test arrangement. Stripa Project Technical Report TR 85-11. Svensk Kärnbränslehantering AB.

/9/ **Johannesson L-E, Börgesson L, Sandén T, 1995**. Compaction of bentonite blocks. SKB TR 95-19. Svensk Kärnbränslehantering AB.

9 Techniques for preparing and applying clay/ballast mixtures

This chapter describes methods for preparing, applying and compacting clay/ballast mixtures. Examples are given from large-scale field tests like the Stripa and Äspö Projects.

9.1 General

Methods tested so far for backfilling of repositories with clay/ballast mixtures require mixing of clay and ballast material to a desired consistency. The mixing procedure can be varied to some extent but the methods to put the material on site can be very different: application in horizontal layers and layerwise compaction are standard procedures, while application and compaction in inclined layers is a recently tested, alternative method. A third procedure mentioned and briefly described in Chapter 8 is to prepare highly compacted blocks of bentonite or smectitic mixtures. All three techniques will be described and commented on in this chapter. There is a fourth method as well that involves blowing of backfill material by using shotcrete techniques as in Stripa BMT experiment, where it was used for bringing in a mixture of 20% MX-80 and graded ballast /1/. It was concluded to yield too low densities but the method has been found to work if highly compacted smectite-rich pellets are used as demonstrated in current NAGRA research. In recent years application and compaction of natural clay (Friedland Ton) in dried and ground form has also been tested.

In this chapter we will confine ourselves to describe materials and methods that have been thoroughly investigated in SKB's R&D work.

9.2 Definitions

The composition of clay/ballast mixtures is often expressed as 10/90, 20/80 etc, representing the ratio of clay and ballast. This terminology is practical since it refers to the weight of the components with their natural water contents but it is not perfectly accurate since the content of water is not indicated. The true ratio of the respective solid materials must hence be known for any sort of preparation of backfills.

9.3 Mixing procedures

9.3.1 Equipment

Mixing of various components to obtain the required homogeneity of backfill in a repository can be made by use of mixers of the type employed for preparing concrete. Free-fall mixers and mixing procedures applied in the Stripa and Forsmark projects /1, 2/ serve well for preparation of dry mixtures of bentonite and ballast but more intense mechanical agitation and better homogeneity is obtained by using mixers with a vertical axis and with blades attached both to the axis and to the inner side of the confining steel container (Swedish: "tvångsblandare"). This sort of equipment was chosen for a recently completed field experiment at Äspö in Sweden in which about 2000 m^3 of mixtures of crushed rock and bentonite were prepared. The photo and graphs in Chapter 9.3 were supplied by Clay Technology, which was responsible for this test.

The mixing was made by use of a mobile station equipped with hoppers for the ballast (Figure 9-1). The MX-80 bentonite used for the project was delivered in 25 kg paper bags and moved by an auger from a small hopper to the mixer. Bentonite was brought in first into the mixer followed by ballast and finally water, all the components being weighed automatically to reach the specified composition. As in the Stripa case the dust formed in the handling and mixing of bentonite as well as in the application in a TBM drift at 400 m depth was insignificant and required no special protection. The grain size distribution of the components are shown in Figures 9-2 and 9-3.

Figure 9-1. *Mobile station for producing larger quantities of thoroughly mixed bentonite/ballast material (100 m^3 per day). NCC was the construction company.*

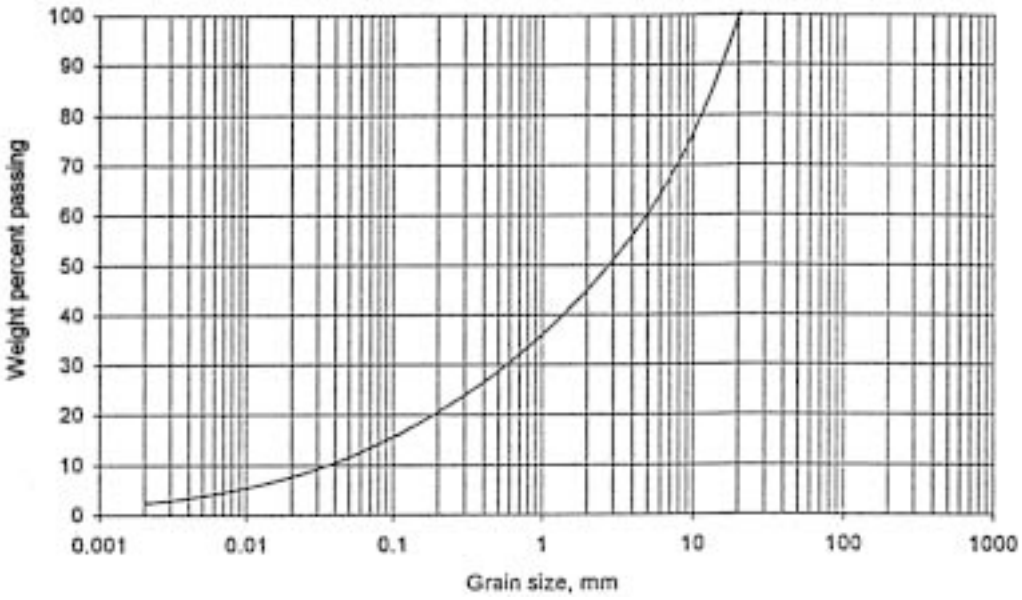

Figure 9-2. *Generalized grain size distribution of the ballast (crushed TBM muck).*

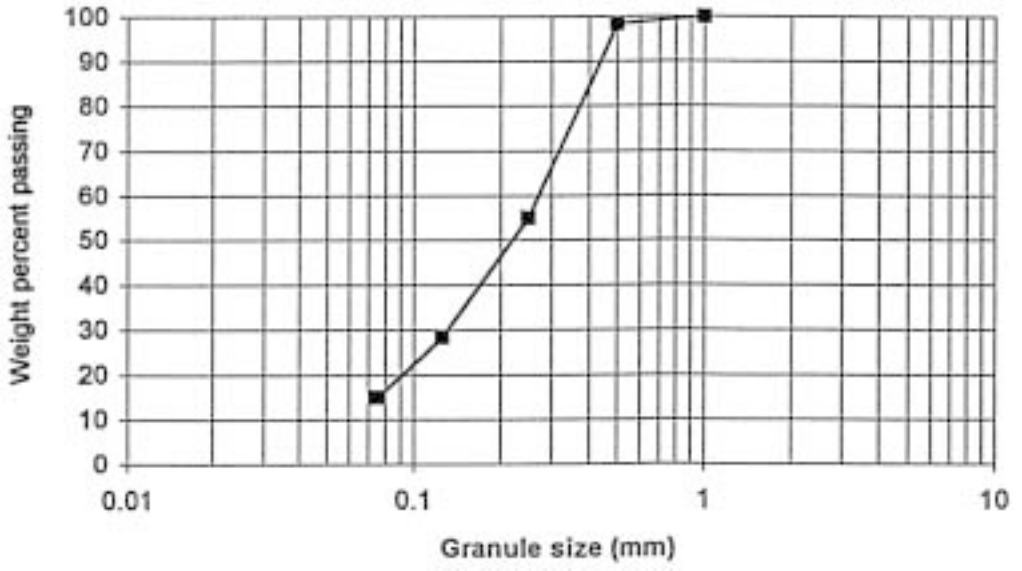

Figure 9-3. *Size distribution of the MX-80 powder grains (granules) for the Äspö backfilling experiments.*

9.3.2 Compactability and quality checking

Laboratory compaction naturally precedes the selection of components and composition of the backfill but additional half-scale compaction tests should be made in conjunction with the start of preparing materials for full-scale application because the mixing and compaction processes are scale-dependent. Thus, slight adjustment of the composition, especially with respect to the water content, may be required for fulfilling density criteria.

In the Äspö case the compaction properties of the bentonite/backfill were as shown in Figure 9-4. These curves illustrate a typical behavior of bentonitic backfills, namely that there are two density maxima, one for practically dry components and one at the optimum water content. A common observation is that the water content can be varied within a relatively large interval without affecting the density very much.

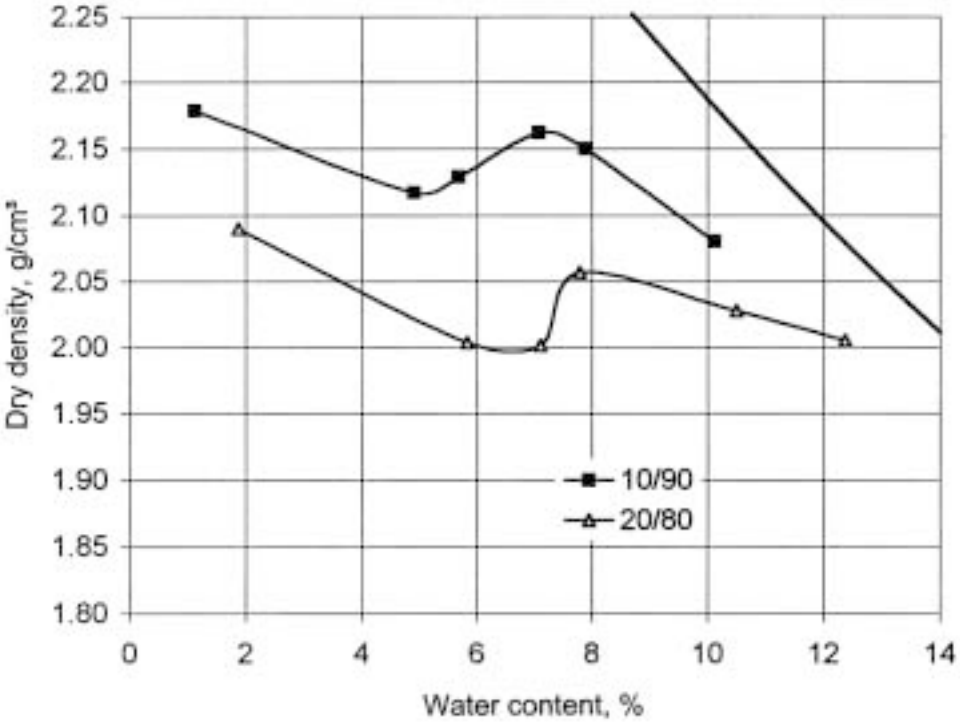

Figure 9-4. *Compaction curves of 10/90 and 20/80 mixtures of MX-80 bentonite and crushed TBM muck using modified Proctor technique. The solid curve represents the theoretical maximum density at complete water saturation.*

9.4 Application of clay/ballast mixtures

9.4.1 Application and compaction of horizontal layers

General

The following general procedure is recommended on the basis the Stripa BMT experiment, which was made in drift with rather little inflowing groundwater (30 liters per day in the 11 m long drift):

1. The material is applied and distributed in layers with a thickness that is related to the compaction capacity of the vibratory machines, which are rollers or vibratory plates. In general, 10/90 mixtures compacted by 400–700 kg vibratory plates (Figure 9-5) should have a maximum thickness of 0.25 m in order to reach 100% Proctor density (cf Section 7). If 5 t vibrating rollers (Figure 9-6) can be used the thickness can be 0.3–0.5 m and a dry density of 2000 kg/m^3 can then be obtained. More bentonite-rich material must be applied in thinner layers for reaching this density and if the clay content exceeds 30% other tools, like vibratory pad- or sheep-foot rollers should be used /3/.

2. The layers are compacted by a certain, specified number of runs, usually 6–10 of the compaction machine.

3. The density is recorded by sampling ("balloon") technique and preferably also by radiometric methods for determining the density distribution laterally and as a function of depth.

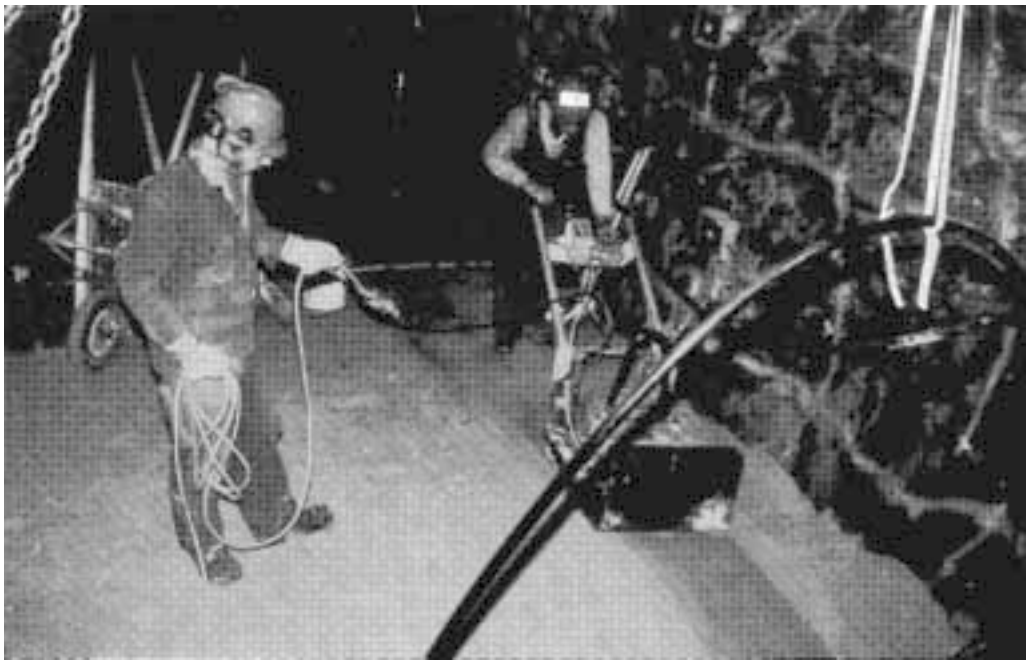

Figure 9-5. *Compaction of 10/90 bentonite/ballast mixtures. Upper: 400 kg vibratory plate /1/. Lower: 4.7 t vibratory roller.*

Figure 9-6. *Compaction by use of a 4.7 t vibratory roller in a TBM tunnel.*

Density variations

Experiments have demonstrated that the density of layers compacted by vibratory machines is highest at the top and drops somewhat with depth. Layers compacted by vibratory rollers usually get a lower density in the most shallow part as a consequence of the combined effects of shearing and unloading.

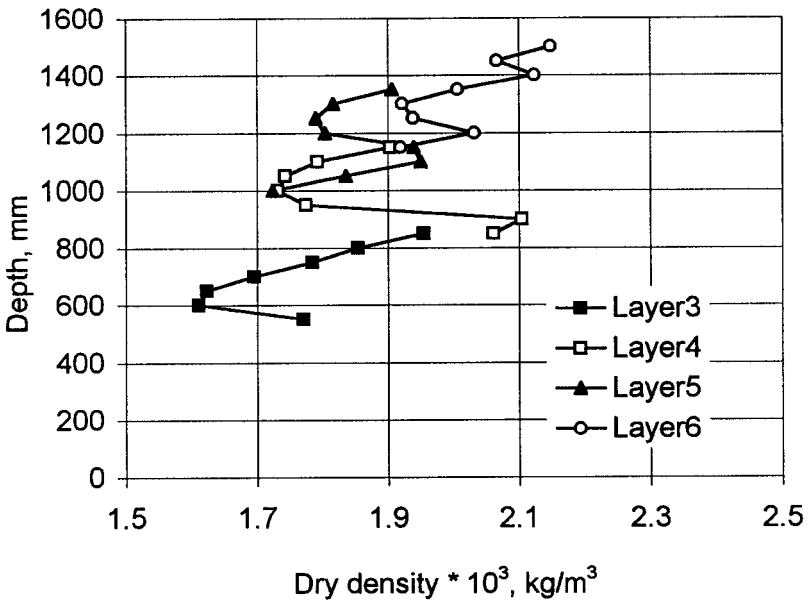

Figure 9-7. *Example of density variation. Layers of 10/90 mixture of MX-80 and crushed TBM muck compacted by vibratory roller /4/.*

Application

The need for applying the material in sufficiently thin layers to reach a uniform density throughout each layer must be underlined. Effective compaction commonly reduces the original layer thickness to 60–70% of this value, which means that a 0.25 m layer becomes 0.15–0.18 m thick /1/.

Effective compaction of backfills in drifts and tunnels cannot be made close to the rock, especially in blasted rooms with their irregular profile it is difficult to bring plates and rollers sufficiently near the rock. Special techniques like compaction by use of pneumatically tampers help to raise the density of the mass next to the rock but experience shows that a peripheral zone with a significantly lower density than in the central part of the mass remains. For 10/90 mixtures the difference in dry density may be 300 kg/m^3.

Application and compaction of the backfill in horizontal layers cannot be made higher up in drifts and tunnels than to a distance of about 1.6–1.8 m from the roof. The rest of the space must be filled with some other method like the ones described below.

9.4.2 "Sideways" application and compaction of inclined layers

Backfilling by pushing the material and compacting it to form inclined layers has been tested in a recently completed test at Äspö using crushed TBM muck and various mixtures of such muck and MX-80 bentonite. The principle can be used for backfilling of the upper part of a drift (Figure 9-8) or of the entire section. If heavy vibrating plates are used (cf Figure 9-8) the compaction effect is not very different from when ordinary application in horizontal layers with subsequent vertical compaction is used. Figure 9-10 shows that even backfills poor in clay adheres to the rock if it is wet.

Figure 9-9 shows recorded densities of inclined layers of 10% MX-80 bentonite and 90% crushed TBM muck. The original thickness was 0.3 m and the dry density in the interval 2000–2250 kg/m^3 except for the material closer than about 1 m from the wall of the blasted tunnel, which was about 5 m high and wide. Here, the dry density was locally as low as 1630 kg/m^3, corresponding to 2030 kg/m^3 at water saturation.

The technique for "sideways" application and compaction has been used successfully also for mixtures of 30% MX-80 and 70% crushed rock but the densities were significantly lower. The same experience was also obtained from tests with Friedland Ton, which was relatively coarsely granulated and wetted to 12–14% water content for avoiding too much dusting. The latter tests showed that the dry density could not be raised to more than about 1300 kg/m^3 with the available compaction equipment. More effective compaction requires use of rammers or pad- or sheep-foot tools.

The experience from the Stripa and Äspö field tests shows that the amplitude and frequency of the vibrators and the equipment for operating them have to be adapted to the respective type of backfill material and shape of the room to be backfilled. It seems necessary to develop vibrators with a possibility to vary the frequency and also to make them exert a higher pressure on the fill if the backfill has a higher clay content than 15–25%.

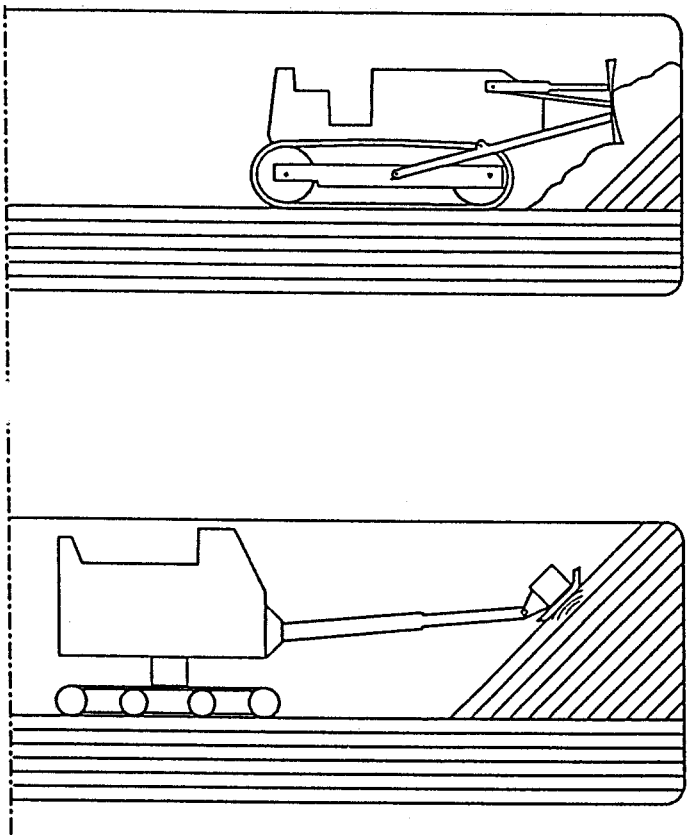

Figure 9-8. *Example of "sideways" backfilling and compaction. The lower picture shows a 700 kg vibrator plate mounted on a tractor for compaction of inclined backfill layers. The plate was electrically powered and could be tilted, turned and pushed to produce 30–40° inclination of the slope.*

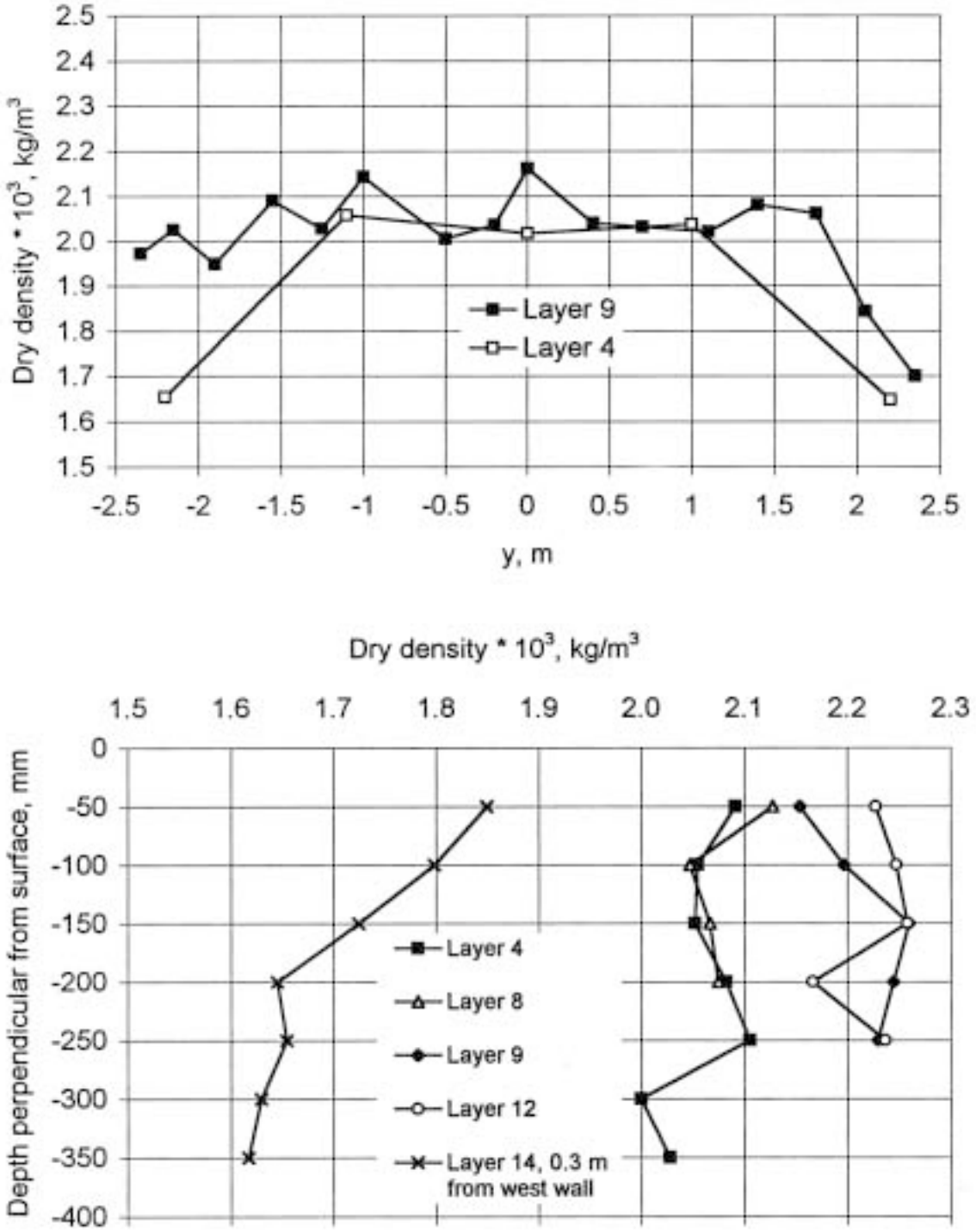

Figure 9-9. *Density variation in 10/90 mixture of crushed TBM muck and MX-80 bentonite at sideways application and compaction. 700 kg plate vibrator, 0.3 m thick layers applied. Upper: Variation across the diameter of the drift at mid-height. Lower: Variation normally to the layers. The left curve represents a layer applied on soft rock fill.*

Figure 9-10. *Excavation of 10/90 backfill in backfilling experiment at Äspö. The backfill material adheres to the rock at wet spots.*

9.4.3 Application by blowing

A possible technique for backfilling of drifts and tunnels that has been tried at Stripa for backfilling the upper part of a blasted drift is to blow ("shotcrete") the material into the space, as indicated in Figures 9-11 and 9-12 /1/. The grain size composition of the 20/80 mixture is shown in Figure 9-13. A small amount of angular quartzite (4–8 mm) had to be added in order to clean the nozzle. The water ratio was 15%.

This technique was concluded to give a too low average density (ρ_d =1200 kg/m^3) and too large variations in density, i.a. a dry density as low as 800 kg/m^3 at the roof, for being accepted in its present form. It has to be further developed to be ranked as candidate method, for instance so that coarse bentonite pellets can be blown in, possibly in combination with compaction using pneumatic tools.

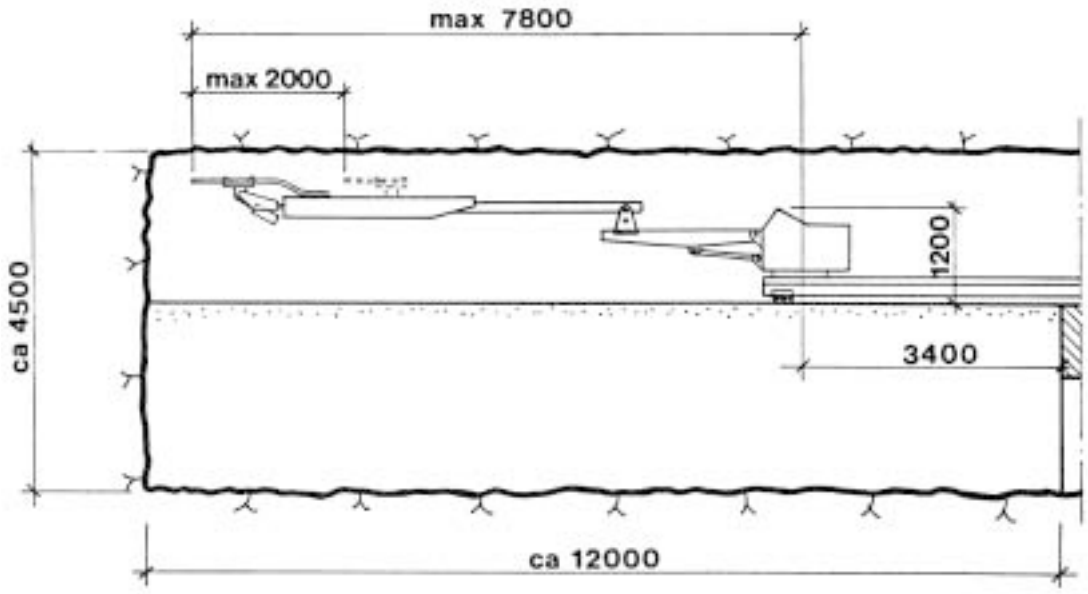

Figure 9-11. *Schematic picture of robot for shotcreting 20/80 bentonite backfill. Dimensions in mm /1/.*

Figure 9-12. *Blowing of 20/80 mixture near the roof of the drift /1/.*

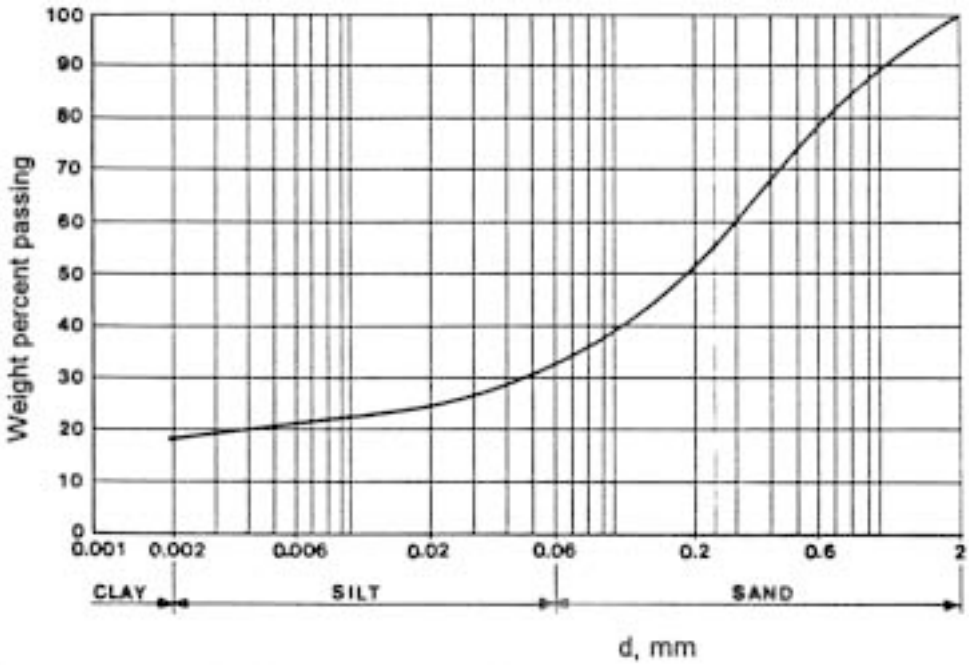

Figure 9-13. *Grain characteristics of the blown backfill with 20% MX-80 and 80% graded ballast of glacial origin /1/.*

9.4.4 Manufacturing and application of precompacted blocks

It has long been realized that air-dry powder of other minerals than smectite can be compressed to blocks with high density and strength. A recent study /4/ of the possibility of preparing blocks of mixtures of MX-80 bentonite, or a more fine-grained type of bentonite, and three types of ballast materials (Figure 9-14), demonstrated certain important facts:

- Blocks can be prepared with bentonite contents down to 10% if crushed rock is used as ballast component. In practice 20–30% bentonite content is preferable for obtaining strong, manageable blocks.
- Very fine-grained ballast is not suitable.
- The physical properties of the block material are controlled by the density of the clay component.

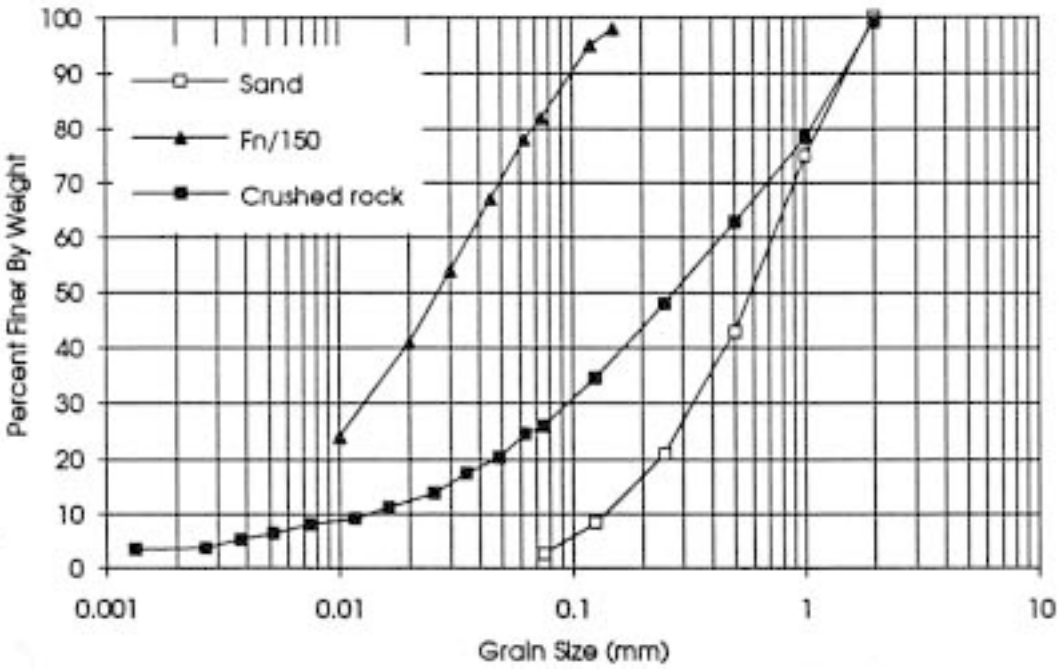

Figure 9-14. *Grain size distribution of the ballast materials for preparation of compacted bentonite/ballast blocks. Fn/150 is a very fine-grained filler-type ballast material /3/.*

If the block masonry (cf Figure 9-1) is left with a gap to the surrounding rock, water will be absorbed spot-wise, and some flow of disintegrated clay emanating from the blocks will take place. This yields variations in density and long time for fluid saturation, which in turn can cause block movements and heterogeneity. These disadvantages can be minimized by injecting a suitable grout in the gap behind a temporary or permanent bulkhead that can resist the grout pressure. The grout should be so composed that it initially has a low viscosity and then undergoes quick strengthening, for instance by mixing in strongly compacted smectite pellets and possibly low-pH cement. If the grout can be made chemically compatible with the block material, which does not offer major difficulties, and has a dry density of 1200–1400 kg/m^3, it will contribute to give an ultimate density of the saturated backfill of 1900 to 2000 kg/m^3, assuming a filling degree of the block units of 90% and their dry density to be around 1900 kg/m^3. This gives the entire backfill a net swelling pressure of a few hundred kPa and a bulk hydraulic conductivity of less than E-10 m/s. The major function of the grout is that it causes the block masonry to mature uniformly while it becomes consolidated under the swelling pressure of the maturing block system.

Backfilling of tunnels by using blocks requires very rational procedures and since no large-scale application of block-filling has been made so far, an optimum technique is not yet known. A combination of several techniques, as indicated in Figure 9-15, may turn out to be at optimum.

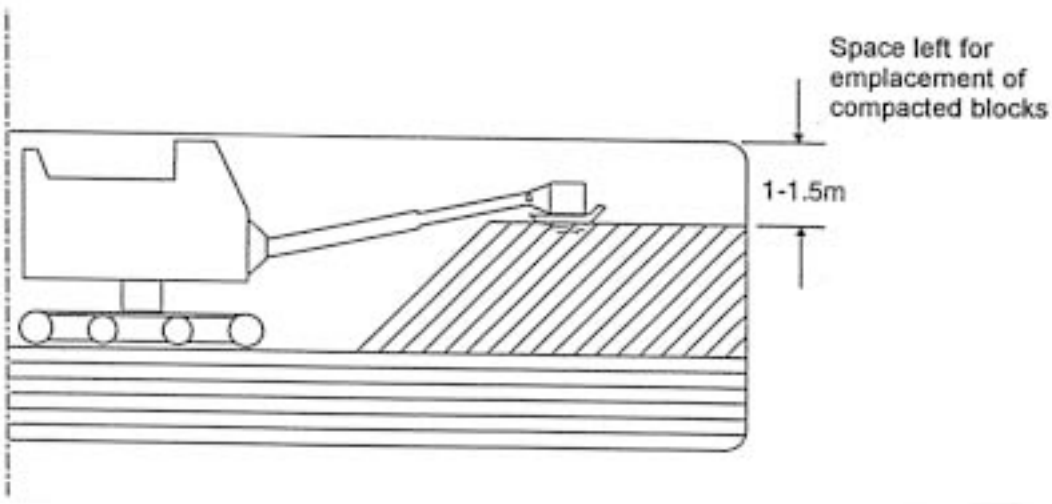

Figure 9-15. *Schematic picture of combination of backfilling techniques, i.e. bottom bed of horizontally applied layers, central fill of sideways application and compaction saving a space for block application.*

9.5 Importance of inflowing water for successful backfilling

A most important factor for successful application of smectitic backfills is the inflow of water into the tunnels and shafts that are to be filled. Experience indicates that it has to be limited to about 0.05 liters per minute and meter length of the room, which requires sealing of fracture zones by grouting or employing sealing methods. The above-mentioned technique to make masonries of units of compacted blocks and fill the gap with clay grout in short tunnel segments would offer a possibility to overcome difficulties with water inflow and disintegration of the backfilled material especially in TBM-tunnels since the required bulkhead can then be rather simple.

9.6 References

/1/ **Pusch R, Nilsson J, Ramqvist G, 1985**. Final Report of the Buffer Mass Test – Volume I: scope, preparative field work, and test arrangement. Stripa Project Technical Report 85-11. Svensk Kärnbränslehantering AB.

/2/ **Cederström M, Frykstedt L, 1984**. Packningsförsök med bentonit/ballast-blandningar. SKBF/KBS Arbetsrapport SFR 84-03. Svensk Kärnbränsle-hantering AB.

/3/ **Forsblad L, 2000.** Packning. Svensk Byggtjänst. ISBN 91-7732-932-0.

/4/ **Börgesson L, Johannesson L-E, Fredrikson A, 1993.** Laboratory investigations of highly compacted sand/bentonite blocks for backfilling. Compaction technique, material properties and repository function. SKB Djupförvar Projekt Rapport PR 44-93-010. Svensk Kärnbränslehantering AB.

ISSN 1404-0344

CM Digitaltryck AB, Bromma, 2002